



MONASH University

**Ventilation-Induced Brain Injury
in Preterm Neonates:
Mechanisms and Potential Therapies**

Chan Yan Yee Kyra

BBioMedSci(SchProg), BBioMedSc(Hons)

A thesis submitted for the degree of Doctor of Philosophy at
Monash University in 2020

Department of Obstetrics and Gynaecology, Faculty of Medicine, Nursing and Health Sciences
The Ritchie Centre, Hudson Institute of Medical Research
Melbourne, Australia

© Chan Yan Yee Kyra (2020).

I certify that I have made all reasonable efforts to secure copyright permissions for third-party content included in this thesis and have not knowingly added copyright content to my work without the owner's permission.

Figures created with BioRender.com were exported under a paid subscription.

This page is intentionally blank.

To you.

The proof that the little prince existed is that he was enchanting, that he laughed, and that he was looking for a sheep. When someone wants a sheep, it is proof that they exist.

- **Antoine de Saint-Exupéry**, *The Little Prince*

Contents

CONTENTS	I
GENERAL DECLARATION	V
FUNDING ACKNOWLEDGEMENT	VI
RESEARCH DISSEMINATIONS	VII
PEER-REVIEWED PUBLICATIONS	VII
PRESENTATIONS	VIII
AWARDS AND RECOGNITION	XI
ACKNOWLEDGEMENTS	XIII
THESIS SUMMARY	XVII
LIST OF	XX
UNITS, SYMBOLS, AND ABBREVIATIONS	XX
CHAPTER ONE: INTRODUCTION	1
1.1. PRETERM BIRTH	1
1.1.1. <i>Neurodevelopmental morbidities associated with preterm birth</i>	1
1.2. FETAL BRAIN DEVELOPMENT AND VULNERABILITY OF THE IMMATURE BRAIN	3
1.2.1. <i>Gliogenesis and myelination</i>	4
1.2.2. <i>Vascularisation</i>	5
1.2.3. <i>Neurovascular unit</i>	6
1.2.3.1. Neurovascular coupling and cerebral autoregulation	6
1.2.3.2. The blood-brain barrier and neurovascular permeability	7
1.3. VENTILATION OF THE PRETERM NEONATE	8
1.3.1. <i>Requirement for assisted ventilation in the delivery room</i>	8
1.3.2. <i>Requirement for assisted ventilation in the NICU</i>	10
1.3.3. <i>Aspects of providing ventilation that may cause injury</i>	10
1.3.3.1. Ventilation-induced lung injury	11
1.3.3.2. Effects of poorly controlled ventilation in the delivery room on the brain	13
1.3.3.3. Effects of prolonged controlled ventilation in the NICU on the brain	14
1.4. VENTILATION-INDUCED BRAIN INJURY (VIBI)	15
1.4.1. <i>Haemodynamic pathway of injury</i>	16
1.4.1.1. Haemodynamic instability due to altered cerebral autoregulation	16
1.4.1.2. Altered blood-brain barrier	17
1.4.2. <i>Inflammatory pathway of injury</i>	17
1.4.3. <i>Neuropathology in preclinical studies</i>	19
1.4.4. <i>Potential management strategies and treatments</i>	21
1.4.5. <i>Summary of VIBI</i>	23
1.5. UMBILICAL CORD BLOOD (UCB)	23
1.5.1. <i>UCB composition</i>	23
1.5.2. <i>Umbilical cord blood cells and neonatal brain injury</i>	25
1.6. SUMMARY AND THESIS AIMS	26
CHAPTER TWO: GENERAL METHODOLOGY	30
2.1. ANIMAL ETHICS AND WELFARE	30
2.2. EXPERIMENTAL DESIGN – BRAIN INJURY 24 H AFTER INJURIOUS VENTILATION (CHAPTERS 3 & 4)	30

2.2.1.	<i>Fetal surgery</i>	31
2.2.2.	<i>Injurious ventilation strategy</i>	32
2.2.3.	<i>Surgical wound closure and post-surgery monitoring</i>	33
2.2.4.	<i>Umbilical cord blood cell preparation and administration (Chapter 4 only)</i>	33
2.2.5.	<i>Lamb delivery and stabilisation</i>	34
2.2.6.	<i>Lamb monitoring during magnetic resonance imaging</i>	34
2.2.7.	<i>Blood samples</i>	34
2.2.8.	<i>Physiological data collection and analysis</i>	35
2.3.	EXPERIMENTAL DESIGN — BRAIN INJURY FOLLOWING 24 H IN UTERO VENTILATION (CHAPTER 5)	35
2.3.1.	<i>Fetal surgery</i>	36
2.3.2.	<i>Maternal surgery</i>	37
2.3.3.	<i>Ewe recovery and post-surgical care</i>	37
2.3.4.	<i>In utero ventilation</i>	38
2.3.5.	<i>Blood samples</i>	38
2.3.6.	<i>Physiological data collection and analysis</i>	39
2.4.	TISSUE COLLECTION AND HANDLING (ALL CHAPTERS)	39
2.4.1.	<i>Cerebrospinal fluid collection</i>	39
2.4.2.	<i>Removal of brain from skull</i>	40
2.4.3.	<i>Right hemisphere collection</i>	40
2.4.4.	<i>Left hemisphere collection</i>	40
2.5.	MOLECULAR ANALYSES.....	41
2.5.1.	<i>Enzyme-linked immunosorbent assay</i>	41
2.5.2.	<i>RT-qPCR by Fluidigm</i>	42
2.5.2.1.	RNA preparation	42
2.5.2.2.	cDNA preparation	43
2.5.2.3.	Quantitative real-time polymerase chain reaction (qPCR) by Fluidigm (Chapters 3 & 4)	44
2.6.	HISTOLOGICAL AND IMMUNOHISTOCHEMICAL ANALYSES	46
2.6.1.	<i>Tissue fixation, processing, embedding, and sectioning</i>	46
2.6.2.	<i>Histological staining</i>	46
2.6.3.	<i>Immunohistochemistry staining</i>	46
2.6.4.	<i>Regions of interest</i>	50
2.6.5.	<i>Quantitative analyses</i>	52
2.6.5.1.	Haematoxylin and Eosin.....	52
2.6.5.2.	Ionised calcium-binding adapter molecule-1 (Iba-1)	53
2.6.5.3.	Sheep serum	54
2.6.5.4.	Oligodendrocyte transcription factor (Olig2).....	55
2.6.5.5.	Myelin basic protein (MBP).....	56
2.6.5.6.	Glial fibrillary acid protein (GFAP).....	57
2.7.	STATISTICAL ANALYSES	57
CHAPTER THREE: ISOLATING PATHWAYS OF ACUTE VIBI		58
3.1.	INTRODUCTION	58
3.2.	METHODS	59
3.2.1.	<i>Instrumentation and injurious ventilation strategy</i>	60
3.2.2.	<i>Lamb delivery and subsequent monitoring</i>	61
3.2.3.	<i>Brain collection</i>	61
3.2.4.	<i>Reverse-transcription real-time quantitative PCR</i>	62
3.2.5.	<i>Immunohistochemistry</i>	62
3.2.6.	<i>Quantitative immunohistochemical analysis</i>	62
3.2.7.	<i>Plasma protein analysis</i>	63
3.2.8.	<i>Statistical analysis</i>	64
3.3.	RESULTS.....	65
3.3.1.	<i>Physiological parameters</i>	65
3.3.2.	<i>Injurious ventilation and carotid blood flow</i>	67

3.3.3.	<i>Plasma cytokine levels.....</i>	69
3.3.4.	<i>Gene expression levels in the PVWM and SCWM.....</i>	70
3.3.5.	<i>Immunohistochemical assessment of brain injury</i>	71
3.4.	DISCUSSION	75
3.5.	CONCLUSION.....	79
CHAPTER FOUR: EARLY UCBC EXACERBATES ACUTE VIBI		80
4.1.	INTRODUCTION	80
4.2.	METHODS	81
4.2.1.	<i>Instrumentation and injurious ventilation strategy.....</i>	82
4.2.2.	<i>Umbilical cord blood cells treatment.....</i>	82
4.2.3.	<i>Lamb delivery and subsequent monitoring</i>	83
4.2.4.	<i>Brain collection</i>	83
4.2.5.	<i>Plasma protein analysis.....</i>	84
4.2.6.	<i>Reverse-transcription real-time quantitative PCR</i>	84
4.2.7.	<i>Immunohistochemistry.....</i>	84
4.2.8.	<i>Quantitative immunohistochemical analysis.....</i>	85
4.2.9.	<i>Statistical analysis</i>	85
4.3.	RESULTS.....	87
4.3.1.	<i>Physiological and ventilation parameters</i>	87
4.3.2.	<i>UCB cell treatment increased systemic inflammation.....</i>	88
4.3.3.	<i>Gene expression levels of inflammatory cytokines.....</i>	90
4.3.4.	<i>UCB cell treatment increased microgliosis</i>	91
4.3.5.	<i>UCB cell treatment altered blood brain barrier integrity</i>	93
4.3.6.	<i>UCB cell treatment reduced the number of oligodendrocytes</i>	96
4.3.7.	<i>Gene expression levels of markers of cell death.....</i>	97
4.4.	DISCUSSION	98
4.5.	CONCLUSION.....	102
CHAPTER FIVE: VIBI FROM PROLONGED VENTILATION		104
5.1.	INTRODUCTION	104
5.2.	METHODS	105
5.2.1.	<i>Instrumentation.....</i>	106
5.2.2.	<i>Ventilation strategy and blood gas sampling.....</i>	106
5.2.3.	<i>Brain collection</i>	106
5.2.4.	<i>Histological staining and analysis.....</i>	107
5.2.5.	<i>Immunohistochemistry.....</i>	107
5.2.6.	<i>Quantitative immunohistochemical analysis.....</i>	108
5.2.7.	<i>Plasma protein analysis.....</i>	108
5.2.8.	<i>Statistical analysis</i>	109
5.3.	RESULTS.....	110
5.3.1.	<i>Lamb characteristics, ventilation parameters, and arterial blood gas parameters</i>	110
5.3.2.	<i>Plasma and CSF cytokine levels</i>	112
5.3.3.	<i>Assessment of gross neuropathology.....</i>	115
5.3.4.	<i>Iba-1 positive microglia in the PVWM and SCWM</i>	115
5.3.5.	<i>Sheep serum immunoreactivity in the PVWM and SCWM</i>	117
5.3.6.	<i>Olig2-positive oligodendrocytes in the PVWM and SCWM</i>	118
5.4.	DISCUSSION	119
5.5.	CONCLUSION.....	122
CHAPTER SIX: GENERAL DISCUSSION		123
6.1.	OVERVIEW	123
6.2.	TIDAL VOLUME BELOW A THRESHOLD DOES NOT INDUCE VIBI	125

6.3.	DOES LUNG INJURY PREDICT BRAIN INJURY?	126
6.3.1.	<i>Role of the haemodynamic and inflammatory pathways to VIBI</i>	126
6.4.	EARLY UCB CELL THERAPY IN CONJUNCTION WITH MECHANICAL VENTILATION IS UNFAVOURABLE.....	128
6.5.	THE INFLUENCE OF THE PLACENTA	129
6.6.	LIMITATIONS	130
6.6.1.	<i>Clinical relevance of the fetal ventilation model</i>	130
6.6.2.	<i>Low tidal volumes</i>	131
6.6.3.	<i>Brain regions of interest and pathways of injury investigated</i>	131
6.6.4.	<i>Inherent issues with using sheep</i>	132
6.7.	FUTURE DIRECTION.....	132
6.7.1.	<i>Umbilical cord blood cells and mechanical ventilation</i>	132
6.7.2.	<i>Further characterisation of the pathology and pathways of VIBI</i>	133
6.7.3.	<i>Examining placental factors</i>	133
6.8.	CONCLUSION.....	133
REFERENCES.....		134
AFTERWORD		153
APPENDICES.....		155
APPENDIX I		156
APPENDIX II		186
APPENDIX III		205

General Declaration

This thesis is an original work of my research and contains no material which has been accepted for the award of any other degree or diploma at any university or equivalent institution and that, to the best of my knowledge and belief, this thesis contains no material previously published or written by another person, except where due reference is made in the text of the thesis.

Chan Yan Yee Kyra

02 July 2020

Funding Acknowledgement

This research was supported by the Department of Obstetrics & Gynaecology, the Faculty of Medicine, Nursing and Health Sciences, and Monash University through the Co-Funded Monash Graduate Scholarship, Faculty Graduate Research International Scholarship, Monash International Postgraduate Research Scholarship, and Monash University Graduate Research Completion Award.

Research Disseminations

Peer-Reviewed Publications

Asterisk denotes equal contribution

Publications arising from this thesis

1. **Chan KYY**, Miller SL, Schmölzer GM, *Stojanovska V, *Polglase GR. Respiratory support of the preterm neonate: lessons about ventilation-induced brain injury from large animal models. [Submitted to *Front Neurol*, resubmitted after peer review on 18/06/2020]

N.B. This manuscript has since been accepted and published in *Front Neurol* 2020;**11**:862.

Publications arising from collaboration, in relation to this thesis

1. Smith MJ, **Chan KYY**, Papagianis PC, Nitsos I, Zahra VA, Allison BJ, Polglase GR, McDonald CA. Umbilical cord blood cells do not reduce ventilation-induced lung injury in preterm lambs. *Front Physiol* 2020;**11**:119.
2. Alahmari DM, **Chan KYY**, Stojanovska V, LaRosa DA, Barton SK, Nitsos I, Zahra VA, Barbuto J, Farrell M, Yamaoka S, Pearson JT, Polglase GR. Diffusion tensor imaging detects ventilation-induced brain injury in preterm lambs. *PLoS One* 2017;**12**(12):e0188737.

Additional publications during candidature

1. Allison BJ, LaRosa DA, Barton SK, Hooper SB, Zahra VA, Tolcos M, **Chan KYY**, Barbuto J, Inocencio IM, Moss TJM, Polglase GR. Dose-dependent exacerbation of ventilation-induced lung injury by erythropoietin in preterm newborn lambs. *J Appl Physiol* 2019;**126**(1):44-50.
2. **Chan KYY**, LaRosa DA, Tolcos M, Li A, Zahra VA, *Polglase GR, *Barton SK. Optimizing the dose of erythropoietin required to prevent acute ventilation-induced cerebral white matter injury in preterm lambs. *Dev Neurosci* 2017;**39**(1-4):298-309.

Presentations

Presenting author underlined

Invited Presentations

1. **Chan KYY**. (2019). What happens to the developing brain when we help our most vulnerable babies breathe? Invited talk at the *2019 AusCP-CTN Hot Topics in Cerebral Palsy Research Forum*, Melbourne, VIC, Australia.
2. **Chan KYY**. (2019). Ventilation-induced brain injury in the preterm infant: what we know and where to go from here. Invited talk at *Centre for Neuroscience Imaging Research, Sungkyunkwan University*, Suwon, South Korea.

Accepted Conference Abstracts

1. **Chan KYY**, Zahra VA, Stojanovska V, Nitsos I, Allison BJ, Polglase GR. (2020). Neuropathology in the very immature ovine brain following prolonged in utero ventilation. *24th Perinatal Society of Australia and New Zealand (PSANZ) Annual Congress*, Sydney, NSW, Australia. [Poster/Conference postponed/Abstract to be published in *J Paediatr Child Health*]
2. **Chan KYY**, Zahra VA, Stojanovska V, Nitsos I, Allison BJ, Polglase GR. (2019). Neuropathology in the very immature ovine brain following prolonged in utero ventilation. *Students of Brain Research (SOBR) 2019 Student Symposium*, Melbourne, VIC, Australia. [Poster]
3. Stojanovska V, Staindl EM, **Chan KYY**, Stanojkovic D, Nitsos I, Zahra VA, Hooper SB, Galinsky R, Polglase GR. (2019). Intrauterine inflammation inhibits breathing movements in fetal lambs. *46th Annual Meeting of The Fetal and Neonatal Physiological Society*, Marysville, VIC, Australia. [Oral]
4. **Chan KYY**, Zahra VA, Stojanovska V, Papagianis PC, Li A, Nitsos I, LaRosa DA, Miller SL, Alahmari DM, Polglase GR, McDonald CA. (2019) Early administration of umbilical cord blood cells increases ventilation-induced brain injury in preterm lambs. *10th International Brain Research Organisation (IBRO) World Congress of Neuroscience*, Daegu, South Korea. [Poster/Published abstract in *IBRO Reports*; **6**: S82]
5. Polglase GR, **Chan KYY**, Stojanovska V, Barton SK, Nitsos I, Zahra VS, Hooper SB, James Pearson JT, Alahmari DM. (2019). Diffusion tensor imaging detects ventilation-induced brain injury in preterm lambs. *Annual Pediatric Academic Societies Meeting*, Baltimore, MD, United States. [Poster]

6. Smith M, Nitsos I, Papagianis PC, **Chan KYY**, Zahra VA, Allison BJA, Polglase GR, McDonald CA. (2019). Umbilical cord blood cells do not reduce ventilation induced lung injury in preterm infants. *23rd Perinatal Society of Australia and New Zealand (PSANZ) Annual Congress*, Gold Coast, QLD, Australia. [Oral]
7. **Chan KYY**, Zahra VA, Stojanovska V, Papagianis PC, Li A, Nitsos I, LaRosa DA, Miller SL, Alahmari DM, Polglase GR, McDonald CA. (2018). Early administration of umbilical cord blood cells increases inflammation and blood-brain barrier breakdown in injuriously ventilated preterm lambs. *38th Annual Scientific Meeting of the Australasian Neuroscience Society*, Brisbane, QLD, Australia. [Oral]
8. Polglase GR, **Chan KYY**, Stojanovska V, Barton SK, Nitsos I, Zahra VA, James Pearson JT, Alahmari DM. (2018). Diffusion tensor imaging detects ventilation-induced brain injury in preterm lambs. *38th Annual Scientific Meeting of the Australasian Neuroscience Society*, Brisbane, QLD, Australia. [Oral]
9. Stojanovska V, Galinsky R, Staindl EM, Zahra VA, **Chan KYY**, Stanojkovic D, Nitsos I, Hooper SB, Polglase GR. (2018). Intrauterine inflammation is associated with high PGE₂ expression and microgliosis in brainstem respiratory centre. *38th Annual Scientific Meeting of the Australasian Neuroscience Society*, Brisbane, QLD, Australia. [Poster]
10. **Chan KYY**, Nitsos I, Zahra VA, LaRosa DA, Stojanovska V, Miller SL, Alahmari DM, Polglase GR, McDonald CA. (2018). Early administration of umbilical cord blood cells increases systemic inflammation and blood-brain barrier breakdown in injuriously ventilated preterm lambs. *11th Hershey Conference on Developmental Brain Injury*, Pacific Grove, CA, United States. [Poster]
11. Alahmari DM, **Chan KYY**, Stojanovska V, Barton SK, Nitsos I, Zahra VA, Barbuto J, Pearson JT, Polglase GR. (2018). Diffusion tensor imaging detects ventilation-induced brain injury in preterm lambs. *11th Hershey Conference on Developmental Brain Injury*, Pacific Grove, CA, United States. [Poster]
12. **Chan KYY**, Nitsos I, Zahra VA, LaRosa DA, Stojanovska V, Miller SL, Alahmari DM, Polglase GR, McDonald CA. (2018). Early administration of umbilical cord blood cells increases systemic inflammation and blood-brain barrier breakdown in injuriously ventilated preterm lambs. *32nd Fetal and Neonatal Workshop of Australia and New Zealand*, Queenstown, OTA, New Zealand. [Oral]

13. Smith M, Polglase GR, McDonald CA, Papagianis PC, Nitsos I, Zahra VA, **Chan KYY**. (2018). Do umbilical cord blood cells reduce ventilation induced lung injury in preterm infants? *32nd Fetal and Neonatal Workshop of Australia and New Zealand*, Queenstown, OTA, New Zealand. [Oral]
14. **Chan KYY**, Nitsos I, Zahra VA, LaRosa DA, Stojanovska V, McDonald CA, Miller SL, Alahmari DM, Polglase GR. (2017). How does initiating mechanical ventilation in the delivery room affect the preterm brain? *Monash Health Translational Precinct Research Week*, Melbourne, VIC, Australia. [Poster]
15. **Chan KYY**, Nitsos I, Zahra VA, LaRosa DA, Stojanovska V, McDonald CA, Miller SL, Alahmari DM, Polglase GR. (2017). Isolating effects of the initiation of ventilation on the preterm lamb brain. *3rd Annual Monash University Clinical Schools Translational Research Symposium*, Melbourne, VIC, Australia. [Poster]
16. **Chan KYY**, Nitsos I, Zahra VA, LaRosa DA, Stojanovska V, McDonald CA, Miller SL, Alahmari DM, Polglase GR. (2017). How does initiating mechanical ventilation in the delivery room affect the preterm brain? *8th Annual Australian Society for Medical Research (ASMR) Victoria Student Research Symposium*, Melbourne, VIC, Australia. [Poster]
17. **Chan KYY**, Nitsos I, Zahra VA, LaRosa DA, Stojanovska V, McDonald CA, Miller SL, Alahmari DM, Polglase GR. (2017). Isolating effects of the initiation of ventilation on the preterm lamb brain. *31st Fetal and Neonatal Workshop of Australia and New Zealand*, Canberra, ACT, Australia. [Oral]
18. **Chan KYY**, LaRosa DA, Tolcos M, Li A, Zahra VA, Barton SK, Polglase GR. (2016). Optimising the dose of erythropoietin required to prevent ventilation-induced brain injury. *Monash Health Translational Precinct Research Week*, Melbourne, VIC, Australia. [Poster]
19. **Chan KYY**, LaRosa DA, Tolcos M, Li A, Zahra VA, Barton SK, Polglase GR. (2016). Optimising the dose of erythropoietin required to prevent ventilation-induced brain injury in preterm lambs. *Students of Brain Research (SOBR) 2016 Student Symposium*, Melbourne, VIC, Australia. [Oral]

Awards and Recognition

2020

Monash University Graduate Research Completion Award, Monash University

The Graduate Research Completion Award provides financial support to students in the final stages of thesis preparation who have been significantly impacted during the COVID-19 situation.

Early Career Research Travel Award, Perinatal Society of Australia and New Zealand (PSANZ)

2019

Young Investigator Training Program, International Brain Research Organisation (IBRO)

The Young Investigator Training Program (YITP) is a prestigious award that supports a week-long immersion in leading neuroscience laboratories prior to the quadrennial World Congress of Neuroscience. The award also fully supports attendance at the conference. In 2019, sixty awardees were selected from 500 international applications to participate in the program preceding the 10th IBRO World Congress of Neuroscience in Daegu, South Korea.

Three-Minute Thesis People's Choice Award, The Ritchie Centre

Student Travel Award, Australasian Neuroscience Society (ANS)

2018

Outstanding Young Investigator – Trainee Award, The Hershey Conference

The Young Investigator Trainee Award is a travel stipend, not limited to young investigators from the United States of America, that fully supports attendance at the biannual Hershey Conference. In 2018, two awardees were selected for the inaugural award to attend the 11th Hershey Conference on Developmental Brain Injury in Pacific Grove, California, United States.

Senior PhD Student Travel Award Top-up, The Ritchie Centre

Monash Graduate Education Travel Grant, Monash University

2017

Monash International Postgraduate Research Scholarship, Monash University

The Monash International Postgraduate Research Scholarship (MIPRS) funded by Monash University is a competitive university-wide tuition scholarship that meets the full cost of international course tuition fees and standard Overseas Student Health Cover. (July 2017 – July 2020)

2016

Faculty Graduate Research International Scholarship by the Faculty of Medicine, Nursing and Health Sciences, Monash University

The Faculty Graduate Research International Scholarship (FGRIS) funded by the enrolling faculty (Medicine, Nursing and Health Sciences) and the enrolling academic unit (Department of Obstetrics & Gynaecology) is a competitive faculty-wide tuition scholarship that meets the full cost of international course tuition fees. (October 2016 – July 2017)

Co-Funded Monash Graduate Scholarship, Monash University

The Co-funded Monash Graduate Scholarship (CF-MGS) funded by Monash University and the enrolling faculty/academic unit (Medicine, Nursing and Health Sciences/Department of Obstetrics & Gynaecology) is a competitive university-wide stipend scholarship awarded to international students undertaking a higher degree by research. (October 2016 – April 2020)

Acknowledgements

The best view comes after the hardest climb, and while no one could do the climbing for me, I am where I am only because of the support I have received along the way. After all, science is not something you do alone. The premise of scientific research is that it is incremental, and it is unquestionably on the shoulders of giants that this thesis has come to fruition. In particular, I would like to thank my supervisors Dr Graeme Polglase, Dr Vanesa Stojanovska, and Dr Suzie Miller for their encouragement and generous professional support.

To Graeme, my tallest giant –

You have always cared for me as a person, even when I was the worst, sassiest, procrastinating student. To you, it was never (entirely) about me ticking boxes or winning awards; it was if I was confident and happy. Yet, you have celebrated each of my successes like a proud parent trying to play it cool. You have kept every single promise even as my academic goals constantly evolved, and I cannot adequately express how grateful I am.

You've taught me that seemingly futile journeys and processes can and will teach me important lessons I'd otherwise miss, and that is a life lesson I will carry with me beyond the confines of science. In the most terrifying moments, I'll remember you asking "but have you tried" and let the fear empower me instead. Grae, I'm not saying that I couldn't have done this without you; I'm saying that I wouldn't have wanted to do this with anyone else. Thanks for everything.

To Vanesa –

You have been more excited about my achievements than I have, and you constantly remind me of how deserving I am of them. I truly appreciate your honesty about my progress and for unabashedly sharing your journey as a scientist. Thank you for not giving up on me.

To Suzie –

With you, I have never felt that my opinions did not matter. You have never hesitated when I reached out for help and I genuinely value your guidance. Thank you.

To Val –

You have been instrumental to my growth and have gone above and beyond to make sure that I stay afloat. I owe so much of what I know to your teaching and there are not enough 'thank you's I can say to express my gratitude. Thanks for being on my side.

To Sam –

None of this thesis would have happened without your mentorship 4 years ago. In S12E24 of Grey's Anatomy, when Amelia was panicking before the wedding, Meredith told her, "if you want to freak out and call it off, if you want to run, I'll drive the getaway car. Just let me know what you need. I'm here for you." You have always been that person to me, thank you.

To my wonderful MBI family –

Thank you for the work that makes up half of this thesis. Paris – thanks for your patience and supervision through the early mornings and dreaded nights when I had no idea what I was doing. Jade – I'm glad the PM parties were with you.

To the loveliest IUV gang –

You were my hype men when I was too overwhelmed to see the cool science we were doing. Beth – you are an inspiration and it was from you that I ascertained the worth of my 'yes' and value of my presence. Kaz – you were always there with the answers. Dal and Ilias – I cannot thank the both of you enough for your assistance with surgeries and animal work, and for always pausing what you're doing to check that I'm doing okay. Thank you all so much.

To the Hooper Group –

You are family. Stuart – thank you for welcoming me into your lab group; it has been an absolute privilege and pleasure. Caroline – thanks for taking the burden of administrative work off my shoulders. Kelly – you have said all the things I needed to hear, before I knew I needed to hear them. Thank you so, so much. Ali – thanks for all your assistance. Anja – you have always been generous with your knowledge, thanks for reminding me that I have the capacity to educate and that I shouldn't undermine what I know. Rob – I've learnt from you that there is strength in admitting "it's not okay, but we can fix it". That means a lot to me.

To the PhD students before me –

You have made this journey infinitely less daunting. Mikee – you have been there from the start. Thank you for adopting this little sister with open arms. I owe you so many. Shreya – my Gambling Den 3. Aidan – your support makes up for all the broken streaks. Ben Nowotny – reading your thesis reflections prompted me to see myself as a person who has grown with my science rather than a scientist who has lost her person. I really needed that, thanks. To the 2017 ASMR SRS organising committee – signing up for that was one of the best decisions I made in my PhD. Those boardgame nights kept me sane and listening to your PhD struggles and life plans made me feel grounded and not alone. Thy – you are an amazing, brilliant human. Hidaya – you are essential. To the IBRO YTTP group – it was with you that

I re-found the sparkle in my eyes. Those weeks in Suwon and Daegu have meant the world. To Immanuel – tack för allt.

To Anna and Tayla –

It's been such fun completing my PhD alongside you two marvellous scientists and I wouldn't have had it any other way. The small things were always the big things to me. I'm pretty bummed Savoy's will never taste as good. Anna Maria – you unfailingly know what to say. Tayla Rose Penny – you spark so much joy.

To all other students and staff of The Ritchie Centre, Hudson Institute, and Monash –

I am aware that there are numerous others who have no doubt been a part of this story but whom I have not been able to personally credit. It is incredibly empowering yet humbling to work alongside you folks. Yen and Amy – I really appreciate all your help. Caroline Gargett – thanks for your invaluable feedback. Special thanks to the precious few who religiously stock up the snack drawer/feed me and even more those whose cars run on friendship and not petrol. Anqi – your presence is reassuring. Nhi – thanks for always showing up. Ingrid and Sharmony – you've made me recall all the joys when I first started, reminders I desperately needed to make it across the finish line. Thank you.

To people in my life who have known me from an identity apart from my PhD –

I am incredibly blessed that my village is the size of the world. Most of you have not directly contributed to this thesis, but I am certain that all of you pulled me through this candidature in one way or another, so thank you. To MG who first taught me that I can do all things and to all the friendships made in that decade that have survived another. Charlotte – we seem to always be in different parts of the world, yet it never feels that way. Thanks for being present. To my Gambling Den 1, Meddies, Westers – you have watched me grow up and have shaped the Melbourne I now hold dear. The past decade has been one crazy ride, thanks for sticking through. Yen – you deserve all the credit for putting BME on my radar; without that first step, none of this would have happened. Jia – this should be obvious, but it isn't always: please don't ever become a stranger.

To my family –

Nothing will ever make up for the time I have spent away, and I am immensely thankful that you have never asked for more than I could give. Daddy and Mummy – 所有的勇敢都來自你們對我的愛。 You brought me up to believe that I can do anything and everything I want, that I am not limited by my gender, race, age, or even myself. Your faith in my dreams and insane trust in me were what kickstarted this entire Melbourne journey. This thesis is as much mine as it is yours. Hong Kit and Yan Kei – the world is your oyster; it doesn't owe you anything, but it has everything to offer. And I will always have your backs.

Behind the science in this thesis is the summation of all these encounters, interactions, mentorships, lessons, stories, love, and grace. I know I have not come this far only to come this far. But before I move on to the next stage of my career and life, I think it's befitting to complete this chapter with a beautiful book as such:

Thesis Summary

Ventilation-induced brain injury (VIBI) refers to neuropathology resultant from respiratory support such as mechanical ventilation. The overarching theme of this thesis is VIBI in preterm infants – a unique population at an increased risk because of their high requirement for respiratory support and the heightened vulnerability of their immature brains at birth.

A significant number of preterm neonates will require respiratory support at birth, in the delivery room and subsequently in the neonatal intensive care unit (NICU), as their lungs are too underdeveloped for efficient gas exchange. While necessary, the initiation and maintenance of respiratory support can be inadvertently injurious to the immature brain. There are currently no effective preventive measures or treatments for brain injury resultant from this life-sustaining but potentially injurious intervention. This thesis investigates the pathways by which injurious ventilation impairs the immature brain and the effectiveness of umbilical cord blood (UCB) cells as a potential treatment.

Chapters Three and Four of this thesis focus on VIBI resultant from acute injurious ventilation, akin to ventilation with poorly controlled and/or excessive tidal volumes (V_T) a newborn might receive in the delivery room. Chapter Three seeks to clarify the relative contribution of the two major pathways of acute VIBI: cerebral inflammation and haemodynamic instability. This was possible using a fetal head-out ventilation model where manipulating placental circulation in one group isolated the haemodynamic pathway of injury. I found that injurious ventilation, regardless of placental circulation, did not increase systemic inflammation or any investigated histological markers of brain injury. Relative to previous findings whereby brain injury was observed after 15 min of injurious ventilation in preterm lambs, it appears that the early markers of cerebral inflammation and injury previously assessed at 2 h post-ventilation do not progress to gross injury at 24 h. However, the V_T obtained during injurious ventilation of these lambs were lower than desired, suggesting instead that V_T below a certain threshold may not result in VIBI. The absence of overt brain injury in the ventilated animals may also be attributed to limitations of our experimental model, discussed in detail within Chapter Three. Briefly, all animals (controls and ventilated) underwent magnetic resonance imaging after delivery, during which they were anaesthetised and sustained on mechanical ventilation. Although a gentle ventilation strategy was used, this may have inadvertently contributed to a baseline brain injury in all lambs, potentially masking the effects of the injurious ventilation 24 h prior.

Chapter Four investigates the efficacy of early UCB cell administration in preventing or reducing VIBI. UCB cells have shown neuroprotective potential with anti-inflammatory properties. Using the same fetal ventilation model as above, I administered 80 million UCB cells directly to the fetus 1 h after injurious ventilation onset. Instead of reducing severity of white matter injury, early UCB cell administration increased systemic and cerebral inflammation, compromised cerebral blood vessel integrity, and increased white matter injury. Thus, while my ventilation strategy in Chapter Three did not induce detectable systemic or cerebral inflammation, it appears to have created an environment that, in the presence of UCB cells, is pro-injury. Essentially, the data suggest that 1 h after injurious ventilation is an inappropriate timing for UCB cell administration in the context of VIBI. This is the first time UCB cells have been investigated in conjunction with mechanical ventilation in a preterm large animal model. As UCB therapies progress to clinical trials in preterm infants, many of whom will require mechanical ventilation in the delivery room, my findings highlight the urgent need to scrutinise the use of UCB cells in relation to mechanical ventilation.

Following results from Chapter Three, I investigated whether an extended period of standard (gentle, not intentionally injurious) ventilation was more damaging than a short period of injurious ventilation in the preterm neonate. Despite this being an obvious area of research, clinical observations have been limited by challenges in determining whether brain injury in preterm infants is due solely or predominantly to ventilation or confounded by ongoing clinical management. As such, neuropathology from long-term ventilation has not been comprehensively characterised.

Chapter Five explores the role of prolonged mechanical ventilation in VIBI progression. Using a model of *in utero* ventilation (IUV), I found that continuous ventilation for 24 h transiently increased systemic inflammation in preterm fetuses but had no effects on assessed histopathology in cerebral white matter. As with Chapter Three, the V_T achieved in these animals were lower than desired, implying yet again that a threshold V_T for VIBI may exist.

In trying to interpret results from all the chapters together, it became apparent that the haemodynamic and inflammatory pathways of VIBI are intricately interlinked.

Overall, my research to date has the potential to impact management and treatment of ventilated preterm infants with a focus on improving neurodevelopmental outcomes. I suggest that improved monitoring of V_T in the delivery room and maintaining low V_T during extended periods of ventilation in the NICU may reduce the risk of VIBI. Further, I propose that the inflammatory and haemodynamic pathways of VIBI are more intricately interlinked than previously understood. This has major implications for therapy development. Although my investigated therapy (UCB cells) in Chapter Four exacerbated rather than reduced acute VIBI, this study provides vital groundwork to understanding the

interaction of UCB therapy and mechanical ventilation. Additionally, it reinforces the importance of thorough preclinical investigations. My studies in this thesis emphasise the need and value of established animal models to study VIBI, in the context of both acute and chronic mechanical ventilation of preterm infants.

List of

Units, Symbols, and Abbreviations

Units

°C	degree Celsius; unit of temperature
<i>g</i>	relative centrifugal force
g	gram; unit of mass
h	hour; unit of time
IU	international unit
l	litre; unit of volume
M	molar; unit of concentration
m	metre; unit of length
m ²	square metre; unit of area
min	minute; unit of time
mmHg	millimetres of mercury; unit of pressure
s	second; unit of time
T	tesla; unit of magnetic induction

Prefixes

k	kilo	10 ³
m	milli	10 ²
c	centi	10 ⁻²
μ	micro	10 ⁻⁶
n	nano	10 ⁻⁹

Symbols

α	alpha
&	and
~	approximately
β	beta
©	copyright
Δ	delta
=	equal to
>	greater than
<	less than
/	per
%	percentage
±	plus or minus
®	registered trademark
™	unregistered trademark

Abbreviations

ABC	avidin-biotin complex
ANOVA	analysis of variance
BBB	blood-brain barrier
BDNF	brain-derived neurotrophic factor
BPD	bronchopulmonary dysplasia
BSA	bovine serum albumin
CBF	cerebral blood flow
cDNA	<i>see DNA</i>
CNS	central nervous system
CP	cerebral palsy
CSF	cerebrospinal fluid
C _T	cycle threshold
DAB	3,3'-Diaminobenzidine
DMSO	dimethyl sulfoxide
DNA	deoxyribonucleic acid
cDNA	complementary DNA
DTI	diffusion tensor imaging
EDTA	ethylenediaminetetraacetic acid
e.g.	<i>exempli gratia</i> (for example)
ELBW	extremely low birth weight
ELISA	enzyme-linked immunosorbent assay
EPC	endothelial progenitor cells
EPO	erythropoietin
et al.	<i>et alia</i> (and others)
FBS	fetal bovine serum
FiO ₂	fraction of inspired oxygen
FOV	field(s) of view
GA	gestational age
GDNF	glial cell line-derived neurotrophic factor
GFAP	glial fibrillary acidic protein
GM	grey matter

hAECs	human amnion epithelial cells
HRP	horse radish peroxidase
HSC	haematopoietic stem cells
Iba-1	ionised calcium-binding adapter molecule 1
ID	internal diameter
i.e.	<i>id est</i> (that is)
Ig	immunoglobulin
IL	interleukin
i.m.	intramuscular
i.v.	intravenous
IUV	<i>in utero</i> ventilation
IVH	intraventricular haemorrhage
JAM	junctional adhesion molecule
MBP	myelin basic protein
mRNA	<i>see RNA</i>
MRI	magnetic resonance imaging
MRS	magnetic resonance spectroscopy
MSC	mesenchymal stromal cells
N	number
N.B.	<i>nota bene</i> (note well; take note)
NBF	neutral buffered formalin
NeuN	neuronal nuclei
NGS	normal goat serum
NICU	neonatal intensive care unit
OD	outer diameter
Olig2	oligodendrocyte transcription factor 2
p	p-value; probability value in statistical hypothesis testing
PaCO ₂	partial pressure of carbon dioxide dissolved in arterial blood
PaO ₂	partial pressure of oxygen dissolved in arterial blood
PBCC	physiological-based cord clamping
PBF	pulmonary blood flow
PBS	phosphate-buffered saline

PCR	polymerase chain reaction
qPCR	quantitative real-time PCR
RT-qPCR	reverse transcription qPCR
PEEP	positive end-expiratory pressure
pH	measure of acidity or basicity
PIP	peak inspiratory pressure
PPV	positive pressure ventilation
PVL	periventricular leukomalacia
PVWM	periventricular white matter
qPCR	<i>see PCR</i>
ROS	reactive oxygen species
Rov	recombinant ovine
RNA	ribonucleic acid
mRNA	messenger RNA
RT-qPCR	<i>see PCR</i>
SaO ₂	oxygen saturation measured by blood analysis
SCWM	subcortical white matter
SD	standard deviation
SEM	standard error of the mean
SpO ₂	oxygen saturation measured by pulse oximetry
TMB	tetramethylbenzidine
TNF	tumour necrosis factor
Tregs	regulatory T cells
UCB	umbilical cord blood
UCBC	umbilical cord blood cells
VEGF	vascular endothelial growth factor
V _T	tidal volume
VIBI	ventilation-induced brain injury
VILI	ventilation-induced lung injury
VLBW	very low birth weight
WM	white matter

Note on gene and protein nomenclature

This thesis follows the general guidelines of the National Centre for Biotechnology Information (NCBI) Gene Database^a and the Human Genome Organisation (HUGO) Gene Nomenclature Committee (HGNC)^b for gene and protein nomenclature. For genes, only Latin letters and Arabic numerals are used, a space separates a letter and number in full names (e.g. interleukin 1 alpha), and the space is omitted in symbols. Gene symbols are italicised (e.g. *IL1A*). Where an alias has been used, the official gene name and symbol have also been provided. The formatting of symbols for RNA and cDNA follow the same conventions. RT-qPCR nomenclature follows the recommendation of The Minimum Information for Publication of Quantitative Real-Time PCR Experiments (MIQE) guidelines.^c

For protein nomenclature, Greek letters are written in full in lower case and a hyphen is included in the space that separates a letter and number in full names (e.g. interleukin-1 alpha). Protein symbols are identical to their corresponding gene symbols but are not italicised (e.g. IL1A). However, more commonly, the abbreviated name rather than protein symbol has been used in text. In abbreviated protein names, Greek letters are used and a hyphen separates a letter and number (e.g. IL-1 α).

Note on anatomical terms

In this thesis, ‘temporal lobe’ refers to tissue of the lamb brain taken at the level of the hippocampal formation, which includes the temporal lobe (see Section 2.6.4).

^a Gene [Internet]. Bethesda (MD): National Library of Medicine (US), National Center for Biotechnology Information (2004). Accessible at <<https://www.ncbi.nlm.nih.gov/gene/>>

^b Yates B. *et al.* Genenames.org: the HGNC and VGNC resources in 2017. *Nucleic. Acids. Res.* **45**:D619-625 (2017). Accessible at <<https://www.genenames.org/>>

^c Bustin S.A. *et al.* The MIQE guidelines: minimum information for publication of quantitative real-time PCR experiments. *Clin. Chem.* **55**:611-622 (2009).

Chapter One: Introduction

This chapter contains content included in a manuscript under review (Appendix I):

Chan KYY, Miller SL, Schmölzer GM, *Stojanovska V, *Polglase GR. Respiratory support of the preterm neonate: lessons about ventilation-induced brain injury from large animal models. [Submitted to *Front Neurol*, resubmitted with revisions after peer review on 18/06/2020]

N.B. This manuscript has since been accepted and published in *Front Neurol* 2020;**11**:862.

1.1. Preterm Birth

Preterm birth, defined as birth prior to 37 completed weeks of gestation, affects 15 million live births globally each year and is a major cause of perinatal mortality and morbidity.^{1,2} Many complications associated with prematurity are due to an interruption of normal organ development that would otherwise proceed to term *in utero*. For this reason, the distinction of babies by gestational age (GA) at birth – extremely preterm (<28 weeks), very preterm (28-<32 weeks), and moderate to late preterm (32-<37 weeks) – helps to identify infant populations which are most at risk of complications related to preterm birth.³ Reducing preterm birth is challenging as a significant proportion of spontaneous preterm labour cases have unidentified causes.¹ Advancements in neonatal healthcare have increased survival rates of preterm infants, especially those born at the lower limit of viability (22-25 weeks).¹⁻⁴ Unfortunately, improvements in the survival of preterm neonates have outpaced prevention of morbidities and many surviving preterm infants suffer long-term complications including neurologic consequences.⁵⁻⁸

1.1.1. Neurodevelopmental morbidities associated with preterm birth

Preterm birth is a major risk factor for brain injury. The annual rate of brain injuries occurring during or soon after birth among preterm infants is estimated to be 25.88 per 1000 live preterm births, more than 7 times higher than that of term infants.⁵ This rate has stayed fairly consistent from 2010 to 2015,⁵ highlighting the urgent need to devise ways to prevent or reduce brain injury in this population. Cerebral pathologies in preterm infants commonly present as intracranial haemorrhages (including intraventricular and periventricular haemorrhages), periventricular leukomalacia (PVL), and other white matter injury.^{5,9,10} Approximately 6% of very and extremely preterm infants have severe grade cerebral haemorrhages (grades 3 and 4)^{5,11} while the rates of cystic PVL is 1.1-1.8%.^{2,5} The prevalence of cystic PVL has decreased in the past decades and the most common form of white matter injury in

preterm infants now is diffuse white matter gliosis without focal lesions.^{2,10} Preterm infants are also likely to have altered white matter microstructure compared to their term counterparts.^{12,13} Importantly, these detectable abnormalities are predictors of subsequent neurodevelopmental morbidity in preterm infants.^{14,15}

Adverse neurodevelopmental outcomes are common in preterm infants, affecting nearly 1 million preterm infants who survive the neonatal period (first 28 days after birth) worldwide.¹⁶ These include varying severity of cognitive, motor, sensory, social, and behavioural deficits which may compromise quality of life of these individuals.^{17–19} In very and extremely preterm infants especially, the rate of survival with neurodevelopmental impairments is not decreasing.⁸

Doyle *et al.* evaluated neurosensory outcomes at two years of age of extremely preterm infants born at 22–27 weeks GA in the state of Victoria, Australia.¹⁸ Of the cohort (n=531 assessed from three eras: 1991–1992, 1997, 2005), 44.6% showed mild to severe developmental delay and 48.4% had mild to severe disability.¹⁸ When assessed at eight years of age, the 2005 cohort of children did not show better neurodevelopmental outcomes, whereby 14% were diagnosed with cerebral palsy (CP), highlighting that improved neonatal care over the years have not translated to improved outcomes.²⁰ It is indeed concerning that a baby born <32 weeks GA in high-income regions has only a 53% chance of surviving the neonatal period without later neurodevelopmental impairment.¹⁶ While moderate to late preterm infants – the largest and fastest growing subset of preterm neonates^{1,2} – are more mature in development at birth, their brains are still in a critical developmental time period and remain at risk of injury.²¹ Compared to term infants, late preterm infants have been found to have a three-fold increased risk of developing CP and a greater risk for developmental delay and learning difficulties at school age.^{21,22} Importantly, the impact of these morbidities extends beyond the neonatal period and the individual, persisting through childhood and early adulthood.^{19,23}

Economically, the cost associated with preterm birth is considerably high on individuals and the public sector.²⁴ Neonatal hospitalisation costs increase significantly with decreasing GA, in part due to the medical resources required and length of neonatal intensive care unit (NICU) stay.^{24–26} Additionally, part of the economic burden is attributed to long-term care, in particular due to neurodevelopmental disabilities, of surviving very and extremely premature babies. The financial cost of CP was A\$1.47 billion in Australia in 2007, with an additional A\$2.4 billion attributed to lost wellbeing²⁷ while the average lifetime cost of CP in individuals in Denmark is estimated at €830,000 (~A\$1.4 million), consisting largely of social costs including specialised education.²⁸ It is obvious that neurological morbidities associated with preterm birth puts a huge economical strain on society.

Altogether, there is an urgent need to reduce the burden of adverse neurodevelopmental outcomes in preterm babies by reducing the incidence of brain injury itself. The underlying cause of brain injury is the immature brain, since key neurodevelopmental events which occur *in utero* are interrupted by preterm birth.

1.2. Fetal brain development and vulnerability of the immature brain

Brain development occurs throughout gestation and continues into early adulthood. Preterm babies born during critical developmental windows are at risk of interrupted normal brain development and altered developmental trajectories.²⁹ These include progressive events such as neurogenesis, axonal and dendritic development, synaptogenesis, gliogenesis, and vascularisation, as well as regressive events such as synapse elimination, axon pruning, and apoptosis.³⁰

Between 23-32 weeks GA, key neurodevelopmental processes that are occurring include gliogenesis, the maturation of oligodendrocytes, and the establishment of the blood-brain barrier (BBB) [Fig. 1.1].³⁰ In addition, defence and repair mechanisms in the immature brain may be inadequate to prevent and/or repair damage sustained from insults,²⁹ thereby also contributing to subsequent neurodevelopmental impairments.

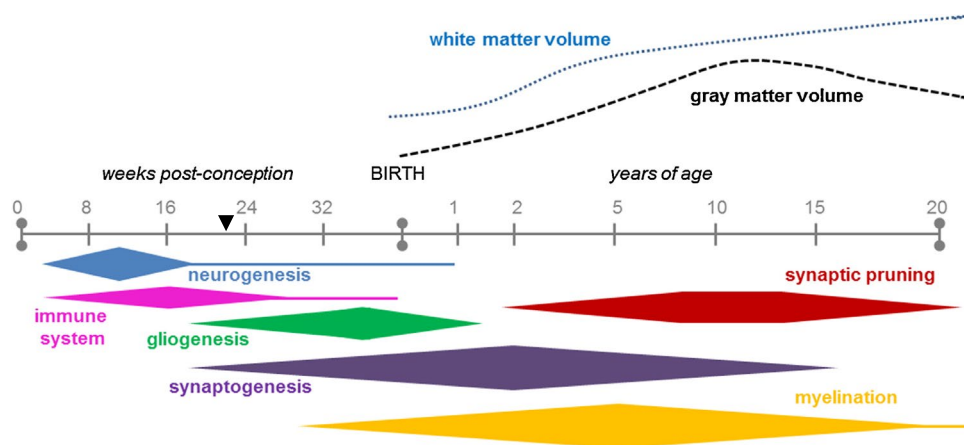


Figure 1.1. Timeline of main fetal and postnatal neurodevelopment events in humans.

The black arrowhead at 22 weeks marks the lowest possible gestational age of an extremely preterm infant because prior to then the lungs are too underdeveloped to support survival. To the right of that are processes likely to be compromised or altered following preterm birth. *Reproduced with permission from Semple et al., 2013³⁰ with minor adaptations.*

1.2.1. Gliogenesis and myelination

Preterm birth at <32 weeks GA coincides with gliogenesis and synaptogenesis.^{30,31} Glial cells are specialised support cells crucial for normal nervous system development and function.³² The three main types of glia in the central nervous system (CNS) are microglia, astrocytes, and oligodendrocytes.

Microglia are resident macrophages of the brain that also have roles in development.^{31,33} Amoeboid and intermediate microglial clusters are detected in the brain parenchyma from as early as 5.5 weeks GA.^{31,34} These cells localise around blood vessels from 10 weeks GA in the expanding intermediate zone of the forebrain (future white matter) then subsequently extend to the grey matter anlagen.^{34,35} The heterogeneous subpopulations of microglia continue to develop and proliferate alongside neurons and, by 35 weeks GA, are present in the CNS as well-differentiated, ramified microglia in the resting phenotype.^{31,34–36} Microglia are crucial for normal brain development and have been associated with neuronal migration and cell death, phagocytosis of cell debris, angiogenesis, axonal development, and synaptic pruning.^{32,33,36–38} Furthermore, microglia are involved in vasculogenesis and BBB development in the embryonic brain.³⁸ Besides regulating homeostasis through surveillance and scavenging functions, microglia can change activation states in pathological conditions to take on a spectrum of functional phenotypes.^{32,33,36,37}

Astrocytes develop later in gestation than microglia, often after initial neurogenesis in many CNS regions.³⁹ Astrocytes are the most abundant cell type within the CNS and can be classified into two main populations: protoplasmic astrocytes found mainly in grey matter and fibrous astrocytes predominantly in white matter.³² Both astrocyte types are in extensive contact with blood vessels and contribute to angiogenesis.³⁹ There are no astrocytes present in the developing brain when it is first vascularised, suggesting that they do not participate in the early stages of BBB development.^{40,41} However, as brain development progresses, mature astrocytes produce factors that regulate BBB function and integrity.⁴⁰ Astrocytes also play important roles in neuronal survival and axonal guidance, to regulate the extracellular environment, and to maintain brain metabolic homeostasis.³²

Given the vital homeostatic roles of microglia and astrocytes, it is obvious that any interruption or impairment in the development of these cells due to preterm birth can impact brain function. Importantly, both microglia and astrocytes are able to take on a reactive phenotype after an insult.^{37,42} This shift to reactive phenotypes further diverts from the crucial developmental roles in addition to potentiating a harmful inflammatory environment.¹⁰ Much about the phenotypic characteristics of microglia have been inferred from peripheral macrophages – an M1 polarisation is pro-inflammatory with killing or growth-inhibitory capacity while an M2 polarisation is anti-inflammatory with growth-promoting capacity.³⁷ An increase in microglia activation can upset the balance of pro- and anti-

inflammatory factors, eventuating in a prolonged inflammatory environment that may cause injury to oligodendrocytes, neurons, and other cells.³⁷ Microgliosis and astrogliosis can be pathogenic or protective; regardless, an imbalance of pro- and anti-inflammatory factors is detrimental to the immature brain.^{37,42} In particular, injury to cells of the oligodendrocyte lineage cells can lead to white matter injury which is commonly linked to neurodevelopmental impairments in preterm infants.¹⁰

Oligodendrocytes are the myelinating glial cells in the CNS. The concentric wrapping of oligodendrocytes around neuronal axons forms an insulating layer (myelin sheath) that facilitates efficient action potential propagation.⁴³ Oligodendrocyte precursor cells emerge after neurogenesis, between 20–24 weeks GA, pre-oligodendrocytes ensheath axons from 24–32 weeks GA, and the process of myelination continues through postnatal life to late adolescence.^{10,30,43} Hence, in the preterm infant, oligodendrocyte development and maturation are incomplete and at a stage of development that is extremely vulnerable to injury.⁴³ Notably, myelination differs between cerebral regions, and the subventricular zone of the periventricular white matter (PVWM) where oligodendrocyte precursor cells reside is most commonly affected in preterm brain injury. Furthermore, the myelination process requires adequate access to substrates from blood vessels; therefore, white matter development is especially vulnerable to hypoxic-ischaemic episodes or when cerebral blood flow (CBF) is interrupted.

1.2.2. Vascularisation

Development of the brain vasculature occurs primarily through vasculogenesis and angiogenesis.^{32,44} Vasculogenesis refers to development of vessels from *in situ* differentiation of mesoderm-derived angioblasts into endothelial cells^{44,45} whereas angiogenesis, primarily responsible for vascularisation of the brain, is the development of new vessels from pre-existing vessels.^{32,45} Branches of newly formed vessels anastomose with adjacent vessel sprouts to make up a capillary network in the ventricular zone of the developing brain.^{45,46} Grey matter vascularity begins to mature from 16 weeks GA, arterial development in other brain regions such as the brainstem, cerebellum, basal ganglia, and diencephalon occurs between 20–28 weeks GA, while white matter vascularity only increases after 32 weeks GA.^{47,48} These vessels are composed of fenestrated endothelial cells that have no BBB properties – a vital complexity of the CNS vasculature.^{40,46} As endothelial cells penetrate neural tissue, they gradually lose fenestrations and develop specialised structural and functional BBB properties (discussed further in Section 1.2.3.2).^{40,46}

For preterm infants, incomplete vascularisation and the underdevelopment of penetrating vessels at the time of birth put watershed regions and deep cerebral structures at an increased risk of hypoxic ischaemic injury.^{49,50} For example, injury is common in white matter along the lateral ventricle between the distal fields of the middle cerebral and anterior cerebral arteries (frontal white matter).⁵⁰ The immaturity or

absence of deep and short penetrating vessels may relate in part to the vulnerability of the PVWM and subcortical white matter (SCWM) respectively in extremely preterm infants.⁵⁰ Furthermore, newly-formed blood vessels are fragile and have a higher tendency of rupturing during surges in blood flow, which can result in haemorrhagic brain injury.^{51,52} In preterm infants, intraventricular haemorrhage (IVH) which originate within the germinal matrix – an area rich in proliferating neuronal and glial progenitor cells – may impact development and migration of these cells within the immature brain.¹⁴ Additionally, immature vessels may not be sufficiently muscularised. Smooth muscle cells associated with the endothelium are responsible for local constriction or dilation of the blood vessels.⁵³ Neurovascular coupling – the process where local blood flow increases to meet the metabolic demand of neuronal activities – may be compromised, leading to inadequate sustenance of neuronal activity and function (discussed further in Section 1.2.3.1).^{9,52}

1.2.3. Neurovascular unit

The endothelial cells of cerebral capillaries along with pericytes, astrocytes, and basal lamina are collectively known as the neurovascular unit [Fig. 1.2].^{40,46,54} The neurovascular unit is important in regulating neurovascular coupling (discussed in Section 1.2.3.1).⁴⁶ Within the neurovascular unit, the endothelial cell layer physically forms the BBB, although the dynamic interaction of all cells within the neurovascular unit is vital to maintain BBB integrity.^{40,45,46,54}

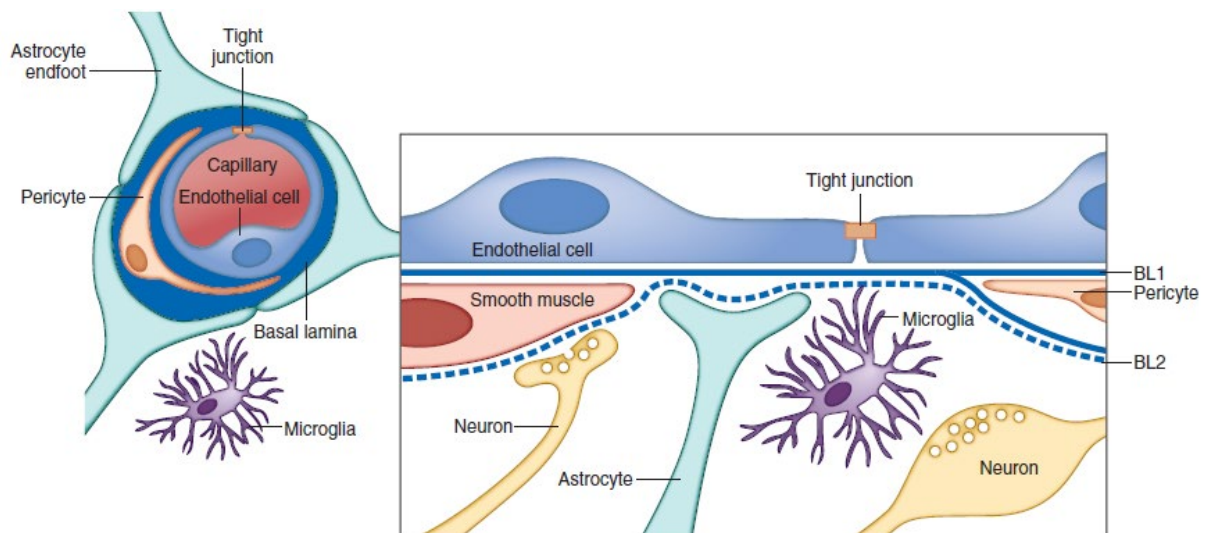


Figure 1.2. Components of the neurovascular unit. *Reproduced with permission from Badaut et al., 2017.*⁴⁶

1.2.3.1. Neurovascular coupling and cerebral autoregulation

The ability of the neurovascular unit to alter CBF is vital to meet demands of neuronal activity and accommodate changes in systemic pressure. Neurovascular coupling refers to an increase in cerebral

perfusion, and hence oxygen and glucose, in response to and to support increased neuronal activity.⁴⁰ Cerebral autoregulation involves the alteration of cerebral vasculature resistance in response to changing perfusion pressures, to maintain homeostasis of cerebral perfusion.⁵⁵ While the stimuli are different, both processes involve constriction and dilation of arteries and arterioles, with input from glial and neuronal cells in proximity with vasculature, to alter CBF.^{53,55}

The diameter of local cerebral blood vessels are regulated by vasoactive neurotransmitters and peptides released by neuronal axonal projections and astrocytic end feet onto arteriolar smooth muscle cells.^{46,53} Furthermore, astrocytes have their end feet in close contact with brain endothelial cells, and because of this proximity to the blood vessels and neurons, can act as important metabolic sensors.⁴⁰ Pericytes have been suggested to play an important role in regulating blood flow in capillaries.⁵³

1.2.3.2. The blood-brain barrier and neurovascular permeability

The BBB segregates the brain parenchyma from the systemic circulation. Contrary to previous understanding that the BBB of a preterm infant is incomplete, it is now thought that the barrier is structurally intact but is either functionally immature or functionally adapted to the fetal environment and hence not well modulated in a preterm neonate.⁴¹ The structural integrity of the BBB is conferred mainly by tight junction proteins which are present early in development.^{40,41,54} Other junctional proteins include adherens junction and gap junction proteins [Fig. 1.3].⁵⁴

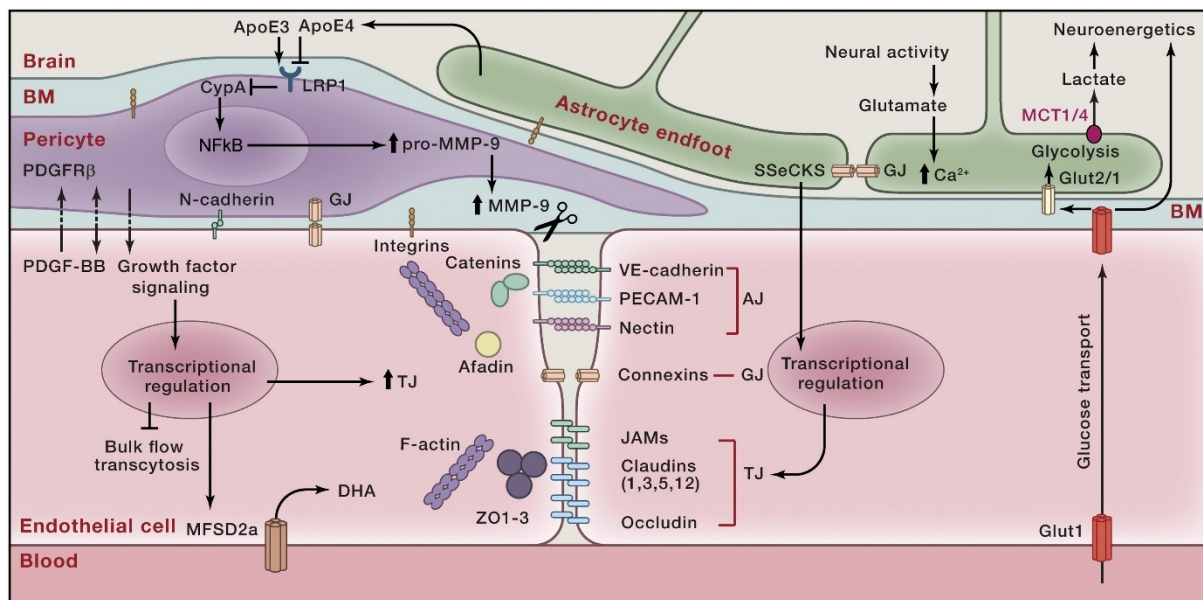


Figure 1.3. Illustration of the physical components of the blood-brain barrier. Endothelial cells are connected by adherens junction (AJ) proteins, gap junction (GJ) proteins, and tight junction (TJ) proteins. The expression of tight junction proteins is regulated by pericytes and astrocytes which are in close association with the endothelial cells. *Reproduced with permission from Zhao et al., 2015.*⁵⁴

Adherens junctions and junctional adhesion molecules (JAMs) regulate trans-endothelial migration of lymphocytes from blood into the CNS.⁵⁴ Furthermore, transmigration of peripheral immune cells into the CNS is restricted due to low expression of leukocyte adhesion molecules on brain endothelial cells, compared to non-neuronal endothelial cells.⁴⁰

Tight junction proteins include the cytosolic plaque protein zonulae occludens and transmembrane proteins such as the claudin family members, occludin, and JAMs.^{40,54} Together, these tight junction proteins, especially claudins, restrict paracellular diffusion of molecules into the CNS.⁴⁰ The key claudins of the BBB are claudin-1, claudin-3, claudin-5, and claudin-12.^{45,54,56} Claudin-5, the major constitutive claudin at the BBB, is expressed in cerebral vessels as early as 12 weeks GA and is uniformly expressed in the cortex, white matter, and germinal matrix between 16 to 40 weeks GA in a linear manner.⁵⁷⁻⁵⁹ The expression of tight junction proteins is regulated by pericytes and astrocytes which are in close association with the endothelial cells.⁵⁴ Tight junction proteins are dynamic and have the ability to relocate under various stimuli such as inflammation.⁵⁶ The ratio and distribution of tight junction proteins affect the strength and integrity of the BBB.⁵⁶ For example, redistribution of claudin-5 and occludin by caveolae-mediated endocytosis is associated with loosening of endothelial cell adhesions and formation of paracellular gaps.⁵⁶

However, in the preterm neonate, physiologic and metabolic regulation of the BBB by astrocytes, pericytes, and endothelial enzyme systems are likely adapted for *in utero* development and may contribute to BBB disruption.⁴¹ The consequence of this is that the BBB integrity of a preterm neonate may be more prone to compromise, allowing inflammatory or neurotoxic substances from the periphery to infiltrate the brain, leading to injury.

Given the inherent risk of brain injury following preterm birth, it is unsurprising that additional interventions with the potential to impact key neurodevelopmental events in the immature brain can worsen disability. Mechanical ventilation is one such intervention.

1.3. Ventilation of the preterm neonate

Preterm infants often require respiratory support due to reduced respiratory drive, weak chest muscles and flexible ribs, inadequate alveolarisation, insufficient surfactant production, and impaired lung liquid clearance. Approximately 60-95% of very and extremely preterm infants will require respiratory support during their neonatal period, whether in the delivery room or subsequently in the NICU or both.^{3,60-66}

1.3.1. Requirement for assisted ventilation in the delivery room

Most infants can independently transition from fetal to newborn life, but many preterm infants will require assistance for this physiologically challenging process. The youngest infants often have difficulty

achieving a successful transition and with each decreasing week of GA, the need for resuscitation in the delivery room and the degree of the required respiratory support increases.⁶⁷ Neonatal transition involves cardiovascular adaptations and, more importantly, respiratory adaptations since the newborn is no longer supported by the placenta for oxygenation.⁶⁸

The initiation of assisted ventilation in the delivery room aims to help the newborn overcome the first step of respiratory transition, which is to clear airway liquid and establish lung aeration for effective gas exchange.^{69–71} Infants who cannot spontaneously breathe at birth will require positive pressure ventilation (PPV), delivered using a T-piece resuscitator, flow-inflating bag, or self-inflating bag.^{69–71} PPV is usually first delivered non-invasively via a face mask and infants who are still unable to initiate stable respiration are intubated.^{69,72} Extremely preterm infants may be electively intubated in the delivery room in some centres. In a small proportion of infants, failure to achieve adequate lung aeration in the face of falling heart rate may necessitate chest compressions and adrenaline administration during resuscitation.⁶⁹

Depending on GA, approximately 34 – 85% of preterm infants require PPV with intubation to establish lung aeration immediately after birth in the delivery room.^{3,63–66} In the United States, a study conducted on extremely preterm infants born at centres of the *Eunice Kennedy Shriver* National Institute of Child Health and Human Development (NICHD) Neonatal Research Network found that despite decreasing percentages of infants requiring intubation in the delivery room over the past two decades, the average percentage of extremely preterm infants who required this intervention in 2012 remains a staggering 65%.³ A similar trend was observed in North American hospitals in the Vermont Oxford Network where delivery room intubation rates decreased from 58.3% in 2000 to 54.5% in 2009, whereby more than half the very low birth weight (VLBW) preterm infants still required invasive respiratory support immediately after birth.⁶³ More recently, a study from South Korea reported that between 2013–2014, 88.3% of VLBW preterm infants received PPV and 77.7% required intubation in the delivery room.⁶⁵ In Australia and New Zealand, 31.6% of very and extremely preterm babies registered to the Australian and New Zealand Neonatal Network (ANZNN) in 2017 required endotracheal intubation in the delivery suite.⁶⁴ Although a much lower percentage than the other studies, this is more than triple the requirement of term babies in the same cohort (9.2%).⁶⁴ Notably absent from these statistics are the infants who required non-invasive forms of ventilation in the delivery room, meaning the total percentage of preterm infants who need respiratory support immediately after birth is substantially higher.

1.3.2. Requirement for assisted ventilation in the NICU

Preterm infants often continue to require respiratory support after transfer to the NICU. Approximately 79.6-95.0% of very and extremely preterm infants require invasive mechanical ventilation in the NICU.^{61,64,73} In moderate to late preterm infants, the requirement for assisted ventilation, not necessarily invasive, is up to 91.3%.⁶⁴ The cumulative duration of ventilation required differs, with the median duration ranging from 2-19 days, depending on the GA of the infant at birth and study periods.^{60,61,74,75} In general, the lower the GA of the infant at birth, the longer the duration of ventilation required.^{61,64,73,74} A cohort study in South Korea reported that 38.5% of VLBW preterm infants received >7 days of mechanical ventilation.⁷³ Importantly, the trends for long-term respiratory support in preterm infants do not seem to be decreasing.^{64,74}

1.3.3. Aspects of providing ventilation that may cause injury

Despite it being a necessary life-sustaining intervention, assisted ventilation is linked to long-term morbidities in the preterm infant, specifically respiratory and neurodevelopmental outcomes. There are two key aspects of providing assisted ventilation to preterm infants that influence injury: 1) how ventilation is administered and 2) for how long. These factors are crucial determinants of the degree of pulmonary inflammation and injury (ventilation-induced lung injury; VILI). Importantly, the initiation of VILI has systemic consequences and can initiate downstream pathways to elicit brain injury.

1.3.3.1. Ventilation-induced lung injury

Mechanical ventilation can injure the immature lungs of preterm infants, primarily by atelectrauma, volutrauma, and biotrauma [Fig. 1.4].^{70,76–78}

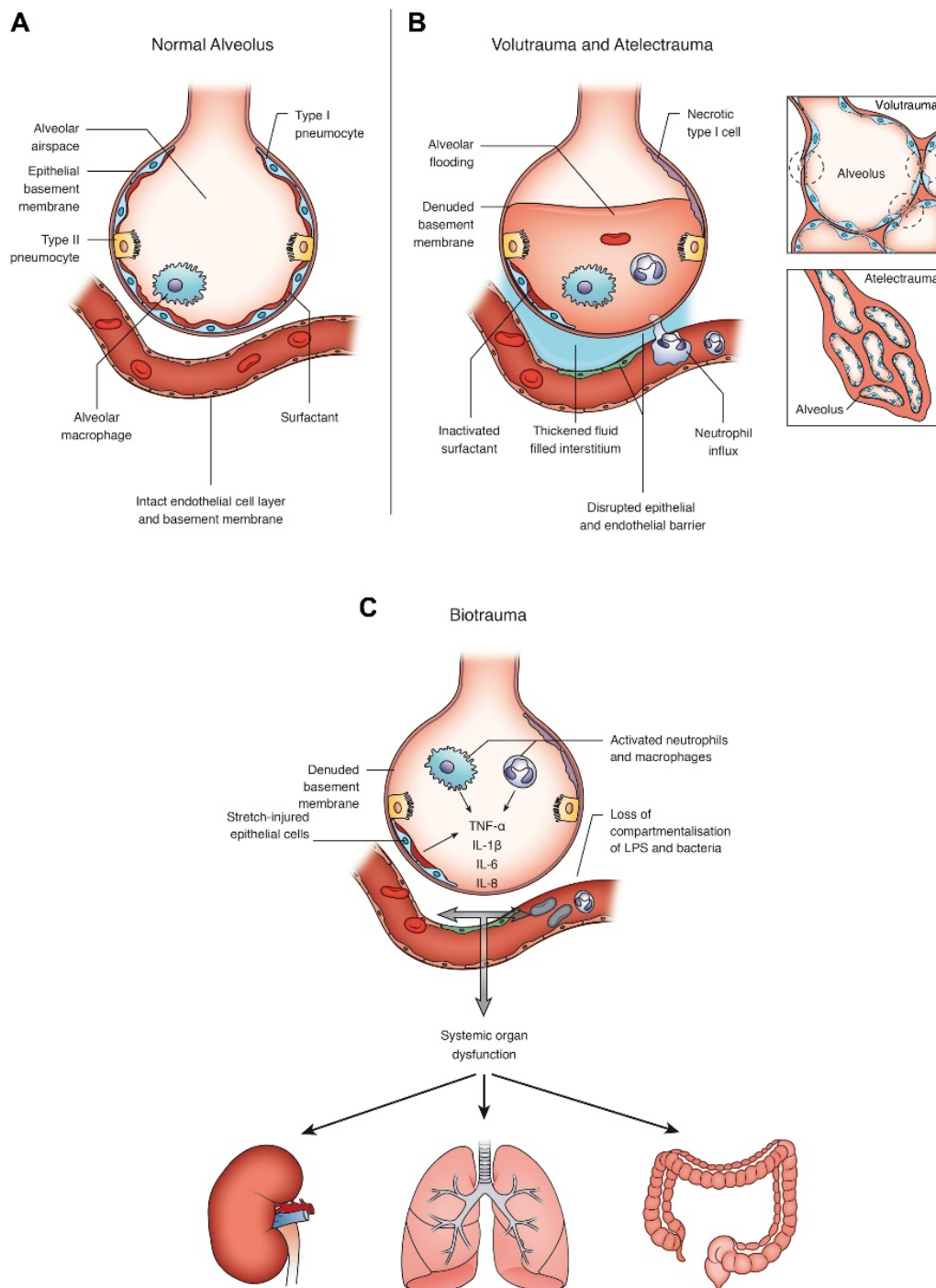


Figure 1.4. Key mechanisms of ventilation-induced lung injury. (A) The normal alveolus and (B-C) the damaged alveolus following injurious ventilation. *Reproduced with permission from Curley et al., 2016.*⁷⁶

Atelectrauma refers to injury from cyclic collapse and reopening of alveoli and airway units due to inadequate volumes below the functional residual capacity.^{70,76–78} An example of atelectrauma is when insufficient positive end-expiratory pressure (PEEP) is applied during ventilation.^{70,76–78} Volutrauma refers to injury when the lungs are overdistended by volumes exceeding total lung capacity.^{70,76–78} An example of this is in response to excessively high tidal volume (V_T), which has been found to be a major cause of lung inflammation and injury in the preterm infant.^{79,80} As few as six manual inflations of high V_T are enough to induce injury in immature, surfactant-deficient lungs of preterm lambs.⁸¹

Clinical trials have found that variable V_T and PEEP during neonatal resuscitation in the delivery room can exceed recommended limits.^{82–84} Current neonatal resuscitation guidelines in the delivery room rely on visual assessment of chest rise to deliver an adequate V_T during PPV where pressure monitoring is unavailable.^{69,85,86} Besides the subjective nature of this procedure, there is reduced ability to observe changes in chest wall movement when a preterm infant is covered to maintain thermoregulation during resuscitation, stabilisation, and transportation.⁸⁶

Schmölzer *et al.* reported delivery of V_T during mask ventilation ranging from 0–31 ml/kg in preterm infants, with 85% of babies receiving a V_T higher than the recommended 5–7 ml/kg.⁸⁷ Similarly, van Vonderen *et al.* observed inspired V_T of 7.9–22.6 ml/kg and expired V_T of 6.8–15.4 ml/kg in extremely preterm infants.⁸⁸ Although larger V_T during face mask ventilation have been proposed to account for distention of the upper respiratory tract and to ensure adequate ventilation of distal airways, overdistension of the trachea potentially increases the risk of inflammation and injury.⁸⁸ The above studies could not measure volume directed to the lungs. However, van Vonderen *et al.* also observed V_T of 3.9–9.6 ml/kg during endotracheal tube ventilation which is still slightly higher than suggested volumes.⁸⁸ Prophylactic pulmonary surfactant treatment can increase the uniformity of inflation and partially mitigate the early biomarkers of lung injury but high V_T remains a risk for developmentally small lungs of preterm infants.^{78,89} Importantly, even if appropriate volumes are applied, mechanical stretch itself can activate an immune response in immature respiratory units.⁷⁶

The biological response to atelectrauma and volutrauma is known as biotrauma.⁷⁶ Biotrauma refers to the release of inflammatory mediators following mechanical injury of the alveoli [Fig. 1.4C].^{76,77} Mechanical or oxidative damage of airway and epithelium upregulates the expression and release of pro-inflammatory cytokines such as interleukin(IL)-1 beta (IL-1 β) and tumour necrosis factor (TNF).^{76,77} This in turn stimulates the upregulation of monocyte-derived chemokines in the alveolar epithelium for leukocyte recruitment, which is facilitated by the breakdown of the alveolar-capillary barrier.⁷⁶ For example, monocyte chemoattractant protein-1 (MCP1, *alias CCL2 [C-C motif chemokine ligand 2]*) recruits neutrophils and macrophages into the lung.⁹⁰ Pro-inflammatory cytokines released by activated

neutrophils and macrophages can enter the systemic circulation and have adverse effects on other organs.⁷⁶ Even short periods of mechanical ventilation have been associated with increased systemic plasma levels of IL-1 β , IL-6, and IL-8 in preterm infants,^{91,92} which in turn have been associated with later development of chronic lung disease in extremely preterm infants.^{91,93} Furthermore, prolonged ventilation can lead to chronic pulmonary and systemic inflammation.⁹⁴ Importantly, systemic inflammation secondary to lung injury can initiate cerebral inflammation which is a major cause of brain injury.⁹

1.3.3.2. Effects of poorly controlled ventilation in the delivery room on the brain

The intensity of delivery room resuscitation for infants who cannot spontaneously breathe (as discussed in Section 1.3.1) has been suggested to affect short- and long- term neurodevelopmental outcomes, although its exact impact remains unclear. Increased intensity of delivery room resuscitation increases the risk of IVH and white matter injury in moderately preterm infants.⁶⁷ In very and extremely preterm infants, higher observed rates of brain injury and CP were reported with increasing levels of delivery room resuscitation but these differences did not persist after the rates were adjusted, suggesting that more intense delivery room resuscitation does not necessarily predict neurodevelopmental impairments.⁹⁵ Nevertheless, it is important to note that regardless of the intensity of resuscitation, PPV in this setting is likely the least controlled respiratory support a neonate will ever receive, and suboptimal delivery of ventilation has proven to be injurious to the immature brain.^{87,96–98} Early PPV in the delivery room, both non-invasively via a face mask and through invasive intubation, has been associated with the development of severe IVH.^{97–99}

Further, ventilation-induced brain injury (VIBI) in the delivery room may be a downstream consequence of VILI. As mentioned above, it is challenging even for experienced clinicians to accurately estimate the V_T delivered^{85,87} and a noticeably expanded chest wall from PPV may itself be a sign of lung overdistension. Indeed, excessively high V_T causes volutrauma which is a major cause of lung inflammation and injury.^{70,77–80} Inappropriate ventilation pressures and volumes can also trigger the haemodynamic pathway of brain injury by altering pulmonary and cerebral haemodynamics.⁹⁶ Together, these factors contribute to a suboptimal ventilation situation that leads to injury of the lung and, consequently, the brain.⁹⁶ Preterm infants <33 weeks GA who developed IVH were found to have been resuscitated with a greater number of inflations resulting in $V_T > 6$ ml/kg in the delivery room, compared to infants who did not develop IVH.⁹⁹ Undeniably, the use of excessive V_T has dire consequences on the immature brain; preterm infants <29 weeks GA who received unintentional high V_T ventilation (>6 ml/kg, where median normal V_T is 4.2–5.8 ml/kg) in the delivery room had a nearly four-fold higher incidence of IVH than infants who received normal V_T (<6 ml/kg; 51% vs 13%).^{97,100}

1.3.3.3. Effects of prolonged controlled ventilation in the NICU on the brain

Compared to the initiation of PPV in the delivery room, PPV in the NICU is much more controlled with sophisticated equipment and vigilant monitoring of ventilation parameters.¹⁰¹ The precise effect of ventilation on the immature brain in the NICU setting has not been thoroughly investigated. Confounding factors such as analgesia and anaesthetics,^{102–104} oxygenation,¹⁰⁵ and a plethora of other NICU interventions for a range of primary and/or secondary complications need to be considered; these are challenging to account for in clinical studies that aim to isolate the effects of ventilation. However, it is known that the duration of ventilation is an important determinant of neurodevelopmental morbidities.¹⁰⁵ The length of ventilation, which is inversely related to GA at birth,¹⁰⁶ correlates with poorer outcomes, particularly for the white matter of the brain.^{60,62,75,105}

In a retrospective analysis of extremely low birth weight (ELBW) infants, most of whom were extremely preterm, only 24% of infants who were ventilated for ≥ 60 days and 7% of those ventilated for ≥ 90 days survived without neurodevelopmental impairments.⁶⁰ All infants who had been ventilated for ≥ 120 days and survived suffered some form of neurodevelopmental impairment.⁶⁰ Indeed, the cumulative duration of mechanical ventilation has been associated with increased odds of PVL and/or IVH.^{61,62,73,98} Additionally, prolonged periods of mechanical ventilation increases the risk of CP and attention deficit hyperactivity disorder in ELBW infants.¹⁰⁷

Attempts to shift management encouraging earlier extubation or less invasive ventilation strategies have not translated to improved neurological outcomes in preterm infants.¹⁰⁸ Furthermore, limiting the duration of mechanical ventilation to reduce complications is not always feasible with preterm infants. Therefore, it is imperative to devise treatments for unavoidable brain injury from prolonged respiratory support.

Our improved understanding of respiratory transition and lung function has led to significant advances in neonatal respiratory care, many of which aim to reduce the risk of chronic lung diseases and adverse neonatal outcomes. However, a significant proportion of preterm infants still develop long-term neurodevelopmental morbidities due to ventilation-induced injury. Thus, there is an urgent need to better understand the mechanisms behind VIBI.

1.4. Ventilation-induced brain injury (VIBI)

VIBI refers broadly to pathology within the brain after mechanical ventilation. Various methods of respiratory support have been linked to cerebral inflammation and neuropathologies in preterm infants, including cystic PVL, diffuse white matter injury, and IVH.^{97,98,105,107,109}

Several explanations have been put forward to link ventilation and brain injury. Studies in ventilated preterm lambs have identified two major pathways of acute VIBI: cerebral inflammation and haemodynamic instability.^{80,96,110,111} Both pathways are proposed to be downstream effects of the pulmonary consequences following ventilation [Fig. 1.5].^{80,96,110} Incidentally, these key pathways mirror those of preterm brain injury – suggesting compounded risk of injury in preterm infants. The relative contribution of each pathway of injury is unknown. This information may be useful for developing targeted treatments.

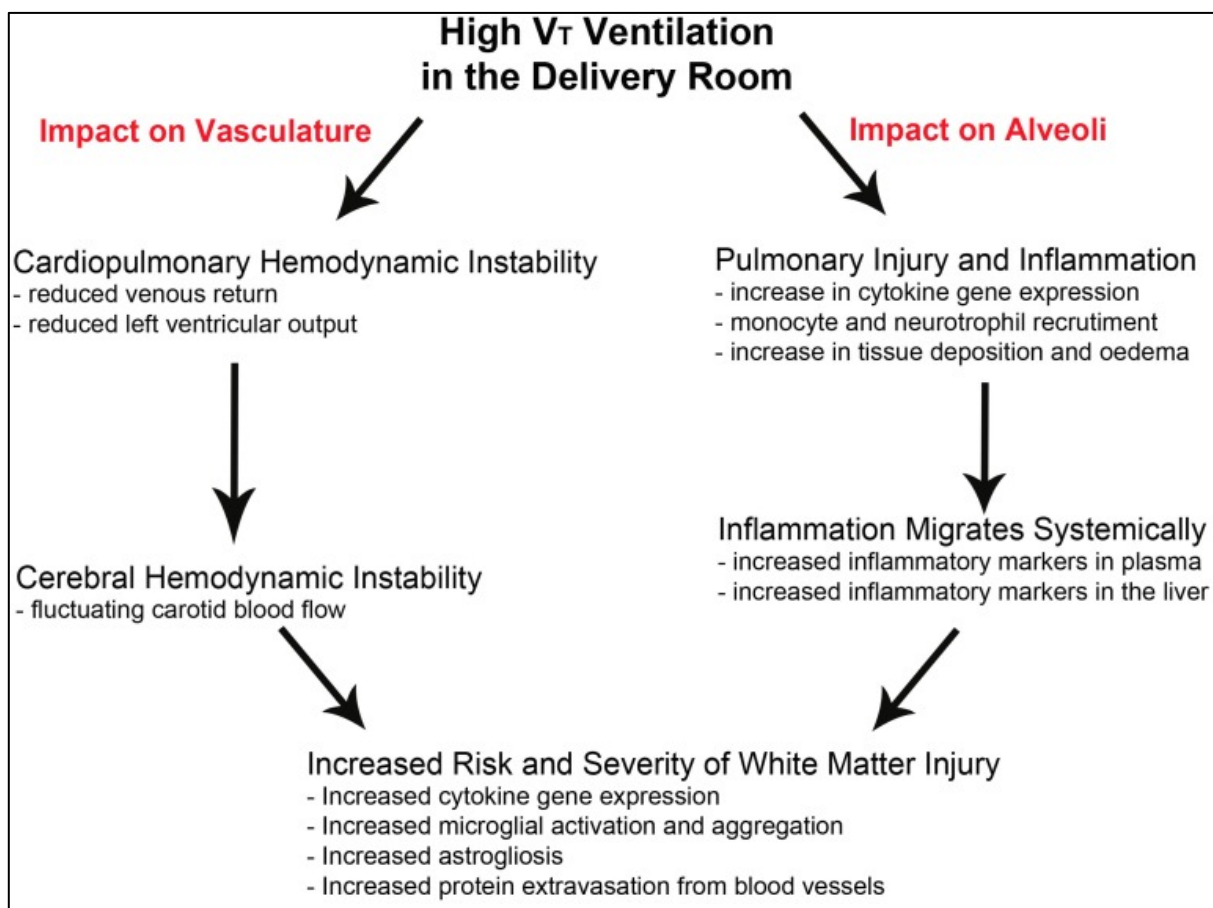


Figure 1.5. Proposed mechanisms of ventilation-induced brain injury. The initiation of injurious high tidal volume (V_T) ventilation causes pulmonary inflammation which migrates systemically to the brain. Simultaneously, fluctuating carotid blood flow causes alterations to cerebral blood flow. These two pathways independently or converge to increase the risk and severity of white matter injury. *Reproduced from Barton et al., 2015⁹⁶ under the terms of the Creative Commons Attribution 4.0 International License.*

1.4.1. Haemodynamic pathway of injury

The initiation of ventilation causes significant alterations to pulmonary blood flow and, as a result, CBF.^{80,110} In PPV, applying a high pressure into the airways decreases pulmonary capillary transmural pressure, causing compression of intra-alveolar capillaries, hence increasing capillary resistance and decreasing pulmonary blood flow.^{80,96,112} This reduces pulmonary venous return and left ventricular output, and consequently alters CBF.^{80,96,110} Prolonged CBF fluctuations for more than 10 to 20 s constitutes cerebral haemodynamic instability.¹¹³

Arterial blood pressure variability within a physiological range is not usually a problem in term infants because it is compensated by pressure-flow autoregulation to sustain a stable CBF.⁵⁵ This involves constriction and dilation of arteries to alter cerebral vasculature resistance in response to changing perfusion pressures.^{50,55} However, preterm infants are exceptionally susceptible to cerebral haemodynamic perturbations, in part due to underdeveloped vascular development.^{9,50} The immaturity or absence of muscles in penetrating cerebral arterioles contributes to susceptibility of the preterm infant to pressure-passive cerebral regulation,^{9,52,114} which has been associated with increased risks for subsequent PVWM injury.⁵⁰ In addition, poorly muscularised vessels are prone to rupture during surges in arterial blood flow⁵² while an interruption in oxygenation can result in hypoxic-ischaemic injury.⁴⁹ Venules and veins are also susceptible to rupture following changes in blood pressure, contributing to BBB disruption.¹¹⁵

1.4.1.1. Haemodynamic instability due to altered cerebral autoregulation

While there is a lack of consensus on the state of cerebral autoregulation in preterm infants, prematurity and ventilation likely affect it. The autoregulatory plateau, bounded by lower and upper limits of arterial pressure, has been postulated to be narrower with decreasing GA.^{55,116,117} The exact limits of the autoregulatory pressure plateau in premature infants remain contentious and perhaps depend to a large extent on the GA of the infant.¹¹⁶ Papile *et al.* showed that CBF autoregulation is present and intact in preterm fetal sheep (118-122 days GA; 0.79 gestation) to maintain CBF of 75-86 ml/min/100g within mean arterial blood pressure boundaries of 45-80 mmHg.¹¹⁸ Even though the lower limit of autoregulation is similar to that of near-term and term lambs, the upper limit is ~15 mmHg lower, supporting the notion that the range of autoregulation in the preterm lamb is narrower.^{118,119} The resting mean arterial blood pressure of the preterm lamb also lies closer to the lower limit of autoregulation,^{9,118} meaning that it is relatively easier for hypotension beyond the autoregulatory plateau compared to its term counterpart.⁹ Altogether, the cerebral circulation in preterm infants is extremely sensitive to even minor changes in systemic blood pressure. Even if cerebrovascular autoregulation is intact, severe

systemic hypotension or cerebral vasoconstriction can still result in significantly compromised CBF.⁹ Moreover, an intervention such as mechanical ventilation is likely to alter cerebral autoregulation.

Despite having established functional cerebral autoregulation in fetal preterm-equivalent sheep (110 days and 118-122 days GA)^{118,120}, it was absent in ventilated preterm lambs (127-132 days GA).¹²¹ The authors suggested that cerebral autoregulation may have been affected by preterm delivery and subsequent treatments reflective of clinical care, including ventilation.¹²¹ Pressure-passive circulation increases and the resulting cerebral haemodynamic instability escalates brain injury in the preterm infant, especially in arterial end vascular zones.⁹ Hypoperfusion in periventricular zones where there is a high concentration of oligodendrocyte precursor cells, which are highly vulnerable to hypoxia, increases the risk of myelination deficits and has been associated with diffuse white matter gliosis.^{9,49,116} The risk of synaptic dysfunction is also increased as neurons in areas of low CBF lose dendritic spines.⁵³ Without adequate energy (adenosine triphosphate; ATP) supply, microglia cannot be activated in the presence of insults.⁵³ Conversely, high CBF and CBF that rapidly oscillates between low and high flows increase the risk of haemorrhagic injury due to rupture of vessels.^{9,52,116} Approximately 91% of babies with respiratory distress syndrome who had fluctuating CBF after 12 h of life subsequently had IVH.¹²²

1.4.1.2. Altered blood-brain barrier

Compromised BBB integrity and the resulting increased permeability are known contributors of preterm brain injury and VIBI.⁹⁶ Indeed, BBB permeability increases during PPV.^{123,124} High mean arterial blood pressure beyond the cerebral autoregulatory range during PPV in newborn piglets increased BBB permeability to small water-soluble molecules (Na⁺-fluorescein).¹²³ Prolonged duration of ventilation has also been shown to increase regional BBB permeability, such as in the cerebral cortex, thalamus, and hippocampus, in preterm lambs.¹²⁴ Furthermore, compromised cerebral vasculature introduces systemic cytokines and peripheral immune cells into the CNS when the structural component of the BBB is breached.¹²⁵

1.4.2. Inflammatory pathway of injury

The main mechanisms in the inflammatory pathway of VIBI are upregulation of pro-inflammatory cytokines and activation of glial cells within immature white matter [**Fig. 1.6**].⁹ Mechanical ventilation initiates a profound pulmonary inflammatory response that migrates systemically^{91,94,126} and subsequently elicits localised cerebral inflammation.^{80,96,110} Indeed, mechanical ventilation elevated levels of systemic pro-inflammatory cytokines (IL-1 β , TNF) and downregulated levels of anti-inflammatory cytokines (IL-10) in late preterm and term infants after 2 h.⁹¹ Circulating phagocytes were activated by 12-24 h after the onset of ventilation, suggesting a rapid systemic inflammatory response, in very

preterm infants with respiratory distress syndrome.¹²⁶ Moreover, prolonged ventilation for 2 weeks contributes to systemic inflammation in extremely preterm infants, indicated by elevated levels of circulating pro-inflammatory cytokines (IL-1 β , IL-6, IL-8, TNF).⁹⁴ Systemic inflammation is a challenge to the CNS, much more to the susceptible immature brain of preterm infants. Studies have shown that the PVWM and SCWM regions in the brain are particularly vulnerable to inflammatory injury following ventilation.^{80,96,110}

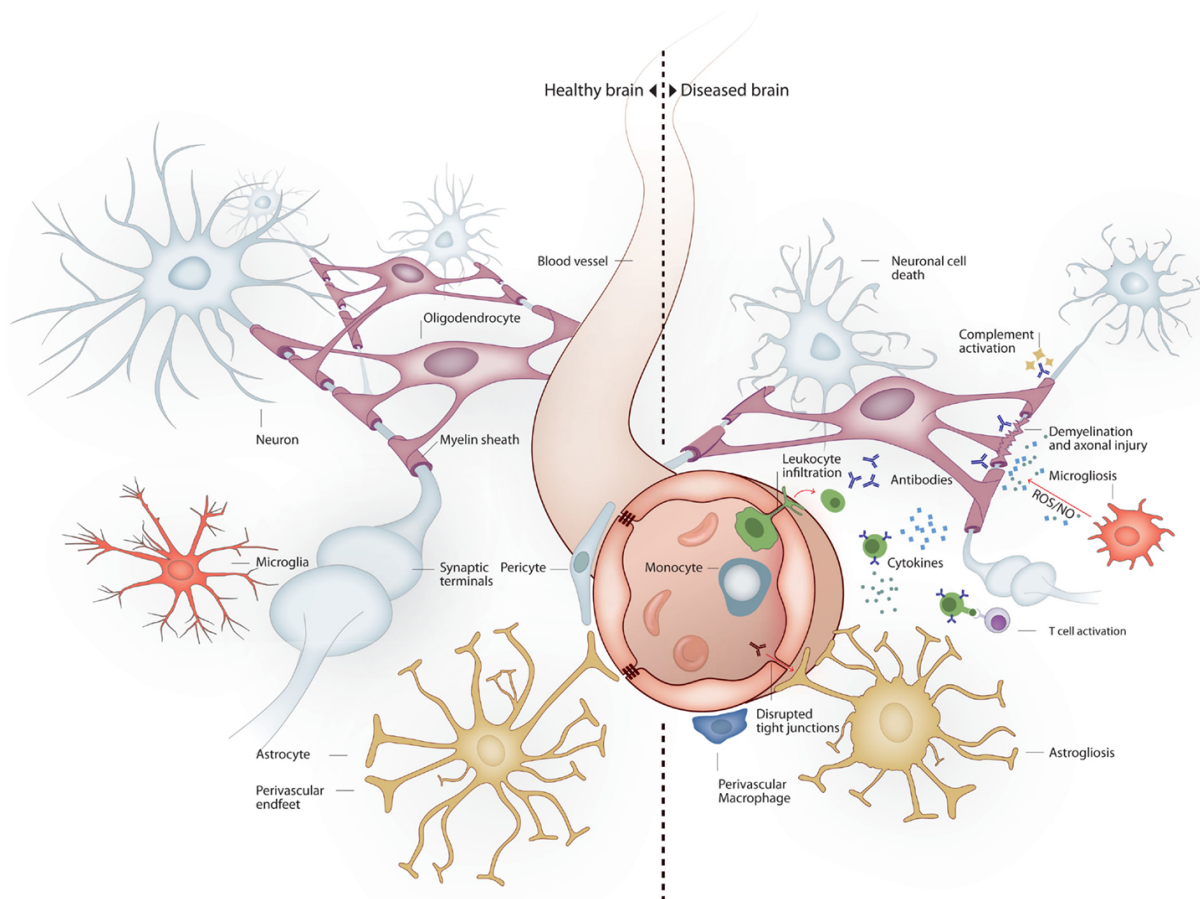


Figure 1.6. Cerebral inflammatory response to systemic inflammation. In the disease state, localised cerebral inflammation results in microglialosis, astroglialosis, disruptions in tight junctions, a compromised blood-brain barrier, and demyelination. *Figure reproduced from Sankowski et al., 2015¹²⁷ under the terms of the Creative Commons Attribution 4.0 International License.*

Inflammatory cytokines have been postulated to cross the BBB by saturable transport.¹²⁸ Moreover, ventilation-induced compromise in BBB function may aid infiltration of systemic circulating inflammatory proteins and peripheral leukocytes into the brain parenchyma of preterm infants.¹²⁵ Inflammatory conditions may in turn further disrupt the BBB by altering expression of tight junction proteins and inducing expression of cell surface adhesion molecules of endothelial cells.^{29,129} This further facilitates immune cell infiltration into the CNS.²⁹ Clinical systemic inflammatory conditions such as

bronchopulmonary dysplasia (BPD), sepsis, and necrotising enterocolitis in preterm infants have been associated with an increased risk of neurodevelopmental impairments.^{42,127,130} This might be mediated by localised cerebral inflammation, when recruited microglia and astrocytes cause injury to oligodendrocytes in the developing brain, resulting in white matter abnormalities.^{29,125,127,131}

1.4.3. Neuropathology in preclinical studies

VIBI in the preterm neonate can lead to devastating lifelong neurological impairment. Some aspects of this injury have been characterised in preclinical studies and will be discussed here as cerebral changes due to either acute injurious ventilation or prolonged ventilation.

To represent poorly regulated V_T in the delivery room, lambs in these studies were exposed to 15 min of PPV with stepwise increments of V_T to achieve a high target V_T of 10–15 ml/kg, which is 2–3 times the normal V_T of lambs for that GA (125 days of term 148 days; ~5–7 ml/kg).^{80,96,110,132–137} High V_T ventilation caused a robust pulmonary inflammatory response which increased systemic and cerebral inflammation, characterised by elevated *IL6* and *IL8* messenger ribonucleic acid (mRNA) levels in the PVWM and SCWM of the brain in ventilated preterm lambs.^{110,133,135} Increased microglial activation and aggregation as well as a higher incidence of vascular protein extravasation (indicative of a compromised BBB) and cerebral haemorrhage in the same regions were also observed [Fig. 1.7].^{110,133,136} Acute injurious ventilation did not alter expression of myelin basic protein (MBP; oligodendrocyte and myelin marker) in the internal capsule or neuronal nuclei (NeuN; neuronal marker) in the thalamus¹³⁸ and did not increase inflammation or injury in grey matter.¹³⁹

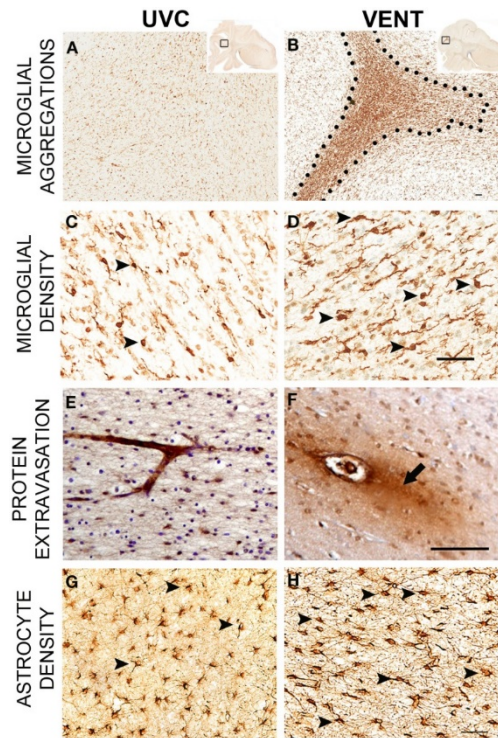


Figure 1.7. Pathology of acute ventilation-induced brain inflammation and injury 2 h after injurious ventilation. Compared to unventilated control (UVC) lambs, preterm lambs ventilated with high tidal volume (VENT) have (A,B) larger, denser microglial aggregations, (C, D) increased microglial density, (E, F) increased protein extravasation, and (G, H) increased astrogliosis in the subcortical white matter of the parietal lobe. Scale bar = 50 μ m. *Reproduced from Barton et al., 2015⁹⁶ under the terms of the Creative Commons Attribution 4.0 International License.*

Importantly, pathology resultant from injurious ventilation can be visualised using non-invasive imaging such as MRI^{111,134,140} and correlated with histopathology.¹³⁸ Magnetic resonance spectroscopy (MRS) detected acute changes in brain metabolite peak-area ratios (lactate/creatine and lactate/choline) in preterm lambs that received high V_T ventilation although macroscopic injury was absent.¹³⁴ Alterations in MRS-detected metabolite levels relate to neuronal damage and potentially predict subsequent neurodevelopmental impairments.^{141,142} Notably, these MRS changes were observed within 90 min of ventilation onset.¹³⁴ Recent findings suggest that MRS-detectable changes persist 24 h after injurious ventilation.¹¹¹ Diffusion tensor imaging (DTI) perhaps offers the most sensitive measures of early brain injury. DTI detected decreased diffusivity measures in the frontal white matter (axial, radial, and mean) and internal capsule (axial) in preterm lambs 24 h after injurious ventilation.¹¹¹ These parameters have been suggested to correlate with axonal loss and myelination deficits.¹¹¹

Long-term ventilation studies in preterm baboons and lambs suggest that the brain injury underlying neurodevelopmental impairments in chronically ventilated preterm infants involves subtle diffuse white and grey matter lesions, often without intraventricular or germinal matrix haemorrhage and overt lesions or infarcts.^{105,143–146} Preterm baboons (125 days of term 185 days; 0.68 gestation) were cared for with similar interventions to that of preterm infants in the NICU, including mechanical ventilation using a gentle strategy to maintain V_T at 4–6 ml/kg with adequate chest motion.^{144,147} While not investigating injury from ventilation per se, the brain injury observed in these animals was not from any direct insult nor influenced by potentiating conditions associated with preterm birth nor an adverse uterine environment. The subtle neuropathologies from preterm birth and subsequent intensive care alone closely resemble what is observed clinically.^{143,144,146,148} After 14 days of ventilator support, preterm baboon brains showed delayed gyrification,^{145,146} reduced brain weight,^{143,145,146} reduced white and grey matter volumes,^{143,145} increased white and grey matter injury,¹⁴⁴ increased astrogliosis in the forebrain,¹⁴³ increased ramified microglia,¹⁴³ and a reduction of oligodendrocytes^{143,145} compared to gestation-matched controls. These histopathological indices correlated with microstructural and macrostructural changes detected by *ex vivo* MRI of immersion fixed brains.¹⁴⁸ Baboons have also been used to investigate different modes of ventilatory support including high frequency oscillation¹⁴³ and continuous positive airway pressure.¹⁴⁹

Preterm lambs (125 days of term 145 days; 0.85 gestation) ventilated with a gentle strategy (V_T at 5–7 ml/kg) had increased *IL8* and connective tissue growth factor (*CTGF*) mRNA levels and decreased vascular occludin protein density in the white matter after 2 h.¹⁵⁰ In another study, preterm lambs of similar GA (126 days) ventilated for 2 h, 6 h, or 24 h (V_T at 7–8 ml/kg) showed no changes in *IL1B*, *IL6*, *IL8* and *TNF* mRNA levels in the PVWM when compared to unventilated controls, across all ventilation durations.¹⁵¹ Histologically, preterm lambs that received 24 h of ventilation had increased astrogliosis within cortical grey matter but otherwise no apparent neuropathology or changes in glial cell populations compared to unventilated control lambs.¹⁵²

1.4.4. Potential management strategies and treatments

There is presently no cure for preterm brain injury. Current clinical trials for preterm brain injury rarely account for ventilation as a covariate. It is unlikely that a single strategy will prevent or reduce VIBI. The key might lie in a multipronged approach that involves reducing the requirement for or duration of respiratory support, optimising how PPV is administered to avoid adverse effects, and reducing the sequelae of unpreventable adverse effects of PPV.

In the delivery room, therapies such as caffeine may help to improve respiratory efforts of preterm infants, potentially reducing the need for invasive respiratory support.¹⁵³ Indeed, spontaneous

respiratory drive is a determinant of effective use of gentle non-invasive respiratory support.¹⁵⁴ Gentle ventilation strategies do not completely mitigate injury but result in less brain inflammation and vascular extravasation by improving cerebral haemodynamic stability.^{80,110,134,155} Similarly, physiological-based cord clamping (PBCC) can stabilise pulmonary, systemic, and cerebral circulation in preterm^{156,157} and near-term lambs,¹⁵⁸ essentially mitigating the haemodynamic pathway of injury, but it is unlikely to prevent VIBI resultant from the inflammatory pathway. PBCC refers to delaying umbilical cord clamping until lung aeration has been established in the newborn, either by stimulating spontaneous breathing or providing respiratory support, prior to umbilical cord clamping.^{156–158} These studies indicate that our current efforts to minimise the need for respiratory support and, where respiratory support is necessary, improve the way PPV is administered are inadequate to prevent VIBI. There is an apparent need to devise a therapy that targets both pathways of VIBI, with a focus on modulating inflammation.

To date, animal experiments have investigated short-term effects of erythropoietin (EPO) and human amnion epithelial cells (hAECs) as prophylactic postnatal treatments for VIBI resultant from acute volutrauma.^{133,135,159} These treatments have proposed mechanisms of action that make them ideal candidates for neuroprotection. EPO has anti-inflammatory, anti-apoptotic, and neurotrophic properties while hAECs are anti-inflammatory and reparative.¹⁶⁰

When administered to preterm lambs that received 15 min of injurious high V_T ventilation, single early low doses of human recombinant EPO (300 IU/kg and 1000 IU/kg) did not reduce or exacerbate lung and brain injury,^{159,161} suggesting that EPO doses presently used in clinical trials appear to be safe for preterm infants receiving respiratory support. However, they appear to not be efficacious as a therapy for VIBI given the lack of therapeutic potential observed. High doses of EPO of 3000 IU/kg and 5000 IU/kg increased cerebrospinal fluid EPO levels to “neuroprotective levels” (>100 mU/ml¹⁶²) within 2 h of administration.^{133,159} These high doses respectively had a protective effect on BBB integrity¹⁵⁹ and differential regional effects on white matter¹³³ despite both doses amplifying lung inflammation and injury.^{161,163} Together, these data highlight a complex dose response with distinct effects on the lungs and brain, indicating that further investigation is required to elucidate the efficacy of EPO in the context of a preterm infant requiring respiratory support.

In a similar study, preterm lambs that received high V_T ventilation were administered an intratracheal infusion of 9×10^7 hAECs before ventilation onset and an additional intravenous dose of 9×10^7 hAECs within 5 min of delivery (total 1.8×10^8 hAECs).^{135,164} The cells were able to enter the brain within 2 h of administration, as detected by fluorescent cell labelling in the frontal and parietal PVWM and SCWM.¹³⁵ Cell administration reduced microgliosis and vascular protein extravasation,¹³⁵ potentially

as a downstream effect of reduced pulmonary inflammation.¹⁶⁴ However, hAECs did not stabilise haemodynamic transition or modulate systemic inflammation within the brief period of the experiment, and conversely they induced an increase in pro-inflammatory cytokine mRNA levels within the brain.^{135,164} Further long-term effects of hAECs on acute VIBI have not been investigated to accurately determine the interaction of hAECs and ventilation on the preterm brain.

Chronic ventilation studies in animals have so far focused on treatments to reduce lung rather than brain injury. Sheep fetuses ventilated *in utero* for 12 h and administered an intratracheal infusion of 3×10^7 hAECs and an intravenous dose of 3×10^7 hAECs at 3 h and 6 h after ventilation onset (total 1.2×10^8 hAECs) demonstrated a reduction in VILI,¹⁶⁵ and as such may have the potential to reduce VIBI. However, this remains a speculation.

1.4.5. Summary of VIBI

In the background of incomplete brain development, the brain of a preterm infant is highly susceptible to injury following insults that increase cerebral inflammation and haemodynamic instability. Mechanical ventilation, which many preterm infants will be exposed to, has the propensity to amplify these pathways of injury. VIBI can manifest as early on as the initiation of ventilation in the delivery room and the neonatal period when the infant is in the NICU.

There are currently no preventative therapies or cures and existing therapies only aim to manage sequelae of brain injury. Given the increasing number of surviving preterm infants, the incidence of VIBI is likely to rise. Thus, there is an urgent need to elucidate the underlying causes of VIBI and identify targeted treatments accordingly, so as to prevent VIBI or promote repair of damaged brain tissue.

1.5. Umbilical cord blood (UCB)

Therapies involving stem cells – cells with the capacity for self-renewal and differentiation¹⁶⁶ – have recently emerged as a promising candidate for neuroprotective treatment. While the optimal source of stem cells is not known, stem cells derived from the umbilical cord and placenta can be collected non-invasively after birth and have shown lower immunogenicity than cells derived from adult tissue (e.g. bone marrow).^{166–169} Cells derived from umbilical cord blood (UCB) have been investigated as a potential treatment for neurological conditions.^{169,170}

1.5.1. UCB composition

For therapeutic use, UCB is first processed to remove erythrocytes, platelets, and plasma, then the remaining fraction of nucleated cells is cryopreserved (herein referred to as UCB cells).¹⁷¹ Because this

fraction contains variable proportions of constituent cells, there is increasing interest to isolate individual cell populations before cryopreservation.^{167,171} UCB cells consist of granulocytes (neutrophils, basophils, eosinophils), lymphocytes (T cells, B cells, natural killer cells), monocytes, and approximately 2-10% stem and progenitor cells.^{169,170,172} The heterogeneity of cells in UCB implies a range of potential mechanisms of action by which UCB can protect or repair the brain with the principle action to modulate inflammation.¹⁶⁷ In particular, monocytes and monocyte-derived suppressor cells, regulatory T cells (Tregs), and a subset of stem and progenitor cells have been proposed to be of therapeutic benefit in the context of neonatal brain injury [Fig. 1.8].¹⁷¹

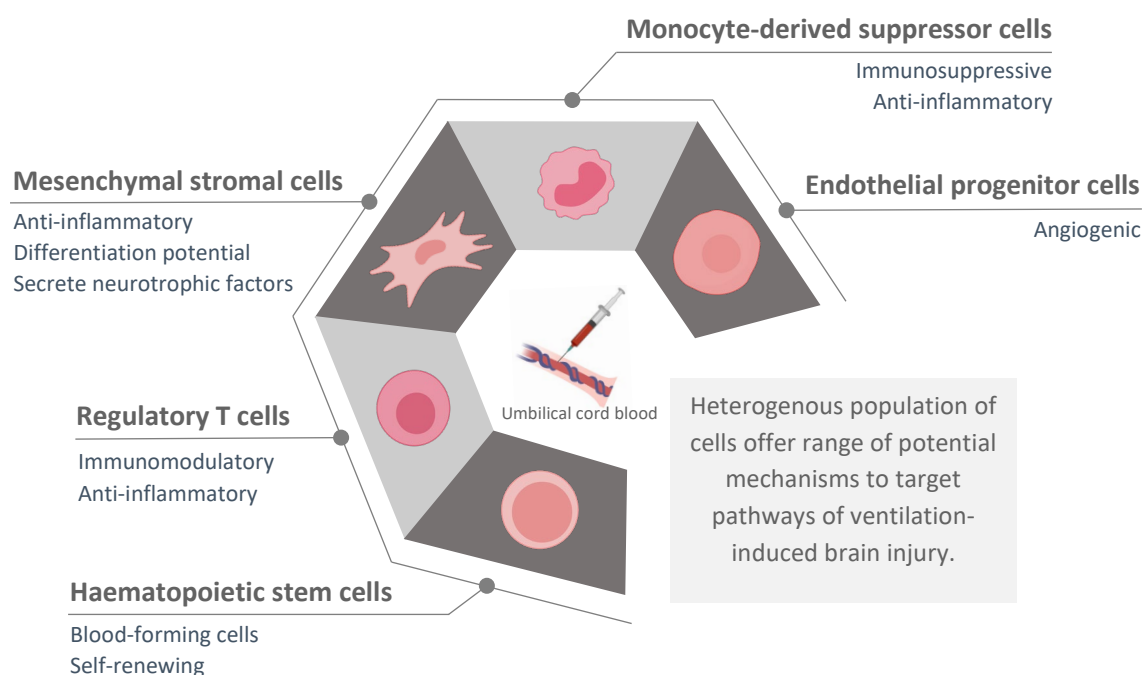


Figure 1.8. Potential therapeutic cell types in umbilical cord blood. *Original figure using information from McDonald et al., 2017.*¹⁷¹

Tregs found in UCB express naïve T-cell markers and together with monocytes and monocyte-derived suppressor cells help to modulate immune responses.^{171,173} Both Tregs and monocytes have anti-inflammatory subsets and given the abundance of these cell types in UCB, this may suggest that a main effect of UCB cell therapy is in mediating inflammation.¹⁷¹

The three principal types of stem cells found in UCB are endothelial progenitor cells (EPC), haematopoietic stem cells (HSC), and mesenchymal stromal cells (MSC).^{171,174,175} EPCs are vasculogenic and have been shown to promote the growth of new vessels and repair damaged vessels in mice.¹⁷⁶ In addition to their angiogenic properties, EPCs derived from human UCB have been shown to promote differentiation of other progenitor cells through paracrine signalling *in vitro*.^{171,177} HSCs are

CD34⁺ cells that can mature into various blood cell lineages.^{169,171} HSCs account for approximately 0.5-1.0% of UCB mononuclear cells,¹⁶⁸ and have been shown to reduce neural damage after stroke in adult rodents, although not as well as whole UCB mononuclear fraction.¹⁷² MSCs make up a small proportion of stem cells in UCB and are not necessarily present; they were found in only 10-30% of human term UCB samples.^{171,178} MSCs produce immunoregulatory factors upon stimulation by inflammatory mediators to reduce immune cell activation.¹⁷⁹ MSCs can also secrete factors that promote tissue repair and growth while decreasing cell death.¹⁷⁹ For example, IL-6 released by MSCs reduced apoptosis of astrocytes in neonatal rats with hypoxic-ischemic brain damage.¹⁸⁰ Additionally, *in vitro* experiments have found that MSCs can differentiate into various cell types including neurons, astrocytes, and oligodendrocytes following neural induction.^{181,182}

1.5.2. Umbilical cord blood cells and neonatal brain injury

The potential of UCB cells to prevent and reduce neonatal brain injury has been widely investigated in preclinical and clinical studies.^{167,175,183} It is not known how rapidly UCB cells are cleared when administered systemically or if these cells can freely cross the BBB into the brain.¹⁷⁰ Given that BBB integrity of the preterm brain is often compromised, and that leukocyte infiltration is not uncommon in disease, it is likely that at least some UCB cell types enter the brain parenchyma. Aridas *et al.* noted a sparse distribution of autologous UCB mononuclear cells in the brains of newborn lambs 60 h after intravenous administration¹⁸⁴ while Li *et al.* found limited numbers of allogeneic UCB cells in the brains of lambs with hypoxic-ischaemic injury 10 days after administration.¹⁸⁵ Regardless, the presence of UCB cells and engraftment within the brain parenchyma may not be essential for neuroprotection.^{169,171,186,187} UCB cells may be able to modulate injury by acting on upstream injury pathways, targeting the pulmonary or systemic systems. Indeed, UCB cells administered to rabbit kittens reduced motor deficits associated with CP although the cells could not be detected within the brain parenchyma 24 h after administration.¹⁸⁶ Similarly, in an adult rat model of stroke, UCB cells combined with mannitol (BBB permeabiliser) reduced cerebral infarcts and motor and cognitive deficits despite not being detected in the brains of the animals.¹⁸⁷ The benefits of UCB cell therapy may instead be attributed to the release of trophic factors such as glial cell line-derived neurotrophic factor (GDNF) and brain-derived neurotrophic factor (BDNF) which can cross the BBB under the right conditions.^{169,171,187} It is unclear if these trophic factors are released by the administered UCB cells themselves or by endogenous cells upon stimulation by the UCB cells.¹⁷¹

The range of mechanisms of action of UCB cells show promise in ameliorating VIBI, by modulating the inflammatory pathway of injury. However, the potential of UCB cells to protect against VIBI has not been evaluated.

1.6. Summary and thesis aims

Following advancements in neonatal healthcare, there is ubiquitous consensus that the aim of neonatal resuscitation should go beyond survival and focus on preserving quality of life of surviving preterm infants. However, it remains a great challenge to identify strategies for better neurodevelopmental outcomes. Risk factors such as the mode and duration of mechanical ventilation are potentially modifiable, but we need to understand if improving these aspects of care sufficiently prevents VIBI, and if not, effort needs to be put into developing practical preventative or treatment strategies. Recognising the consequences and understanding the injury pathways of acute injurious and prolonged mechanical ventilation will aid in this goal.

As such, the overall aim of this thesis is to provide insight into the mechanisms of VIBI and to evaluate the therapeutic benefits of existing treatments, such as UCB cells, that target these pathways of injury. This is broken down to three specific aims and hypotheses as follows:

Aim 1 (addressed in Chapter 3)

Aim 1A: To establish the pattern of brain injury within the PVWM and SCWM of preterm lambs 24 h after 15 min of injurious ventilation.

Aim 1B: To determine the relative contributions of the two major pathways of VIBI: cerebral inflammation and haemodynamic instability.

To address Aim 1, an ovine fetal head-out ventilation model was used with four experimental groups [Fig. 1.9].

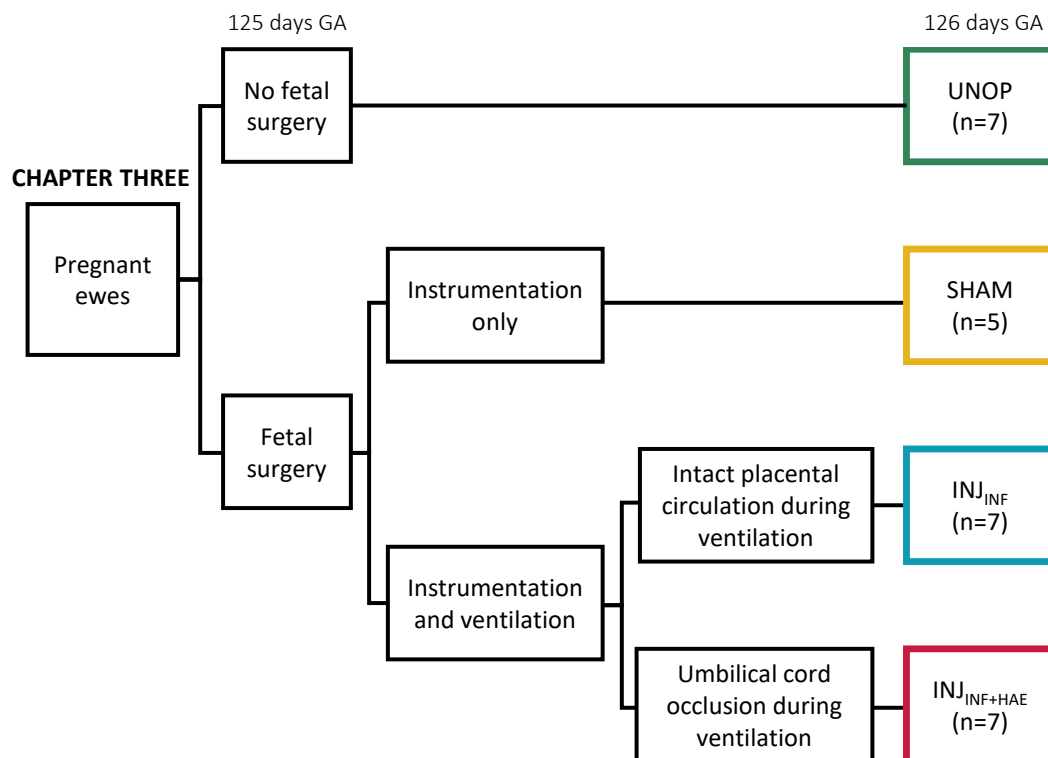


Figure 1.9. Experimental groups for Chapter 3, to investigate the relative contribution of the pathways of acute ventilation-induced brain injury in preterm sheep.

Hypotheses for aim 1

I hypothesised that high V_T ventilation would result in PVWM and SCWM injury detectable by molecular and histological analyses 24 h after the insult. Further, inflammation was hypothesised to be the dominant pathway of injury.

Aim 2 (addressed in Chapter 4)

To determine if UCB cells prevent or reduce PVWM and SCWM injury in preterm ventilated lambs by attenuating cerebral inflammation.

To address Aim 2, an ovine fetal head-out ventilation model was used. The UCB cells-treated group was compared against animals from Chapter 3 [Fig. 1.10].

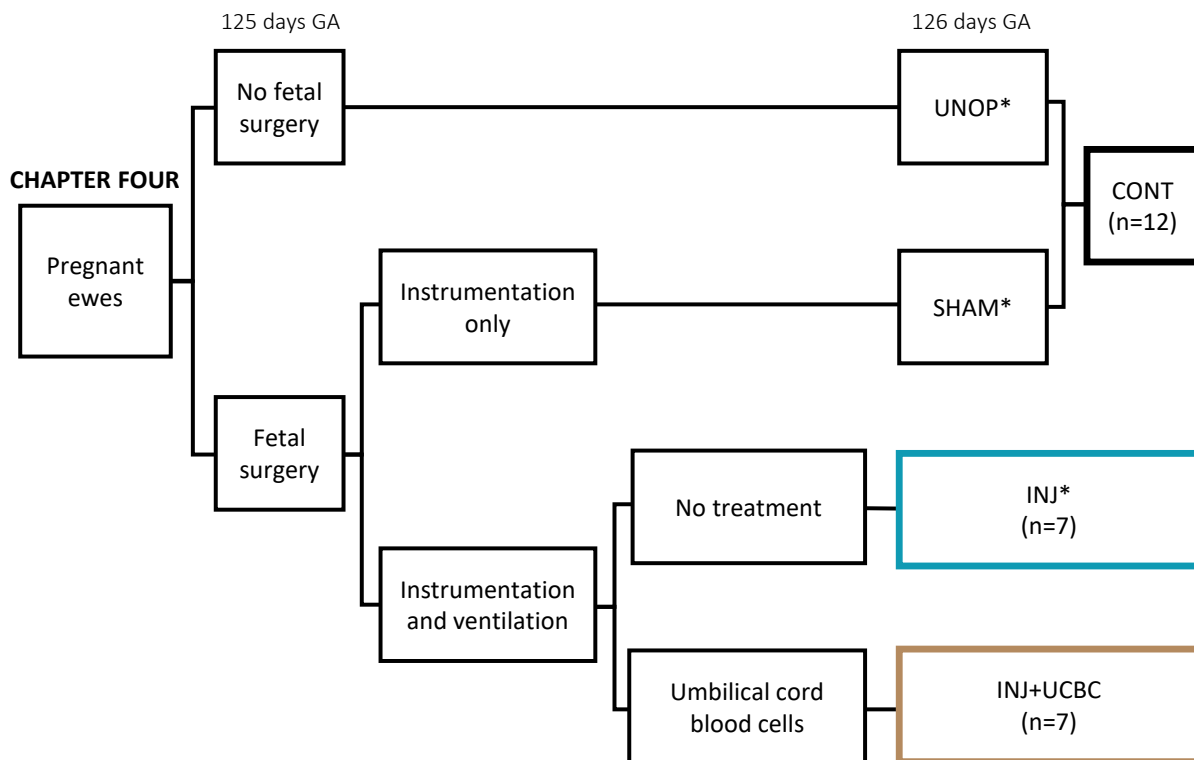


Figure 1.10. Experimental groups for Chapter 4, to investigate the effects of umbilical cord blood cells on periventricular and subcortical white matter injury in preterm sheep following injurious ventilation. Ventilation was conducted with intact placental circulation. Umbilical cord blood cells were administered 1 h after the initiation of injurious ventilation. Asterisk denotes common experimental groups to Chapter 3.

Hypothesis for aim 2

I hypothesised that early administration of UCB cells would reduce ventilation-induced cerebral white matter injury, assessed by molecular and histological means, 24 h after the high V_T ventilation insult.

Aim 3 (addressed in Chapter 5)

To establish the pattern of injury within the PVWM and SCWM in preterm-equivalent fetal sheep after 24 h of ventilation.

To address Aim 3, an ovine *in utero* ventilation model was used with two experimental groups [Fig. 1.11].

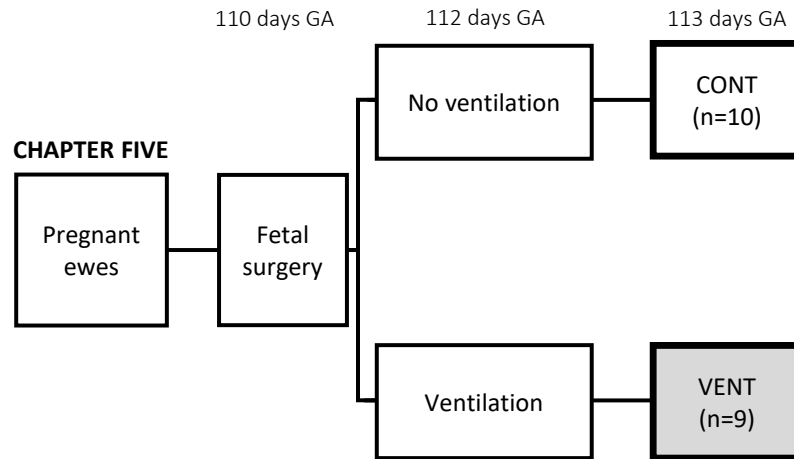


Figure 1.11. Experimental groups for Chapter 5, to investigate periventricular and subcortical white matter pathology after 24 h of ventilation in preterm-equivalent sheep fetuses.

Hypothesis for aim 3

I hypothesised that continuous ventilation for 24 h would result in reproducible PVWM and SCWM injury in the immature brain, which can be detected by molecular and histological analyses.

Chapter Two: General Methodology

Sheep were used in all the experiments in this thesis. The pregnant sheep and fetus tolerate surgery well, meaning surgical intervention is unlikely to initiate preterm delivery. This is advantageous for experiments requiring instrumentation of the fetus. Moreover, the size of a preterm lamb is similar to that of a neonate, allowing the use of ventilators that closely mimic clinical settings. Sheep are precocial and the ovine fetal brain developmental milestones are comparable to that of humans. Ovine brain development has been extensively characterised. The appropriateness of using sheep as a model for VIBI is discussed further in Appendix I (Review).

2.1. Animal ethics and welfare

All experimental procedures were approved by the Monash Medical Centre Animal Ethics Committee A, Monash University, and were conducted in accordance with the National Health and Medical Research Council of Australia's guidelines.

2.2. Experimental design – Brain injury 24 h after injurious ventilation (Chapters 3 & 4)

Date-mated pregnant Border-Leicester ewes were delivered from Monash Animal Research Platform (MARF) Gippsland Field Station to MARF Clayton prior to transfer to the Monash Biomedical Imaging (MBI) facility to allow graded acclimatisation. A total of 31 pregnant ewes with singleton or twin fetuses were delivered to MBI at least two days prior to experimental surgery. Ewes were housed with a companion sheep at room temperature under a 12 h light/dark cycle and their pens were cleaned daily. Ewes had constant access to drinking water, were fed chaff daily, and were fasted at least 16 h prior to surgery. General wellbeing of the ewes was monitored and noted daily; all ewes were deemed healthy for participation in the studies.

Lambs were randomised to one of five groups:

- 1) Unoperated control (**UNOP**; n=7): Lambs did not undergo fetal surgery or ventilation and were used to control for the surgical intervention.
- 2) Sham surgery control (**SHAM**; n=5): Lambs underwent fetal surgery, were instrumented and intubated, but did not receive mechanical ventilation to control for the experimental intervention.

- 3) Injurious ventilation (**INJ/INJ_{INF}**; n=7): Lambs received 15 min of high V_T ventilation, with intact placental circulation, to initiate predominantly the inflammatory pathway of VIBI.
- 4) Injurious ventilation with umbilical cord occluded (**INJ_{INF+HAE}**; n=7): Lambs received 15 min of high V_T ventilation during which the umbilical cord was occluded. The removal of the placental circulation simulates umbilical cord clamping to initiate the haemodynamic pathway of VIBI in addition to the inflammatory pathway. The umbilical cord occlusion was released after the 15 min of injurious ventilation and placental blood flow to the fetus was restored.
- 5) Injurious ventilation with umbilical cord blood cell treatment (**INJ+UCBC**; n=7): Lambs received 15 min of high V_T ventilation, with intact placental circulation. Lambs were administered 80 million allogeneic UCB cells 1 h post-ventilation.

The experimental protocol spanned two days. Fetal surgery was performed on the first day (except UNOP) and the ewe was allowed to recover for 24 h. The fetus was monitored via arterial blood gases during this 24 h. On the second day, all lambs were delivered and underwent magnetic resonance imaging (MRI) of the brain. Immediately after MRI, lambs were euthanised (sodium pentobarbitone >100 mg i.v.; Valabarb Euthanasia Solution; Jurox, NSW, Australia) for tissue collection. Ewes were euthanised (overdose of sodium pentobarbitone i.v.; Valabarb) after delivery of the lambs.

2.2.1. Fetal surgery

Sterile fetal surgery was conducted at 125 ± 1 days gestation (mean \pm SD; term ~148 days). The ventral surface of the ewe's neck was shorn to expose the jugular vein. The ewe was anaesthetised by intravenous (i.v.) injection of thiopentone sodium into the jugular vein (20 mg/kg i.v.; Jurox, NSW, Australia). Upon sedation, the ewe was transferred onto the surgical table, placed in the supine position, intubated with an endotracheal tube (ID 8.0 mm; Smiths Medical, UK), ventilated (EV500 Anaesthesia ventilator; ULCO Medical, NSW, Australia), and maintained on anaesthesia via inhaled isoflurane (1.5-2.5% in oxygen; Bomac Animal Health, NSW, Australia) for the entirety of the experiment. Wellbeing of the ewe was constantly monitored to ensure adequate anaesthesia throughout the experiment. Prophylactic antibiotics (1 g Ampicillin i.v.; Alphapharm, NSW, Australia and 500 mg Engemycin i.v.; Coopers Animal Health, VIC, Australia) were administered via the maternal jugular vein at least 30 min before the surgical procedure.

The right flank and abdomen of the ewe were shorn and thoroughly cleaned using multiple applications of chlorhexidine (0.5% w/v in 70% ethanol; Johnson & Johnson Medical, Australia), triplicate washes with Betadine surgical scrub (7.5% w/v povidine-iodine; Faulding, Australia), and finally sprayed with

Betadine antiseptic solution (10% w/v povidine-iodine; Faulding, Australia) to cover the entire surgical site. Sterile drapes were placed over the ewe, exposing only the immediate incision site. All surgical instruments used were sterile. Operators performing the surgery were surgically scrubbed in. The surgical scrub procedure involves decontaminating the hands and arms (chlorhexidine; 0.5% w/v in 70% ethanol and Betadine surgical scrub; 7.5% w/v povidine-iodine), donning a sterile surgical gown, and a pair of sterile gloves.

Local anaesthetic (12.5 mg bupivacaine hydrochloride; Marcaine; Astra Zeneca, NSW, Australia) was subcutaneously injected at the abdominal incision site on the ewe prior to incision. A midline laparotomy was performed to expose the uterus, and the fetal head and neck were exteriorised. Polyvinyl catheters (ID 0.86 mm, OD 1.52 mm; Dural Plastics & Engineering, NSW, Australia) were inserted in the left carotid artery and jugular vein of the fetus. An ultrasonic flow probe (3PS; Transonic Systems, NY, USA) was placed around the right carotid artery to monitor carotid blood flow. For INJ_{INF+HAE} lambs, an occluder was placed around the umbilical cord (Chapter 3).

The fetal chest was exteriorised and the fetus was intubated with a cuffed endotracheal tube (ID 4.0–4.5 mm; Smiths Medical, UK) and lung liquid was passively drained. SHAM animals remained intubated and exteriorised for 15 min without mechanical ventilation. The umbilical cord occluder was inflated when ventilation commenced and removed at the end of the ventilation period to restore placental blood flow to the fetus (INJ_{INF+HAE} only). INJ animals received 15 min of injurious ventilation as described below.

2.2.2. Injurious ventilation strategy

Ventilation was conducted for 15 min under sterile conditions using a neonatal positive pressure ventilator (Babylog 8000+, Dräger, Lübeck, Germany) with a sterile circuit using heated, humidified air (Fisher and Paykel Healthcare, Auckland, New Zealand). The weight of the fetus was estimated using historical age-matched fetal data to determine a target V_T of 12–15 ml/kg. Ventilation was initiated with a peak inspiratory pressure (PIP) of 40 cmH₂O, positive end expiratory pressure (PEEP) of 5 cmH₂O, fraction of inspired oxygen (FiO_2) at 0.21, inspiratory time 0.6 s, and expiratory time 0.6 s. PIP was adjusted to an upper limit of 45 cmH₂O to escalate V_T to 10 ml/kg by 10 min and 12–15 ml/kg by 15 min. Sustained inflations (maximum set PIP for 5 s) were used to recruit the lung.

2.2.3. Surgical wound closure and post-surgery monitoring

After ventilation, the fetus was extubated. Flow probes were removed and the incision site in the neck was sutured closed before the fetus was returned to the uterus. Fetal catheters were affixed with three-way taps and externalised through the ewe's right flank via a small incision to allow periodic blood sampling and administration of UCB cells (Chapter 4). The abdominal and flank incisions were sutured closed and the incision sites were irrigated with Marcaine (Astra Zeneca, NSW, Australia). Additional analgesia was provided to the ewe via buprenorphine (0.3 mg i.m.; Temgesic; Reckitt Benckiser, UK) and a transdermal fentanyl patch (75 µg/h; Janssen-Cilag, NSW, Australia) was applied for post-surgical pain relief.

The ewe was returned to a mobile pen and regularly monitored for 24 h. Ewes had access to chaff immediately after surgery and were provided water once they were alert and had good neck tone. Ewes were fasted for at least 8 h prior to delivery the following day but still had access to drinking water.

2.2.4. Umbilical cord blood cell preparation and administration (Chapter 4 only)

At 1 h post-ventilation, 80 million allogeneic UCB cells were administered to the fetus via the jugular vein catheter. The cells were suspended in 3 ml of phosphate-buffered saline (PBS; Gibco, MA, USA) which was administered slowly over 2 min. The catheter was flushed with 3 ml of sterile heparinised saline to ensure all the cells were administered.

UCB cells were obtained from healthy term lambs (141 days gestation) undergoing procedures in a separate study, using UCB collection and UCB cells preparation protocols as previously described.^{184,188,189} Briefly, approximately 90-100 ml of cord blood was collected via the two umbilical veins of each lamb. The mononuclear cell layer was obtained by centrifuging the blood at $1000 \times g$ for 12 min with no brake and the buffy coat was collected and washed in PBS. Red blood cells were lysed by combining cells with lysis buffer (ammonium chloride, potassium bicarbonate, and ethylenediaminetetraacetic acid [EDTA] in MilliQ water). The lysis reaction was stopped with excess media (16.5% fetal bovine serum [FBS] in DMEM:F13; Gibco). Cells were centrifuged at $400 \times g$ for 5 min, supernatant was aspirated, and the cells resuspended in media. Cells were manually counted and their viability was assessed using trypan blue exclusion dye (Gibco) and a haemocytometer. UCB cells were cryopreserved in dimethyl sulfoxide (10% DMSO, Sigma-Aldrich, MO, USA in FBS) and stored in liquid nitrogen before retrieval for administration. On the day of experiment, the cells were rapidly thawed in a 37°C water bath, washed with media, re-suspended in PBS and recounted, then kept on ice until administration.

2.2.5. Lamb delivery and stabilisation

At 24 h post-ventilation, ewes were anaesthetised again as described above, and the fetus was delivered via caesarean section at the same incision site as made previously. A transcutaneous oximeter (Masimo, CA, USA) was attached to the fetus's tail to monitor oxygen saturation level and heart rate. UNOP lambs were instrumented with arterial and venous polyvinyl catheters prior to delivery.

All lambs were dried, intubated, and stabilised with a gentle ventilation strategy (Babylog 8000+, Dräger). Ventilation was initiated in volume-guarantee mode set at 7 ml/kg, maximum PIP 40 cmH₂O, PEEP 5 cmH₂O, inspiratory time 0.6 s, and expiratory time 0.6 s. FiO₂ was set initially at 0.4 but adjusted to maintain arterial oxygen saturation (SaO₂) between 88-95% and partial pressure of carbon dioxide (PaCO₂) between 45-55 mmHg. Intratracheal surfactant (240 mg; Curosurf[®]; Chiesi Pharmaceuticals, Parma, Italy) was administered within the first 10 min of ventilation to improve lung compliance. Sustained inflations at 35 cmH₂O for 5 s duration were applied to recruit the lung if necessary. Once the lambs were stabilised (within 15 min of ventilation onset), the umbilical cord was clamped and the lambs were transferred to an MR-compatible ventilator (Pneupac[®] babyPAC[™]; Smiths Medical, UK) using the same ventilator settings on the Dräger ventilator as a reference.

2.2.6. Lamb monitoring during magnetic resonance imaging

Lambs were transferred supine to a 3T MRI system (Magnetom Skyra; Siemens, Erlangen, Germany). Lambs were kept warm with a hot water bottle and sedated (5-15 mg/kg Alfaxan in 5% glucose; Jurox, NSW, Australia) for the duration of imaging. The total acquisition time was approximately 40 min. Brain MRI included structural imaging sequences, diffusion tensor imaging (DTI), susceptibility-weighted imaging, and single-voxel magnetic resonance spectroscopy (MRS). Results of the MRI have been reported¹¹¹ and do not form part of this thesis (Appendix II).

2.2.7. Blood samples

Arterial blood (~0.3 ml) was collected via the carotid artery catheter and analysed to monitor the wellbeing of fetuses (ABL80 FLEX; Radiometer Medical ApS, Denmark). Blood gas sampling was conducted during fetal surgery, injurious ventilation, up to 24 h post-ventilation, and after delivery until the lamb was euthanised [Fig. 2.1]. Lambs in the UNOP group did not undergo fetal surgery and recovery; '24 h' in Fig. 2.1 represents 'PRE T=0' in this group. Plasma collection (~3 ml of blood, centrifuged at 4°C, 3000 × g, 10 min to separate the plasma layer) was conducted before commencement of ventilation (PRE), at 15 min, 1 h, 3 h, 6 h, 12 h, and 24 h after ventilation, and at the end of MRI [Fig. 2.1].

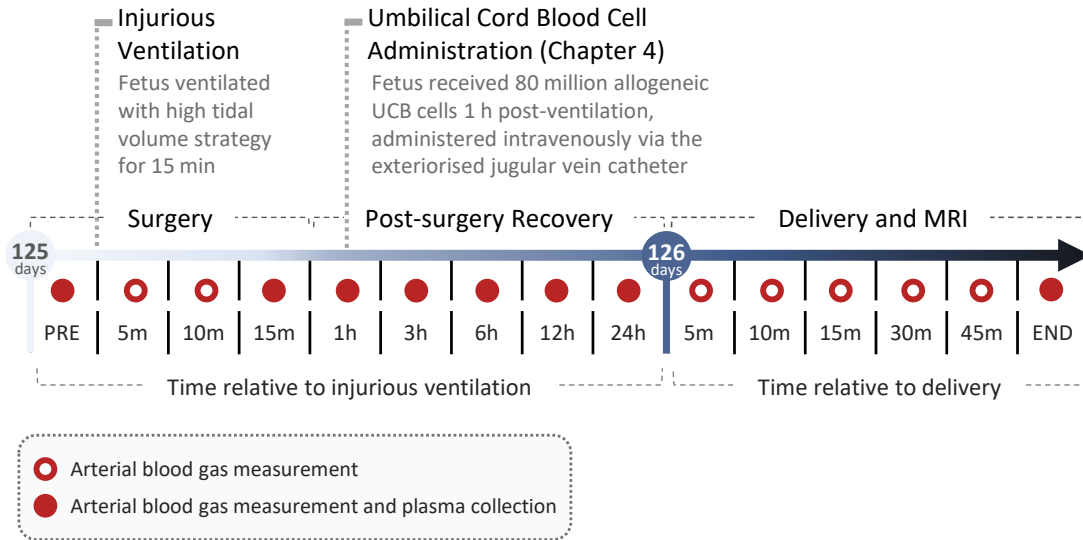


Figure 2.1. Experimental timeline for Chapters 3 and 4. Arterial blood was collected at specific time points during the experiment for blood gas measurement (open circle) and collection for cytokine analysis (filled circle). Term pregnancy in sheep is ~148 days of gestation.

2.2.8. Physiological data collection and analysis

Fetal heart rate, carotid blood flow, carotid arterial pressure, and ventilator outputs were recorded in real-time throughout the 15 min injurious ventilation period (Powerlab; ADInstruments, NSW, Australia). Physiological data were extracted and analysed in 10 s epochs for every minute of recording (LabChart; ADInstruments, NSW, Australia). Maximum V_T was divided by the body weight of individual lambs and expressed as V_T/kg . Carotid blood flow was divided by the brain weight of individual lambs and expressed as $\text{ml}/\text{min}/100\text{g}$.

The brain was collected for analysis as discussed below (see Section 2.4).

2.3. Experimental design –

Brain injury following 24 h *in utero* ventilation (Chapter 5)

Date-mated pregnant Border-Leicester ewes were delivered from MARP Gippsland Field Station to MARP Clayton prior to transfer to the Monash Medical Centre (MMC) B-block animal facility to allow acclimatisation. A total of 19 pregnant ewes with singleton or twin fetuses were delivered to MMC B-block at least two days prior to experimental surgery. Ewes were housed in neighbouring pens under a 12 h light/dark cycle and their pens were cleaned daily. Ewes had constant access to drinking water, were fed chaff daily, and were fasted at least 16 h prior to surgery. The general wellbeing of ewes was monitored and noted daily; all ewes were deemed healthy for participation in the studies.

Fetal sheep were randomised to one of two groups:

- 1) Sham control (**CONT**; n=10): Fetuses underwent fetal surgery, were instrumented, but did not receive ventilation.
- 2) *In utero* ventilation (**VENT**; n=9): Fetuses received 24 h of gentle ventilation whilst *in utero*.

The experimental protocol spanned four days. Fetal surgery was performed on the first day and the ewe was allowed to recover for at least 36 h. On day 3, ventilation was initiated in VENT fetuses for 24 h, during which the ewe was allowed to eat and movement was not restrained. Fetal wellbeing for both groups was monitored via arterial blood gases and physiological measurements. At the end of the ventilation period, ewes were euthanised (overdose of sodium pentobarbitone i.v.; Valabarb). The fetuses were immediately removed from the ewe for post-mortem tissue collection. Sodium pentobarbitone readily crosses the placenta to kill the fetus; additional sodium pentobarbitone was administered directly to the fetus otherwise.

2.3.1. Fetal surgery

Sterile fetal surgery was conducted at 110 ± 1 days gestation (mean \pm SD; term ~148 days). The ewe was anaesthetised as above (Section 2.2.1). The fetal head and neck were exposed for catheterisation of the left carotid artery and jugular vein as described above (Section 2.2.1). An additional polyvinyl catheter (ID 2.6 mm, OD 4.2 mm) was secured to the exterior of the fetus to allow administration of antibiotics to the amniotic sac and to correct for fetal pressure for physiological recordings.

A tracheostomy was performed on the fetus to secure a modified reinforced endotracheal tube (ID 4.0 mm; Medtronic, MN, USA) in the lower trachea. This was then connected to a saline-filled large-bore ventilation tube (ID 6.4 mm, OD 12.7 mm) with a catheter (ID 3.2 mm, OD 6.4 mm) attached to the other end. A separate saline-filled catheter (ID 3.2 mm, OD 6.4 mm) was inserted into the upper trachea. The two catheters were exteriorised via the right flank of the ewe and then connected to create a tracheal loop to allow normal flow of lung liquid [**Fig. 2.2**].

Fetal arterial and venous catheters were exteriorised via the ewe flank incision. The abdominal and flank incisions were sutured closed and the incision sites were irrigated with Marcaine (Astra Zeneca, NSW, Australia).

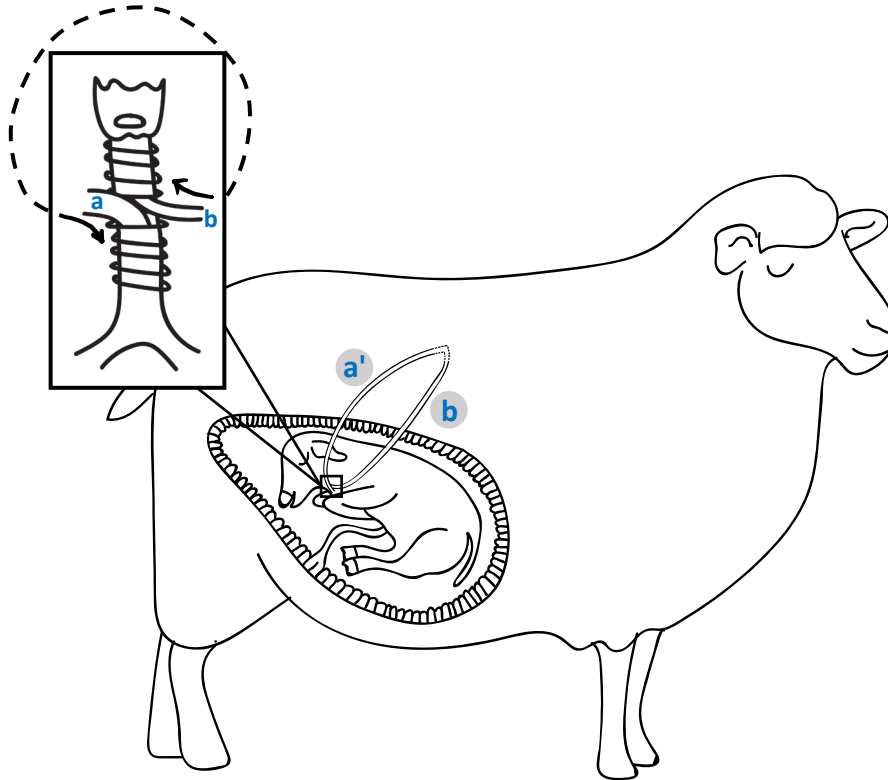


Figure 2.2. Set-up of tracheal loop. A modified reinforced endotracheal tube (**a**) was inserted in the lower trachea and connected to a saline-filled large-bore ventilation tube and catheter on the other end (**a'**). A separate saline-filled catheter (**b**) was inserted into the upper trachea. The catheters were exteriorised via a flank incision and connected to create a tracheal loop. Before ventilation commenced, the large ventilation tube (**a'**) was disconnected from the tracheal loop, lung liquid was passively drained, and the tube was connected to a neonatal ventilator.

2.3.2. Maternal surgery

During surgery, a small incision was made in the maternal neck for catheterisation of the right jugular vein. A polyvinyl catheter (ID 2.6 mm, OD 4.2 mm) was inserted towards the direction of the heart to allow post-surgery administration of maternal antibiotics. The incision site was sutured closed and irrigated with Marcaine (Astra Zeneca, NSW, Australia).

2.3.3. Ewe recovery and post-surgical care

Analgesia was provided to the ewe via a transdermal fentanyl patch (75µg/h; Janssen-Cilag, NSW, Australia) for post-surgery pain relief. The ewe was returned to a mobile pen and closely monitored for the first 4 h post-surgery. Ewes were fed chaff immediately after surgery and were provided water once they were alert and showed good neck tone. Wellbeing of the ewe was monitored daily.

On days 2 and 3 (i.e. post-surgery days 1 and 2), antibiotics were administered to the ewe (1 g Ampicillin and 5 ml Engemycin i.v.) and fetus (100 mg Ampicillin i.v.) via their respective jugular vein catheters. Ampicillin was also administered to the amniotic fluid (400 mg). An arterial blood sample was taken from the fetus on day 2 to check the wellbeing of the fetus.

2.3.4. *In utero* ventilation

At 112 ± 1 days gestation, 2 days post-surgery, the large ventilation tube [Fig. 2.2(a')] was disconnected from the tracheal loop, lung liquid was passively drained, and the tube was connected to a neonatal ventilator (Babylog 8000+, Dräger, Lübeck, Germany). Ventilation was initiated in volume-guarantee mode set at 5 ml/kg, maximum PIP 45 cmH₂O, PEEP 5 cmH₂O, inspiratory flow of 10 l/min, rate of 60 inflations/min, and FiO₂ at 0.21. Ventilator parameters were adjusted when necessary during the ventilation period to achieve a target V_T of 3-5 ml/kg but limited to a PIP of 45 cmH₂O. Sustained inflations were applied to recruit the lung if necessary. Fetal wellbeing was monitored via physiological measurements and arterial blood gas results at regular intervals (see Section 2.3.5).

2.3.5. Blood samples

Arterial blood (~0.3 ml) was collected via the fetal carotid artery catheter and analysed (ABL90; Radiometer Medical ApS, Denmark) to monitor the wellbeing of fetuses. Arterial blood gas monitoring and plasma collection (~3 ml of blood, centrifuged at 4°C, 3000 × *g*, 10 min to separate the plasma layer) was conducted before commencement of IUUV (PRE), and at 15 min, 1 h, 3 h, 6 h, 9 h, 12 h, and 24 h after IUUV [Fig. 2.3]. Additional blood gas monitoring was performed at post-surgery day 1, 30 min and 45 min after IUUV, and when deemed necessary to ensure fetal wellbeing [Fig. 2.3].

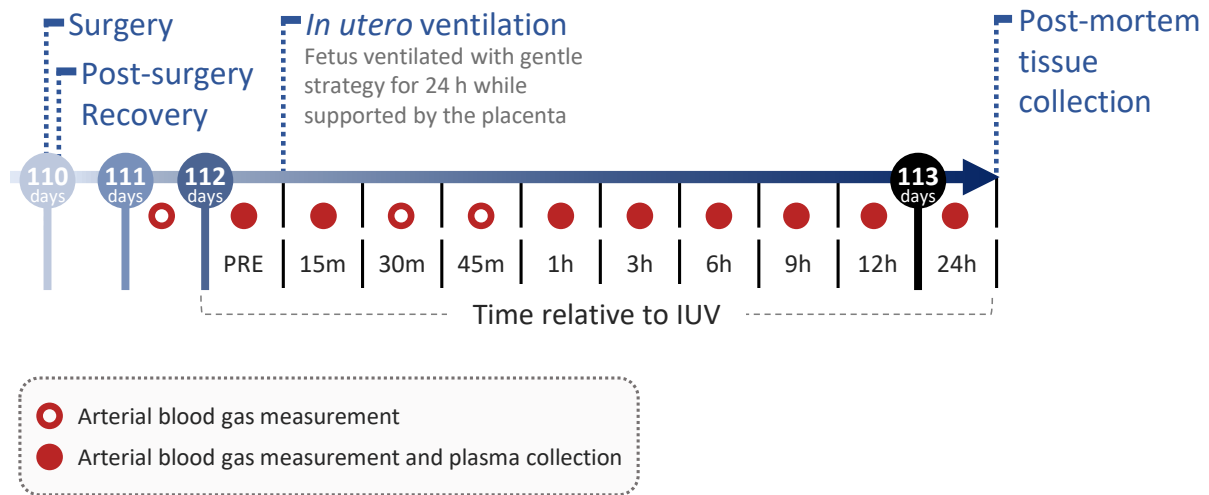


Figure 2.3. Experimental timeline for Chapter 5. Arterial blood was collected at specific time points during the experiment for blood gas measurement (open circle) and collection for cytokine analysis (filled circle). Term pregnancy in sheep is ~148 days of gestation.

2.3.6. Physiological data collection and analysis

Ventilator output, carotid arterial pressure, and amniotic fluid pressure were measured and recorded in real-time throughout the 24 h ventilation period (Powerlab; ADInstruments, NSW, Australia).

The brain was collected for analysis as discussed below.

2.4. Tissue collection and handling (all chapters)

At post-mortem examination, lamb body weight and organ weights were recorded. The brain and lungs were collected for analysis.

2.4.1. Cerebrospinal fluid collection

Cerebrospinal fluid (CSF) was collected immediately following euthanasia, prior to brain collection, and was frozen in liquid nitrogen. The lamb's neck was flexed at the atlanto-occipital joint such that its head was perpendicular to the cervical vertebral column. The head was palpated to identify anatomical landmarks, and a needle (21G; Sigma-Aldrich) was advanced slowly into the cisterna magna to obtain CSF. Samples containing blood were centrifuged (4°C , $3000 \times g$, 10 min) to separate CSF from blood cells before freezing. Xanthochromia in the supernatant CSF was noted.

2.4.2. Removal of brain from skull

At post-mortem, a scalpel incision was made through the skin from the front of the skull to midway down the back of the lamb's neck followed by a perpendicular incision between its ears. The skull and attached meninges were then carefully peeled back using rongeurs, starting from the nasion in a rostral to caudal manner. Once the brain and part of the spinal cord were exposed, the cervical spinal cord and cranial nerves on the ventral side of the brain were severed to allow the brain to be removed. The brain was weighed and immediately placed on ice, ventral side down.

The cerebellar peduncles were severed to separate the cerebellum which was then dissected in half along the sagittal plane. The brainstem was dissected below the inferior colliculi and the cerebrum was halved along the medial longitudinal fissure. The right cerebellum, right forebrain, and entire brainstem were immersion fixed in 10% neutral buffered formalin (NBF; Amber Scientific, WA, Australia) overnight. The left cerebellum and left forebrain were placed on ice for dissection. For Chapter 5, the right brainstem was immersion fixed in 10% NBF and the left brainstem was placed on ice for dissection.

2.4.3. Right hemisphere collection

The right hemisphere of the lamb's brain was immersion fixed in 10% NBF and kept at 4°C overnight. The right forebrain was then cut coronally into 5 mm blocks (8-9 blocks per animal) and placed into mega cassettes. The brainstem and right cerebellum were each placed in a mega cassette. All mega cassettes were placed in fresh 10% NBF for 6 days, after which the brain tissue was processed and paraffin-embedded.

2.4.4. Left hemisphere collection

The left hemisphere of the lamb's brain was cut coronally into blocks (8-9 blocks per animal) starting from the ansate sulcus and fanned out [Fig. 2.4]. Regions of the corpus callosum, hippocampus, periventricular white matter (PVWM), subcortical white matter (SCWM), and grey matter (GM) were cut out from the sections, snap frozen in liquid nitrogen, and transferred to cryovials. The remaining tissue was cut up and collected as a representation of 'Frontal' (until section before lateral ventricle), 'Parietal', and 'Occipital' (from section after hippocampus) lobes. The choroid plexus, cerebellar white matter, and cerebellar GM were also snap frozen.

The brain was kept chilled during this process to minimise tissue degradation. All cryovials containing the frozen tissue were subsequently stored at -80°C.

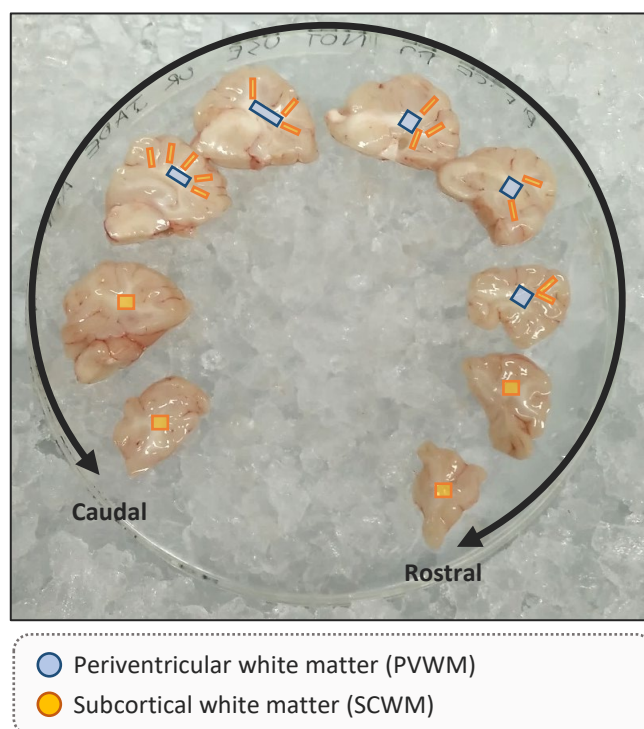


Figure 2.4. Dissection of the left hemisphere of the preterm lamb brain for molecular analysis. The left hemisphere was cut coronally and fanned out on ice, rostral side down. The periventricular white matter (PVWM; blue boxes) and subcortical white matter (SCWM; orange boxes) regions were dissected and snap frozen for molecular analysis in Chapters 3 and 4.

2.5. Molecular analyses

2.5.1. Enzyme-linked immunosorbent assay

Plasma protein levels of interleukin(IL)-6 and IL-8 were determined by ovine-specific enzyme-linked immunosorbent assay (ELISA). Antibodies and standards used are detailed in **Table 2.1**. Briefly, 96-well flat-bottom plates (Nunc MaxiSorp; Invitrogen, Thermo Fisher Scientific, USA) were incubated with respective coating antibodies (diluted in carbonate buffer pH 9.6) at 4°C overnight. Wells were washed and blocked (Dulbecco's PBS; Gibco, 1% BSA) for 1 h at room temperature. To generate a standard curve, recombinant ovine (rov) IL-6 and IL-8 proteins were serially diluted 1:2 in diluting buffer (PBS, 0.1% BSA, 0.05% Tween 20) down the first 2 columns of the ELISA plate. Standards were included and a 4-parameter standard curve was generated for every ELISA plate used ($R^2 > 0.99$ for all). Experimental plasma samples (diluted 1:1 in diluting buffer) were added into duplicate wells. The plates were incubated for 1 h at room temperature. After washing, appropriate cytokine-specific detecting antibodies were added, and plates were incubated for 1 h at room temperature. After further washing, horseradish peroxidase (HRP) conjugated swine anti-rabbit immunoglobulin was added, and plates were incubated for 1 h at room temperature. Plates were then washed and incubated with

tetramethylbenzidine (TMB) chromogen solution (Invitrogen, USA) in the dark for 15–20 min at room temperature. Reactions were stopped with the addition of 0.5M sulfuric acid (H₂SO₄). Plates were read on a plate reader (SpectraMax i3; Molecular Devices, CA, USA) at 450 nm to determine optical density.

Cytokine levels were measured for all time points and reported normalised to baseline values.

Table 2.1. Details of reagents used in enzyme-linked immunosorbent assays (ELISAs) for detection of pro-inflammatory cytokines.

Target	Reagent details	Clone/type	Dilution	Source
IL-6	<i>rov</i> IL-6 (cytokine standard)	N/A	N/A	Kingfisher ^a RP0367V-005
	Mouse anti-ovine IL-6 mAb (coating)	4B6, isotype IgG1	1:200	Bio-Rad ^b MCA1659
	Rabbit anti-ovine IL-6 pAb (detecting)	N/A	1:500	Bio-Rad ^b AHP424
	Swine anti-rabbit Ig/HRP pAb	N/A	1:2000	DAKO ^c P0217
IL-8	<i>rov</i> IL-8 (cytokine standard)	N/A	N/A	Kingfisher ^a RP0488V-005
	Mouse anti-ovine IL-8 mAb (coating)	8M6, isotype IgG2a	1:1000	Bio-Rad ^b MCA1660
	Rabbit anti-ovine IL-8 pAb (detecting)	N/A	1:4000	Bio-Rad ^b AHP425
	Swine anti-rabbit Ig/HRP pAb	N/A	1:2000	DAKO ^c P0217
<i>HRP</i> horse radish peroxidase, <i>Ig</i> immunoglobulin, <i>IL</i> interleukin, <i>rov</i> Recombinant ovine, <i>mAb</i> Monoclonal antibody, <i>pAb</i> Polyclonal antibody ^a Kingfisher: Kingfisher Biotech, Inc., MN, USA ^b Bio-Rad: Bio-Rad Laboratories, Inc., CA, USA ^c Dako: Agilent Technologies, Inc., CA, USA				

2.5.2. RT-qPCR by Fluidigm

2.5.2.1. RNA preparation

Ribonucleic acid (RNA) was extracted from brain tissue so that reverse transcription real-time quantitative polymerase chain reaction (RT-qPCR) could be performed to quantify the expression of genes of interest.

Total RNA was extracted from the PVWM and SCWM using the RNeasy Midi RNA Extraction Kit (Qiagen, VIC, Australia) as per manufacturer's instructions. Briefly, 100–150 g of frozen tissue was homogenised in Buffer RLT (with 1% β-Mercaptoethanol) using a rotor-stator homogenizer (Ultra-Turrax T-25; Janke & Kunkel, IKA-Laboritechnik, Germany). The supernatant was transferred to a

new tube, an equivalent volume of 70% ethanol was added, and the solution was vigorously shaken to resuspend any precipitates. Immediately after, the sample was applied to an RNeasy midi column, centrifuged for 5 min at $4800 \times g$, and flow-through was discarded. This process was repeated until all supernatant had passed through the column.

Deoxyribonucleic acid (DNA) digestion was performed using the RNase-free DNase Set. Buffer RW1 was added into the RNeasy column and centrifuged for 5 min at $4800 \times g$. Each membrane was treated with 20 μ l Dnase 1 stock solution in 140 μ l Buffer RDD to remove any DNA contamination. The column was left to incubate at room temperature for 15 min, then 2 ml of Buffer RW1 was added to each column and left to stand at room temperature for a further 5 min. The column was centrifuged for 5 min at $4800 \times g$ and flow-through was discarded. Buffer RPE (diluted with 4 volumes of ethanol) was added to the column to remove traces of salts from previous buffers. The column was centrifuged for 2 min at $4800 \times g$ and flow-through was discarded. Another 2.5 ml of Buffer RPE was added to the column and centrifuged for 5 min at $4800 \times g$ to dry the RNeasy silica-gel membrane. This ensured no residual ethanol that may interfere with downstream reactions was present.

The RNeasy column was transferred to a new 15 ml collection tube for elution. 120 μ l of RNase-free water was pipetted directly onto the membrane. The column was left to stand for 1 min and then centrifuged for 3 min. The second elution step was performed using the first eluate to obtain a higher final RNA concentration.

Gel electrophoresis was used to validate the quality of extracted RNA and check for DNA contamination. A spectrophotometer (Nanodrop, ThermoScientific, USA) was used to measure RNA purity and concentration. RNA was stored at -80°C until further use.

2.5.2.2. cDNA preparation

RNA was reverse-transcribed into complementary DNA (cDNA) as per protocols of the SuperScript® III First-Strand Synthesis System for RT-PCR kit (Invitrogen, CA, USA). Briefly, RNA was diluted with sterile RNase-free water in a nuclease-free microcentrifuge tube to achieve a target concentration of 50 ng/ μ l and 1 μ l of random hexamers and 1 μ l of 10mM deoxyribonucleotides (dNTP) mix were added. The solution was heated at 65°C for 5 min to denature the RNA, then incubated on ice for at least 1 min. Reagents 4 μ l 5X First-Strand Buffer, 1 μ l 0.1M dithiothreitol (DTT), and 1 μ l RNaseOUT™ Recombinant RNase Inhibitor were added to the tube and 1 μ l SuperScript™ III Reverse Transcriptase was added directly to each solution and mixed by gently pipetting up and down. The samples were incubated at room temperature for 5 min, 50°C for 60 min, and finally at 70°C for 15 min to inactivate the reaction. The cDNA was stored at -20°C until further use.

2.5.2.3. Quantitative real-time polymerase chain reaction (qPCR) by Fluidigm (Chapters 3 & 4)

Samples of cDNA were provided to the Monash Health Translation Precinct (MHTP) Medical Genomics Facility for high throughput PCR using the microfluidic technology Fluidigm Access Array System (Fluidigm Corporation, CA, USA) with TaqMan probes and primers (Thermo Fisher Scientific, MA, USA). A minus-reverse transcriptase control (-RT; no Superscript III added during cDNA preparation) was provided for every batch of cDNA made.

Briefly, all samples were checked for quality by qPCR (ABI 7900 HT; Thermo fisher Scientific, MA, USA) using predesigned primers in combination with Sybr chemistry. The level of fluorescence was detected and plotted against the number of cycles to produce an amplification curve for each sample. A fluorescence threshold was set and the number of cycles required for each sample to reach the threshold was determined (cycle threshold; C_T). A -RT control sample with a C_T value difference of <10 cycles with the cDNA samples indicated potential genomic DNA contamination.

Samples were processed on the Fluidigm BioMark™ HD system in which they were loaded on a 48.48 (Chapter 3) or 192.24 (Chapter 4) Dynamic Array integrated fluidic circuit for amplification to determine the relative gene expression levels of pro-inflammatory cytokines, tight junction proteins, markers of cell death, factors of angiogenesis, and markers of neuronal and glial activity, specifically: *IL1B*, *IL6*, *IL8*, *IL10*, *TNF*, *CCL2*, *TGFB1*, *OCLN*, *CLDN1*, *P53*, *CASP3*, *VEGFA*, *VEGFR1*, *NOX2*, *HIF1A*, and *ANGPT1* [Table 2.2]. *RPS18*, which encodes ribosomal protein S18 of the 40S ribosomal subunit, was used as a reference gene as it is expressed constitutively and stably at various developmental stages of the ovine brain.¹⁹⁰

The integrated fluidic circuit was then placed in the Biomark™ HD system for thermal cycling. Fluorescence was detected in real-time and the final output file consisted of amplification curves, C_T data, and a colour-coded heat map. Gene expression levels were quantified using the $\Delta\Delta C_T$ method.¹⁹¹ The expression of all genes was normalised to *RPS18* for each sample, then expressed relative to the control group.

Table 2.2. Details of genes investigated using RT-qPCR by Fluidigm. Gene names and symbols have been validated on the National Center for Biotechnology Information (NCBI) Gene database. The TaqMan assay ID for each probe is provided; target-specific sequences of TaqMan assays are not available due to non-disclosure policies.

Reason for assessment	Gene name	Gene symbol	TaqMan Assay ID	Used in
Reference gene	Ribosomal protein S18	RPS18	Oa04906333_g1	Chapters 3 and 4
Cytokines	Interleukin 1 beta	IL1B	Oa04656322_m1	Chapters 3 and 4
	Interleukin 6	IL6	Oa04656315_m1	
	Interleukin 8	IL8	Bt03211906_m1	
	Tumour necrosis factor	TNF	Oa04655425_g1	
	Interleukin 10	IL10	Oa03212724_m1	Chapter 4 only
	C-C motif chemokine ligand 2	CCL2	Oa04677078_m1	
	Transforming growth factor beta 1	TGFB1	Oa04259484_m1	
Tight junction proteins	Occludin	OCLN	Oa04728970_m1	Chapters 3 and 4
	Claudin 1	CLDN1	Oa03217991_m1	
Markers of cell death	Tumor protein p53	P53	Oa03223218_g1	Chapters 3 and 4
	Caspase 3	CASP3	Oa04817361_m1	
Mediators of angiogenesis	Vascular endothelial growth factor A	VEGFA	Oa04653812_m1	Chapter 4 only
	Vascular endothelial growth factor receptor 1 <i>alias fms related receptor tyrosine kinase 1</i>	VEGFR1 <i>alias FLT1</i>	Oa04694159_m1	
	NADPH oxidase 2 <i>alias cytochrome b-245 beta chain</i>	NOX2 <i>alias CYBB</i>	Oa04793417_m1	
	Hypoxia inducible factor 1 subunit alpha	HIF1A	Oa04877334_m1	
	Angiopoietin 1	ANGPT1	Oa04757067_m1	

2.6. Histological and immunohistochemical analyses

2.6.1. Tissue fixation, processing, embedding, and sectioning

Tissue was processed and embedded by Monash Histology Platform - Monash Health Translational Precinct (MHP-MHTP) Histology Node.

Briefly, tissue was dehydrated in a series of increasing concentrations of ethanol, transferred to xylene to displace the ethanol, and then infiltrated with paraffin wax (Histokinette, Hendrey Relays and Electrical Equipment Ltd, UK). Processed tissue was mounted in paraffin wax for sectioning. Tissue sections were cut using a rotary microtome (Reichert-Jung Biocut 2030, Leica, Germany) to include PVWM and SCWM for immunohistochemical analyses. Four blocks from each animal were sectioned to represent the frontal, parietal, temporal, and occipital lobes. Sections were cut at 8 μ m thickness, placed in a 40°C waterbath, mounted onto slides (Superfrost plus, Thermo Scientific, Germany), and left to dry in a 37°C oven overnight.

2.6.2. Histological staining

Haematoxylin and eosin (H&E) staining was carried out to visualise gross structures of the brain and neuropathology. Slides were baked at 60°C for 30 min to adhere sections to slides, then immersed in xylene (2 \times 5 min) to remove paraffin wax. Sections were rehydrated in a graded series of ethanol (100%, 100%, 70%) and PBS. Sections were stained with regressive Harris haematoxylin (Amber Scientific, WA, Australia), washed under running tapwater to stop the action of haematoxylin, differentiated in acid ethanol, washed under running tapwater, dipped into Scott's tapwater (1 min) to produce a more pronounced blue stain, counterstained with Eosin (Eosin 1% aqueous solution; Amber Scientific), and washed in water to remove excess reagents. Sections were dehydrated in ethanol of increasing concentrations (70%, 100%, 100%) and xylene. Coverslips were adhered to each slide with DPX mountant (Merck, Darmstadt, Germany) for microscopy.

2.6.3. Immunohistochemistry staining

Slides were baked at 60°C for 30 min to adhere sections to slides, then immersed in xylene (2 \times 5 min) to remove paraffin wax. Sections were rehydrated in a graded series of ethanol (100%, 100%, 70%) and PBS.

Sections were stained with the following primary antibodies: rabbit anti-ionised calcium-binding adapter molecule 1 (Iba-1; 1:1500, WAKO Pure Chemical Industries, Osaka, Japan) to identify microglia, rabbit anti-sheep serum (1:1000, Sigma-Aldrich) to identify vascular leakage, mouse anti-oligodendrocyte transcription factor 2 (Olig2; 1:1000, Merck) to identify cells in the oligodendrocyte

lineage, rat anti-myelin basic protein (MBP; 1:200, Merck) to quantify myelin density, and mouse anti-glial fibrillary acidic protein (GFAP; 1:400, Sigma-Aldrich) to identify astrocytes. Sections were reacted in two batches according to lobes (frontal and parietal, and temporal and occipital) with positive control slides included to allow comparisons of variability. Staining was absent when the primary antibody was omitted. The reagents used are summarised in **Table 2.3**.

Prior to incubation with anti-Iba-1, sections were pre-treated with citric acid buffer (pH 6.0) in a microwave oven at high power for 9 min and power was gradually reduced for the next 7 min to maintain a simmer. Sections were then incubated at room temperature with 0.3% hydrogen peroxide (H_2O_2) in PBS for 20 min to block endogenous peroxidase activity followed by 4% bovine serum album (BSA) in PBS for 30 min to prevent non-specific binding.

Prior to incubation with anti-sheep serum, sections were incubated at room temperature with 3% H_2O_2 in PBS for 20 min to block endogenous peroxidase activity followed by 2% fish gelatin in casein-blocking buffer (CAS-block; Invitrogen, CA, USA) for 90 min to prevent non-specific binding.

Prior to incubation with anti-Olig2, sections were pre-treated with citric acid buffer (pH 6.0) in a microwave oven at high power (3×5 min) to reach boiling temperature. Sections were then incubated at room temperature with 3% H_2O_2 in PBS for 10 min to block endogenous peroxidase activity followed by 5% normal goat serum (NGS) and 1% BSA in PBS with 0.3% Triton-X100 for 60 min to prevent non-specific binding.

Prior to incubation with anti-MBP, sections were pre-treated with citric acid buffer (pH 6.0) in a microwave oven at high power for 9 min and power was gradually reduced for the next 7 min to maintain a simmer. Sections were then incubated at room temperature with 1% H_2O_2 in methanol for 30 min to block endogenous peroxidase activity followed by 3% NGS in PBS for 1 h to prevent non-specific binding.

Prior to incubation with anti-GFAP, sections were pre-treated with citric acid buffer (pH 6.0) in a microwave oven at high power (3×3 min) to reach boiling temperature. Sections were then incubated at room temperature with 0.3% H_2O_2 in 50% methanol for 20 min to block endogenous peroxidase activity followed by 5% NGS in PBS for 30 min to prevent non-specific binding.

Sections were incubated with primary antibody overnight at 4°C . Secondary antibody biotinylated goat anti-rabbit immunoglobulin G (IgG; 1:200, Vector Laboratories, CA, USA), goat anti-mouse IgG (1:200, Vector Laboratories, CA, USA), or goat anti-rat IgG (1:200, Vector Laboratories, CA, USA) were used accordingly and reacted using the Vectastain Elite ABC Kit (avidin-biotin complex; Vector Laboratories, USA). Sections were incubated with diaminobenzidine (DAB) chromogen with H_2O_2

which caused a colour reaction allowing antigens in the tissue to be visualised. Where required, sections reacted with anti-sheep serum and anti-Olig2 were counterstained with 20% haematoxylin (Amber Scientific) to visualise unreacted background for general orientation.

All sections were dehydrated in ethanol of increasing concentrations (70%, 100%, 100%) and xylene. Coverslips were adhered to each slide with DPX mountant (Merck) for microscopy.

Table 2.3. Details of reagents used in immunohistochemical analyses.

Labeling for	Antigen retrieval	Block	1° Antibody			2° Antibody		
			Antibody	Dilution	Source	Antibody	Dilution	Source
Microglia	0.01M Citric acid buffer	1) 0.3% H ₂ O ₂ in PBS 2) 4% BSA in PBS	Rabbit α -Iba-1	1:1500	WAKO ^a 019-19741	Goat anti-rabbit IgG	1:200	Vector ^d BA-1000
Vascular leakage	N/A	1) 3% H ₂ O ₂ in PBS 2) 2% fish gelatin in CAS-block	Rabbit α -sheep serum	1:1000	Sigma-Aldrich ^b S4265	Goat anti-rabbit IgG	1:200	Vector ^d BA-1000
Oligodendrocytes	0.01M Citric acid buffer	1) 3% H ₂ O ₂ in PBS 2) 5% NGS and 1% BSA in 0.3% TX-PBS	Mouse α -Olig2	1:1000	Merck ^c MABN50	Goat anti-mouse IgG	1:200	Vector ^d BA-9200
Myelinating oligodendrocytes	0.01M Citric acid buffer	1) 1% H ₂ O ₂ in 100% methanol 2) 3% NGS in PBS	Rat α -MBP	1:200	Merck ^c MAB395-1ML	Goat anti-rat IgG	1:200	Vector ^d BA-9400
Astrocytes	0.01M Citric acid buffer	1) 0.3% H ₂ O ₂ in 50% methanol 2) 5% NGS in PBS	Mouse α -GFAP	1:400	Sigma-Aldrich ^b G3893	Goat anti-mouse IgG	1:200	Vector ^d BA-9200

BSA bovine serum albumin; *CAS-block* casein blocking buffer; *GFAP* glial fibrillary acidic protein; *H₂O₂* hydrogen peroxide; *Iba-1* ionised calcium-binding adapter molecule 1; *IgG* immunoglobulin G; *MBP* myelin basic protein; *N/A* not applicable; *Olig2* oligodendrocyte transcription factor 2; *PBS* phosphate-buffered saline; *TX* triton X-100;

^a Wako: Wako Pure Chemical Industries, Osaka, Japan

^b Sigma-Aldrich: Sigma-Aldrich, MA, USA

^c Merck: Merck, Darmstadt, Germany

^d Vector: Vector Laboratories, CA, USA

2.6.4. Regions of interest

The PVWM and SCWM regions from four blocks of the right hemisphere of each animal were analysed. The selection of blocks encompasses the frontal, parietal, temporal, and occipital lobes to be representative of the whole brain. Anatomical landmarks were identified using brain atlases, primarily The Sheep Brain Atlas at Michigan State University.¹⁹² For this thesis, regions of interest were sampled as follows [Fig. 2.5]:

The frontal block was the first block rostral to the ansate sulcus, at the level of the anterior horn of the lateral ventricle, corresponding to sections 520-560 in The Sheep Brain Atlas at Michigan State University.¹⁹² The frontal PVWM was bounded by the apex of the lateral ventricle and the depth of the diagonal, ectomarginal, and cingulate sulci.¹⁹³ This region comprises both the medial and lateral PVWM and excludes the subventricular zone.¹⁹³

The parietal block was 1-2 blocks caudal to the ansate sulcus, at the level of the body of the lateral ventricle and somatosensory cortices, corresponding to sections 840-880 in The Sheep Brain Atlas at Michigan State University.¹⁹² The parietal PVWM was bounded by the apex of the lateral ventricle and the depth of the diagonal, ectomarginal, and cingulate sulci.¹⁹³ This region comprises both the medial and lateral PVWM and excludes the subventricular zone.¹⁹³

The temporal lobe of sheep is relatively small and not easily differentiated from the frontal and parietal lobes due to the absence of a defined sylvian fissure. Blocks at the level of the hippocampal formation that include the temporal lobe, corresponding to blocks 1080-1200 in The Sheep Brain Atlas at Michigan State University,¹⁹² were considered representative of that section of the brain and are referred to as the 'temporal' region in this thesis. The temporal PVWM was bounded by the lateral aspect of the lateral ventricle to the temporal horn.

The occipital block was 1-2 blocks at the caudal end of the left hemisphere, beyond the posterior horn of the lateral ventricle. This block was analysed for SCWM only.

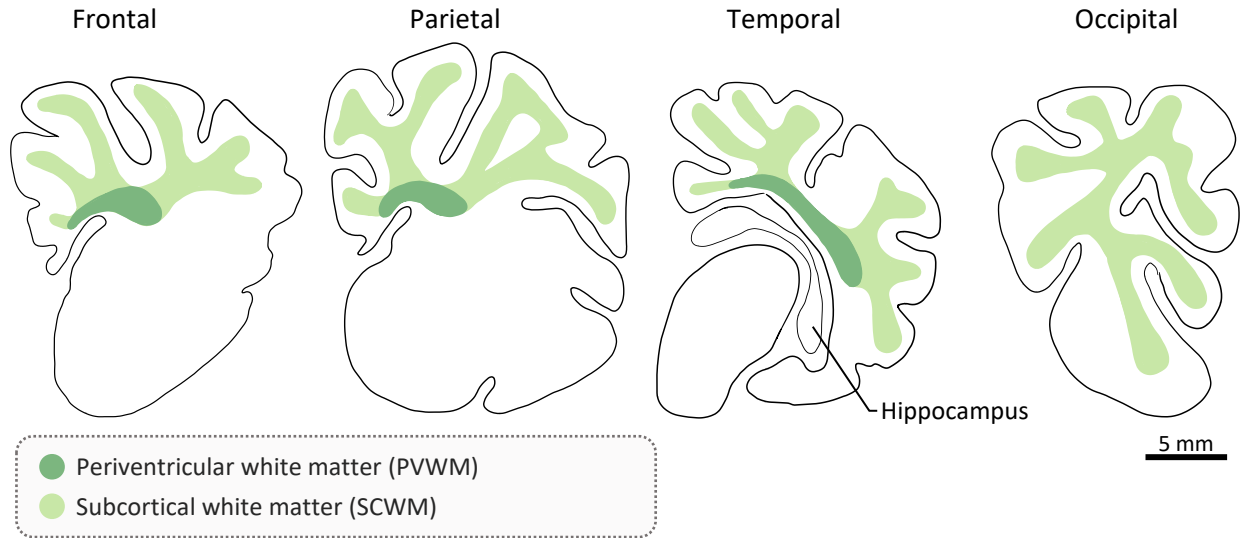


Figure 2.5. Regions in the right hemisphere of the preterm lamb brain for immunohistochemical analysis. Illustration of the total white matter area for immunohistochemical analysis (green), and the boundaries of the PVWM region (dark green) and SCWM region (light green) in the frontal, parietal, temporal, and occipital lobes of the preterm lamb brain. Scale bar = 5mm.

2.6.5. Quantitative analyses

2.6.5.1. Haematoxylin and Eosin

Sections were viewed under the microscope (BX-41 Laboratory Microscope, Olympus Corporation, Tokyo, Japan) and scored according to the presence of cystic lesions/parenchymal damage, compromised vessel integrity, hypercellularity in the PVWM and SCWM, and disrupted cytoarchitecture in the cortex. Each category was scored on a scale of 0-2 based on severity and a mean of all categories was calculated as a final score for each section. A mean of all lobes was calculated for each animal and then collectively averaged for each experimental group.

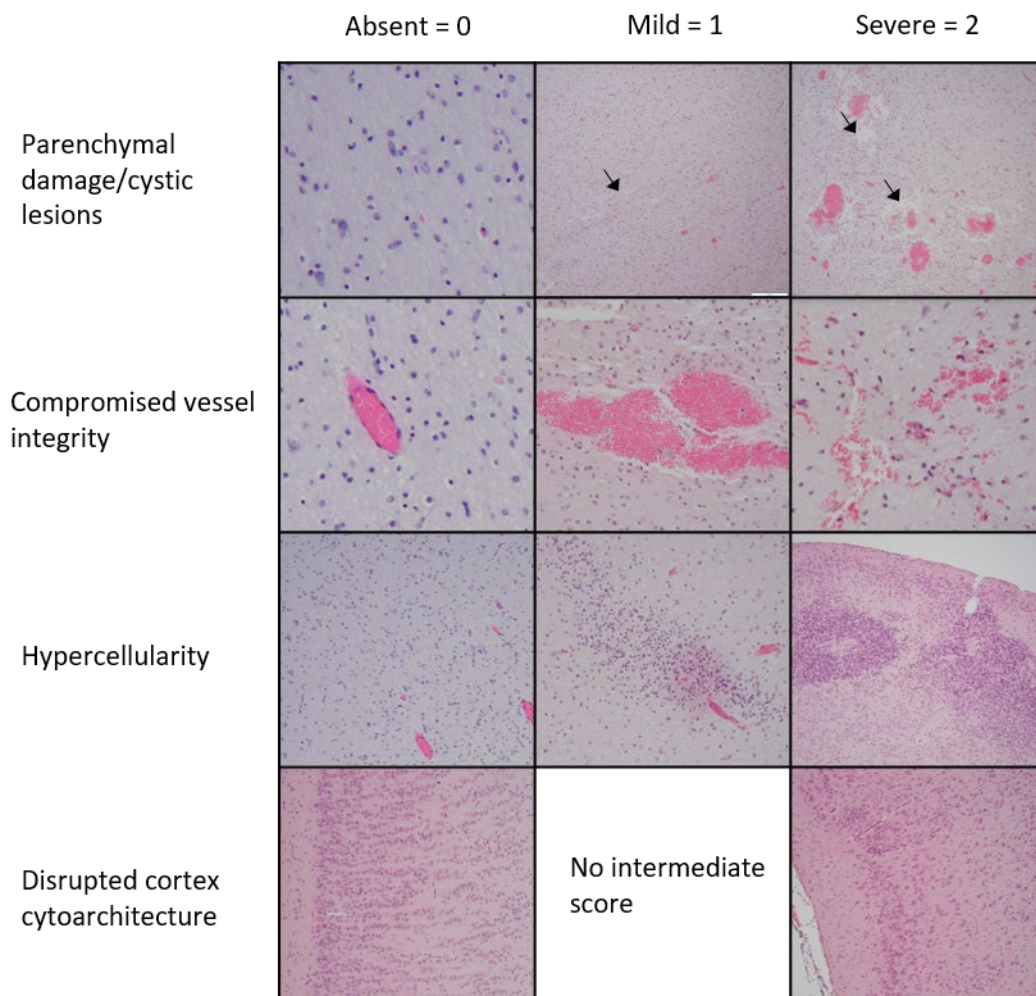


Figure 2.6. Scoring rubric of haematoxylin and eosin staining. Brain sections were scored for severity of the presence of cystic lesions/parenchymal damage, compromised vessel integrity, hypercellularity in the PVWM and SCWM, and disrupted cytoarchitecture in the cortex.

2.6.5.2. Ionised calcium-binding adapter molecule-1 (Iba-1)

Iba-1 is expressed in macrophages of monocytic lineage.¹⁹⁴ Among cell types in the central nervous system, Iba-1 is expressed by microglia and its expression is upregulated in reactive microglia.¹⁹⁴ Slides were scanned by Monash Histology using an eSlide capturing device (Aperio Scanscope AT Turbo; Aperio Technologies, CA, USA). The area of Iba-1 positive microglial aggregations within the PVWM and SCWM of each section was assessed using ImageScope (Aperio Technologies). For each section, aggregation areas were summed and divided by the total area of PVWM or SCMW of the section, data expressed as a percentage (%). The fraction areal coverage of Iba-1 immunoreactivity within an aggregation was assessed using a set intensity threshold with Fiji is Just ImageJ (FIJI; ImageJ, NIH Image, MD, USA).

Areal density (cells/mm²) of Iba-1 positive microglia was quantified in three non-overlapping FOV in the PVWM and six non-overlapping FOV from two separate gyri in the SCWM, avoiding microglial aggregations, using ImageScope (Aperio Technologies); n=9 FOV per section, FOV=0.14 mm². Microglia were distinguished based on morphology (ramified microglia were characterised by long cellular processes while amoeboid microglia by round, densely stained soma with resorbed processes).¹⁹⁵ The ratio of amoeboid-to-total microglia was determined and expressed as a percentage (%).

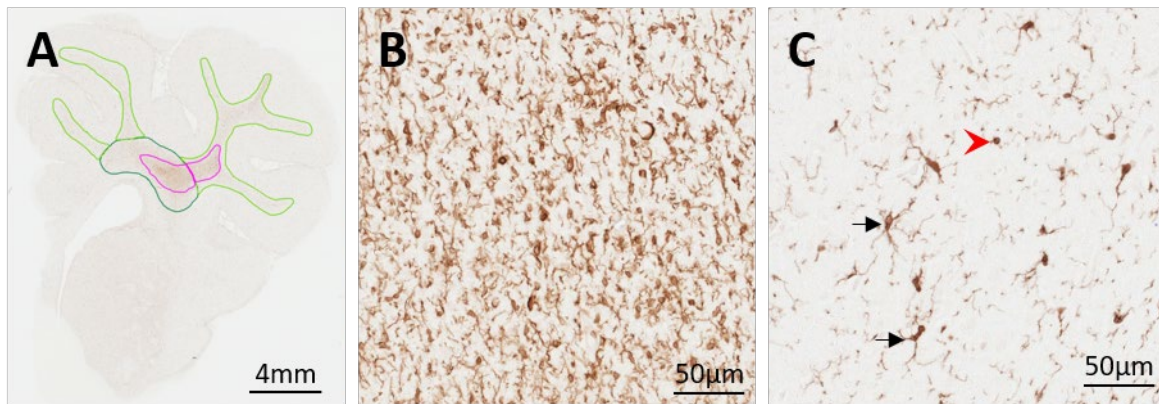


Figure 2.7. Representative images of Iba-1 immunoreactivity. (A) The area of Iba-1 positive microglial aggregations was assessed within the white matter. Iba-1 positive microglial aggregations were traced on brain sections. The number of Iba-1 positive microglial aggregations (purple outline) were quantified. The percentage area within the PVWM (dark green outline) and SCWM (light green outline) occupied by the microglia were quantified. Scale bar = 4mm. (B) Microglia density within each aggregation was quantified as a fraction areal coverage (%) using a set intensity threshold. (C) The number of ramified microglia (black arrow) and amoeboid microglia (red arrowhead) were quantified in white matter regions away from the microglia aggregations. Scale bar = 50µm.

2.6.5.3. Sheep serum

The anti-sheep serum antibody detects proteins within serum, the most abundant being albumin, which cannot readily cross the blood-brain barrier (BBB) due to their large size. Thus, the presence of such proteins outside the vasculature may indicate a disruption of the endothelial cell membrane and compromised BBB integrity.¹⁹⁶ Slides were viewed under the microscope (BX-41 Laboratory Microscope, Olympus Corporation). The entire WM area was scanned under the microscope and blood vessel profiles with protein extravasation were quantified and expressed as total number of vessel profiles with protein extravasation within the PVWM and SCWM.

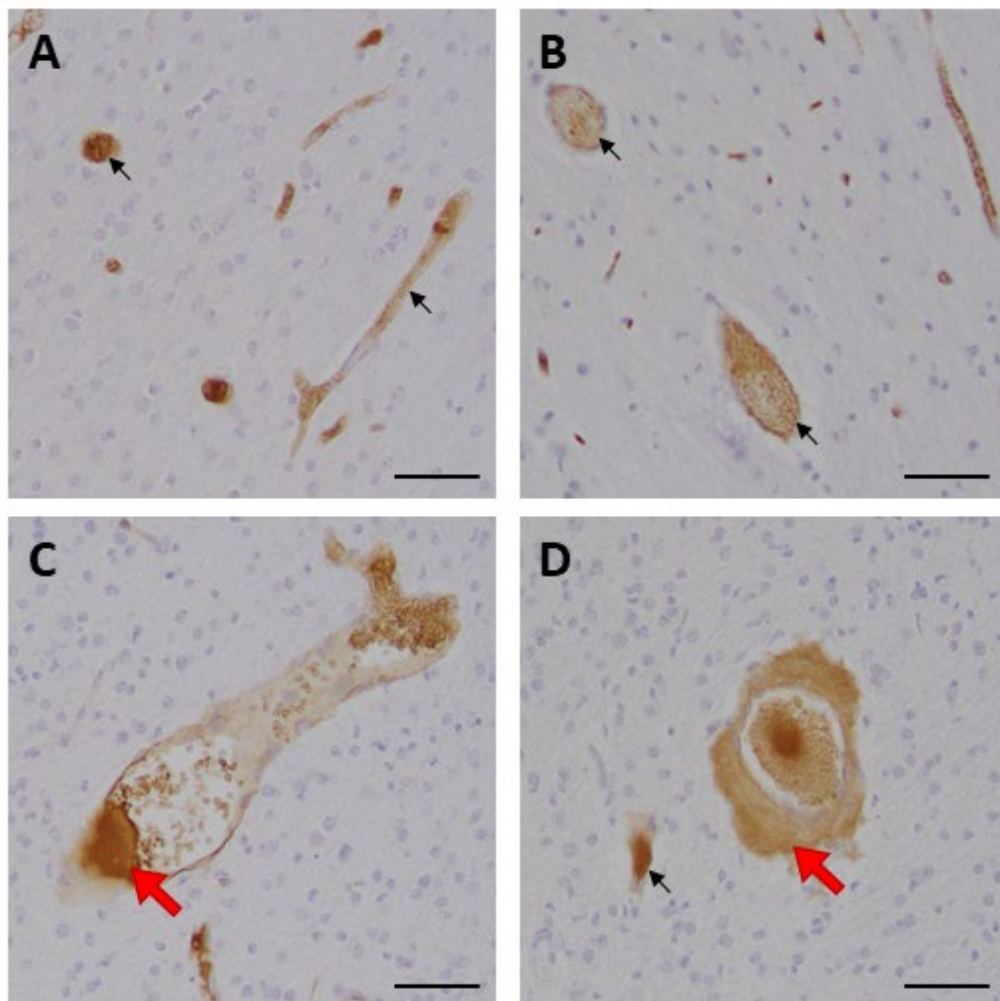


Figure 2.8. Representative images of sheep serum immunoreactivity. (A-D) The number of vessel profiles with protein extravasation and disrupted epithelium (red arrows) were quantified. Black arrows indicate intact vessel profiles. Sections were counterstained with haematoxylin for general tissue orientation. Scale bar = 50 μ m.

2.6.5.4. Oligodendrocyte transcription factor (Olig2)

Olig2 is a pan-oligodendrocyte marker that identifies all cells present in the oligodendrocyte lineage.^{43,197} Slides were viewed and imaged under the microscope with a mounted camera (BX-41 Laboratory Microscope, Olympus Corporation). Areal density (cells/mm²) of Olig2-positive cells was quantified in three non-overlapping FOV in the PVWM and six non-overlapping fields from two separate gyri in the SCWM using FIJI (ImageJ); n=9 FOV per section, FOV=0.14mm².

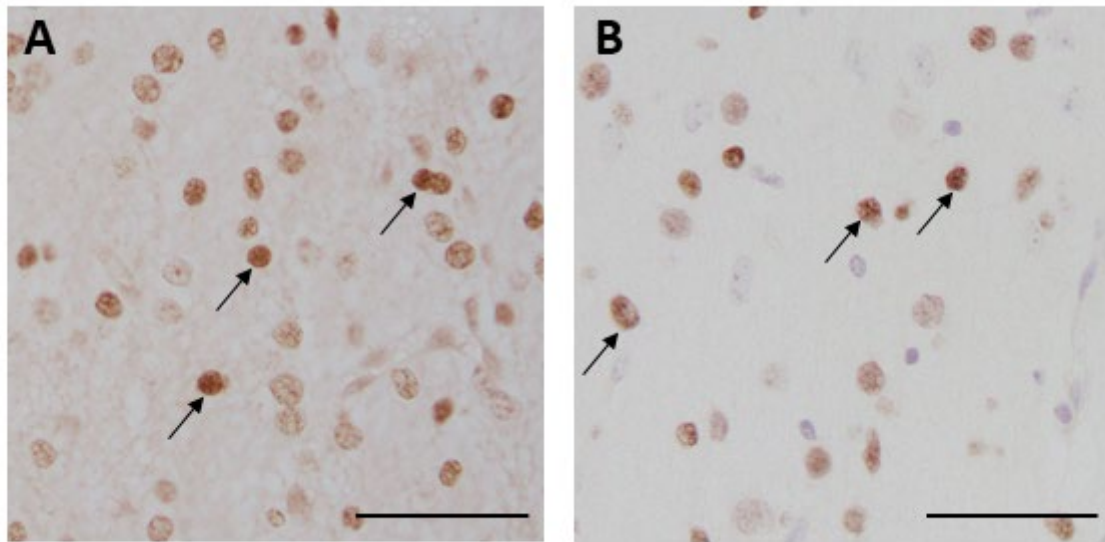


Figure 2.9. Representative images of Olig2 immunoreactivity. The areal density of Olig2-positive cells (arrows) was quantified in **(A)** sections without counterstain, as used in Chapters 3 and 4 and **(B)** sections counterstained with haematoxylin (purple cells in the background) for general tissue orientation, as used in Chapter 5. Scale bar = 50µm.

2.6.5.5. Myelin basic protein (MBP)

MBP, a membrane-associated protein that constitutes myelin, was used as a marker for myelinating oligodendrocytes.^{43,198} Slides were viewed and imaged under the microscope with a mounted camera (BX-41 Laboratory Microscope, Olympus Corporation). Images were taken from three non-overlapping FOV in the PVWM and six non-overlapping fields from two separate gyri in the SCWM, from the frontal lobe section only; n=9 FOV per section, FOV=0.14mm². The areal coverage of MBP immunoreactivity within these FOV was assessed using a set intensity threshold with FIJI (ImageJ).

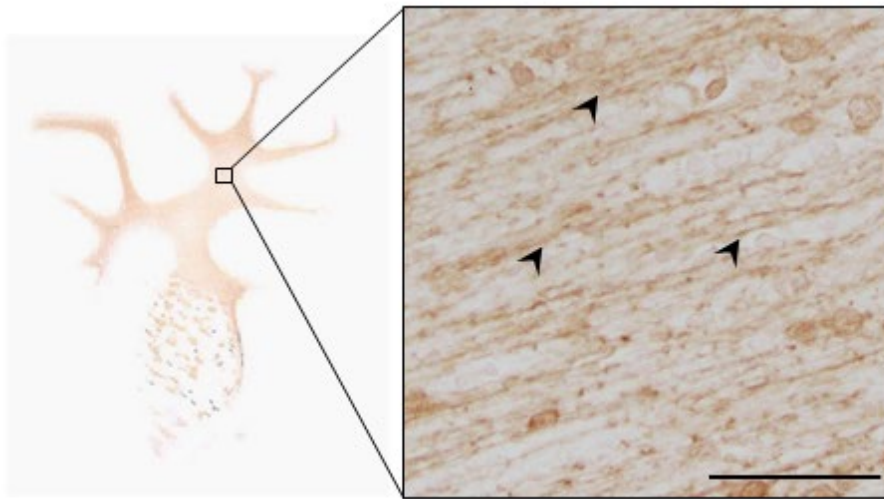


Figure 2.10. Representative images of MBP immunoreactivity. The area occupied by myelinated fibers (arrows) was quantified using a set intensity threshold. Scale bar = 50μm.

2.6.5.6. Glial fibrillary acid protein (GFAP)

GFAP is a marker of astrocytes, expressed predominantly in the main astrocytic processes.³⁹ GFAP expression is upregulated in reactive astrogliosis.³⁹ Slides were scanned by Monash Histology using an eSlide capturing device (Aperio Scanscope AT Turbo; Aperio Technologies). Images of three non-overlapping FOV in the PVWM and six non-overlapping FOV from two separate gyri in the SCWM were taken (Aperio Imagescope) for quantification of the area coverage of GFAP-positive astrocytes, data expressed as a percentage (FIJI; ImageJ); $n=9$ FOV per section, $FOV=0.14\text{mm}^2$.

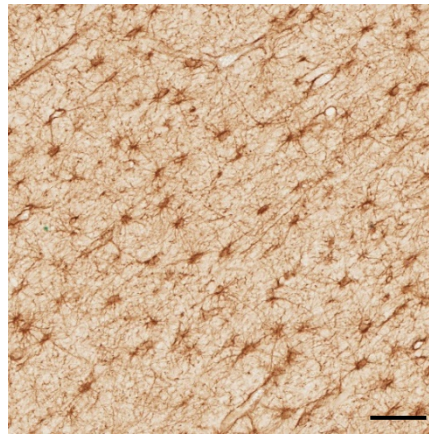


Figure 2.11. Representative image of GFAP immunoreactivity. The area occupied by astrocyte cell bodies and processes was quantified using a set intensity threshold. Scale bar = $50\mu\text{m}$.

2.7. Statistical analyses

Fetal characteristics data were analysed using a one-way analysis of variance (ANOVA; Chapters 3 and 4; Graphpad Prism 8.1.2; GraphPad Software, CA, USA) or independent T-test (Chapter 5; Graphpad Prism 8.1.2). Data are presented as mean \pm standard deviation (SD).

Serial physiological and molecular (ELISA) data were analysed using a two-way repeated measures ANOVA with *post hoc* Holm-Sidak test to compare indices between groups and over time (Sigmaplot; Systat Software Inc., CA, USA).

The statistical tests used for molecular (qPCR) and immunohistochemical data varied between chapters. All data were assessed with the Shapiro-Wilk Test for normality, then compared using either a one-way ANOVA with *post hoc* Holm-Sidak test (≥ 3 groups, parametric), Kruskal-Wallis Test with *post hoc* Dunn's Test (≥ 3 groups, non-parametric), independent T-Test (2 groups, parametric), or Mann-Whitney U Test (2 groups, non-parametric) (Graphpad Prism 8.1.2).

Statistical significance was accepted at $p < 0.05$. Data are presented as mean \pm standard error of the mean (SEM) unless otherwise stated.

Chapter Three: Isolating Pathways of Acute VIBI

In this study, I sought to examine the pathways of brain injury following acute injurious ventilation in preterm lambs. I utilised the head-out ventilation model described in Chapter 2 (Section 2.2). Briefly, the fetus is partially exteriorised, injuriously ventilated, returned to the uterus, and brain injury is examined 24 h later. Returning the fetus to the uterus, where it is supported by placental circulation, removes the need for subsequent ventilation to sustain the animal, as in postnatal studies. This allows the injury and mechanisms from the initial injurious ventilation period to be studied in isolation, without the influence of prolonged ventilation.

The findings in this chapter are incremental to results from the imaging aspect of this study, which have been published and are provided in Appendix II.

3.1. Introduction

Preterm infants (<37 completed weeks gestation) are at high risk of brain injury during or soon after birth, leading to life-long morbidities including the motor deficit cerebral palsy (CP).¹⁹⁹ There is an urgent need to investigate and address the causes of brain injury to improve neurodevelopmental outcomes of preterm infants. The initiation of positive pressure ventilation (PPV) in the delivery room is often poorly controlled⁸⁷ and has been associated with haemorrhagic and diffuse white matter injury^{97,98} collectively termed ventilation-induced brain injury (VIBI). The major pathways of acute VIBI have been identified as cerebral inflammation and haemodynamic instability,⁹⁶ consistent with the main causes of preterm brain injury.²⁰⁰

The inflammatory pathway of VIBI is postulated to be a downstream consequence of ventilation-induced lung injury.⁹⁶ In the delivery room, inadvertent excessive tidal volume (V_T ; volutrauma) applied during PPV initiates a profound pulmonary inflammatory response. This triggers systemic and subsequently cerebral inflammation, characterised by upregulation of pro-inflammatory cytokines messenger ribonucleic acid (mRNA) levels (e.g. interleukin 6 [*IL6*] and interleukin 8 [*IL8*]) and activation of glial cells, predominantly within the white matter of the preterm brain.^{96,110,133,135} An altered microenvironment and the activation of microglia and astrocytes contribute to the loss of cells in the oligodendrocyte lineage and failure to mature towards myelinating cells, which in turn contributes to hypomyelination and diffuse white matter injury that can underlie long-term neurological sequelae such as CP.^{9,201}

The haemodynamic pathway of VIBI refers to irregular variations in pulmonary blood flow and, as a result, instability of left ventricular output and subsequently cerebral blood flow (CBF).^{80,110} During PPV, pressure applied into the airways compresses alveolar capillaries, altering pulmonary blood flow, pulmonary venous return and hence cardiac output.¹¹⁰ While arterial blood pressure variability within a physiological range is usually compensated by pressure flow cerebral autoregulation to sustain a stable CBF, this is not always the case in preterm infants.^{9,55,116} The autoregulatory plateau of preterm infants is suggested to be narrower and longer, in part due to underdeveloped cerebral vasculature.^{55,116} CBF fluctuations for a period longer than 10 to 20 s constitutes cerebral haemodynamic instability.¹¹³ Cerebral haemodynamic instability increases the risk of haemorrhagic injury such as intraventricular haemorrhage which, even at lower grades and in the absence of detectable white matter injury, has been associated with poor neurodevelopmental outcomes in preterm infants.^{9,14}

Despite having identified the two major pathways of VIBI, little is known about the relative contributions of each pathway and this has hindered development of targeted therapies. Our group has recently reported, based on diffusion tensor imaging (DTI) analysis, that the haemodynamic pathway has an additive effect on the inflammatory pathway on injury progression.¹¹¹ In the current study, I aimed to examine molecular and immunohistochemical indices of inflammation and injury in cerebral white matter. I hypothesised that white matter injury in preterm lambs exposed to both inflammatory and haemodynamic instability pathways of injury would be worse than that of lambs exposed to the inflammatory pathway alone. Furthermore, previous studies have evaluated acute VIBI only to 2 h after the initiation of injurious ventilation.^{96,110,133,135} In this study, I also aimed to evaluate if these initial changes in neuroinflammatory cell populations persist or progress to 24 h.

3.2. Methods

The detailed experimental methodology used in this study is provided in Chapter 2. Below is a concise overview. Experimental procedures were approved by the Monash Medical Centre Animal Ethics Committee A, Monash University, and were conducted in accordance with guidelines established by the National Health and Medical Research Council of Australia.

Animals were randomised to one of four groups:

- 1) Unoperated control (**UNOP**; n=7): Lambs did not undergo fetal surgery or ventilation and were used to control for the surgical intervention.
- 2) Sham surgery control (**SHAM**; n=5): Lambs underwent fetal surgery, were instrumented and intubated, but did not receive mechanical ventilation to control for the experimental intervention.

- 3) Injurious ventilation (**INJ_{INF}**; n=7): Lambs received 15 min of high V_T ventilation, with intact placental circulation, to initiate predominantly the inflammatory pathway of VIBI.
- 4) Injurious ventilation with umbilical cord occluded (**INJ_{INF+HAE}**; n=7): Lambs received 15 min of high V_T ventilation during which the umbilical cord was occluded. The removal of the placental circulation simulates umbilical cord clamping, critical for initiating the haemodynamic pathway of VIBI in addition to the inflammatory pathway.

3.2.1. Instrumentation and injurious ventilation strategy

Anaesthesia was induced in pregnant ewes at 125 ± 1 days gestation (mean \pm SD; term ~148 days) by intravenous injection of thiopentone sodium (20 mg/kg; Jurox, NSW, Australia). Ewes were then intubated with an endotracheal tube (ID 8.0 mm; Smiths Medical, MN, USA) and maintained on an inhalational anaesthetic (isoflurane 1.5-2.5% in oxygenated air; Bomac Animal Health, NSW, Australia). A midline laparotomy was performed to expose the uterus. The head and neck of the fetus were exteriorised for introduction of polyvinyl catheters (ID 0.86 mm, OD 1.52 mm; Dural Plastics & Engineering, NSW, Australia) into the left carotid artery and jugular vein. An ultrasonic flow probe (3PS; Transonic Systems, NY, USA) was placed around the right carotid artery to monitor carotid blood flow. The fetal chest was exteriorised and the fetus was intubated with a cuffed endotracheal tube (ID 4.0-4.5 mm; Smiths Medical) and lung liquid was passively drained. SHAM animals remained intubated and exteriorised for 15 min without mechanical ventilation.

Ventilation was conducted under sterile conditions using a neonatal positive pressure ventilator (Babylog 8000+, Dräger, Lübeck, Germany) as described previously.¹¹¹ Briefly, the exteriorised fetus was ventilated for 15 min with a high V_T strategy targeting 12-15 ml/kg known to cause ventilation-induced brain pathology.^{110,133,134} **INJ_{INF+HAE}** animals were ventilated with the umbilical cord occluder inflated with saline to remove placental circulation and to simulate cardiovascular instability following umbilical cord clamping. The occluder cuff was deflated and removed at the end of the 15 min injurious ventilation and placental blood flow was restored to the fetus.

After the 15 min of ventilation, the carotid flow probe was removed, and the fetus was extubated and returned to the uterus. The fetal jugular vein and carotid artery catheters were externalised through the ewe's flank via a small incision to allow periodic blood sampling. All incision sites were sutured closed and the ewe and fetus were allowed to recover. Analgesia was provided to the ewe via buprenorphine (0.3 mg i.m.; Temgesic; Reckitt Benckiser, UK) and a transdermal fentanyl patch (75µg/h; Janssen-Cilag, NSW, Australia) for post-surgery pain relief. At regular intervals over the subsequent 24 h, fetal arterial blood was sampled (ABL80 FLEX; Radiometer Medical ApS, Denmark) to ensure fetal wellbeing and collected in heparin tubes for plasma cytokine analysis.

3.2.2. Lamb delivery and subsequent monitoring

At 24 h post-ventilation, ewes were anaesthetised as above, and the fetus was exteriorised via the same incision site. A transcutaneous oximeter (Masimo, CA, USA) was attached to the fetal tail to monitor oxygen saturation level and heart rate. UNOP lambs were instrumented with arterial and venous polyvinyl catheters prior to delivery.

All lambs were dried, intubated, and stabilised with a gentle ventilation strategy (Babylog 8000+, Dräger). Ventilation was initiated in volume-guarantee mode set at 7 ml/kg, maximum peak inspiratory pressure (PIP) 40 cmH₂O, positive end expiratory pressure (PEEP) 5 cmH₂O, inspiratory time 0.6 s, and expiratory time 0.6 s. Fraction of inspired oxygen (FiO₂) was set initially at 0.4 but adjusted accordingly to maintain arterial oxygen saturation (SaO₂) between 88-95% and partial pressure of carbon dioxide (PaCO₂) between 45-55 mmHg. Intratracheal surfactant (240 mg; Curosurf®; Chiesi Pharmaceuticals, Parma, Italy) was administered within the first 10 min of ventilation onset to improve lung compliance. Sustained inflations at 35 cmH₂O for 5 s durations were applied to recruit the lung if necessary.

Once the lambs were stabilised (within 15 min of ventilation onset), the umbilical cord was clamped and the lambs were placed on a magnetic resonance imaging (MRI)-compatible ventilator (Pneupac® babyPAC™; Smiths Medical, UK). The MRI acquisition protocol has previously been reported¹¹¹ and is not the focus of this study, although the paper is included as Appendix II in this thesis and I will reflect on these results in the discussion of this chapter. Lambs were euthanised (sodium pentobarbitone >100 mg i.v.; Valabarb; Jurox, NSW, Australia) for tissue collection after MRI scanning (total acquisition time 40 min). Ewes were euthanised (as above) immediately after delivery of the lambs.

3.2.3. Brain collection

At autopsy, the brain was removed from the skull and the cerebrum halved along the medial longitudinal fissure. The periventricular and subcortical white matter (PVWM; SCWM) were dissected from the left cerebral hemisphere and snap-frozen in liquid nitrogen. The right cerebral hemisphere was immersion fixed in 10% neutral buffered formalin (NBF; Amber Scientific, WA, Australia) overnight. The right hemisphere was then cut coronally into 5 mm blocks (8-9 blocks/animal), post-fixed in 10% NBF for 6 days, processed, and paraffin-embedded. Serial sections (8 µm) were cut from one block each at the level of frontal, parietal, temporal, and occipital lobes for immunohistochemical analysis.

3.2.4. Reverse-transcription real-time quantitative PCR

Tissue from the PVWM and SCWM of the left hemisphere were separately homogenised, and RNA from each region was extracted (RNeasy Midi RNA Extraction Kit; Qiagen, VIC, Australia) and reverse-transcribed into cDNA (SuperScript® III First-Strand Synthesis System for RT-PCR kit; Invitrogen). Genes of interest were measured by quantitative PCR using the Fluidigm Biomark™ HD system (Fluidigm Corporation, CA, USA). Relative mRNA expression of key inflammatory interleukins (IL 1 alpha [*IL1A*], IL 1 beta [*IL1B*], *IL6*, tumour necrosis factor [*TNF*]), tight junction proteins (occludin [*OCLN*], claudin 1 [*CLDN1*]), and markers of cell death (p53 [*P53*] and caspase 3 [*CASP3*]) were measured. Samples were run in quadruplicates and the average was taken. The expression of all genes was normalised to ribosomal protein S18 (*RPS18*) expression using the $2^{-\Delta\Delta C_t}$ method for each sample, expressed relative to the UNOP group.

3.2.5. Immunohistochemistry

Coronal sections from comparable sites of the frontal, parietal, temporal, and occipital lobes (4 slides/animal) were stained with rabbit anti-ionised calcium binding adapter molecule-1 (Iba-1; 1:1500, Wako Pure Chemical Industries, Osaka, Japan) to identify microglia, rabbit anti-sheep serum (1:1000, Sigma-Aldrich, MO, USA) to identify vascular extravasation of protein, mouse anti-oligodendrocyte transcription factor-2 (Olig2; 1:1000, Merck, Darmstadt, Germany) for oligodendrocytes, rat anti-myelin basic protein (MBP; 1:200; Merck) to quantify myelin density, and mouse anti-gial fibrillary acidic protein (GFAP; 1:400, Sigma-Aldrich) to identify astrocytes. Prior to incubation with anti-Iba-1, anti-Olig2, anti-MBP, and anti-GFAP, sections were pre-treated with citrate buffer (pH 6.0) in a microwave oven. Sections were incubated with secondary antibody biotinylated goat anti-rabbit, goat anti-mouse, or goat anti-rat immunoglobulin G (IgG; 1:200; Vector Laboratories, CA, USA) and reacted using the Vectastain Elite ABC Kit (Vector Laboratories). Sections reacted with anti-sheep serum were counterstained with 20% haematoxylin. Staining was absent when the primary antibody was omitted.

3.2.6. Quantitative immunohistochemical analysis

Analyses were conducted at equivalent sites within the cerebral white matter of sections from the frontal, parietal, temporal, and occipital lobes of each lamb. Non-overlapping fields of view in the PVWM were taken medial to lateral from the ventricle, and fields in the SCWM were obtained from alternating gyri starting from the second gyrus closest to the midline. For all indices, a mean of all lobes was calculated for each animal and then collectively averaged for each treatment group. Slides were coded and the observer (KC) was blinded to the treatment.

The proportion of PVWM and SCWM occupied by Iba-1-positive microglial aggregations was assessed using ImageScope (Aperio Technologies, CA, USA); individual aggregation areas were summed then divided by the total area of PVWM or SCWM of the section, data expressed as a percentage. The fraction areal coverage (%) of Iba-1 immunoreactivity within an aggregation was assessed using a set intensity threshold (FIJI; ImageJ, NIH Image, MD, USA).

Areal density (cells/mm²) of Iba-1-positive microglia were quantified in 3 non-overlapping fields in the PVWM and 6 non-overlapping fields in the SCWM from 2 separate gyri, avoiding microglial aggregations, using ImageScope (Aperio Technologies). Microglia were distinguished based on morphology (ramified microglia were characterised by long cellular processes while amoeboid microglia by round, densely stained soma with resorbed processes).¹⁹⁵

Areal density (cells/mm²) of Olig2-positive oligodendrocytes were quantified in 3 non-overlapping fields in the PVWM and 6 non-overlapping fields in the SCWM from 2 separate gyri, using FIJI (ImageJ).

Blood vessel profiles with protein extravasation were quantified and expressed as total number of vessel profiles with protein extravasation within the PVWM and SCWM.

Area coverage (%) of MBP immunoreactivity (myelin) and GFAP immunoreactivity (astrocytes) were assessed in 3 non-overlapping fields in the PVWM and 6 non-overlapping fields in the SCWM from 2 separate gyri from the frontal lobe sections only, using a set intensity threshold (FIJI). For assessments in the frontal lobe only, a mean was calculated for each treatment group.

3.2.7. Plasma protein analysis

Arterial blood was collected via the fetal carotid artery catheter before injurious ventilation (T=0), at the end of injurious ventilation (15 min), and post-surgery until delivery (1 h, 3 h, 6 h, 12 h, 24 h). Plasma proteins (IL-6 and IL-8) were quantified using a sandwich enzyme-linked immunosorbent assay (ELISA). 96-well flat-bottom plates (Nunc Maxisorp™; Thermo Fisher Scientific, MA, USA) were coated with mouse anti-ovine IL-6 (1:200, Bio-Rad Laboratories, CA, USA) or mouse anti-ovine IL-8 (1:1000, Bio-Rad) antibodies and incubated overnight at 4°C. The next day, plasma samples were diluted with an equal part of diluting buffer (PBS, 0.1% BSA, 0.05% Tween 20) and incubated in duplicates in the 96-well plates for 1 h at room temperature. After washing, the plates were incubated with respective detecting antibodies (rabbit anti-ovine IL-6, 1:200, Bio-Rad; rabbit anti-ovine IL-6, 1:4000, Bio-Rad) for 1 h at room temperature, washed, then incubated with horse radish peroxidase(HRP)-conjugated swine anti-rabbit Ig (1:2000, DAKO, CA, USA) for 1 h at room temperature. After further washing, plates were developed with 3,3', 5,5'-tetramethylbenzidine (TMB

chromogen solution; Invitrogen, CA, USA) for 20 min in the dark at room temperature. Reactions were stopped with the addition of 0.5M H₂SO₄. The plates were read on a SpectraMax i3 microplate reader (Molecular Devices, CA, USA) at 450 nm to determine optical density. Standards (recombinant ovine IL-6 or IL-8; Kingfisher Biotech, MN, USA) were included and a standard curve was generated for every ELISA plate used ($R^2 > 0.99$ for all).

3.2.8. Statistical analysis

Fetal parameters, PCR, and immunohistochemical data were compared using one-way analysis of variance with Holm-Sidak *post hoc* comparison (ANOVA; Graphpad Prism 8.1.2; GraphPad Software, CA, USA). Blood gas, physiological, and ELISA data were compared using two-way repeated measures ANOVA with Holm-Sidak *post hoc* comparison (SigmaPlot; Systat Software Inc., CA, USA). Statistical significance was accepted at $p < 0.05$. Baseline physiological data are presented as mean \pm SD to convey variability in the study cohort. All other data are presented as mean \pm SEM unless otherwise stated.

3.3. Results

3.3.1. Physiological parameters

Blood gas parameters at surgery for all groups (except UNOP) were not different between groups [Table 3.1]. Blood gas parameters during injurious ventilation and over the recovery period up to 24 h were not different between groups [Fig. 3.1]. Physiological parameters after delivery, during the MRI examination, have previously been reported.¹¹¹ Lamb characteristics, including body and brain weights, recorded post-mortem were not different between groups [Table 3.1].

Table 3.1. Lamb characteristics and baseline arterial blood gas parameters. Lamb characteristics at the end of the experiment and fetal arterial blood gas parameters at the start of the experiment were not different between groups. Blood gas parameters were taken before any interventions (i.e. before sterile fetal surgery for all groups except UNOP before delivery). Data are presented as mean \pm SD.

	UNOP	SHAM	INJ _{INF}	INJ _{INF+HAE}
Group characteristics				
Number (n=)	7	5	7	7
Gestational age (d)	126 \pm 1	126 \pm 1	126 \pm 1	126 \pm 1
Sex (% male)	85.7	60.0	71.4	14.3
Birth order 1 st (ratio)	6:1	4:1	7:0	7:0
Body weight (kg)	3.4 \pm 0.4	3.3 \pm 0.2	3.4 \pm 0.5	3.2 \pm 0.4
Brain weight (g)	45.6 \pm 2.6	46.0 \pm 2.5	46.3 \pm 2.4	45.9 \pm 4.2
Arterial blood gas parameters				
pH	7.27 \pm 0.03	7.27 \pm 0.04	7.25 \pm 0.05	7.24 \pm 0.04
PaCO ₂ (mmHg)	59.0 \pm 7.8	64.0 \pm 12.9	57.3 \pm 7.7	63.9 \pm 6.9
PaO ₂ (mmHg)	36.7 \pm 17.7	33.0 \pm 4.8	43.2 \pm 9.9	34.8 \pm 5.3
SaO ₂ (%)	48.2 \pm 23.1	46.4 \pm 12.7	62.6 \pm 11.9	53.6 \pm 19.4

PaCO₂ partial pressure of carbon dioxide; *PaO₂* partial pressure of oxygen; *SaO₂* oxygen saturation.

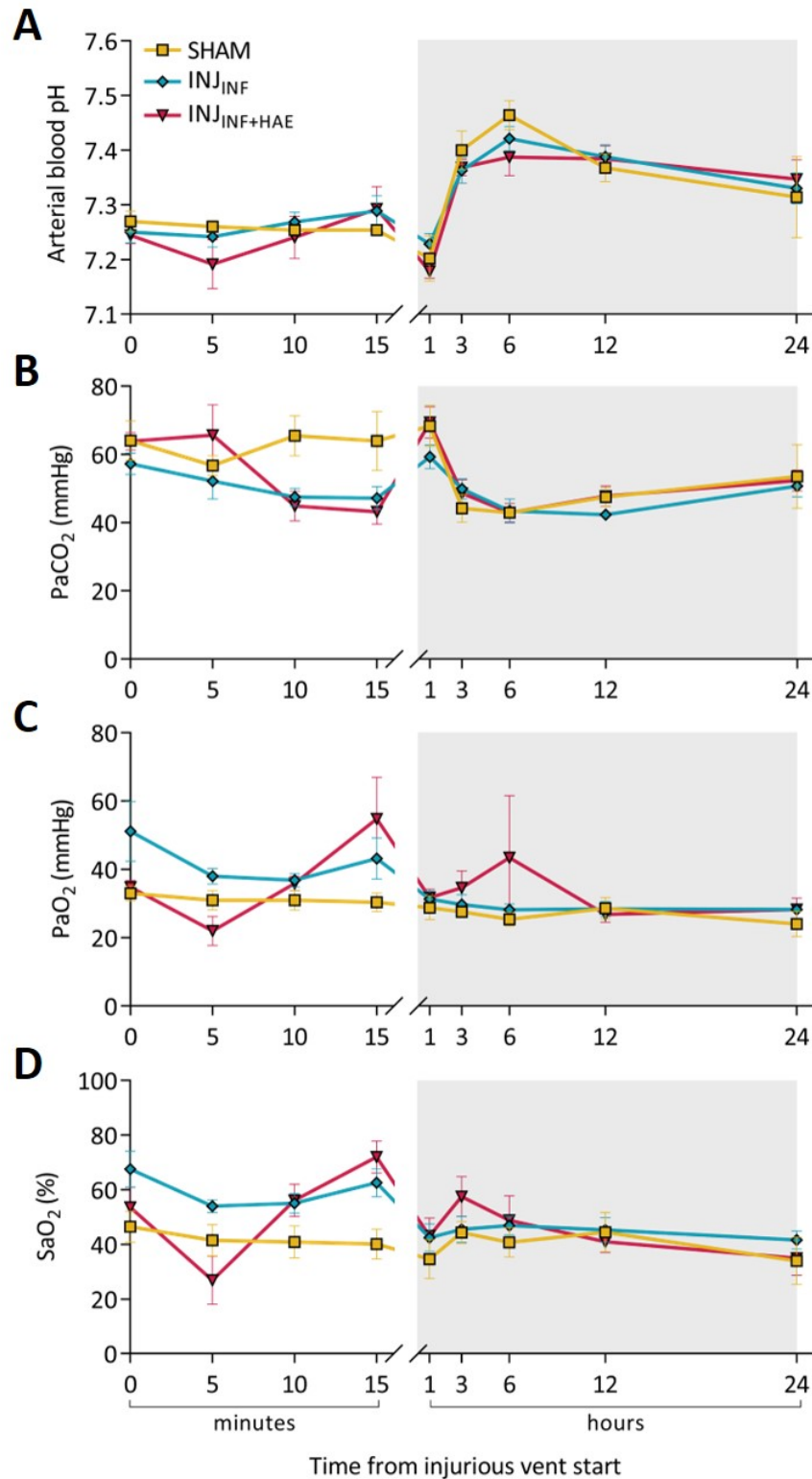


Figure 3.1. Arterial blood gas parameters during the injurious ventilation and recovery periods. (A) pH, **(B)** partial pressure of carbon dioxide (PaCO₂), **(C)** partial pressure of oxygen (PaO₂), and **(D)** oxygen saturation level (SaO₂) at specified time points after commencement of injurious ventilation were not different between SHAM (yellow), INJ_{INF} (blue), and INJ_{INF+HAE} (red) animals. Data presented as mean \pm SEM.

3.3.2. Injurious ventilation and carotid blood flow

V_T increased in both groups over the 15 min duration but failed to reach the target range of 12-15 ml/kg [Fig. 3.2A]. V_T was significantly higher in the INJ_{INF+HAE} group compared to the INJ_{INF} group at 5 min ($p=0.014$) but was not different thereafter. At 15 min, V_T was 8.3 ± 1.7 ml/kg in INJ_{INF} animals and 9.3 ± 1.3 ml/kg in INJ_{INF+HAE} animals.

Carotid blood flow, used as a proxy for CBF,²⁰² was relatively stable and did not change within the SHAM group over the 15 min period the animals were exteriorised but not ventilated (coefficient of variation = 2.5%, Fig. 3.2B, E). Compared to SHAM animals, CBF was more variable in INJ_{INF} animals (coefficient of variation = 15.8%; Fig. 3.2C) and most variable in INJ_{INF+HAE} animals (coefficient of variation = 30.5%; Fig. 3.2D). CBF decreased in both ventilation groups and was significantly lower than baseline (pre-ventilation) levels at 13-15 min ($p<0.05$ for all time points). CBF was higher in INJ_{INF+HAE} than INJ_{INF} animals at 3-5 min ($p<0.05$ for all time points; Fig. 3.2E).

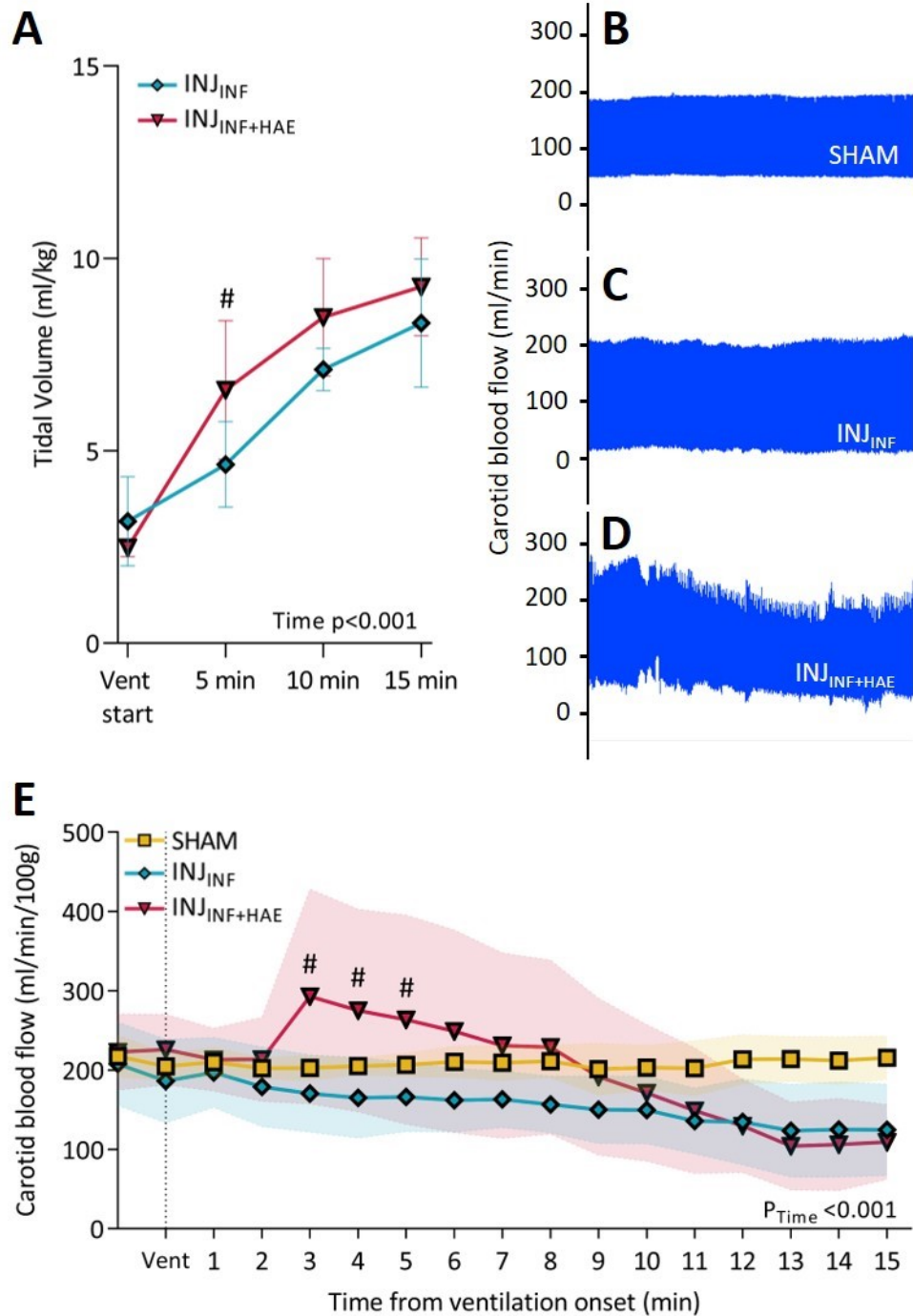


Figure 3.2. Tidal volume and carotid blood flow during injurious ventilation. (A) Tidal volume (V_T) increased over time in INJ_{INF} (blue) and INJ_{INF+HAE} (red) animals. V_T was higher in INJ_{INF+HAE} than INJ_{INF} at 5 min. (B-D) Representative snapshots of carotid blood flow (CBF) where INJ_{INF+HAE} animals that received injurious ventilation with umbilical cord occlusion showed the greatest CBF instability. (E) CBF corrected for brain weight was higher in INJ_{INF+HAE} than INJ_{INF} animals at 3-5 min. Dotted line indicates when injurious ventilation commenced. Data presented as mean \pm SD. # p <0.05 INJ_{INF+HAE} vs INJ_{INF} animals.

3.3.3. Plasma cytokine levels

Plasma IL-6 levels appeared higher in the INJ_{INF+HAE} group compared to INJ_{INF} and SHAM but this failed to reach significance ($p=0.402$; **Fig. 3.3A**). IL-6 levels within the INJ_{INF+HAE} group were significantly higher at 12 h compared to baseline ($p=0.036$) and 15 min ($p=0.022$), but not different between groups.

Plasma IL-8 levels were not different between groups ($p=0.575$; **Fig. 3.3B**) nor did they change within any group throughout the 24 h period.

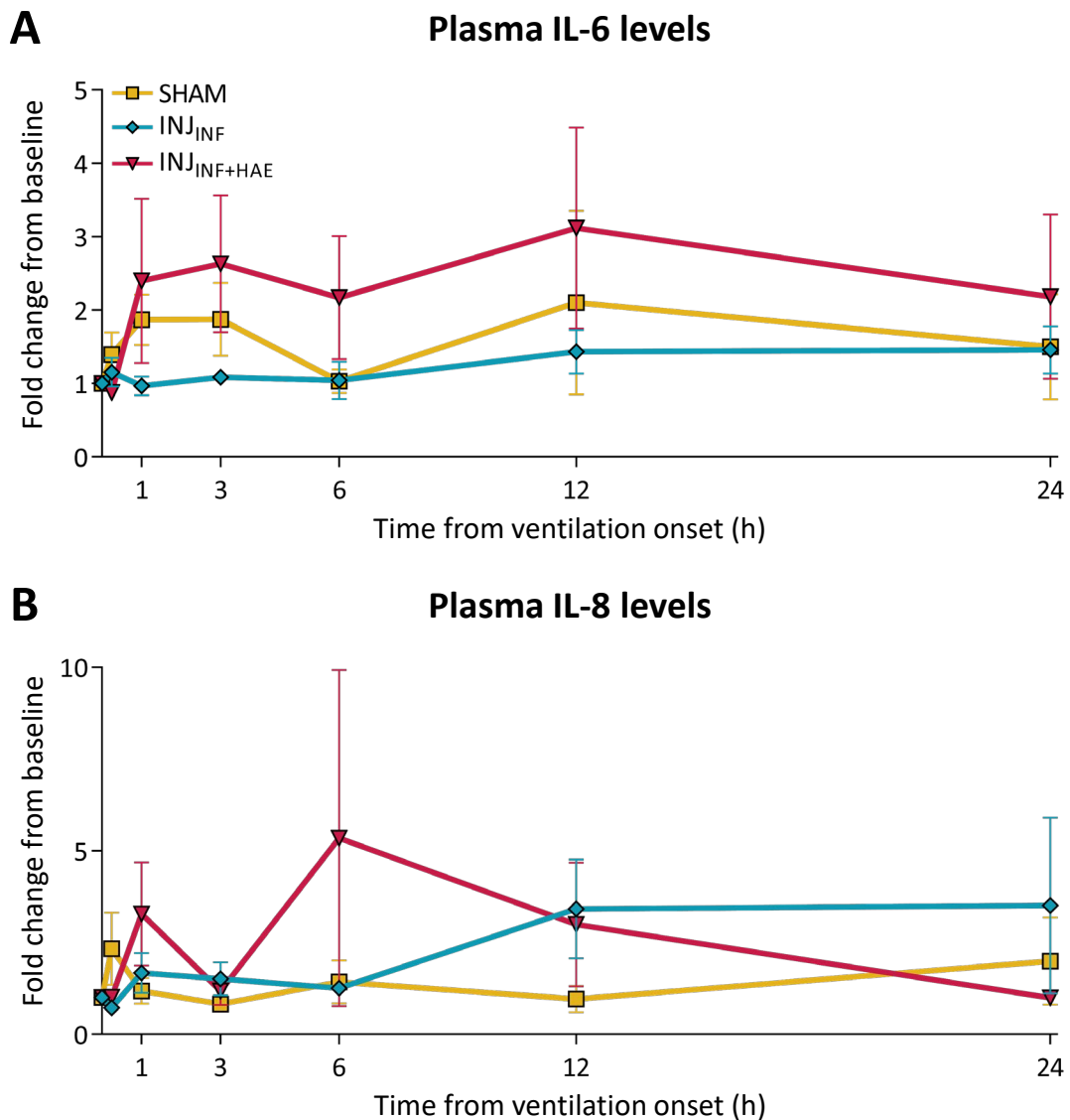


Figure 3.3. Plasma levels of the pro-inflammatory cytokines after injurious ventilation. (A) interleukin(IL)-6 and (B) IL-8 levels were not different between SHAM (yellow), INJ_{INF} (blue), and INJ_{INF+HAE} (red) animals at any assessed time point. Data are not available for unoperated controls that did not receive fetal surgery and instrumentation as plasma could not be obtained. Data presented as mean \pm SEM.

3.3.4. Gene expression levels in the PVWM and SCWM

The mRNA levels of cytokines IL 1 alpha (*IL1A*), IL 1 beta (*IL1B*), IL 6 (*IL6*), and tumour necrosis factor (*TNF*) in the PVWM and SCWM were not different between groups. mRNA levels of tight junction proteins claudin 1 (*CLDN1*) and occludin (*OCN*), and cell death markers p53 (*P53*) and caspase 3 (*CASP3*) in the PVWM [Fig. 3.4A] and SCWM [Fig. 3.4B] were not different between groups.

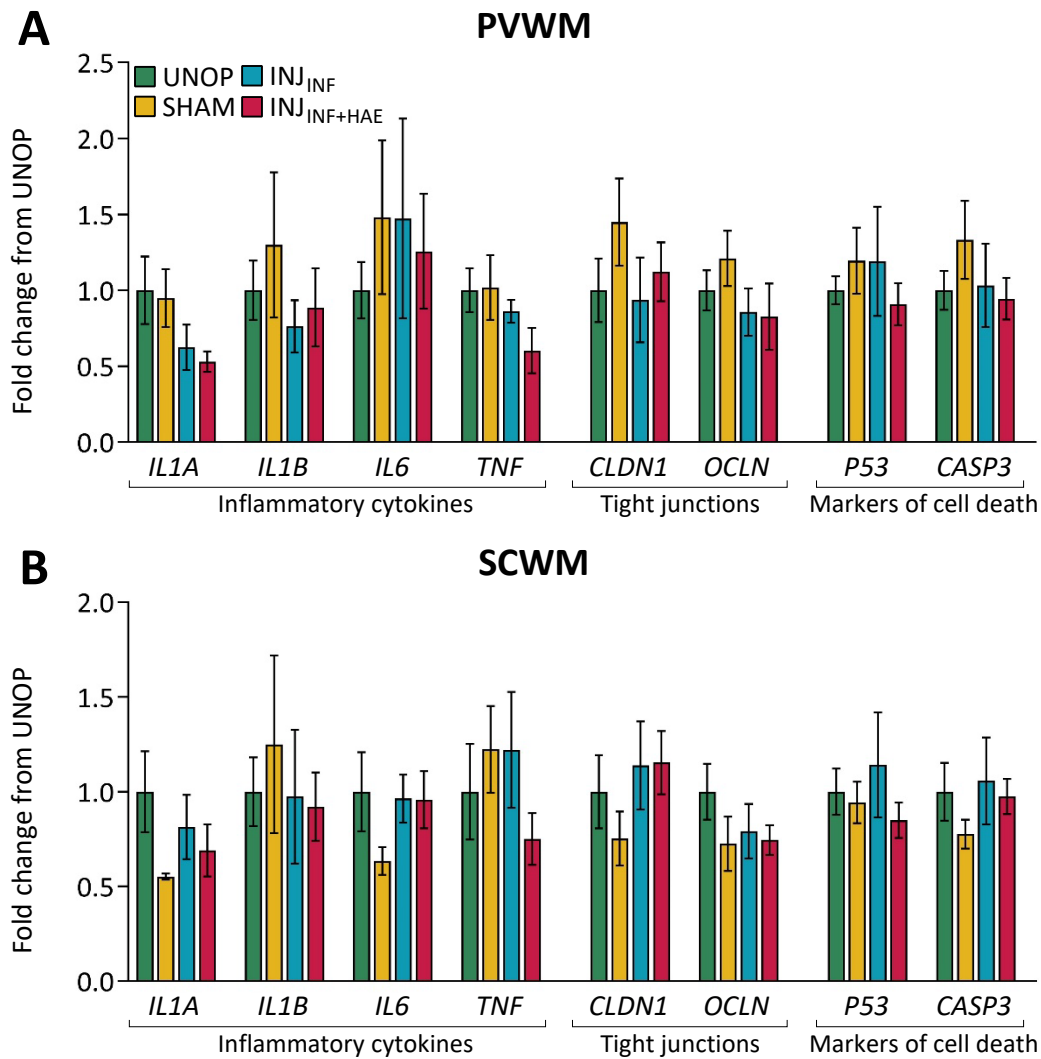


Figure 3.4. Gene expression levels of inflammatory cytokines (interleukin 1 alpha [*IL1A*], interleukin 1 beta [*IL1B*], interleukin 6 [*IL6*], tumour necrosis factor [*TNF*]), tight junction proteins (claudin 1 [*CLDN1*], occludin [*OCN*]), and markers of cell death (p53 [*P53*], caspase 3 [*CASP3*]) in the (A) PVWM and (B) SCWM were not different between groups. Data presented as mean \pm SEM.

3.3.5. Immunohistochemical assessment of brain injury

Quantitative assessment of the resident immune cells of the brain (microglia), blood-brain barrier integrity (protein extravasation), and myelinating cells (oligodendrocytes) showed no differences between all groups.

The number of Iba-1-positive aggregations was not different between groups in the PVWM ($p=0.760$) and SCWM ($p=0.537$; **Fig. 3.5A**). The area occupied by these aggregations within the PVWM and SCWM were not different between groups ($p=0.758$; $p=0.321$; data not presented). The areal density of microglia within these aggregations was not different between groups in both the PVWM ($p=0.480$) and SCWM ($p=0.154$; **Fig. 3.5B**).

The total number of Iba-1-positive microglia was not different between groups in the PVWM ($p=0.833$) and SCWM ($p=0.197$; **Fig. 3.5C**). The areal densities of ramified and amoeboid microglia were not different between groups in the PVWM (ramified $p=0.851$; amoeboid $p=0.597$) and SCWM (ramified $p=0.205$; amoeboid $p=0.937$; data not presented). The percentage of amoeboid microglia was not different between groups in both the PVWM ($p=0.579$) and SCWM ($p=0.802$; **Fig. 3.5D**).

The areal density of olig-2-positive cells was not different between groups in the PVWM ($p=0.829$) and SCWM ($p=0.697$; **Fig. 3.6A**).

The area coverage of MBP-positive cells was not different between groups in the PVWM ($p=0.085$) and SCWM ($p=0.209$) of the frontal lobe [**Fig. 3.6B**].

The number of blood vessel profiles with protein extravasation was not different between groups in the PVWM ($p=0.709$) and SCWM ($p=0.333$; **Fig. 3.7A**).

The area coverage of GFAP-positive astrocytes was not different between groups in the PVWM ($p=0.837$) and SCWM ($p=0.426$) of the frontal lobe [**Fig. 3.7B**].

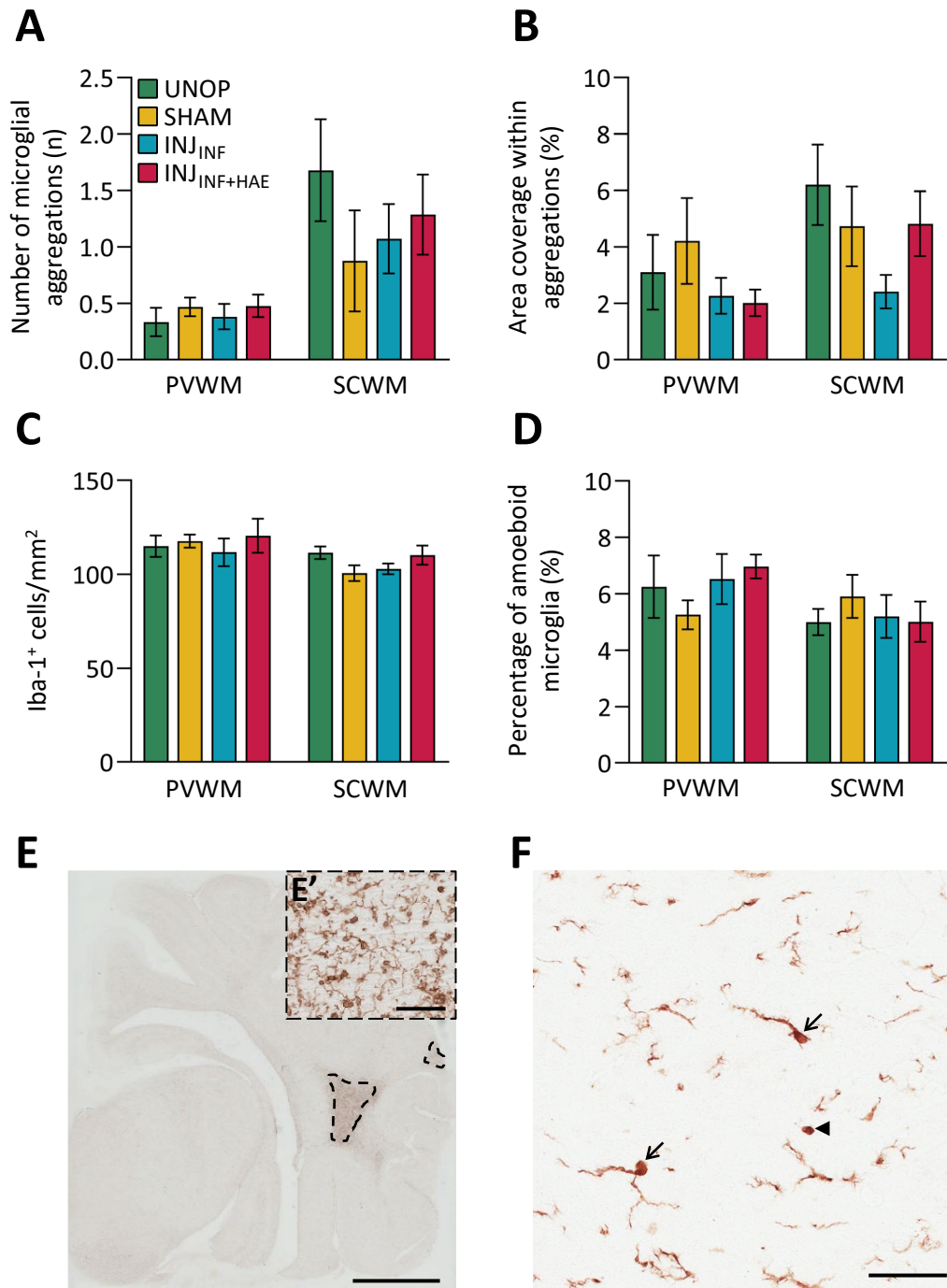


Figure 3.5. Iba-1-positive microglia in the PVWM and SCWM. The (A) number of microglia aggregations, (B) areal density of microglia within aggregations, (C) total number of microglia, and (D) percentage of amoeboid microglia in the PVWM and SCWM were not different between groups. (E) Representative image of microglia aggregations (dotted outline; scale bar = 5mm; insert **E'** shows microglia density within the aggregation, scale bar = 50μm). (F) Representative image of Iba-1-positive cells, arrows indicate ramified microglia and arrowhead indicates amoeboid microglia, scale bar = 50μm. Data presented as mean ± SEM.

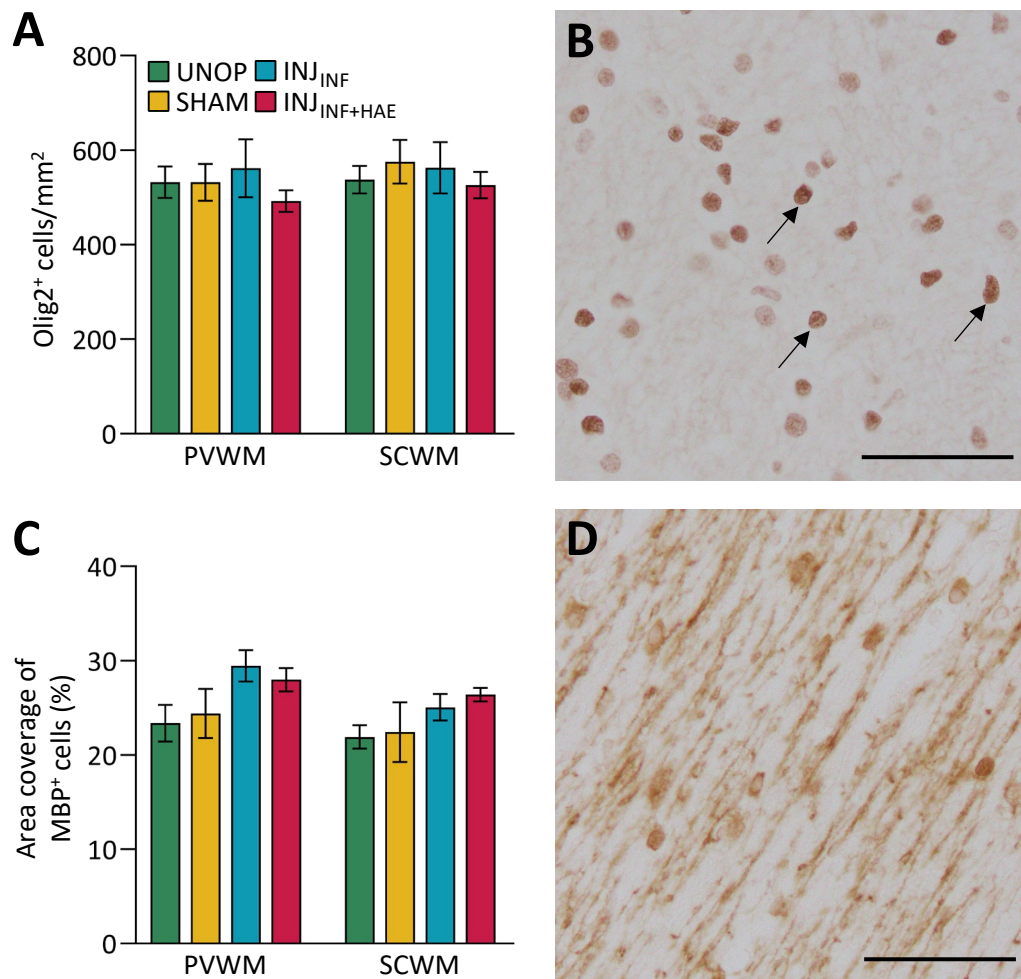


Figure 3.6. Olig2-positive and MBP-positive oligodendrocytes in the PVWM and SCWM. (A) The areal density of Olig2-positive cells in the PVWM and SCWM were not different between groups. (B) Representative image of Olig-2 positive cells (arrows). (C) The area coverage of MBP-positive cells in the PVWM and SCWM were not different between groups. (D) Representative image of MBP staining assessed for myelin density. Scale bar = 50 μ m for all images. Data presented as mean \pm SEM.

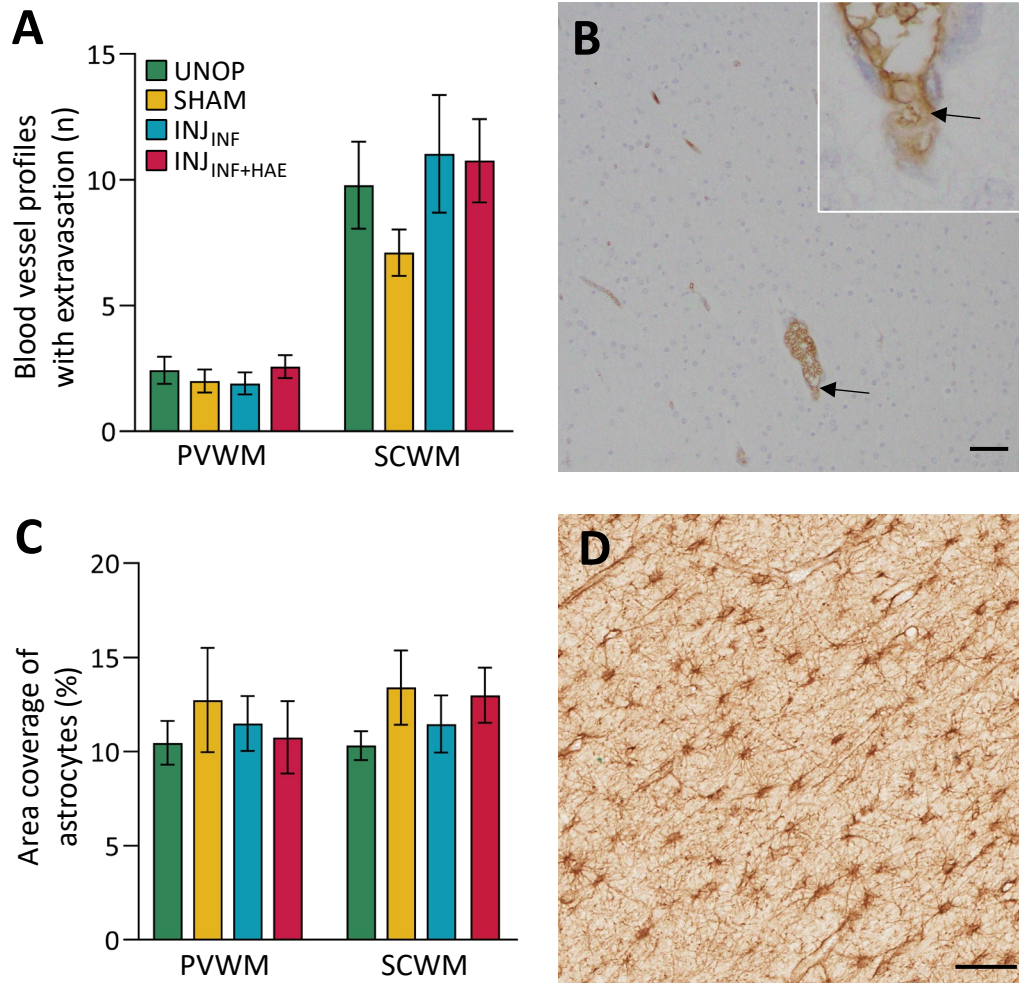


Figure 3.7. Sheep serum immunoreactivity and GFAP-positive astrocytes in the PVWM and SCWM. (A) The number of blood vessel profiles with protein extravasation in the PVWM and SCWM were not different between groups. **(B)** Representative image of sheep serum staining, arrow indicates vessel profile with protein extravasation. **(C)** The area coverage of GFAP-positive cells in the PVWM and SCWM were not different between groups **(D)** Representative image of GFAP staining assessed for area coverage. Scale bar = 50 μ m for all images. Data presented as mean \pm SEM.

3.4. Discussion

Preterm neonates exposed to volutrauma in the delivery room are at increased risk of brain injury, but the aetiology of this brain injury and the relative contribution of pathways to VIBI are not well understood. In the current study, we evaluated brain injury 24 h after injurious ventilation and aimed to determine the relative contributions of the haemodynamic and inflammatory pathways of injury. This study is the first to evaluate histopathology of acute VIBI at this time point. At 0.85 gestation, white matter development in the ovine brain is comparable to that of a late preterm or term human infant.^{203,204} Surprisingly, my results showed no effect of acute injurious ventilation on molecular and histopathological indices of brain injury within the PVWM and SCWM at 24 h.

In studies that have adopted a similar injurious ventilation strategy (15 min of high V_T ventilation) in sheep of similar gestational age, the insult upregulated mRNA gene expression levels of pro-inflammatory cytokines, compromised the blood-brain barrier (BBB), increased microgliosis and astrogliosis, and increased markers of cell death in the PVWM and SCWM of preterm lambs, detectable 90 min to 2 h after ventilation.^{110,133,135} Furthermore, we have previously established that our ventilation strategy in the current study causes significant lung inflammation and structural changes when evaluated at 24 h.¹⁸⁹ Although we failed to reach the target V_T of 12-15 ml/kg, likely because of insufficient surfactant and low pulmonary compliance, the achieved V_T of 7-10 ml/kg is still higher than the normal V_T of 5-7 ml/kg for lambs of this gestational age.^{110,137,205} Following ventilation with intact umbilical cord perfusion, the lungs of some animals in the current study (INJ_{INF} group) had increased inflammatory cell infiltration, increased number of proliferating cells, increased alveolar wall thickness, and decreased secondary septal crests.¹⁸⁹ However, as my plasma cytokine results suggest, this increase in pulmonary inflammation may not have initiated systemic inflammation. The absence of profound systemic inflammation may explain the lack of histological brain injury, since cerebral inflammation in VIBI is postulated to be downstream of profound pulmonary and systemic inflammation.⁹⁶

When evaluating cerebral inflammation, I found no effect of ventilation on mRNA levels of inflammatory cytokines in the PVWM and SCWM. Previous studies have shown elevated *IL6* and *IL8* mRNA levels 2 h after the initiation of injurious ventilation.^{133,135} Given that mRNA is transient, it is possible that changes to mRNA levels resolved over the 24 h period and hence changes were not detected in my tissue. A limitation of this study is that I did not evaluate the products of these genes at a protein level. However, microglia activation was similarly not different between groups. Microglia, the resident immune cells of the central nervous system, are activated when an insult is present, and this is reflected structurally as a change from ramified to amoeboid state.¹⁹⁵ I was not able to differentiate amoeboid microglia on the reactivity spectrum to determine if they were predominantly pro- or anti-

inflammatory. However, previous observations of microglia activation and aggregation 105 min after the onset of acute injurious ventilation have been postulated to indicate or contribute to inflammation.¹³³ The area coverage of astrocytes was also not different between groups. Astrocytes, like microglia, are able to regulate inflammation in the CNS, and hypertrophy of the astrocytic cell body and processes is indicative of astrogliosis.³⁹ This was not observed in this study. Thus, it appears that brief high V_T ventilation, with or without intact placental circulation, has not increased cerebral inflammation when compared to control animals in my study.

Disruption of the BBB and vascular integrity are associated with increased risks of cerebral inflammation as peripheral toxic mediators enter the brain parenchyma.⁹⁶ To evaluate BBB and vascular integrity, I examined mRNA levels of key tight junction proteins claudin 1 (*CLDN1*) and occludin (*OCLN*) in the PVWM and SCWM. These tight junction proteins establish a paracellular barrier vital to BBB integrity.²⁰⁶ No differences in gene expression were found between groups. This is perhaps due to the aforementioned reason of mRNA levels resolving, since previous studies where preterm lambs received high V_T ventilation showed that *CLDN1* mRNA expression was increased in the PVWM and decreased in the SCWM at 2 hours after the initiation of injurious ventilation.¹³³ Another reason may be that tight junction proteins may not be altered during the initial insult, but rather are redistributed or rapidly remodelled to prevent paracellular gap formation.²⁰⁶ I have not investigated the localisation of tight junction proteins with immunohistochemical methods. Instead, I investigated protein extravasation which is a common technique used to identify vascular endothelium disruption, a potential early indicator of BBB compromise and haemorrhage.²⁰⁷ I found no differences between groups, again in contrast to previous studies whereby a higher incidence of vascular extravasation was observed in both the PVWM and SCWM of preterm ventilated lambs.^{110,133} Together, these results suggest that my ventilation strategy did not compromise BBB and vascular integrity in the ventilated animals as compared to their control counterparts, when assessed at 24 h.

I used Olig2 to identify oligodendrocyte lineage cells and found that cell numbers were not altered irrespective of ventilation strategy. Myelin density (MBP immunoreactivity) in the frontal lobe was similarly unaffected by ventilation. The effect of acute injurious ventilation on oligodendrocyte lineage cells has not previously been characterised, although 15 min of high V_T ventilation did not affect myelin density in the PVWM at 90 min after the initiation of ventilation.¹³⁸ Furthermore, regardless of ventilation strategy, mRNA levels of p53 (*P53*) and caspase 3 (*CASP3*) were not altered in the PVWM and SCWM of the lambs in this study, unlike in previous studies where mRNA levels of both markers of cell death were increased in the SCWM of ventilated preterm lambs.¹³³

The ostensible conclusion from the results described above is that the initial 15 min high V_T ventilation in this study, despite causing lung injury,¹⁸⁹ was not as harmful to the immature brain as intended. This may suggest that the presence of lung injury is not necessarily associated with brain injury. However, it is important to note that the animals in this study underwent MRI for detection of brain injury, and DTI colour-mapping detected subtle brain injury in the frontal white matter of ventilated lambs (INJ_{INF} and $INJ_{INF+HAE}$) of this study.¹¹¹ The altered DTI indices are indicative of axonal loss (decreased axial diffusivity) and impairment of myelination (decreased radial diffusivity).¹¹¹ Therefore, an appropriate conclusion may be that the methodology used to detect histological evidence of brain injury following 15 min of injurious ventilation had a limited scope. There may be several explanations: 1) injury was present but not detectable by the techniques I used or in the areas I assessed and hence could not be detected at 24 h, 2) injury was present but was masked by injury caused by subsequent ‘gentle’ ventilation whilst the animals underwent MRI, or 3) injury was not present because of the low V_T applied.

Firstly, I focused on the PVWM and SCWM as these are regions commonly affected in preterm neonates and which have previously been reported to be affected in preterm ventilated lambs. Indeed, our work using DTI colour-mapping in the same animals of the current study detected lower diffusivities, indicative of axonal and myelin loss, in the frontal white matter.¹¹¹ My molecular and immunohistochemical analyses were limited to key markers of neuroinflammation and white matter integrity previously shown to be altered in acute VIBI.^{110,133,135} It is possible that other markers or techniques, such as assessing neuronal and axonal integrity would complement the DTI findings and may detect appreciable differences. In addition, DTI colour-mapping detected subtle injury in the thalamus, internal capsule, and cerebellum¹¹¹ which were not included in the analyses in the current study; VIBI in these regions have yet to be thoroughly interrogated and it is possible that our ventilation strategy adversely affects these structures.

Next, all lambs underwent 1 h of MRI after delivery, during which they were anaesthetised and mechanically ventilated. Even though a gentle ventilation strategy was employed, it is possible that this procedure induced a baseline of subtle injury in all animals which masked changes from the initial injurious ventilation and confounded the results. Indeed, even when gentle or protective ventilation strategies are used, the immature brain remains at high risk of injury.^{155,205} Unfortunately, we did not undertake a control group that did not undergo MRI and therefore were not exposed to the second anaesthesia and ventilation period, and in hindsight this is a major limitation for the histology sub-analysis. Using the same model, Hillman *et al.* previously demonstrated an additive effect of continued ventilation (gentle strategy for 2 h 45 min) to resuscitation injury in the preterm lung, even when the initial resuscitation caused significant injury.²⁰⁵ My findings indicate a need to revisit the contribution

of prolonged mechanical ventilation in the pathogenesis of brain injury in preterm infants. I also recommend that this be considered for future experimental design.

Another explanation to the absence of histological injury might be that the V_T achieved was not high enough to elicit VIBI. In this study, ventilated lambs received V_T of ~7-10 ml/kg while in previous VIBI studies, brain injury was detected in lambs that received V_T of 12-15 ml/kg.^{110,133,134} I speculate that the V_T applied, even though marginally higher than the normal V_T , was insufficient to activate the pathways of VIBI. This warrants further investigation as it implies that appropriate monitoring of V_T in the delivery room may prevent or reduce VIBI.

Due to the abovementioned reasons, it was not possible to compare the INJ_{INF} and $INJ_{INF+HAE}$ groups to address the relative contributions of the two main pathways of VIBI. This study was designed to isolate the two main pathways of VIBI by manipulating placental support. Maintaining placental blood supply during PPV minimises rapid fluctuations in pulmonary and carotid blood flow, thereby reducing the impact of the haemodynamic pathway of VIBI.^{111,205} The expected injury in animals ventilated with intact placental circulation can therefore be attributed primarily to the inflammatory pathway. On the other hand, injury in animals ventilated with the umbilical cord occluded can be attributed to both pathways and comparisons of the two groups would reveal the relative contribution of each pathway to VIBI. The pattern of cerebral haemodynamic instability observed in the $INJ_{INF+HAE}$ animals in this study is consistent with that previously documented in preterm lambs when high V_T ventilation was initiated without placental support.¹¹⁰ The initial rapid increase in CBF was likely in response to the temporary removal of the low resistance placental circulation, which would have increased systemic vascular resistance and blood flow towards the lungs, thus increasing pulmonary blood flow, pulmonary venous return, cardiac output, and consequently CBF. Additionally, umbilical cord occlusion decreases arterial and cerebral oxygen saturation, prompting CBF to increase to maintain adequate cerebral oxygen delivery (autoregulation). The subsequent more gradual decrease of CBF observed in both groups during the ventilation period may be a result of compression of pulmonary capillaries which decreases pulmonary blood flow. In the $INJ_{INF+HAE}$ group, it may also be that cerebral oxygen saturation returned to levels not needing autoregulation compensation in those animals.

DTI analysis of the brains of animals from this study suggests that the haemodynamic pathway has additive effects to the inflammatory pathway on the progression of VIBI.¹¹¹ In $INJ_{INF+HAE}$ animals, IL-6 level was higher at 12 h compared to baseline and 15 min levels although this was not different to the other groups. This may suggest that the haemodynamic pathway is closely linked to the inflammatory pathway. The possibility that the haemodynamic pathway potentially increases systemic inflammation may allude to its role in injury progression. It is unclear how this may occur. However, excessive

haemodynamic shear stress may result in endothelial dysfunction of vascular walls, and potentially induce an inflammatory reaction.²⁰⁸

3.5. Conclusion

In this study, I set out to examine whether the haemodynamic pathway of injury has additive effects to the inflammatory pathway on the progression of VIBI. However, I am not able to report conclusive results due to the lack of histologically-detectable injury in the ventilated lambs. I am also not able to conclude if injury detected at earlier time points in previous studies persist to 24 h, however, it appears that using lower V_T for ventilation does not cause VIBI. Further, my results rationalise the need to investigate the effects of prolonged ventilation on the immature brain of preterm infants.

Chapter Four: Early UCBC Exacerbates Acute VIBI

In this study, I investigated the potential of early administration of umbilical cord blood (UCB) cells to reduce ventilation-induced brain injury (VIBI) in preterm lambs. The effects of early administration of UCB cells on the lungs of the preterm lambs in this study have been published. These findings are complementary to the discussion in this chapter and are provided in Appendix III.

To address the aim of this study, I used the same experimental model as that in Chapter 3. Three groups from Chapter 3 (UNOP, SHAM, INJ_{INF}) were used as comparison groups in this study. This reduced the number of large animals in line with accepted animal ethics principles. It may appear that the experimental model chosen is unjustified given the lack of brain injury in the ventilation groups in Chapter 3. However, the animal experiments in this chapter commenced before the results presented in Chapter 3 were available. Instead, the decision to start experiments on the additional animals in this chapter was made based on preliminary magnetic resonance imaging (MRI) results of those animals (Appendix II). The MRI findings had showed that ventilated animals had worse injury than control animals and supported the use of the model to investigate UCB cells.

4.1. Introduction

Preterm infants (<37 weeks gestation) have a high requirement for respiratory support at birth due to their immature lungs. The initiation of ventilation in the delivery room is sometimes inadvertently injurious because tidal volumes (V_T) are poorly controlled.^{87,88} This often leads to pulmonary inflammation and injury and, consequently, systemic and cerebral inflammation and injury.^{96,110} Indeed, excessive V_T in delivery room resuscitation is associated with an increased risk of haemorrhagic brain injury in preterm infants.⁹⁷

The key pathways of VIBI are postulated to be inflammation and haemodynamic instability, primarily downstream of the pulmonary consequences from ventilation.^{96,110} An additive role of the haemodynamic pathway of injury to the inflammatory pathway has recently been suggested, highlighting the importance of targeting inflammation for effective prevention or treatment of VIBI.¹¹¹ However, such a therapeutic agent has not yet been examined for this purpose.

UCB cells are a therapeutic option that have been examined preclinically as a neuroprotective strategy and have demonstrated strong anti-inflammatory properties.^{185,188,209,210} UCB consists of a heterogeneous population of mononuclear cells and stem and progenitor cells, which have been shown to modulate

neuroinflammation in the preterm brain.^{171,175} In particular, mesenchymal stromal cells (MSCs), monocyte-derived suppressor cells, and regulatory T-cells present within cord blood are strongly linked to immunomodulatory and anti-inflammatory properties.^{171,175} Accordingly, I proposed that administration of UCB cells may attenuate the inflammatory pathway associated with VIBI.

Studies using UCB cells have found that administration 12 h after acute hypoxia-ischaemia reduced cerebral inflammation and injury in the periventricular white matter (PVWM), subcortical white matter (SCWM), and internal capsule of near-term and preterm sheep.^{184,188} In a fetal sheep model of systemic inflammation, UCB cell treatment reduced cell death and inflammation within the white matter, and improved myelination.²⁰⁹ However, the interaction of UCB cells and mechanical ventilation in the preterm cohort has not been investigated. Given that a significant number of preterm infants will require ventilation which increases their risk of white matter injury, it is vital to investigate the use of UCB cells in this context.

In this study, I investigated the effects of early UCB cells administration at 1 h after injurious ventilation on systemic inflammatory cytokine levels and cerebral white matter injury 24 h later. I hypothesised that UCB cells would reduce indices of white matter injury by attenuating systemic and neuro-inflammation.

4.2. Methods

The detailed experimental methodology used in this study is provided in Chapter 2. Below is a concise overview. Experimental procedures were approved by the Monash Medical Centre Animal Ethics Committee A, Monash University, and were conducted in accordance with guidelines established by the National Health and Medical Research Council of Australia.

Animals were randomised to one of the following groups:

- 1) Control (**CONT**; n=12)
 - a. Unoperated control (**UNOP**; n=7): Lambs did not undergo fetal surgery or ventilation and were used to control for the surgical intervention.
 - b. Sham surgery control (**SHAM**; n=5): Lambs underwent fetal surgery, were instrumented and intubated, but did not receive mechanical ventilation to control for the experimental intervention.
- 2) Injurious ventilation (**INJ**; n=7): Lambs received 15 min of high V_T ventilation.
- 3) Injurious ventilation with umbilical cord blood cell treatment (**INJ+UCBC**; n=7): Lambs received 15 min of high V_T ventilation and at 1 h after the initiation of ventilation (referred to as 1 h post-ventilation), 80 million ovine UCB cells were administered intravenously (i.v.).

4.2.1. Instrumentation and injurious ventilation strategy

Pregnant ewes at 125 ± 1 days gestation (mean \pm SD; term ~148 days) were anaesthetised via intravenous injection of thiopentone sodium (20 mg/kg; Jurox, NSW, Australia), followed by tracheal intubation and delivery of inhalational anaesthetic (isoflurane 1.5-2.5% in oxygenated air; Bomac Animal Health, NSW, Australia). A midline laparotomy was performed to expose the head and neck of the fetus for instrumentation of polyvinyl catheters (ID 0.86 mm, OD 1.52 mm; Dural Plastics & Engineering, NSW, Australia) in the left carotid artery and jugular vein. An ultrasonic flow probe (3PS; Transonic Systems, NY, USA) was placed around the right carotid artery to monitor carotid blood flow. The fetal chest was exteriorised, the fetus was intubated with a cuffed endotracheal tube (ID 4.0-4.5 mm; Smiths Medical, UK), and lung liquid was passively drained. SHAM animals remained intubated and exteriorised for 15 min without mechanical ventilation.

Ventilation was conducted under sterile conditions using a neonatal positive pressure ventilator (Babylog 8000+, Dräger, Lübeck, Germany) as described in Chapter 2 (Section 2.2.2). Briefly, the exteriorised fetus was ventilated for 15 min with a high V_T strategy targeting 12-15 ml/kg, which is known to cause ventilation-induced brain pathology (normal V_T 5-7 ml/kg).

After the 15 min period of ventilation, the carotid flow probe was removed, and the fetus was extubated and returned to the uterus. The fetal jugular vein and carotid artery catheters were externalised through the ewe's flank via a small incision to allow for i.v. cell administration and periodic blood sampling respectively. All incision sites were sutured closed and the ewe and fetus were allowed to recover. Analgesia was provided to the ewe via buprenorphine (0.3 mg i.m.; Temgesic; Reckitt Benckiser, UK) and a transdermal fentanyl patch (75 µg/h; Janssen-Cilag, NSW, Australia) for post-surgery pain relief. At 15 min, 1 h, 3 h, 6 h, 12 h, and 24 h post-ventilation, fetal arterial blood was sampled (ABL80 FLEX; Radiometer Medical ApS, Denmark) to ensure fetal wellbeing and collected in heparin tubes for plasma analysis.

4.2.2. Umbilical cord blood cells treatment

At 1 h post-ventilation, 80 million allogeneic UCB cells suspended in 3 ml of phosphate-buffered saline (PBS; Gibco, MA, USA) were administered to the fetus via the jugular vein catheter. The catheter was flushed with 3 ml of sterile heparinised saline to ensure all the cells were administered.

The preparation of UCB cells has previously been reported^{188,189} and is detailed in Chapter 2 (Section 2.2.4). Briefly, cord blood samples were collected from healthy near-term sheep (141 days gestation of term 148 days) at the time of caesarean-section delivery and the cord blood was processed to remove erythrocytes. The remaining UCB cells were assessed for viability, then cryopreserved. On the day of

cell administration, UCB cell samples were rapidly thawed, washed with media, resuspended in PBS (Gibco), and recounted. Cells were kept on ice until administration via the jugular vein catheter.

4.2.3. Lamb delivery and subsequent monitoring

At 24 h post-ventilation, ewes were anaesthetised as above and the fetus was exteriorised via the same incision site. A transcutaneous oximeter (Masimo, CA, USA) was attached to the tail of the fetus to monitor oxygen saturation level and heart rate. UNOP lambs were instrumented with arterial and venous polyvinyl catheters prior to delivery.

All lambs were dried, intubated, and stabilised with a gentle ventilation strategy (Babylog 8000+, Dräger). Ventilation was initiated in volume-guarantee mode set at 7 ml/kg, maximum peak inspiratory pressure (PIP) 40 cmH₂O, positive end expiratory pressure (PEEP) 5 cmH₂O, inspiratory time 0.6 s, and expiratory time 0.6 s. The fraction of inspired oxygen (FiO₂) was set initially at 0.4 but adjusted accordingly to maintain arterial oxygen saturation (SaO₂) between 88-95% and partial pressure of carbon dioxide (PaCO₂) between 45-55 mmHg. Intratracheal surfactant (240 mg; Curosurf®; Chiesi Pharmaceuticals, Parma, Italy) was administered within the first 10 min of ventilation onset to improve lung compliance. Sustained inflations at 35 cmH₂O for 5 s duration were applied to recruit the lung if necessary.

Once the lambs were stabilised (within 15 min of ventilation onset), the umbilical cord was clamped and the lambs were transferred to an MR-compatible ventilator (Pneupac® babyPAC™; Smiths Medical, UK) using the same ventilator settings on the Dräger ventilator as a reference. The MRI acquisition protocol has previously been reported¹¹¹ and is not the focus of this study. Lambs were euthanised (sodium pentobarbitone >100 mg i.v.; Valabarb Euthanasia Solution; Jurox, NSW, Australia) for tissue collection after MRI scanning (total acquisition time 40 min). Ewes were euthanised (overdose of sodium pentobarbitone i.v.; Valabarb) immediately after delivery of the lambs.

4.2.4. Brain collection

The brain was removed from the skull and the cerebrum halved along the medial longitudinal fissure. The periventricular and subcortical white matter (PVWM; SCWM) were dissected from the left cerebral hemisphere and snap-frozen in liquid nitrogen. The right cerebral hemisphere was immersion fixed in 10% neutral buffered formalin (NBF; Amber Scientific, WA, Australia) overnight. The right hemisphere was then cut coronally into 5 mm blocks (8-9 blocks/animal), post-fixed in 10% NBF for 6 days, processed, and paraffin-embedded. Serial sections (8 µm) were cut from one block each at the level of frontal, parietal, temporal, and occipital lobes for immunohistochemical analysis.

4.2.5. Plasma protein analysis

Arterial blood was collected via the fetal carotid artery catheter before injurious ventilation (T=0), at the end of injurious ventilation (15 min), and post-surgery until delivery (1 h, 3 h, 6 h, 12 h, 24 h). Plasma cytokines (interleukin-6 [IL-6] and interleukin-8 [IL-8]) were quantified using a sandwich enzyme-linked immunosorbent assay (ELISA), as described in detail in Chapter 2 (Section 2.5.1). Briefly, 96-well plates were coated with mouse anti-ovine IL-6 (1:200, Bio-Rad Laboratories, CA, USA) or mouse anti-ovine IL-8 (1:1000, Bio-Rad) antibodies. Plasma samples were diluted with an equal part of diluting buffer (PBS, 0.1% bovine serum albumin [BSA], 0.05% Tween 20) and incubated in the 96-well plates. The plates were then incubated with respective detecting antibodies (rabbit anti-ovine IL-6, 1:200, Bio-Rad; rabbit anti-ovine IL-8, 1:4000, Bio-Rad) followed by horse radish peroxidase (HRP)-conjugated swine anti-rabbit immunoglobulin (Ig; 1:2000, DAKO, CA, USA). Plates were developed with 3,3', 5,5'-tetramethylbenzidine (TMB chromogen solution; Invitrogen, CA, USA) and read on a SpectraMax i3 microplate reader (Molecular Devices, CA, USA) at 450 nm to determine optical density. Standards (recombinant ovine IL-6 or IL-8; Kingfisher Biotech, MN, USA) were included and a standard curve was generated for every ELISA plate used ($R^2 > 0.99$ for all).

4.2.6. Reverse-transcription real-time quantitative PCR

Tissue from the PVWM and SCWM of the left hemisphere were separately homogenised, and RNA from each region was extracted (RNeasy Midi RNA Extraction Kit; Qiagen, VIC, Australia) and reverse-transcribed into cDNA (SuperScript® III First-Strand Synthesis System for RT-PCR kit; Invitrogen). Genes of interest were measured by quantitative PCR using the Fluidigm Biomark™ HD system (Fluidigm Corporation, CA, USA). Relative mRNA expression of key inflammatory interleukins, tight junction proteins, mediators of angiogenesis, and markers of cell death were measured, as described in Chapter 2 (Section 2.5.2.3). Samples were run in triplicates and the average was taken. The expression of all genes was normalised to ribosomal protein S18 (*RPS18*) expression using the $2^{-\Delta\Delta C_t}$ method for each sample, expressed relative to the INJ group.

4.2.7. Immunohistochemistry

Coronal sections from comparable sites of the frontal, parietal, temporal, and occipital lobes (4 slides/animal) were stained with anti-ionised calcium binding adapter molecule-1 (Iba-1; 1:1500, Wako Pure Chemical Industries, Osaka, Japan) to identify microglia, anti-sheep serum (1:1000, Sigma-Aldrich, MO, USA) to identify vascular extravasation of protein, and anti-oligodendrocyte transcription factor-2 (Olig2; 1:1000, Merck, Darmstadt, Germany) for oligodendrocytes. Prior to incubation with anti-Iba-1 and anti-Olig2, sections were pre-treated with citrate buffer (pH 6.0) in a

microwave oven. Sections were incubated with secondary antibody biotinylated goat anti-rabbit or goat anti-mouse immunoglobulin G (IgG; 1:200; Vector Laboratories, CA, USA) and reacted using the Vectastain Elite ABC Kit (Vector Laboratories). Sections reacted with anti-sheep serum were counterstained with 20% haematoxylin. Staining was absent when the primary antibody was omitted.

4.2.8. Quantitative immunohistochemical analysis

Analyses were conducted at equivalent sites within the cerebral white matter of sections from the frontal, parietal, temporal, and occipital lobes of each lamb. Non-overlapping fields of view in the PVWM were taken medial to lateral from the ventricle, and fields in the SCWM were obtained from alternating gyri starting from the second gyrus closest to the midline. Slides were coded and the observer (KC) was blinded to the treatment.

The proportion of PVWM and SCWM occupied by Iba-1-positive microglial aggregations was assessed using ImageScope (Aperio Technologies, CA, USA); individual aggregation areas were summed then divided by the total area of PVWM or SCWM of the section, data expressed as a percentage. The fraction areal coverage (%) of Iba-1 immunoreactivity within an aggregation was assessed using a set intensity threshold (FIJI; ImageJ, NIH Image, MD, USA).

Areal density (cells/mm²) of Iba-1-positive microglia was quantified in 3 non-overlapping fields in the PVWM and 6 non-overlapping fields in the SCWM from 2 separate gyri, avoiding microglial aggregations, using ImageScope (Aperio Technologies). Microglia were distinguished based on morphology (ramified microglia were characterised by long cellular processes while amoeboid microglia by round, densely stained soma with resorbed processes).¹⁹⁵

Areal density (cells/mm²) of Olig2-positive oligodendrocytes was quantified in 3 non-overlapping fields in the PVWM and 6 non-overlapping fields in the SCWM from 2 separate gyri, using FIJI (ImageJ, NIH). Blood vessel profiles with protein extravasation were quantified and expressed as total number of vessel profiles with protein extravasation within the PVWM and SCWM. For all indices, a mean of all lobes was calculated for each animal and then collectively averaged for each treatment group.

4.2.9. Statistical analysis

Fetal parameters were compared using a one-way analysis of variance (ANOVA; Graphpad Prism 8.1.2; GraphPad Software, CA, USA). ELISA data were compared using two-way repeated measures ANOVA with Holm-Sidak *post hoc* comparison (SigmaPlot; Systat Software Inc., CA, USA). PCR data was only obtained for INJ and INJ+UCBC animals and have been compared using an independent T-Test (Graphpad Prism 8.1.2). There were no differences in any immunohistochemical indices

between the UNOP and SHAM group, as described in Chapter 3, and they are reported here as a pooled control group (CONT) for comparisons to the INJ and INJ+UCBC groups. All immunohistochemical data were compared using a one-way ANOVA with Holm-Sidak *post hoc* comparison (Graphpad Prism 8.1.2). Statistical significance was accepted at $p < 0.05$. Baseline physiological data are presented as mean \pm SD to convey variability in the study cohort. All other data are presented as mean \pm SEM unless otherwise stated.

4.3. Results

4.3.1. Physiological and ventilation parameters

Blood gas parameters before the initiation of injurious ventilation were not different between groups [Table 4.1]. Arterial blood gas parameters including pH, SaO₂, partial pressure of oxygen (PaO₂), and PaCO₂ during injurious ventilation and up to delivery at 24 h post-ventilation have previously been reported and were not different between groups (Appendix III).¹⁸⁹ Lamb characteristics, and body and brain weights recorded post-mortem were not different between groups [Table 4.1]. A mean \pm SD of 24.5 ± 5.0 million cells/kg was administered to lambs in the INJ+UCBC group at 1 h after the initiation of ventilation.

Ventilation parameters including PIP, mean airway pressure, and V_T during the 15 min injurious ventilation have previously been reported and were not different between groups (Appendix III).¹⁸⁹ At 15 min, mean \pm SD V_T achieved was 8.3 ± 1.7 ml/kg for INJ and 8.5 ± 1.5 ml/kg for INJ+UCBC (p=0.796).

Table 4.1. Lamb characteristics and baseline arterial blood gas parameters. Lamb characteristics recorded at post-mortem examination and fetal arterial blood gas parameters recorded at the start of the experiment were not different between groups. Blood gas parameters were taken before any interventions (i.e. before sterile fetal surgery for all groups except UNOP before delivery). CONT is pooled from UNOP and SHAM. Data are presented as mean \pm SD.

	CONT	INJ	INJ+UCBC
Group characteristics			
Number (n=)	12	7	7
Gestational age (d)	126 \pm 1	126 \pm 1	126 \pm 1
Sex (% male)	75%	71.4%	57.1%
Birth order 1 st (n)	10 (83.3%)	7 (10%)	7 (100%)
Body weight (kg)	3.4 \pm 0.3	3.4 \pm 0.5	3.4 \pm 0.6
Brain weight (g)	45.8 \pm 2.5	46.3 \pm 2.4	45.3 \pm 3.2
V _T at 15 min (ml/kg)	NA	8.3 \pm 1.7	8.5 \pm 1.5
UCB cell dose (cells/kg)	NA	NA	24.5 \pm 5.0 million
Arterial blood gas parameters			
pH	7.27 \pm 0.04	7.25 \pm 0.05	7.27 \pm 0.02
PaCO ₂ (mmHg)	61.3 \pm 10.2	57.3 \pm 7.7	59.2 \pm 4.3
PaO ₂ (mmHg)	35.0 \pm 13.1	43.2 \pm 9.9	34.1 \pm 3.5
SaO ₂ (%)	33.9 \pm 5.8	62.6 \pm 11.9	49.0 \pm 7.7

PaCO₂ partial pressure of carbon dioxide; *PaO₂* partial pressure of oxygen; *SaO₂* oxygen saturation, *UCB* umbilical cord blood; *V_T* tidal volume.

4.3.2. UCB cell treatment increased systemic inflammation

Plasma IL-6 level, expressed as a fold-change from baseline, was the highest at 6 h in INJ+UCBC lambs (5.3 ± 3.2 -fold compared to baseline; $p < 0.05$ compared to all other time points except 3 h), and was significantly higher than INJ ($p = 0.006$) and CONT ($p = 0.007$) lambs [Fig. 4.1A]. CONT consists only of SHAM animals as no plasma was collected from UNOP animals.

Plasma IL-8 level, expressed as a fold-change from baseline, was the highest at 3 h in INJ+UCBC lambs (8.0 ± 4.2 -fold compared to baseline; $p < 0.05$ compared to all other time points), and was significantly higher than INJ ($p < 0.001$) and CONT ($p < 0.001$) lambs [Fig. 4.1B]. CONT consists only of SHAM animals as no plasma was collected from UNOP animals.

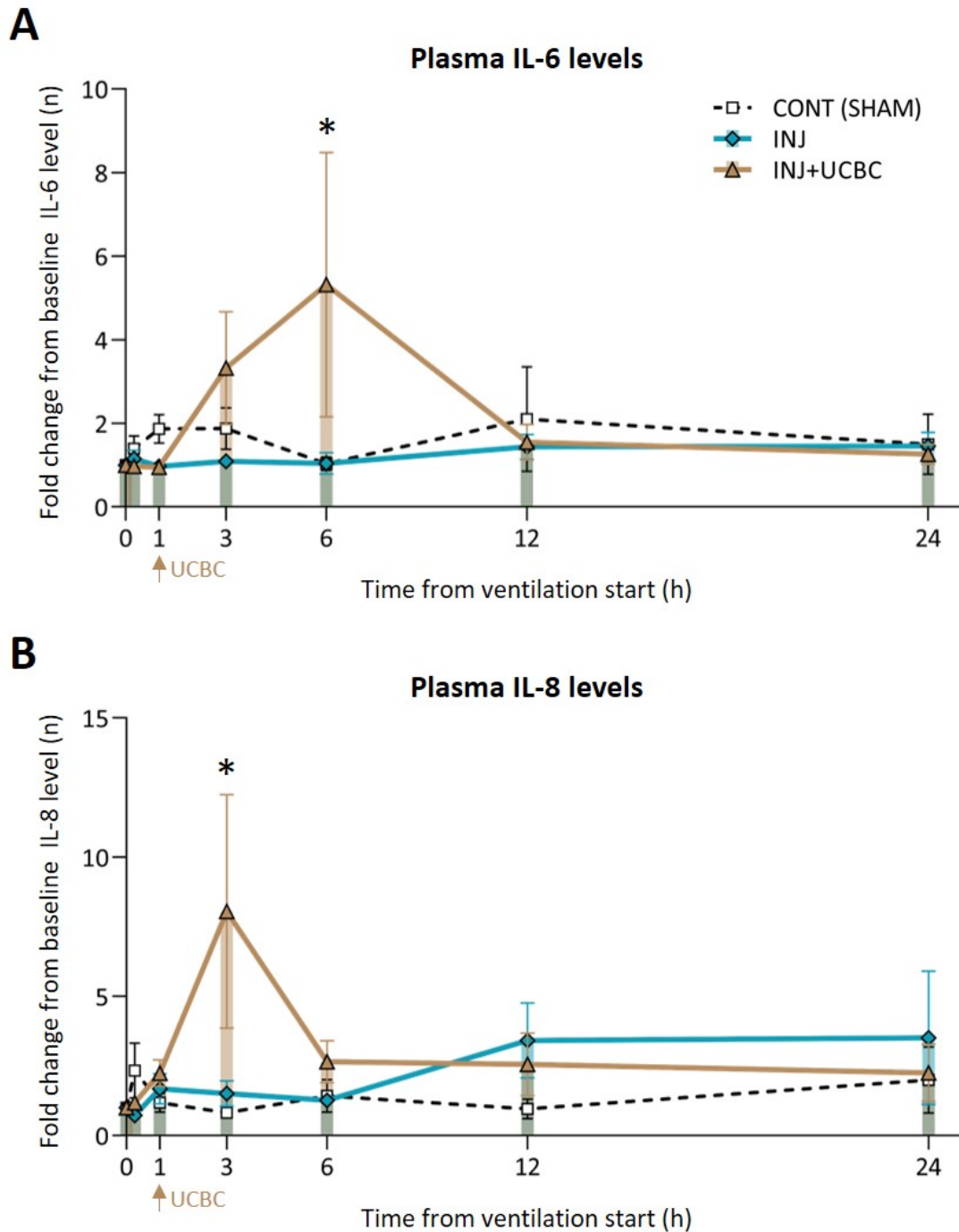


Figure 4.1. Plasma cytokine levels over 24 h. (A) IL-6 levels were not different over time in CONT (white) and INJ (blue). IL-6 levels in INJ+UCBC (brown) was highest at 6 h, and this was higher than CONT and INJ. **(B)** IL-8 levels were not different over time in CONT and INJ. IL-8 levels in INJ+UCBC was highest at 3 h, and this was higher than CONT and INJ. CONT consists only of SHAM animals as no plasma was collected from UNOP animals. Data are presented as mean \pm SEM.

* $p < 0.05$

4.3.3. Gene expression levels of inflammatory cytokines

The mRNA expression of cytokines interleukin 1 beta (*IL1B*), interleukin 6 (*IL6*), interleukin 8 (*IL8*), interleukin 10 (*IL10*), tumour necrosis factor (*TNF*), C-C motif chemokine ligand 2 (*CCL2*), and transforming growth factor beta 1 (*TGFB1*) were not different between INJ and INJ+UCBC lambs in the PVWM [Fig. 4.2A] and SCWM [Fig. 4.2B].

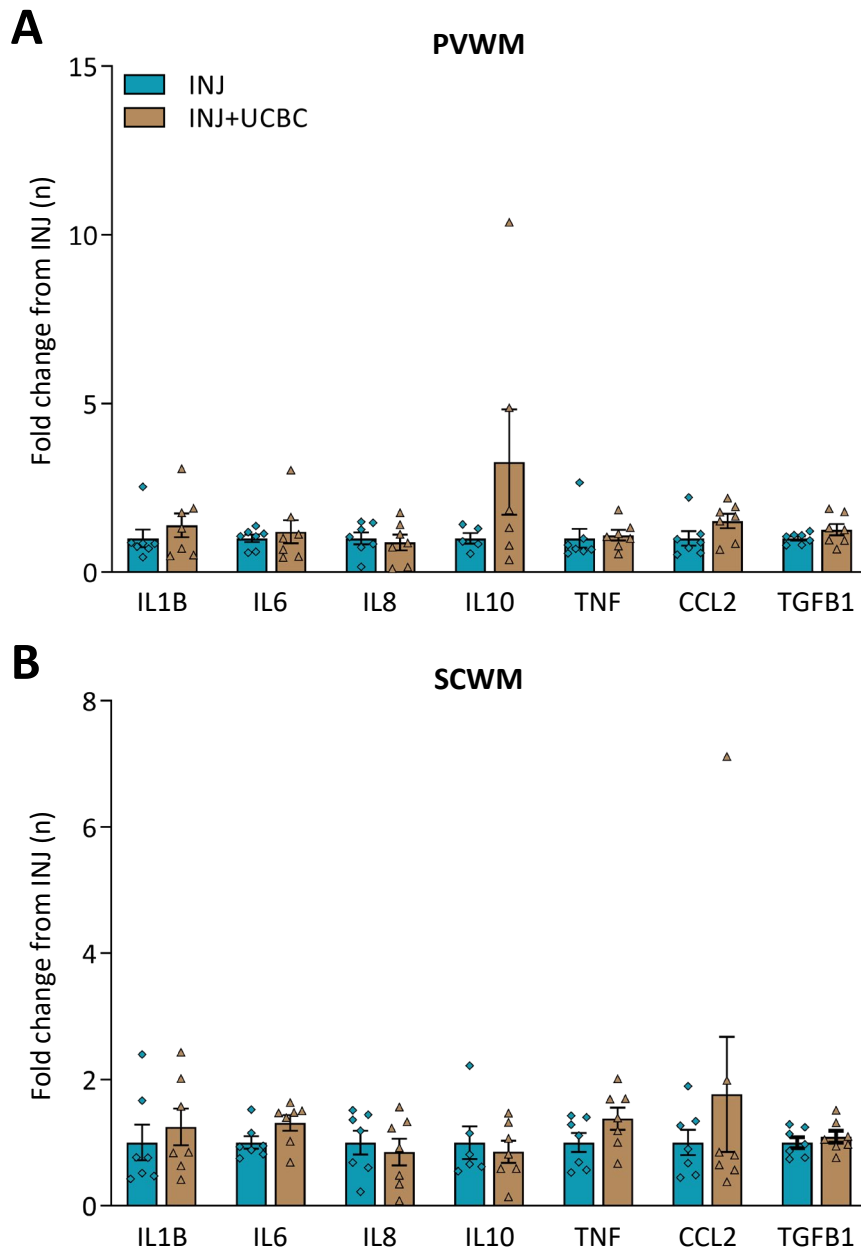


Figure 4.2. Gene expression levels of inflammatory cytokines (*IL1B*, *IL6*, *IL8*, *IL10*, *TNF*, *CCL2*, and *TGFB1*) expressed as a fold change relative to INJ. No differences were observed between INJ (blue) and INJ+UCBC (brown) in the (A) PVWM and (B) SCWM. Data are presented as mean \pm SEM.

4.3.4. UCB cell treatment increased microgliosis

The total number of Iba-1 positive microglia was not different between groups in the PVWM ($p=0.478$). In the SCWM, INJ+UCBC lambs had increased total microglia count compared to CONT ($p=0.003$) and INJ ($p=0.003$; **Fig. 4.3A**). The percentage of amoeboid microglia was not different between groups in the PVWM ($p=0.642$) and SCWM ($p=0.815$; **Fig. 4.3B**).

The number of microglial aggregations was not different between groups in the PVWM ($p=0.940$) and SCWM ($p=0.099$; data not shown). The percentage of white matter occupied by microglial aggregations was not different between groups in the PVWM ($p=0.591$). In the SCWM, INJ+UCBC lambs had an increased percentage white matter occupied by microglial aggregations compared to CONT ($p=0.030$) and INJ ($p=0.030$; **Fig. 4.3C**). The fractional coverage of microglia within aggregations was not different between groups in the PVWM ($p=0.602$). In the SCWM, INJ had decreased fraction coverage of microglia within aggregations compared to CONT ($p=0.048$) and INJ+UCBC ($p=0.020$; **Fig. 4.3D**).

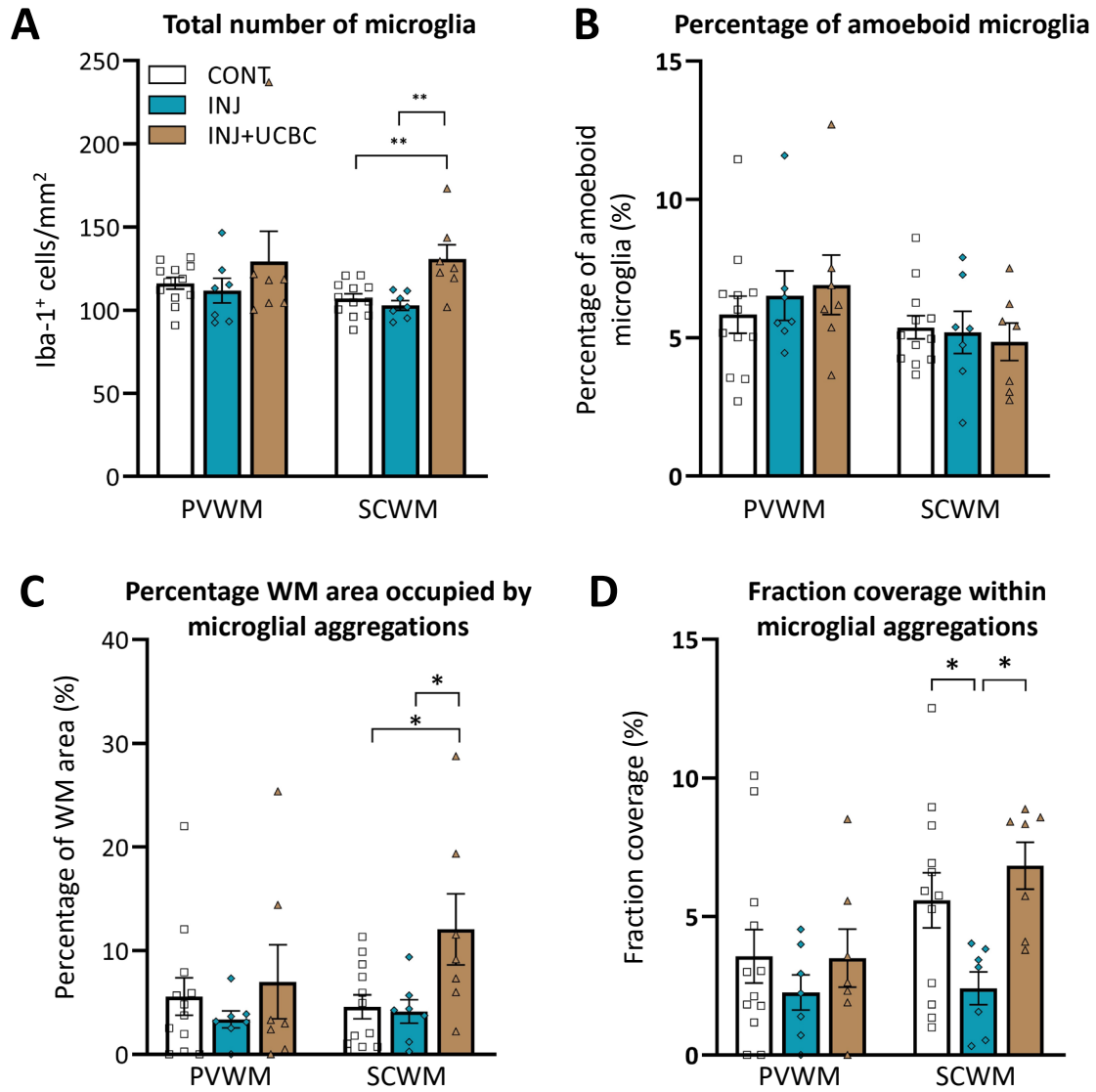


Figure 4.3. Iba-1 immunoreactivity. (A) The total number of microglia was increased in INJ+UCBC (brown) compared to CONT (white) and INJ (blue) in the SCWM. (B) The percentage of amoeboid microglia was not different between groups in both the PVWM and SCWM. (C) The percentage of white matter area occupied by microglial aggregations was increased in INJ+UCBC compared to CONT and INJ in the SCWM. (D) The fraction coverage of microglia within aggregations was decreased in INJ compared to CONT and INJ+UCBC in the SCWM. Data are presented as mean \pm SEM. * $p < 0.05$

4.3.5. UCB cell treatment altered blood brain barrier integrity

In the PVWM, mRNA expression of tight junction proteins occludin (*OCN*) and claudin 1 (*CLDN1*) were not different between INJ and INJ+UCBC lambs. The mRNA expression of mediators of angiogenesis vascular endothelial growth factor A (*VEGFA*), VEGF receptor 1 (*VEGFR1*), angiopoietin 1 (*ANGPT1*), hypoxia-inducible factor 1 subunit alpha (*HIF1A*), and NADPH oxidase 2 (*NOX2*) were not different between INJ and INJ+UCBC lambs [Fig. 4.4A].

In the SCWM, mRNA expression of *CLDN1* was decreased in INJ+UCBC compared to INJ lambs ($p<0.001$). mRNA expression of *VEGFA* was decreased ($p=0.039$) while expression of *ANGPT1* was increased ($p=0.046$) in INJ+UCBC compared to INJ lambs. No other differences were observed [Fig. 4.4B].

The number of blood vessel profiles with protein extravasation was increased in INJ+UCBC compared to INJ ($p=0.021$) and CONT ($p=0.021$) in the PVWM. In the SCWM, the number of blood vessel profiles with protein extravasation was increased in INJ+UCBC compared to CONT ($p=0.018$) [Fig. 4.5].

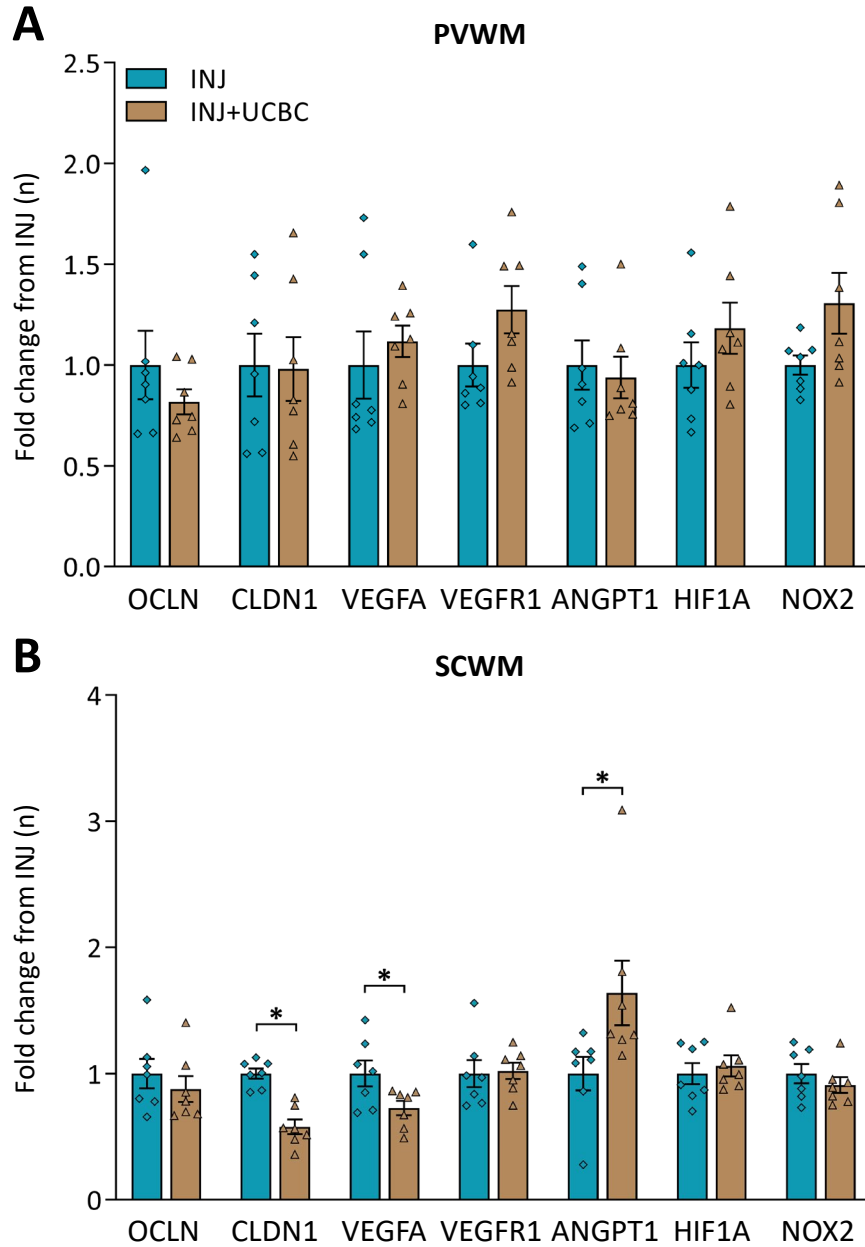


Figure 4.4. Gene expression levels of tight junction proteins (*OCLN* and *CLDN1*) and mediators of angiogenesis (*VEGFA*, *VEGFR1*, *ANGPT1*, *HIF1A*, and *NOX2*) expressed as a fold change relative to INJ. (A) No differences were observed between INJ (blue) and INJ+UCBC (brown) in the PVWM. (B) In the SCWM, INJ+UCBC had decreased *CLDN1* and *VEGFA* expression and increased *ANGPT1* expression. Data are presented as mean \pm SEM. * $p < 0.05$

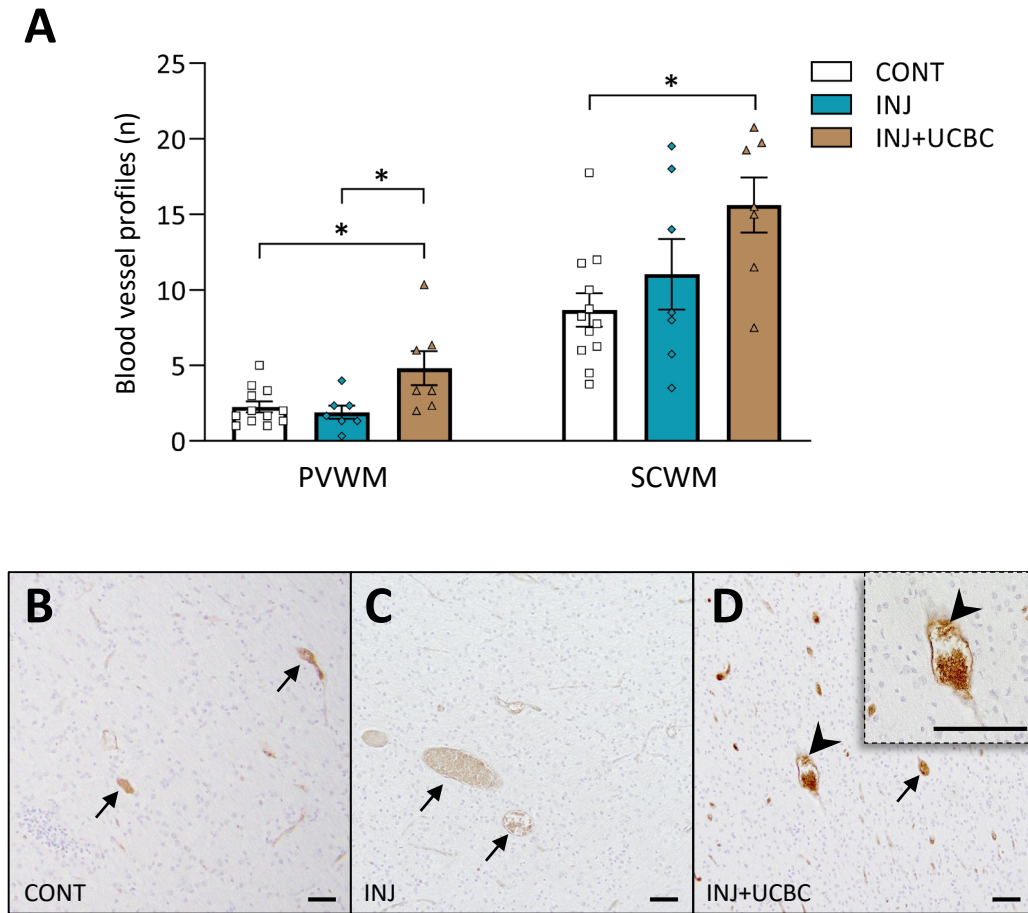


Figure 4.5. Sheep serum immunoreactivity. (A) Vascular protein extravasation was increased in INJ+UCBC (brown) compared to CONT (white) and INJ (blue) in the PVWM. In the SCWM, INJ+UCBC animals had more blood vessel profiles with protein extravasation than CONT animals. Representative images of sheep serum immunohistochemistry in **(B)** CONT, **(C)** INJ, and **(D)** INJ+UCBC. Arrow indicates intact vessels and arrowhead indicates a compromised vessel with protein extravasation, magnified in insert. Scale bar = 50 μ m. Data are presented as mean \pm SEM. * p <0.05

4.3.6. UCB cell treatment reduced the number of oligodendrocytes

The number of Olig2-positive cells was decreased in INJ+UCBC compared to INJ ($p=0.008$) and CONT ($p=0.008$) in the PVWM. The number of Olig2-positive cells was decreased in INJ+UCBC compared to INJ ($p=0.017$) and CONT ($p=0.019$) in the SCWM [Fig. 4.6].

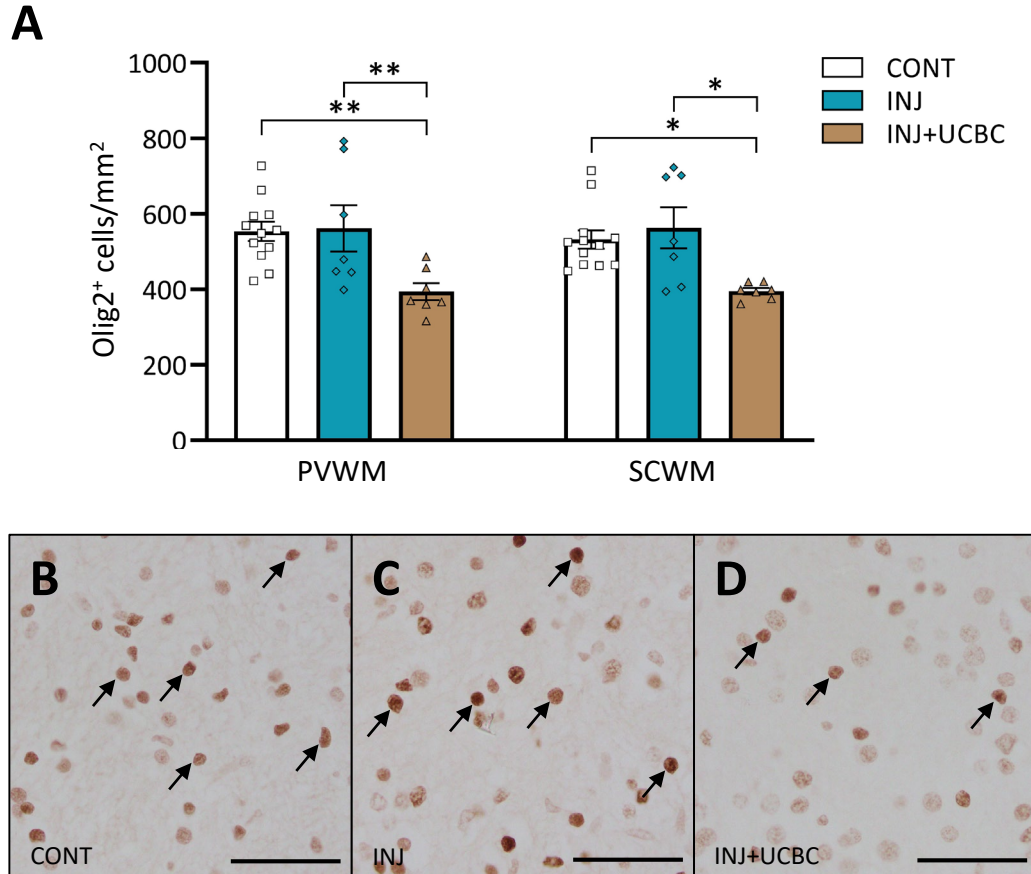


Figure 4.6. Olig2 immunoreactivity. (A) The number of Olig2-positive cells was decreased in INJ+UCBC compared to CONT (white) and INJ in both the PVWM and SCWM. Representative images of Olig2 immunohistochemistry in (B) CONT, (C) INJ, and (D) INJ+UCBC. Arrow indicates Olig2-positive cell. Scale bar = 50 μ m. Data are presented as mean \pm SEM. * $p<0.05$

4.3.7. Gene expression levels of markers of cell death

The mRNA expression of markers of cell death tumour protein p53 (*P53*) and caspase 3 (*CASP3*) were not different between INJ and INJ+UCBC lambs in the PVWM and SCWM [Fig. 4.7].

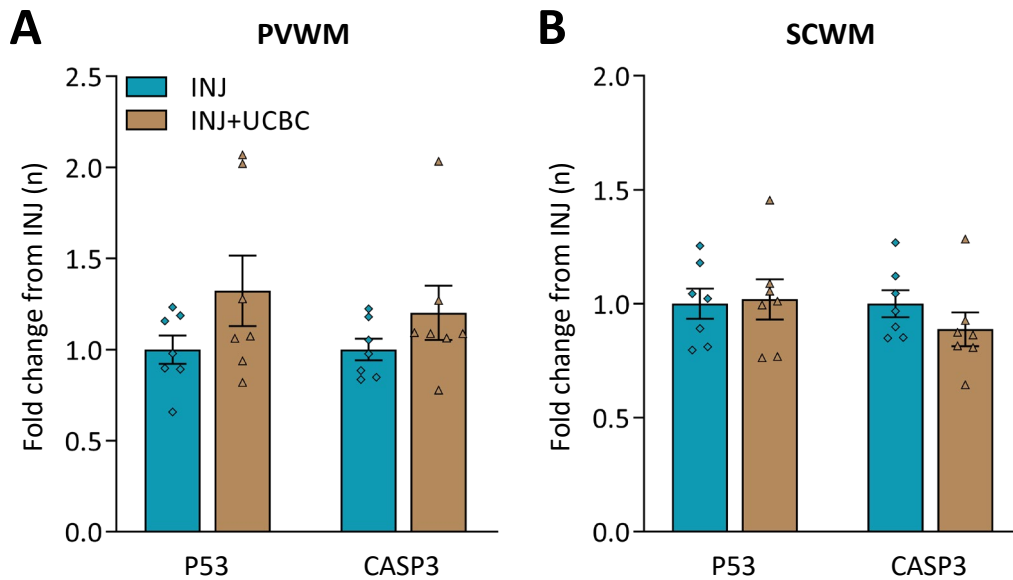


Figure 4.7. Gene expression levels of markers of cell death (*P53* and *CASP3*) expressed as a fold change relative to INJ. No differences were observed between INJ (blue) and INJ+UCBC (brown) in the (A) PVWM and (B) SCWM. Data are presented as mean \pm SEM.

4.4. Discussion

Preterm infants are susceptible to VIBI following delivery room resuscitation. UCB cells have been proposed as a potential therapy for neuroprotection due to their anti-inflammatory, anti-apoptotic, and growth-factor support properties.^{184,185,188,209–211} In this study, I aimed to examine whether UCB cells could prevent or reduce acute VIBI resultant from 15 min of injurious ventilation. I showed for the first time that administration of UCB cells 1 h after the initiation of injurious ventilation has potential adverse effects including increased systemic and cerebral inflammation, decreased BBB integrity, and decreased oligodendrocyte count in the cerebral white matter of preterm lambs when assessed at 24 h.

This study aimed to determine whether the anti-inflammatory properties of UCB cells can protect the immature brain from VIBI caused by high V_T ventilation. The UCB cells were administered intravenously to the fetus 1 h after ventilation onset; this early time point was chosen to try to interrupt the pathways of VIBI before brain injury progression. Specifically, studies found that pro-inflammatory cytokine mRNA levels of *IL1B*, *IL6*, and *MCP1 (CCL2)* in the lungs were upregulated by >20-fold compared to unventilated controls at 1 h after 15 min of injurious ventilation, and these increases were largely resolved by 6 h.²¹² Further, it has been observed that plasma pro-inflammatory cytokine levels (e.g. IL-1 β , IL-8, TNF) are increased in late preterm infants after 2 h of ventilation.⁹¹ The 1 hour time point in this study aimed to dampen the peak of the inflammatory response within the lungs, before profound systemic inflammation. In this study, I chose to give ~25 million cells/kg intravenously to the fetus at 45 minutes after the cessation of ventilation. This treatment dose is based on previous studies where 50 million allogeneic UCB cells in fetal sheep (0.7 gestation; ~30 million cells/kg) and 100 million autologous UCB cells in newborn lambs (0.97 gestation) reduced cerebral inflammation and cell death.^{184,188} Accordingly, a dose of 80 million UCB cells was selected for sheep at 0.85 gestation, targeting 25 million cells/kg based on historical post-mortem lamb weight data. The average dose delivered was 24.5 ± 5.0 million cells/kg, with a range of 18.8–32.7 million cells/kg. Within this range, linear regression analysis showed no correlation between dose and brain injury outcomes.

Unfortunately, as explained in Chapter 3, I was not able to achieve sufficiently high V_T to induce VIBI, and therefore could not appropriately address the aim of this study. Interestingly, what my results do show is that measures of brain inflammation and injury were increased in the UCB cells-treated group. Importantly, all baseline and ventilation parameters of the INJ and INJ+UCBC groups were not different, meaning the brain injury that I have observed is unlikely due to animals in the UCB cells-treated group receiving more injurious ventilation. Moreover, fetuses in both groups remained *in utero* during the 24 h to remove the need for ongoing intensive care, and hence potential confounders to brain injury. Although animals in the INJ group did not receive a vehicle infusion, it is unlikely that the

infusion volume (<1% blood volume by weight) evoked a haemodynamic or physiological response that contributed to the additional inflammation and injury observed in the UCB cells-treated animals. We have shown previously that the lungs of animals in both groups were injured after ventilation and that UCB cells did not reduce lung injury but did not adversely affect lung tissue either (Appendix III).¹⁸⁹

Neuroinflammation is a key mediator of preterm brain injury and VIBI. Neuroinflammation following UCB cells was histologically evident as increased microglia counts and denser microglial aggregations in the SCWM of INJ+UCBC animals. Microglia are the resident immune cells of the central nervous system (CNS). Besides playing an important physiological role in development, microglia help to modulate the microenvironment.³⁸ An increase in microglia activity may be indicative of ongoing inflammation or itself contribute to inflammation.³⁸ Furthermore, *in vitro* studies suggest that microglia activation may be related to BBB disruption.⁴⁰

Compromised cerebral vasculature and BBB integrity are important contributors to preterm brain injury and VIBI. Disruption of vascular integrity can manifest as haemorrhagic injury while increased BBB permeability renders the immature brain vulnerable to infiltration of systemic inflammatory cytokines and leukocytes which may promote a localised cerebral inflammatory response.¹²⁵ The mRNA expression of *CLDN1*, a key tight junction protein, was decreased in the SCWM in the INJ+UCBC compared to the INJ group. This could be an indicator of decreased BBB permeability⁵⁶ although I have not looked at CLDN1 protein levels to confirm this. Histologically, the number of blood vessel profiles with protein extravasation were increased in both the PVWM and SCWM of INJ+UCBC animals. Protein extravasation is an indication of compromised vessel integrity and the presence of serum albumin, which usually cannot cross the BBB into tissue because of its size, can elicit inflammation by activating microglia.²¹³ Additionally, there was an increase in pro-angiogenic factor *ANGPT1* and a decrease in *VEGFA* mRNA levels in the SCWM. An increase in ANGPT1 production by pericytes and astrocytes of the neurovascular unit has been associated with heightening BBB integrity.⁴⁰ UCB cells have been shown to increase *VEGFA* gene expression but not protein expression in the cortex of adult rats after stroke.²¹⁴ It is unclear why I have observed a decrease in *VEGFA* gene expression and if this preceded vascular protein extravasation or was in response to it.

I assessed the total number of oligodendrocytes using the pan-oligodendrocyte marker Olig2 and found that the number of oligodendrocytes was lower in both the PVWM and SCWM in the INJ+UCBC group compared to INJ. This contrasts with previous studies where UCB cells prevented the loss of oligodendrocytes in preterm lambs after hypoxic-ischaemic injury.^{185,188} I suspect that the oligodendrocyte progenitor cells and pre-oligodendrocytes rather than mature and myelinating oligodendrocytes are affected in our study as preliminary myelin basic protein (MBP) analysis has found

no differences between groups (data not shown; PVWM $p=0.951$; SCWM $p=0.726$) – this is an important focus for future investigations. MBP is a major constituent of myelin sheaths and is specifically expressed in mature and myelinating oligodendrocytes in the CNS. Attempts to further characterise the maturational progression of oligodendrocytes with oligodendrocyte markers O1 and O4 were unsuccessful but should be explored in future studies. Additionally, while gene expression levels of markers of cell death were not different between groups, I have not examined apoptosis or cell death histologically and thus cannot speculate if that is a reason for the decrease in oligodendrocytes. Nevertheless, reduced oligodendrocytes may reflect or result in alterations in myelination, which is the underlying cause of white matter injury seen in premature infants.¹⁰

I did not label the UCB cells in this study and hence could not trace if they entered the brain parenchyma. UCB cells have previously been shown to be present in low numbers in the brain after intravenous administration in preterm¹⁸⁸ and near-term¹⁸⁴ lambs. Within the CNS, UCB cells can exert direct effects on the brain although cell engraftment is not necessary to mediate protective effects.^{186,187} Trophic factors (e.g. glial cell line-derived neurotrophic factor [GDNF] and brain-derived neurotrophic factor [BDNF]) secreted by certain cell types within UCB can cross the BBB to also directly affect the brain.¹⁸⁷ However, studies suggest that the main effects of UCB cells are in the periphery, where they modulate systemic inflammation.^{171,187} Hence, I wondered if the increased markers of cerebral injury observed were mediated by changes in systemic inflammation.

I investigated the systemic inflammatory profile by measuring plasma IL-6 and IL-8 levels, for which an upregulation is associated with preterm brain injury.⁴² I initially expected that circulating levels of IL-6 and IL-8 would be increased in response to high V_T ventilation and that UCB cells would decrease levels of these pro-inflammatory cytokines, given the variety of anti-inflammatory cells present within UCB. However, in my model, injurious ventilation alone did not increase systemic inflammation (detailed in Chapter 3), and so it was unexpected to observe an increase in IL-6 and IL-8 levels following early UCB cells administration. Previous studies have found that allogeneic UCB cell therapy 12 h after hypoxia-ischaemia in preterm-equivalent fetal sheep did not change circulating IL-6 levels at 12 h¹⁸⁸ and autologous UCB cell therapy 12 h after birth asphyxia in near-term sheep did not change circulating IL-6 levels at 15 min, 12 h, 24 h, and 36 h after cell administration.¹⁸⁴ My results are comparable in that at the closest similar time points assessed (11 h and 23 h after UCB cells), IL-6 was at baseline levels. My results suggest that IL-6 levels have returned to baseline levels by 12 h after increasing prior. Indeed, the current study provides new information of IL-6 levels at time points prior to 12 h, when systemic inflammation appears to be affected by UCB cell administration. I also assessed IL-8 levels and found a similar pattern – IL-8 levels were increased after UCB cells administration but

returned to baseline levels by 12 h. Given the periodic nature of my blood sampling, I do not know the peak timing of pro-inflammatory cytokine increase or if cytokine levels increased beyond what I have assayed in the time in between measurements. It is important to note that there are key differences between the studies: experimental insult (asphyxia vs VIBI) and, more importantly, the timing of UCB cells administration (12 h vs 1 h post-insult).¹⁸⁴ Regardless, that UCB cell administration following injurious ventilation can increase systemic IL-6 and IL-8 within hours is concerning and requires follow-up investigations.

There is no obvious upstream inflammatory event to account for the elevated systemic inflammation since pulmonary inflammation and injury was not increased in INJ+UCBC compared to INJ animals when assessed at 24 h (Appendix III).¹⁸⁹ The UCB cells likely acted at a systemic level, and so the environment that I have introduced the cells to becomes an important consideration in trying to understand why they have behaved this way. Given that INJ animals had increased lung inflammation and injury¹⁸⁹ but not increased systemic IL-6 and IL-8 compared to CONT animals, it remains unknown if my ventilation strategy caused systemic inflammation not detected by indices I measured or if it simply did not cause systemic inflammation as intended. Accordingly, there are two possibilities to the environment I have introduced the UCB cells to: 1) an undetected mild pro-inflammatory environment or 2) an apparent 'healthy' low- or non-inflammatory environment.

In the first scenario, I speculate that introducing UCB cells in a subclinical inflammatory environment promoted them to take on a pro-inflammatory phenotype, leading to increased systemic IL-6 and IL-8 levels. The concept has been demonstrated previously given that MSCs can polarise to a pro-inflammatory phenotype when exposed to an established inflammatory environment.^{215,216} However, term UCB has been found to contain fewer MSCs than preterm UCB samples, and MSCs are completely absent in 10-30% of human term UCB samples.^{171,178} It is likely that the term UCB cells administered in my study had almost no MSCs. However, even if MSCs were present, their pro-inflammatory activities, such as IL-6 production, have also been suggested to be beneficial in the early phase of inflammation by directing monocytes and macrophages towards anti-inflammatory phenotypes.²¹⁵ Therefore, it is difficult to infer what elevated plasma IL-6 in my study means, although combined with the increased brain injury observed, it is reasonable to postulate that it is detrimental.

In the second scenario, perhaps the introduction of UCB cells has elicited an inflammatory response independent of the actions of the cells. In this study, I administered allogenic UCB cells from near-term sheep and did not assess any cardiovascular parameters in the period after UCB administration. Previous studies have found that autologous UCB cell administration in asphyxiated term lambs did not alter mean arterial pressure,¹⁸⁴ but allogeneic term UCB cell therapy in preterm fetal sheep with hypoxic-

ischaemic injury caused a transient systemic physiological response reflected by elevated mean arterial pressure for 24 h.¹⁸⁵ Given the differences in study designs (source of UCB cells, dose, injury model, fetal or postnatal model, gestational age), more research is required to understand the potential cardiovascular effects of administering UCB cells. Additionally, while I have interpreted the increase in systemic cytokine levels as a potentially adverse upstream event that led to the brain injury observed, increased IL-8 12 days after allogeneic UCB cell treatment has in fact been associated with improved motor function at 6-months post-treatment in children with cerebral palsy.²¹⁷ It has further been suggested that one of the mechanisms underlying the efficacy of UCB cells involves innate immune responses and microglia recruitment.²¹⁷ Longer assessments of the impact of the UCB cells are required to determine whether the acute changes I observed were injurious or beneficial.

Importantly, UCB contains a heterogeneous population of cells. I do not know the proportion of the major cell types (monocyte-derived suppressor cells, regulatory T cells, MSCs, endothelial progenitor cells, and haematopoietic stem cells) administered in the current study. How each subset interacts with mechanical ventilation is poorly understood and it is possible that the detrimental effects observed here are attributed to specific cell types, such as MSCs as mentioned above. It is hence premature to dismiss the efficacy of all cell types within UCB, but certainly caution should be taken in using the whole mononuclear fraction of UCB in similar contexts as that in this study.

Altogether, my findings indicate that introducing UCB cells 1 h post-ventilation has detrimental cerebral effects in fetal sheep. Early administration of UCB cells in conjunction with mechanical ventilation should be avoided until we better understand the interactions of UCB cells and the environment they are put into. I administered UCB cells 1 h post-ventilation with the aim to interrupt the progression of VIBI and prevent or reduce injury manifestation. Previous studies have found that earlier administration of UCB cells at 12 h compared to 5 days post-insult was more efficacious¹⁸⁸ and a delay in peripheral trophic factors entering the brain parenchyma diminishes the neuroprotective capacity of UCB cells.¹⁸⁷ My findings suggest that, in the context of VIBI, earlier may not necessarily be better. Perhaps UCB cells may be efficacious when administered at a later time point as a reparative therapy. This may be the focus of future studies.

4.5. Conclusion

My aim was to investigate the efficacy of UCB cells to reduce VIBI. I demonstrated that a single prophylactic systemic dose of UCB cells caused inflammation and brain injury in white matter regions of preterm ventilated sheep, even in the background of no overt injury caused by the ventilation strategy. While the dose and timing of administration, mechanisms of action of UCB cells, and their interaction

with ventilation require further clarification, I discourage the use of UCB cells immediately after birth, as administered in our study.

Chapter Five: VIBI From Prolonged Ventilation

A future direction from Chapter 3 is to revisit the contribution of prolonged ventilation on cerebral white matter injury as it may play a larger role in ventilation-induced brain injury (VIBI) than previously presumed. However, there are limited approaches to isolate the effects of prolonged ventilation, and preclinical experimental set-ups designed to overcome this have so far focussed on physiology and lung mechanics and injury. Therefore, in this chapter, I sought to examine the effects of 24 h of ongoing ventilation on the cerebral white matter of preterm-equivalent fetal sheep and to determine if an *in utero* ventilation sheep model is suitable to study chronic VIBI.

5.1. Introduction

The majority of very and extremely preterm infants require long periods of respiratory support in the days after birth while in the neonatal intensive care unit (NICU).^{61,64,73} Assisted ventilation is relatively well-controlled in the NICU and ventilatory parameters are less likely to be injurious compared to the initiation of ventilation in the delivery room¹⁰¹ as explored in Chapters 3 and 4. In contrast, ventilation in the NICU tends to be for a much longer duration, with preterm infants receiving an average of 1.0-17.7 days of assisted ventilation, depending in part on the gestational age (GA) at birth.^{64,73,74} The prolonged need for intubation and mechanical ventilation has been associated with increased brain injury and impairments,^{60,62,75,105} for which there are no effective treatments. These include increased risks of periventricular leukomalacia, diffuse cerebral white and grey matter lesions, cerebral palsy, and attention deficit hyperactivity disorder.^{60-62,73,75,98,105,107} Limiting the duration of mechanical ventilation to reduce complications is not always feasible with very and extremely preterm infants, hence there is a real need to understand the aetiology of VIBI in this setting to aid development of therapeutic interventions. However, it is challenging to isolate the effects of prolonged ventilation in clinical studies and most preclinical models currently used. For example, chronic ventilation *ex utero* (after delivery) is accompanied by many interventions required to ensure the very preterm infant or lamb is kept alive, and these may confound an isolated study on VIBI. The novel *in utero* ventilation (IUV) sheep model might be able to address this problem.

The IUV sheep model has been used to study the effects of prolonged ventilation on the immature lungs.^{165,218,219} This model has significant advantages compared to conventional neonatal ventilation animal models, most notably that the effect of the duration of ventilation can be studied in isolation.²¹⁸ While long-term postnatal studies encompass all aspects of NICU management and play important

roles in translational research, they are less informative for investigating the contribution of specific variables because any outcomes assessed are influenced by accompanying interventions. Indeed, the requirement for analgesia and anaesthetics^{102–104}, inotropes,^{220–222} and oxygenation¹⁰⁵ may be confounders to brain injury. Thus, the benefit of the IUV model is that the fetus is supported by the placenta for oxygen and nutrition²¹⁸ and does not require anaesthetics for ethical wellbeing²²³ so that the effects of ventilation can be studied independently.

The other major advantage of the IUV model is that we can study animals at a stage of brain development more closely resembling that of very and extremely preterm human infants. Postnatal studies have been limited by the preterm animal's lung function – in sheep, fetal lungs at 110 days GA are in the mid-late canalicular to saccular stage of development, are relatively surfactant-deficient, and are developmentally similar to that of a 22–26 week human infant.^{224,225} Fetal ovine lungs can conduct gas exchange from about 117 days GA, though not efficiently,^{224,225} and lambs at 125 days GA have more commonly been used in preterm experiments. At 125 days GA, the ovine lung is in the late saccular to alveolar stage of development, in the early stage of surfactant production, and lung development at this stage is comparable to that of a 26–28 week human infant.^{224,225} In sheep, brain development is more advanced in late gestation than the lungs, relative to humans. Thus, in most postnatal preterm sheep studies, white matter development is in fact more comparable to that of a late preterm or term human infant.^{203,204} With IUV, because the fetus remains on placental support for gas exchange, fetuses of younger GA where lung function is inadequate to support life *ex utero* can be used. It is therefore possible to study animals at a stage of brain development more closely resembling that of very and extremely preterm human infants. Despite these strengths of the IUV model, its relevance to investigate VIBI has not been reported.

I aimed to characterise the effects of IUV on the immature brain. I hypothesised that ventilating fetal sheep at 110 days GA (0.75 gestation), equivalent to 30–35 weeks human white matter brain development,^{203,204} *in utero* for 24 h using a strategy that causes ventilation-induced lung injury would result in an increase in systemic and cerebral inflammation, compromise the blood-brain barrier integrity, and alter cell types within cerebral white matter.

5.2. Methods

The detailed experimental methodology used in this study is provided in Chapter 2. Below is a concise overview. Experimental procedures were approved by the Monash Medical Centre Animal Ethics Committee A, Monash University, and were conducted in accordance with guidelines established by the National Health and Medical Research Council of Australia.

Animals were randomised to one of two groups:

- 1) Sham control (**CONT**; n=10): Fetuses underwent fetal surgery, were instrumented, but did not receive ventilation.
- 2) *In utero* ventilation (**VENT**; n=9): Fetuses received 24 h of ventilation whilst *in utero*.

5.2.1. Instrumentation

Pregnant ewes underwent aseptic surgery at 110 ± 1 days gestation (mean \pm SD; term ~148 days). During surgery, the head and neck of the fetus were exteriorised via a midline laparotomy for instrumentation. A tracheostomy was performed on the fetus to secure a modified reinforced endotracheal tube (ID 4.0 mm; Medtronic, MN, USA) in the lower trachea and connected to a saline-filled large-bore ventilation tube (ID 6.4 mm, OD 12.7 mm). A separate saline-filled catheter (ID 3.2 mm, OD 6.4 mm) was inserted into the upper trachea and connected to the ventilation tube externally to create an exteriorised tracheal loop which allowed normal flow of lung liquid.^{165,226} Heparinised polyvinyl catheters were inserted in the left carotid artery and jugular vein (ID 0.86 mm, OD 1.52 mm; Dural Plastics & Engineering, NSW, Australia) and in the amniotic sac (ID 2.6 mm, OD 4.2 mm). All catheters and the tracheal loop were externalised through the ewe's flank via a small incision. The fetus remained *in utero* and the ewe abdomen was sutured closed. Ewes and fetuses were allowed 24–48 h to recover after surgery.

5.2.2. Ventilation strategy and blood gas sampling

At 112 ± 1 days gestation, the ventilation tube was disconnected, lung liquid was passively drained, and the tube was connected to a neonatal ventilator (Babylog 8000+, Dräger, Lübeck, Germany). Fetuses were ventilated with room air for 24 h using a maximum peak inspiratory pressure (PIP) of 45 cmH₂O, positive end-expiratory pressure of 5 cmH₂O, inspiratory flow of 10 l/min, and rate of 60 inflations/min, in reference to previous IUV studies that induced ventilation-induced lung injury.^{165,218,219} Sustained inflations at 35 cmH₂O for 5 s duration were applied to recruit the lung if necessary. Tidal volume (V_T) was monitored to avoid exceeding 5 ml/kg and overinflating the lungs. Fetal arterial blood was sampled regularly throughout the 24 h to assess fetal wellbeing and plasma was collected at specific time points for cytokine analysis (before ventilation [PRE], 15 min, 1 h, 3 h, 6 h, 9 h, 12 h, and 24 h after the commencement of ventilation).

5.2.3. Brain collection

At 24 h from the initiation of ventilation, ewes and fetuses were euthanised (sodium pentobarbitone >100 mg i.v.; Valabarb Euthanasia Solution; Jurox, NSW, Australia). The fetus was

removed from the ewe at autopsy, the fetal brain was removed from the skull, and the cerebrum was halved along the medial longitudinal fissure. The periventricular and subcortical white matter (PVWM; SCWM) were dissected from the left cerebral hemisphere and snap-frozen in liquid nitrogen. The right cerebral hemisphere was immersion fixed in 10% neutral buffered formalin (NBF; Amber Scientific, WA, Australia) overnight. The right hemisphere was then cut coronally into 5 mm blocks (8-9 blocks/animal), post-fixed in 10% NBF for 6 days, processed, and embedded in paraffin. Serial sections (8 μ m) were cut from one block each at the level of frontal, parietal, and temporal lobes for histological and immunohistochemical analysis.

5.2.4. Histological staining and analysis

Coronal sections from comparable sites of the frontal and parietal lobes (2 slides/animal) were stained with haematoxylin (Harris haematoxylin; Amber Scientific, WA, Australia) and eosin (Eosin 1% aqueous solution; Amber Scientific) to examine gross neuropathology. Sections were viewed under the microscope (BX-41 Laboratory Microscope, Olympus Corporation, Tokyo, Japan) and scored according to the presence of cystic lesions/parenchymal damage, compromised vessel integrity, and hypercellularity in the PVWM and SCWM and disrupted cytoarchitecture in the cortex. Each category was scored on a scale of 0-2 based on severity and a mean of all categories was calculated as a final score for each section. A mean of all lobes was calculated for each animal and then collectively averaged for each experimental group. Slides were coded and the observer (KC) was blinded to the experimental groups.

5.2.5. Immunohistochemistry

Coronal sections from comparable sites of the frontal, parietal, and temporal lobes (3 slides/animal) were stained with rabbit anti-ionised calcium binding adapter molecule-1 (Iba-1; 1:1500, Wako Pure Chemical Industries, Osaka, Japan) to identify microglia, rabbit anti-sheep serum (1:1000, Sigma-Aldrich, MO, USA) to identify vascular extravasation of protein, and mouse anti-oligodendrocyte transcription factor-2 (Olig2; 1:1000, Merck, Darmstadt, Germany) for oligodendrocytes. Prior to incubation with anti-Iba-1 and anti-Olig2, sections were pre-treated with citrate buffer (pH 6.0) in a microwave oven. Sections were incubated with secondary antibody biotinylated goat anti-rabbit or goat anti-mouse immunoglobulin G (IgG; 1:200; Vector Laboratories, CA, USA) and reacted using the Vectastain Elite ABC Kit (Vector Laboratories). Staining was absent when the primary antibody was omitted. Sections reacted with anti-sheep serum were counterstained with 20% haematoxylin (Harris haematoxylin, Amber Scientific).

5.2.6. Quantitative immunohistochemical analysis

Analyses were conducted at equivalent sites within the cerebral white matter of sections from the frontal, parietal, and temporal lobes of each lamb. Non-overlapping fields of view in the PVWM were taken medial to lateral from the ventricle, and fields in the SCWM were obtained from alternating gyri starting from the second gyrus closest to the midline. Slides were coded and the observer (KC) was blinded to the experimental groups.

The proportion of PVWM and SCWM occupied by Iba-1-positive microglial aggregations was assessed using ImageScope (Aperio Technologies, CA, USA); individual aggregation areas were summed then divided by the total area of PVWM or SCWM of the section, data expressed as a percentage. The fraction areal coverage (%) of Iba-1 immunoreactivity within an aggregation was assessed using a set intensity threshold (FIJI; ImageJ, NIH Image, MD, USA).

Areal density (cells/mm²) of Iba-1-positive microglia was quantified in 3 non-overlapping fields in the PVWM and 6 non-overlapping fields in the SCWM from 2 separate gyri, avoiding microglial aggregations, using ImageScope (Aperio Technologies). Microglia were distinguished based on morphology (ramified microglia were characterised by long cellular processes while amoeboid microglia by round, densely stained soma with resorbed processes).¹⁹⁵

Areal density (cells/mm²) of Olig2-positive oligodendrocyte was quantified in 3 non-overlapping fields in the PVWM and 6 non-overlapping fields in the SCWM from 2 separate gyri, using FIJI (ImageJ). Blood vessel profiles with protein extravasation were quantified and expressed as total number of vessel profiles with protein extravasation within the PVWM and SCWM. For all indices, a mean of all lobes was calculated for each animal and then collectively averaged for each experimental group.

5.2.7. Plasma protein analysis

Arterial blood was collected via the fetal carotid artery catheter before ventilation (PRE), and at 15 min, 1 h, 3 h, 6 h, 9 h, 12 h, and 24 h after the initiation of ventilation. Plasma proteins (IL-6 and IL-8) were quantified using a sandwich enzyme-linked immunosorbent assay (ELISA). 96-well flat-bottom plates (Nunc MaxiSorp; Invitrogen, Thermo Fisher Scientific, USA) were coated with mouse anti-ovine IL-6 (1:200, Bio-Rad Laboratories, CA, USA) or mouse anti-ovine IL-8 (1:1000, Bio-Rad) antibodies and incubated overnight at 4°C. The next day, plasma samples were diluted with an equal part of diluting buffer (PBS, 0.1% BSA, 0.05% Tween 20) and incubated in duplicates in the 96-well plates for 1 h at room temperature. After washing, the plates were incubated with respective detecting antibodies (rabbit anti-ovine IL-6, 1:200, Bio-Rad; rabbit anti-ovine IL-8, 1:4000, Bio-Rad) for 1 h at room temperature, washed, then incubated with HRP-conjugated swine anti-rabbit Ig (1:2000, DAKO,

CA, USA) for 1 h at room temperature. After further washing, plates were developed with 3,3', 5,5'-tetramethylbenzidine (TMB chromogen solution; Invitrogen, CA, USA) for 20 min in the dark at room temperature. Reactions were stopped with the addition of 0.5M H₂SO₄. The plates were read on a SpectraMax i3 microplate reader (Molecular Devices, CA, USA) at 450 nm to determine optical density. Standards (recombinant ovine IL-6 or IL-8; Kingfisher Biotech, MN, USA) were included and a standard curve was generated for every ELISA plate used ($R^2 > 0.99$ for all).

5.2.8. Statistical analysis

Cohort characteristics were compared using an independent T-test (Graphpad Prism 8.1.2; GraphPad Software, CA, USA). Blood gas parameters and ELISA data were compared using two-way repeated measures analysis of variance (ANOVA) with Holm-Sidak *post hoc* comparison (SigmaPlot; Systat Software Inc., CA, USA). All immunohistochemical data were compared using an independent T-test (Graphpad Prism 8.1.2). Statistical significance was accepted at $p < 0.05$. Baseline physiological data are presented as mean \pm SD to convey variability in the study cohort. All other data are presented as mean \pm SEM unless otherwise stated.

5.3. Results

5.3.1. Lamb characteristics, ventilation parameters, and arterial blood gas parameters

Lamb characteristics, including body and brain weights, recorded post-mortem were not different between groups [Table 5.1]. We noted that there were more animals with a subdural haemorrhage at post-mortem in VENT compared to CONT lambs but this did not reach statistical significance (33% vs 10%; $p=0.303$). Lambs in the VENT group received 21.9 ± 4.7 h (mean \pm SD) of ventilation with a V_T of 2.36 ± 0.78 ml/kg (mean \pm SD).

Baseline blood gas parameters were not different between groups [Table 5.1]. The partial pressure of oxygen (PaO_2), oxygen saturation level (SaO_2), partial pressure of carbon dioxide ($PaCO_2$), and pH changed with time over the 24 h IUV period. PaO_2 and SaO_2 were not different between groups at any assessed time point [Fig. 5.1A, B]. $PaCO_2$ was higher in VENT than CONT animals at 45 min ($p=0.031$; Fig. 5.1C) and pH was lower in VENT than CONT animals at 30 min ($p=0.047$; Fig. 5.1D). No other differences were observed.

Table 5.1. Lamb characteristics and baseline arterial blood gas parameters. Group characteristics recorded at post-mortem examination were not different between CONT and VENT animals. Baseline arterial blood gas measurements obtained before the commencement were not different between groups. Data are expressed as mean \pm SD.

	CONT	VENT
Group characteristics		
Number (n=)	10	9
Gestational age (d)	113 ± 0	113 ± 1
Sex (% male)	50%	55.6%
Body weight (kg)	2.5 ± 0.4	2.4 ± 0.4
Brain weight (g)	35.5 ± 2.9	34.4 ± 1.5
Subdural haemorrhage (% yes)	10%	33.3%
Volume of lung liquid drained (ml)	N/A	102 ± 13
Duration of ventilation (h)	N/A	21.9 ± 4.7
Arterial blood gas parameters		
pH	7.39 ± 0.01	7.40 ± 0.03
$PaCO_2$ (mmHg)	48.6 ± 2.5	48.7 ± 2.4
PaO_2 (mmHg)	21.8 ± 1.4	21.5 ± 2.6
SaO_2 (%)	67.7 ± 5.7	67.4 ± 7.3

PaCO₂ partial pressure of carbon dioxide; *PaO₂* partial pressure of oxygen; *SaO₂* oxygen saturation.

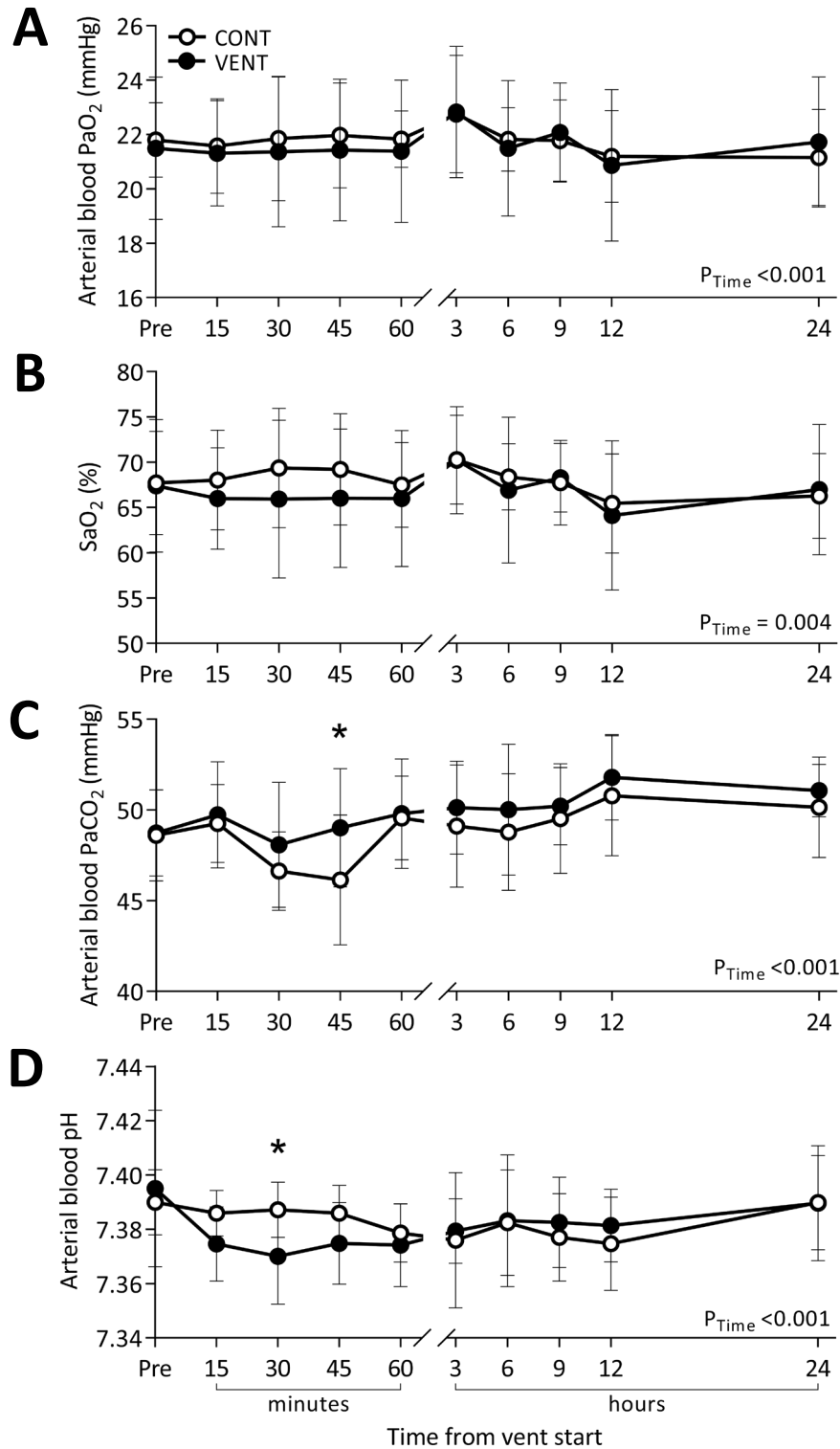


Figure 5.1. Arterial blood gas parameters during 24 h IUUV. The (A) partial pressure of oxygen (PaO_2) and (B) oxygen saturation level (SaO_2) were not different between CONT (open circle) and VENT (filled circle) before (Pre) and at specified time points after the commencement of ventilation. (C) Partial pressure of carbon dioxide (PaCO_2) was higher in VENT than CONT animals at 45 min; no other differences were observed. (D) pH was lower in VENT than CONT animals at 30 min; no other differences were observed. Data presented as mean \pm SD. * $p < 0.05$ between groups.

5.3.2. Plasma and CSF cytokine levels

Plasma IL-6 levels did not change in CONT animals [**Fig. 5.2A**]. In the VENT group, IL-6 levels increased at 6 h (1.8 ± 0.4 -fold) and 9 h (1.8 ± 0.3 -fold) relative to baseline, 15 min, and 24 h levels ($p < 0.05$ for all, **Fig. 5.2A**). Plasma IL-6 levels were higher in VENT than CONT at 6 h ($p < 0.001$), 9 h ($p < 0.001$), and 12 h ($p = 0.045$).

Plasma IL-8 levels did not change in CONT animals [**Fig. 5.2B**]. In the VENT group, IL-8 levels increased at 24 h (5.4 ± 2.0 -fold) relative to all other time points ($p < 0.05$ for all). Plasma IL-8 level was higher in VENT than CONT at 24 h ($p < 0.001$).

Cerebrospinal fluid (CSF) IL-6 and IL-8 levels were not different between groups (IL-6 $p = 0.229$; IL-8 $p = 0.221$; **Fig. 5.3**).

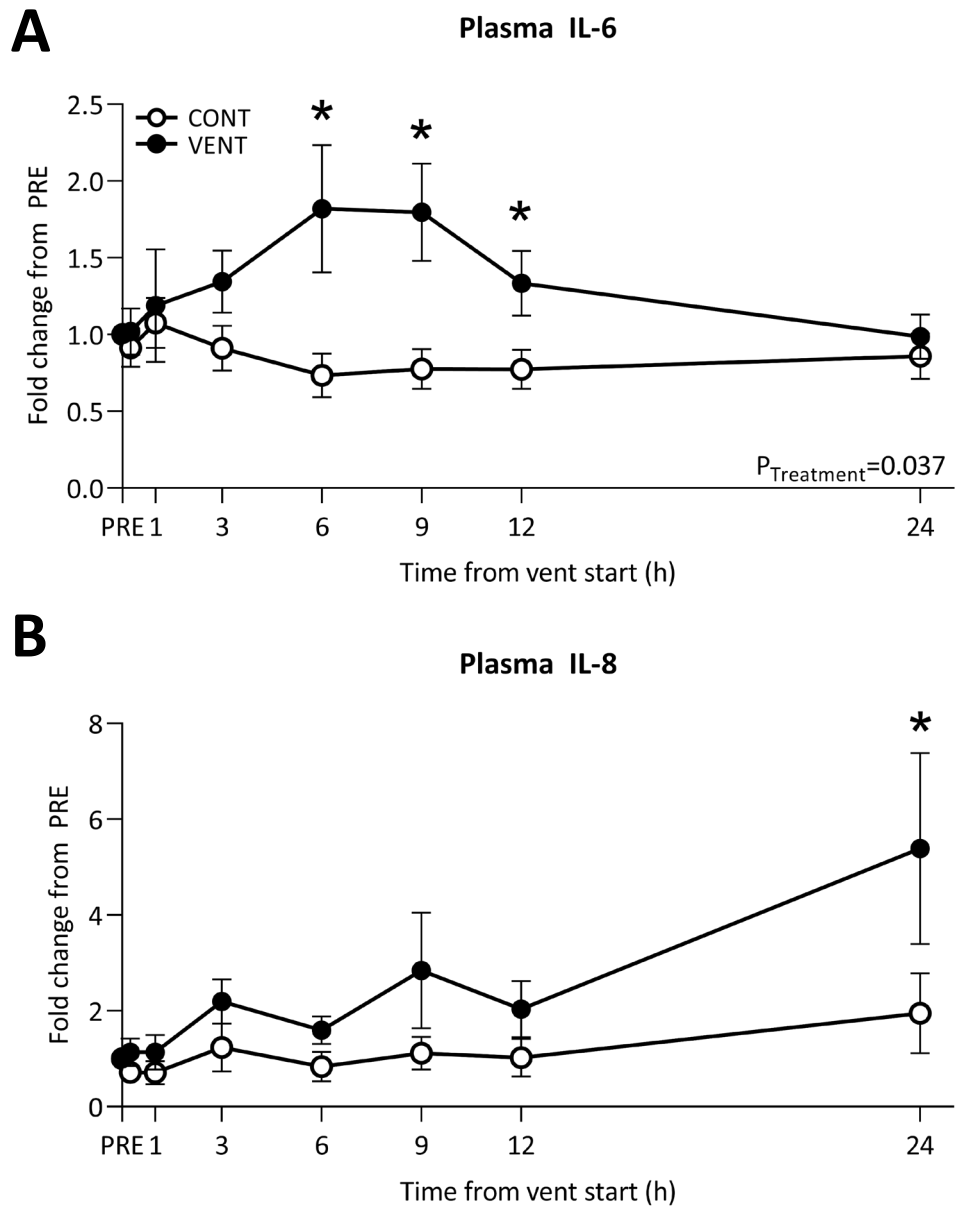


Figure 5.2. Plasma cytokine levels during 24 h IUUV. (A) Plasma IL-6 levels remained unchanged in CONT (open circle) over 24 h and was increased in VENT (filled circle) at 6 h, 9 h, and 12 h. (B) Plasma IL-8 levels remained unchanged in CONT and was increased in VENT at 24 h. Data presented as mean \pm SEM. * $p < 0.05$ between groups.

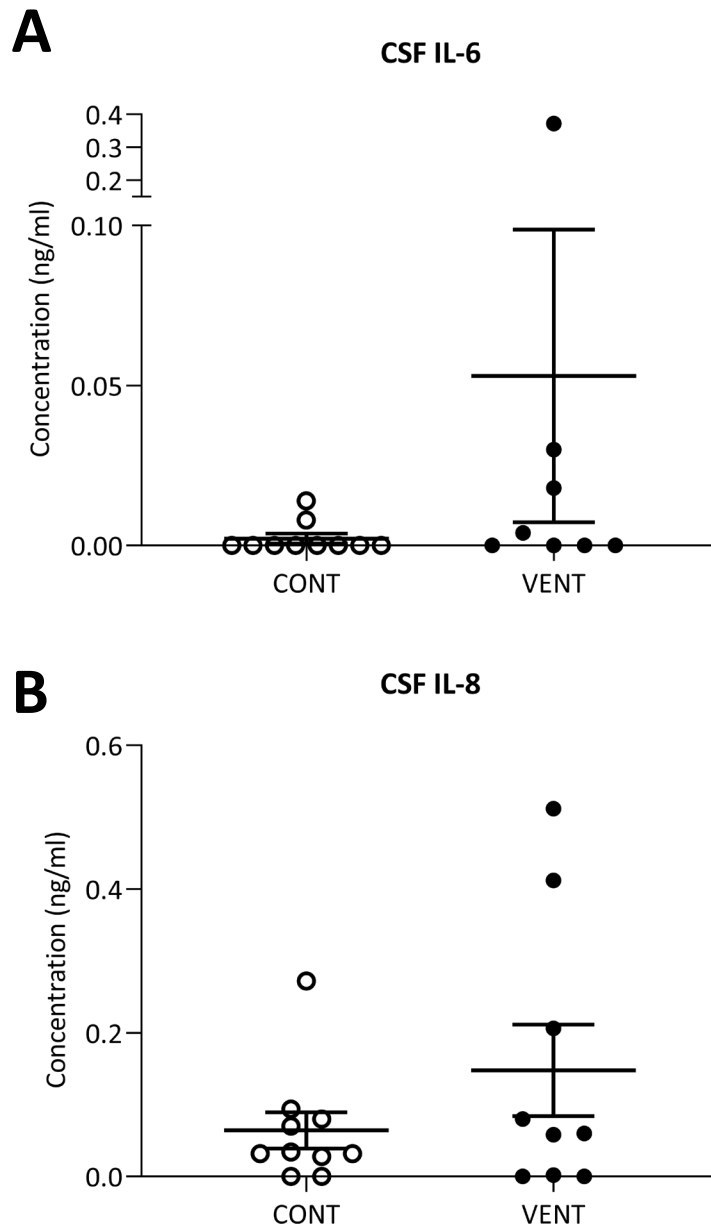


Figure 5.3. Cerebrospinal fluid (CSF) cytokine levels after 24 h IUV. The concentrations of (A) IL-6 and (B) IL-8 in CSF were not different between CONT (open circle) and VENT (filled circle). Data presented as mean \pm SEM.

5.3.3. Assessment of gross neuropathology

Injury scores reflecting parenchymal damage and cystic lesions, compromised vessel integrity, hypercellularity, and disrupted cortex cytoarchitecture were not different between groups [Table 5.2].

Table 5.2. Haematoxylin and eosin analysis. Brain sections were scored from 0 (absent pathology) to 2 (severe pathology) for parenchymal damage, compromised vessel integrity, hypercellularity, and disrupted cortex cytoarchitecture. The individual scores per category and overall injury scores were not different between groups, p-values as indicated. Data are expressed as mean \pm SEM.

	CONT (n=10)	VENT (n=9)	
Parenchymal damage/Cystic lesions	0.05 \pm 0.05	0.05 \pm 0.05	p=0.941
Compromised vessel integrity	0.40 \pm 0.15	0.56 \pm 0.15	p=0.471
Hypercellularity	0.20 \pm 0.08	0.28 \pm 0.09	p=0.525
Disrupted cortex cytoarchitecture	0.30 \pm 0.15	0.11 \pm 0.11	p=0.341
Overall score	0.24 \pm 0.06	0.25 \pm 0.07	p=0.895

Score: 0 = absent, 1 = mild, 2 = severe

5.3.4. Iba-1 positive microglia in the PVWM and SCWM

The number of Iba-1-positive aggregations was not different between groups in the PVWM (p=0.951) and SCWM (p=0.181). The area occupied by these aggregations within the PVWM and SCWM was not different between groups (p=0.457; p=0.475; **Fig. 5.4A**). The areal density of microglia within these aggregations was higher in CONT than VENT in the SCWM (p=0.036); no differences were observed in the PVWM (p=0.543; **Fig. 5.4B**).

The total number of Iba-1-positive microglia was not different between groups in the PVWM (p=0.896) and SCWM (p=0.380; **Fig. 5.4C**). The areal densities of ramified and amoeboid microglia were not different between groups in the PVWM (ramified p=0.670; amoeboid p=0.218) and SCWM (ramified p=0.404; amoeboid p=0.521). The percentage of amoeboid microglia was not different between groups in both the PVWM (p=0.172) and SCWM (p=0.714; **Fig. 5.4D**).

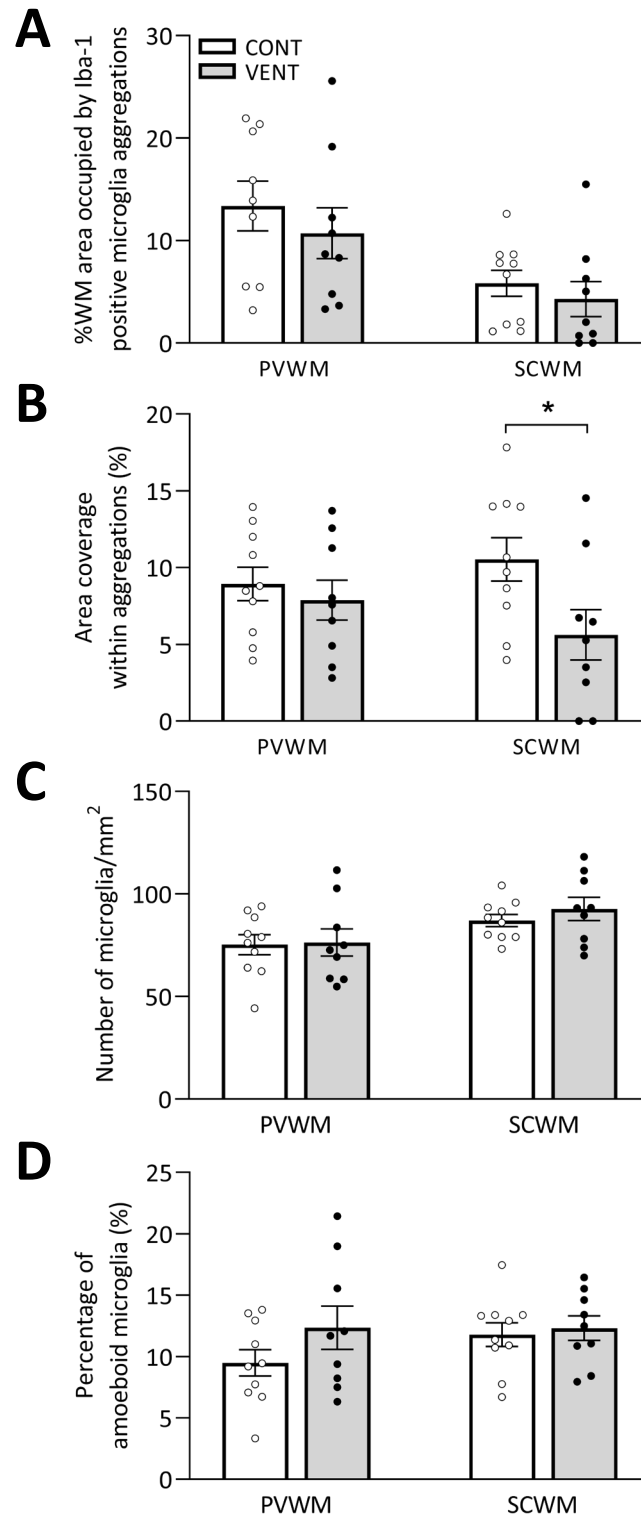


Figure 5.4. Iba-1 positive microglia in the PVWM and SCWM after 24 h IUUV. (A) Percentage area occupied by microglia aggregations, (B) fraction coverage within microglial aggregations, (C) total number of microglia, and (D) percentage of amoeboid microglia. Percentage area, total number of microglia, and percentage amoeboid microglia were not different between CONT (white) and VENT (grey) in the PVWM and SCWM. The fraction coverage within microglial aggregations was higher in CONT than VENT in the SCWM. Data presented as mean \pm SEM. * $p < 0.05$

5.3.5. Sheep serum immunoreactivity in the PVWM and SCWM

The number of blood vessel profiles with protein extravasation was not different between groups in the PVWM ($p=0.282$) and SCWM ($p=0.366$; **Fig. 5.5A**).

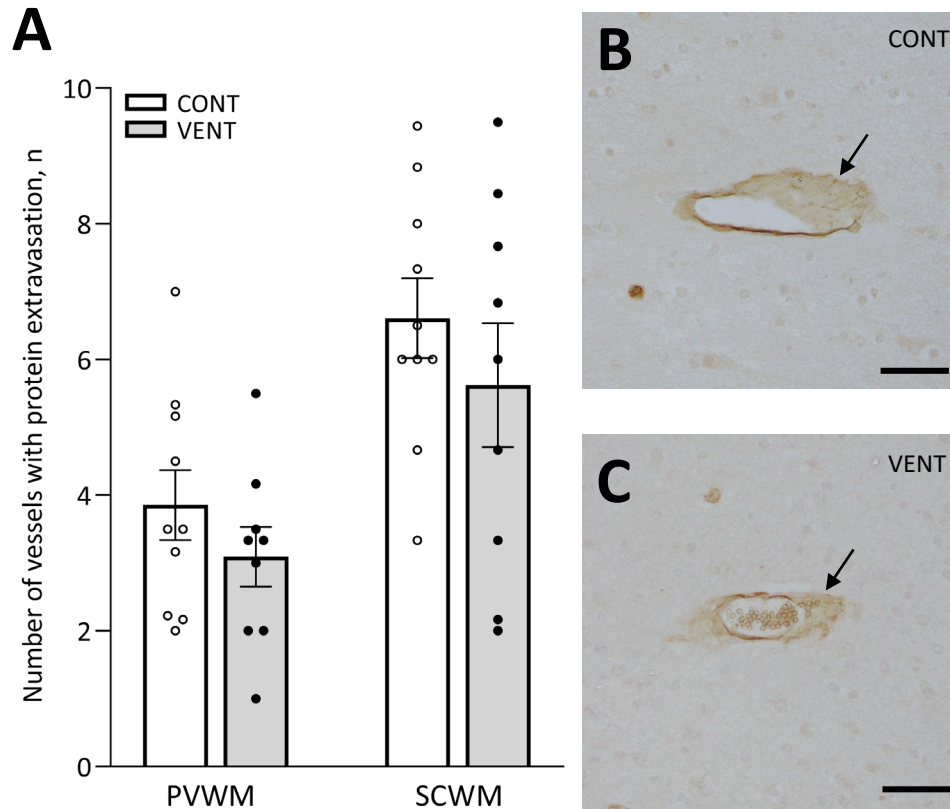


Figure 5.5. Sheep serum immunoreactivity in the PVWM and SCWM after 24 h IUUV. (A) The number of blood vessel profiles with protein extravasation, indicative of compromised blood-brain barrier integrity, were not different between CONT (white) and VENT (grey) in the PVWM and SCWM. (B-C) Representative images, arrows indicate protein extravasation. Scale bar = 50 μm . Data presented as mean \pm SEM.

5.3.6. Olig2-positive oligodendrocytes in the PVWM and SCWM

The areal density of olig2-positive cells was not different between groups in the PVWM ($p=0.302$) and SCWM ($p=0.367$; **Fig 5.6A**).

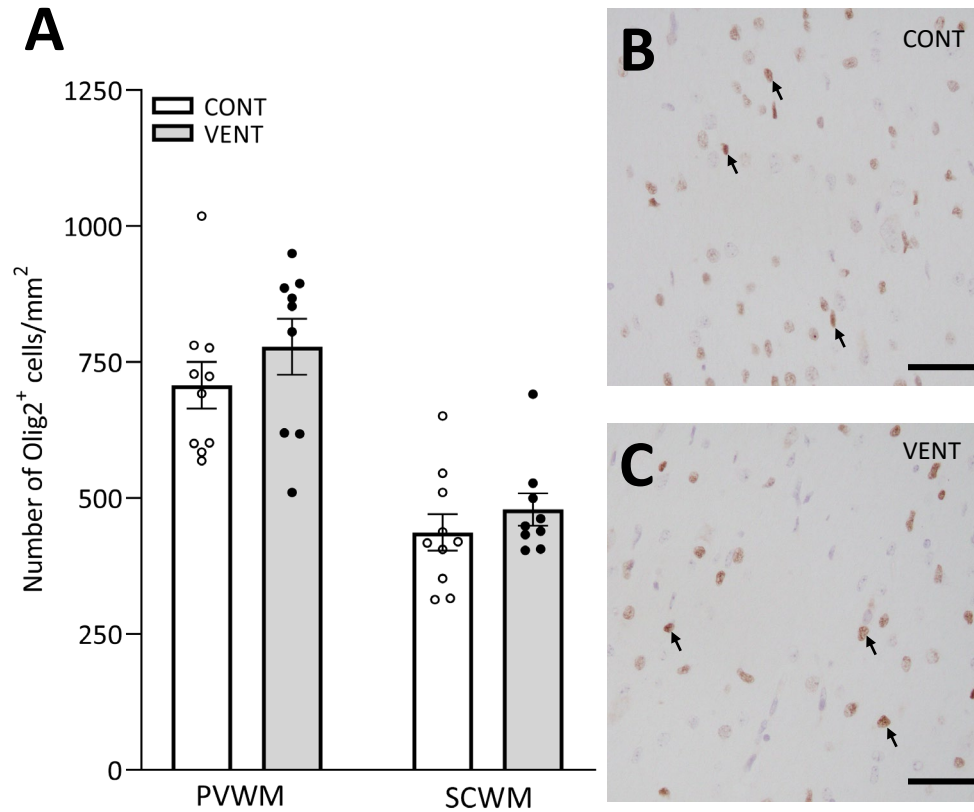


Figure 5.6. Olig2-positive oligodendrocytes in the PVWM and SCWM after 24 h IUV. (A) The areal densities of olig2-positive oligodendrocyte lineage cells were not different between CONT (white) and VENT (grey) in the PVWM and SCWM. (B-C) Representative images, arrows indicate Olig2-positive cells. Scale bar = 50 µm. Data presented as mean ± SEM.

5.4. Discussion

Adverse neurodevelopmental outcome remains a significant burden on our preterm population. While the causes of preterm brain injury are complex, multifactorial, and likely contributed by both antenatal and postnatal compromise, there is a dearth of information on the contribution of prolonged ventilation, which many preterm infants require. In this study, I aimed to establish whether 24 h of standard ventilation (non-injurious) results in white matter brain injury. The ventilation was undertaken with fetal sheep remaining *in utero* to enable me to isolate the effects of ventilation and determine if the IUUV model might be suitable for future chronic VIBI investigations.

For 24 h, fetal sheep supported by the placenta *in utero* were ventilated with a strategy which is not deliberately injurious (i.e. no excessive V_T or pressure) but which inevitably causes damage to the immature lungs.²¹⁸ The IUUV fetal sheep model has previously been shown to induce ventilation-induced lung injury including bronchopulmonary dysplasia (BPD)-like changes in lung morphology,^{165,218,219} but whether this causes brain injury has never been examined. I hypothesised that given the presence of lung inflammation and injury in these studies,^{165,218,219} the immature brain would also be adversely affected by prolonged ventilation. I found that, in the presence of normal blood gases and physiology, prolonged ventilation transiently increased systemic inflammation but did not result in overt brain injury. This is the first study to examine brain histology in fetal sheep ventilated *in utero* at this GA, where brain development approximately corresponds to that of a very preterm human infant in terms of white matter development (~30–35 weeks).^{203,204}

My findings that fetal blood gas levels were not altered by ventilation is consistent with previous studies and reflect that minimal pulmonary gas exchange is occurring in the 113 days GA fetus.^{218,226} I did not measure pulmonary and cerebral blood flow in this study. However, previous studies have found that pulmonary blood flow is not significantly altered after draining lung liquid²²⁶ and IUUV has minimal effects on cerebral perfusion in ovine fetuses.²⁰² Studies evaluating physiological-based cord clamping have similarly found that carotid blood flow remained stable in lambs ventilated with intact umbilical cord circulation.¹⁵⁷ Although that study was conducted in a different context to IUUV, with older lambs (126 days GA) and only a transient period of ventilation,¹⁵⁷ its findings suggest that the placenta prevents haemodynamic instability usually associated with ventilation. Indeed, in Chapter 3, I have shown that ventilating a fetus while attached to the umbilical cord, even with an injurious strategy, does not cause significant fluctuations in carotid blood flow. Taken together, any effects observed in the current study are likely due to the act of ventilation (inflating the fetal lungs) without involvement of haemodynamic instability.

To my knowledge, systemic cytokine profiles after IUV have not previously been investigated. IL-6 and IL-8 are inflammatory mediators that have been associated with preterm brain injury. In postnatal ventilation studies, Malhotra *et al.* found no differences in IL-6 and IL-8 cytokine profiles in the blood (time points of collection not specified) and CSF of preterm but otherwise healthy lambs (125 days GA) that were delivered and supported on ventilation for 24 h compared to unventilated control lambs.¹⁵² In the current study, systemic IL-6 levels were higher than baseline and control animals from 9-12 h. Despite continuous ventilation, systemic IL-6 levels returned to baseline by 24 h. The highest IL-6 level detected after ventilation commenced was 574 ± 0.13 pg/ml at 9 h; the limited reference values for plasma cytokine levels in fetal sheep hinder useful inferences. Nevertheless, increased serum IL-6 levels >100 pg/ml at 12 h of life is associated with severe intraventricular haemorrhage in extremely preterm infants.²²⁷ Elevated systemic IL-6 level in the neonatal period has also been associated with cognitive delay and/or motor deficits at 30 months in term infants at risk of neonatal encephalopathy.²²⁸ In the current study, IL-8 levels increased later at 24 h. In near-term infants, systemic IL-8 level increased after 2 h of intubation and mechanical ventilation.⁹¹ Certainly future experiments with a longer duration will be useful to understand the effects of prolonged ventilation on IL-6 and IL-8 levels and the pattern of upregulation. The levels of IL-6 and IL-8 in CSF were not different between groups, suggesting that these pro-inflammatory cytokines were either not altered within the brain or that altered levels did not persist to 24 h. Increased levels of pro-inflammatory cytokines in CSF are thought to indicate a localised cerebral inflammatory response and have been associated with white matter injury in preterm infants.²²⁹

In the current study, prolonged ventilation did not cause overt histological brain injury or significantly alter blood-brain barrier integrity, microglia reactivity, or the number of oligodendrocytes. This is similar to the abovementioned postnatal ventilation study by Malhotra *et al.* where no apparent neuropathology and changes in microglia and astrocyte reactivity were observed in the PVWM and SCWM of ventilated lambs delivered at 125 days GA.¹⁵² In that study, however, prolonged ventilation significantly increased the number of apoptotic cells (caspase-3-positive) cells in the PVWM.¹⁵² It was speculated that pronounced white matter damage did not occur due to the relative maturity of the white matter at 125 days GA. The oligodendrocyte population progresses from primarily immature oligodendrocytes at 105 days GA in fetal sheep to mature myelinating oligodendrocytes by 120 days GA²⁰⁴ and therefore should be more vulnerable to insults at 113 days GA than at 125 days GA. A much longer period of ventilation for 14 days in preterm baboons induced an increase in ramified microglia and reduction of oligodendrocytes in white matter regions.^{143,145} It may be that 24 h of ventilation was insufficient to induce changes, and a longer cumulative duration of ventilation is needed.

A plausible reason for the lack of brain injury may be that my achieved V_T was considerably lower than previous IUV studies. I achieved V_T of 2.36 ± 0.78 ml/kg (mean \pm SD) despite applying maximum PIP of 45 cmH₂O, whereas previous studies that observed ventilation-induced lung injury in sheep of similar GA attained V_T of 3-5 ml/kg with a maximum PIP of 40 cmH₂O.^{165,218} Fetal posture, which cannot be controlled, may have affected the V_T delivered and distribution of ventilation within the lungs.²²⁶ It is possible that amniotic pressure on the thoracic cavity limited lung expansion, and a larger inspiratory pressure may have been needed to overcome this. However, excessive pressure is itself injurious to the immature lung and I deliberately chose ventilatory parameters to avoid barotrauma and volutrauma. Moreover, my measurement of V_T may be an underestimation given that the flow sensor was attached to the ventilation tubing outside the ewe, instead of at the end of the endotracheal tube at the mouth of the lamb. Importantly, despite the low observed V_T , the lungs of the VENT animals in the current study were significantly injured compared to those of CONT animals (Polglase *et al.*, manuscript in preparation) and the increase in systemic cytokine levels may reflect this.

There are several limitations to my study. Previous studies have shown that there are responders and non-responders to IUV based on pulmonary blood flow changes, though the reasons for this are unknown.²²⁶ I did not measure blood flow in the current study and so could not perform a sub-analysis. I have focused on cerebral PVWM and SCWM in this study as these are regions where brain injury in preterm infants has commonly been observed and which previous studies have focused on. Oligodendrocytes are the most vulnerable cell type in a developing brain of this gestational age.^{203,204} However, it is possible that prolonged ventilation affects other cell types (e.g. neurons, astrocytes) or regions I have not yet examined. This is a focus for future investigations. I investigated a period of 24 h of ventilation as a proof of concept, but human preterm infants are likely to be exposed to longer periods of ventilation in the NICU. Furthermore, perhaps ventilation-induced changes take longer than 24 h to manifest, and so could not be detected in my analyses. Future studies with a longer ventilation period are required to confirm this. In this regard, my study demonstrated that extending the duration of IUV from 12 h (previous studies of lung injury)^{165,218,226} to 24 h was feasible and did not cause undue distress to the ewe and fetus, suggesting that it is conceivable to extend the ventilation period using this model. While this study was not aimed at investigating the pathways of chronic VIBI, it needs to be acknowledged that maintaining placental circulation during ventilation removes the haemodynamic pathway of injury, as explained in Chapter 3. Hence, my findings raise further questions about the involvement of systemic inflammation and haemodynamic instability on chronic VIBI.

5.5. Conclusion

Overall, my findings suggest that the fetal sheep 24 h IUUV model may not yet be an appropriate tool to examine prolonged VIBI. Refinements to the model involving longer ventilation periods and expanding the analysis to other cell types and regions will help to improve relevance of the model. Developing a reliable model of chronic VIBI is necessary to investigate its mechanisms and potential treatments, with the goal of improving the neurodevelopmental outcomes of preterm infants who require long periods of respiratory support.

Chapter Six: General Discussion

6.1. Overview

An estimated 2.4 million babies are born very and extremely preterm at less than 32 weeks gestational age (GA) worldwide each year.¹ Approximately 60-95% of these infants will require respiratory support during their neonatal period, whether in the delivery room, subsequently in the neonatal intensive care unit (NICU), or both.^{3,60-66} This is because their lungs are too immature for efficient gas exchange. Paradoxically, this life-saving respiratory support in the neonatal period can unintentionally cause brain injury and adverse long-term neurodevelopmental outcomes. In the delivery room setting, early positive pressure ventilation (PPV),^{97,98} increasing intensity of resuscitation (non-invasive PPV to invasive PPV to cardiopulmonary resuscitation),^{67,95} and poorly controlled PPV resulting in inappropriate ventilation parameters^{97,100} have been associated with brain injury and long-term neurological deficits. In the NICU, where respiratory support is better controlled and monitored, prolonged duration of invasive PPV has been associated with brain injury and adverse neurodevelopmental outcomes.^{60,62,75,105,107} While it is recognised that the modes and duration of delivery room resuscitation and NICU assisted ventilation are markedly different, the distinct roles each play in the development and progression of ventilation-induced brain injury (VIBI) have scarcely been explored. The mechanisms that mediate VIBI remain elusive and few potential treatments for preterm brain injury have been evaluated in conjunction with mechanical ventilation in either setting. The studies in this thesis aimed to provide insight into the neuropathology and mechanisms of VIBI and to evaluate the therapeutic benefits of treatments that target these pathways (e.g. umbilical cord blood [UCB] cells).

A major issue when associating preterm brain injury directly with an intervention like respiratory support is the inability to isolate the ventilation per se from other potential sources of injury that might already be present antenatally (e.g. chorioamnionitis) and/or in the immediate and long-term postnatal care of a preterm infant. Postnatal sources of injury can occur from respiratory support itself (e.g. oxygen toxicity, atelectrauma) or from other interventions to assist with stabilising multi-organ dysfunction prevalent in immature preterm newborns. To overcome these confounders, I expanded on two ovine fetal ventilation models to investigate VIBI: 1) a head-out ventilation model with a brief injurious ventilation strategy to investigate the mechanisms of acute VIBI in the delivery room and evaluate the use of UCB cells as a treatment, and 2) an *in utero* ventilation (IUV) model with prolonged gentle ventilation to model chronic VIBI in the NICU [Fig. 6.1].

Ventilation-induced brain injury in preterm neonates

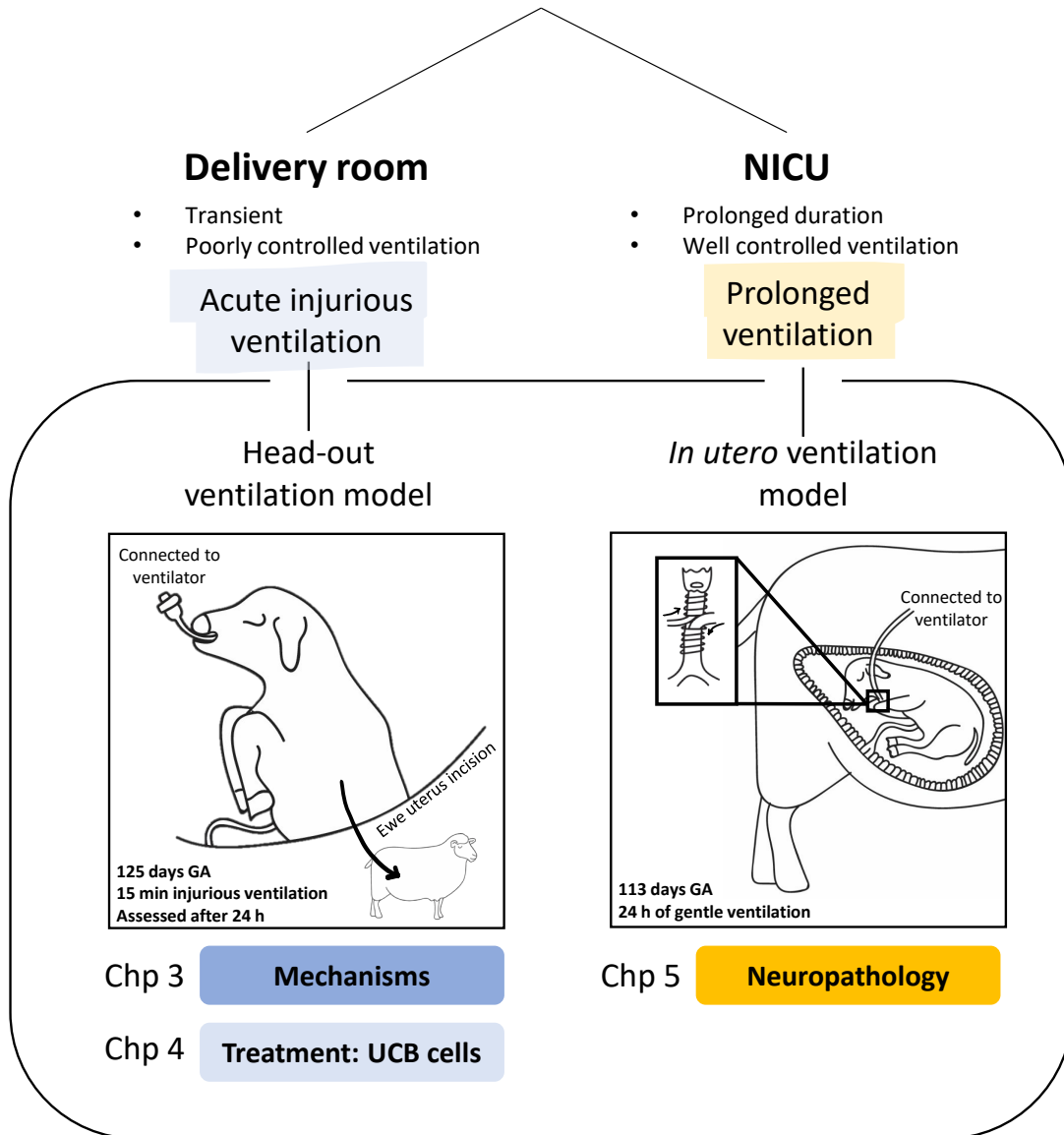


Figure 6.1. Schematic overview of the studies in this thesis. This thesis examined the mechanisms of acute injurious ventilation akin to ventilation strategies that preterm infants may receive in the delivery room, and whether the early administration of umbilical cord blood (UCB) cells showed neuroprotective efficacy. Further, neuropathology after prolonged ventilation was characterised to determine if an *in utero* ventilation model is suitable to mimic prolonged ventilation preterm infants often receive in the neonatal intensive care unit (NICU).

The most important findings of my thesis are the following: In Chapter 3, my results showed that the relative contributions of the inflammatory and haemodynamic pathways of VIBI remain inconclusive. Importantly, while I aimed for high tidal volumes (V_T) to induce acute VIBI, this was not achieved, and my results suggest that the lower V_T was not associated with neuropathology. Thus, V_T below a certain threshold may be less injurious than previously thought. In Chapter 4, I demonstrated that early UCB cell treatment to reduce VIBI actually increased systemic and cerebral inflammation, and adversely affected the blood-brain barrier (BBB), microglia, and oligodendrocytes. Therefore, it appears that the chosen UCB cells treatment regimen (80 million allogeneic term UCB cells administered i.v. 1 h after injurious ventilation) is unfavourable. Lastly, in Chapter 5, I established that prolonged 24 h of ventilation with low V_T increased systemic inflammation but not white matter injury in fetal sheep. Overall, the lack of brain injury observed in my studies raises some interesting possibilities about the role of ventilation in brain injury, as well as the potential role the placenta may play in moderating the effects of VIBI which are discussed below.

6.2. Tidal volume below a threshold does not induce VIBI

Previous studies from our group have shown that high V_T of 10-15 ml/kg immediately at delivery resulted in activation of the haemodynamic and inflammatory pathways that mediate brain injury.^{80,96,110} This finding was important given that the majority of preterm infants receive excessive V_T during delivery room resuscitation⁸⁷ which increases intraventricular haemorrhage (IVH).⁹⁷

I aimed to replicate these high V_T strategies to induce VIBI in Chapters 3 and 4. However, I was unable to achieve the target V_T of 12-15 ml/kg in either study, reaching a mean V_T of only 7-10 ml/kg. Although the animals received V_T that is marginally higher than the normal range (5-7 ml/kg), this was not enough to elicit overt brain injury despite resulting in profound lung injury.¹⁸⁹ This finding raises the possibility that a potential threshold of $V_T \geq 10$ ml/kg is required to induce brain injury in the delivery room in preterm lambs and potentially also in preterm infants. This may have occurred by reducing the impact of the major pathways of preterm brain injury, discussed further in Section 6.3.1.

This result has important clinical implications. The use of respiratory function monitors in the delivery room has long been advocated for, predominately to reduce volutrauma and subsequent ventilation-induced lung injury (VILI).^{230,231} This has been shown to improve short-term respiratory outcomes (reduce oxygen requirement and the need for intubation),²³² but its impact in reducing VIBI has not been established. My results suggest that maintaining a normal or less excessive V_T in the delivery room may prevent or reduce VIBI. The best way to achieve this clinically would be by using respiratory function monitors to maintain and limit lower V_T to fall within a safer range. Importantly, it should be noted that the safe limit in humans is not known. While Mian *et al.* and Pahuja *et al.* showed that V_T

<6 ml/kg was associated with less IVH than >6 ml/kg,^{97,99} a lower V_T (e.g. 5 ml/kg) may be even more beneficial as long as adequate oxygenation can be achieved.

In Chapter 5, the achieved V_T (2–3 ml/kg) was also lower than desired, relative to what previous studies have shown to cause VILI (3–5 ml/kg), although I suspect that this may be due to the placement of the flow sensor on the exteriorised ventilation tubing rather than at the end of the endotracheal tube near to the mouth of the animal where it is normally placed. This would underestimate the actual delivered V_T . Nevertheless, this again supports the notion that it is not inflating immature lungs for an extended duration but *overinflating* them that is the more crucial factor in the pathogenesis of VIBI. Given that the fetus was not dependent on ventilation for survival in my study, I am not able to infer if the low V_T applied is adequate to support respiratory efforts *ex utero* or feasible as a strategy.

6.3. Does lung injury predict brain injury?

Intriguingly, in all chapters, despite the relatively low V_T , our ventilation strategies successfully induced VILI (Appendix III; Polglase *et al.*, manuscript in preparation). VIBI has been proposed to be a downstream consequence of VILI, coordinated through systemic inflammation and perturbed haemodynamics. I propose that the lack of injury from ventilation in Chapters 3 and 5 is due to the modulation or interruption of pathways of VIBI in the fetus, attributed to the intrauterine environment.

6.3.1. Role of the haemodynamic and inflammatory pathways to VIBI

The contribution of the haemodynamic pathway to VIBI was largely neglected in this thesis as most fetuses were ventilated with an intact placental circulation [Fig. 6.2C]. Even in fetuses ventilated with their umbilical cords occluded (INJ_{INF+HAE} group in Chapter 3), carotid blood flow, which is a proxy for cerebral blood flow (CBF),²⁰² was not as variable as previously observed in injuriously ventilated preterm lambs *ex utero* [Fig. 6.2B,D]. Large fluctuations to CBF, especially in preterm infants with compromised cerebral autoregulation, is known to rupture fragile blood vessels and result in haemorrhagic injury.¹¹⁶ Thus, the absence of cerebral haemodynamic instability in my studies may explain the apparent lack of brain injury. Indeed, I did not observe any increase in protein extravasation, an indicator of compromised vasculature and BBB breakdown, in the ventilated groups in Chapters 3 and 5. Importantly, not only would reducing haemodynamic instability prevent cerebrovascular injury, but it can also limit inflammatory consequences upon the brain by preventing BBB disruption. Breakdown of the BBB aids access of systemic circulating inflammatory proteins and peripheral leukocytes into the brain parenchyma of preterm infants to elicit localised inflammation.^{29,125}

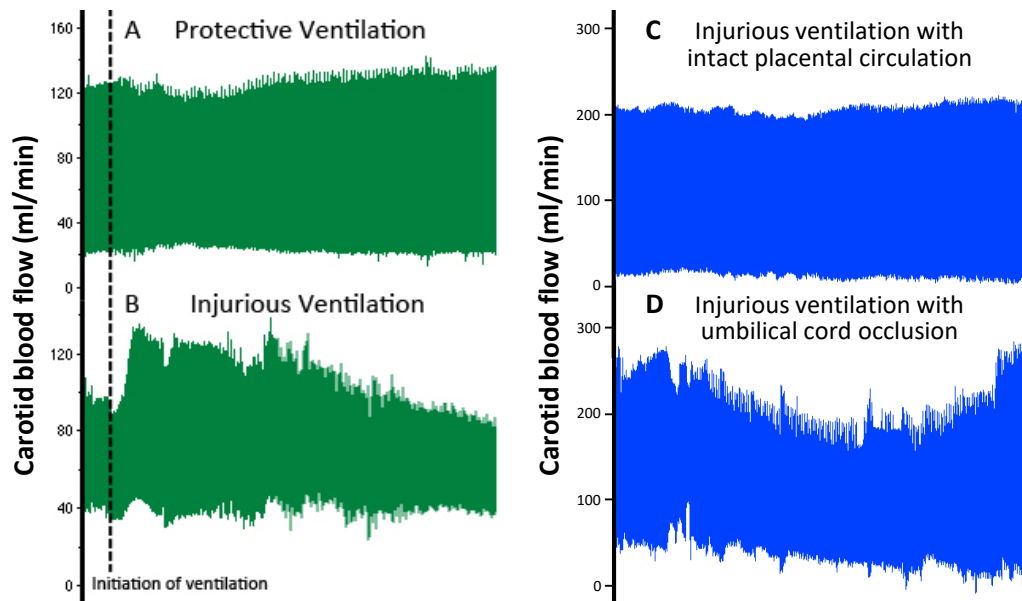


Figure 6.2. Carotid artery blood flow during positive pressure ventilation (PPV). (A-B) In previous studies, PPV initiated using an injurious high tidal volume (V_T) strategy resulted in greater CBF instability in postnatal preterm lambs compared to when a protective ventilation strategy was used. *Reproduced with permission from Polglase et al., 2014⁸⁰ with minor adaptations.* (C-D) In Chapter 3, PPV initiated with an injurious high V_T strategy resulted in greater CBF instability in preterm-equivalent fetal sheep with umbilical cord occlusion compared to when the fetus was connected to intact placental circulation.

The potential reason that CBF was stable was that ventilation, particularly with an intact placental circulation, did not result in an increase in pulmonary blood flow (PBF), which would alter cardiac output and subsequently CBF. Previous research has shown that PBF only increased in 57% of lambs during IUUV, and this only occurred transiently with no differences in PBF observed in any animals after 2 h.²²⁶ Therefore, it is possible that in the fetal ventilation model, the haemodynamic pathway is difficult to initiate, and thus less damaging to the preterm brain by this pathway. Further, PBF is important for the recruitment of inflammatory cells into pulmonary tissue and the translocation of pro-inflammatory mediators to the bloodstream in order to initiate a systemic response. This may explain the lack of a profound systemic response in fetuses where ventilation did not increase PBF. I did not measure PBF in these studies, but a future focus may be to ensure that the haemodynamic pathway is initiated in the fetal ventilation model.

Nevertheless, it raises the question whether an increase in systemic inflammation alone is enough to cause VIBI. In Chapter 3, I showed that systemic interleukin(IL)-6 and IL-8 levels were not altered by injurious ventilation and there was no evidence of BBB compromise (protein extravasation [sheep

serum]). Further, there was no evidence of brain inflammation or injury. In Chapter 5, despite increased circulating IL-6 and IL-8 levels with ongoing ventilation, there remained no evidence of BBB compromise (vascular integrity [H&E] and protein extravasation [sheep serum]), and no evidence of brain inflammation or injury. However, in Chapter 4, an increase in systemic IL-6 and IL-8 levels was accompanied by compromised BBB integrity (protein extravasation [sheep serum]) and cerebral pathology. Taken together, these results imply that increased systemic inflammation (IL-6 and IL-8) itself does not necessarily predict VIBI, unless it also disrupts BBB integrity or BBB integrity is already otherwise compromised. It is unclear whether this indicates that systemic inflammation must be severe enough to adversely alter BBB integrity before it can affect the brain, or if simply a compromised BBB presents an opportunity for circulating immune cells and pro-inflammatory mediators to enter the central nervous system (CNS) and induce cerebral inflammation and injury. Furthermore, the involvement of other cytokines has not been explored in this thesis and is likely crucial to this discussion. Regardless, the importance of the inflammatory pathway to VIBI, particularly systemic inflammation as a conduit in the lung-brain crosstalk, should be further interrogated.

While I have focused on the haemodynamic and inflammatory pathways of VIBI independently in most parts of this thesis, it is essential to acknowledge that these two pathways influence each other. Importantly, my findings suggest that these two pathways of VIBI may be more profoundly interlinked than previously understood.

6.4. Early UCB cell therapy in conjunction with mechanical ventilation is unfavourable

In Chapter 4, I discovered that instead of ameliorating VIBI, UCB cell treatment increased systemic inflammation and exacerbated cerebral white matter injury. The increase in systemic inflammation is not entirely unexpected, given that initiating innate immune responses has been proposed to underlie the efficacy of UCB cells to modulate brain injury.²¹⁷ However, that increased systemic IL-6 and IL-8 levels in my study were accompanied by worsened brain injury is incongruous with numerous other preclinical studies that have demonstrated efficacy of UCB cells in reducing brain injury in sheep^{184,185,188,209} that formed the basis for choosing UCB cells as a treatment in this study. As discussed in Chapter 4, the conflicting findings may be explained by differences in the dosing regimen of UCB cells. Specifically, when and how often we administered the cells (timing), what cells were administered (subtypes within UCB), and how many cells were administered (dose). I have administered my treatment at an early time point (1 h post-ventilation), which coincides with the peak pulmonary inflammatory response after ventilation,²¹² with the intention to interrupt the pulmonary to systemic inflammatory transmission. However, placing the cells in this pro-inflammatory environment may have

pushed the UCB cells to a pro-injury phenotype.^{215,216} This raises the critical concept that the inflammatory state of the newborn should be considered before any treatment is given, especially if the treatment is dynamic and can respond to the microenvironment it is placed in (e.g. stem cells) as it may exacerbate injury rather than reduce it.

Delayed administration may be preferred since ventilation-induced lung inflammation has been shown to resolve by 6 h after injurious ventilation.²¹² Certainly, comprehensive profiles of the pulmonary and systemic inflammatory responses after ventilation may aid in determining an ideal time for UCB administration and are vital areas for future research. Indeed, an in-depth analysis of the pathways of VIBI discussed in Section 6.3.1 and the inflammatory and oxidative stress responses to injurious ventilation over time are required before targeted treatments can be explored.

Regardless, the interaction of UCB cells and mechanical ventilation needs to be thoroughly investigated. This is critical given that the majority of preterm infants born <32 weeks GA, where the majority of cases of brain injury are present, receive substantial respiratory support both in the delivery room and NICU. As the experimental conditions of this study have deliberately deviated from that in the clinical setting, my results should be interpreted with caution. These results certainly should not be extrapolated to preterm infants as is, but they provide a stark reminder that there is a lot that is not known about UCB cells as a potential treatment for brain injury in infants who require respiratory support.

6.5. The influence of the placenta

The main difference between my studies and previous VIBI studies that have investigated neuropathology is that ventilation in most of the previous studies was conducted *ex utero*. The advantage of fetal ventilation models is the ability to isolate the sole effects of ventilation from other potential confounders. In particular, the placenta provides cardiovascular, oxygen, and nutritional support to the fetus throughout the study. Manipulation of umbilical blood flow potentially allows the haemodynamic pathway of VIBI to also be studied. While I discussed above how the placenta may have protected against VIBI by mitigating the haemodynamic and inflammatory pathways of injury, here, I speculate that the intrauterine environment and placenta may further protect the fetus and/or the fetal brain from insults.

It has previously been reported that the ovine fetal lung has capacity for self-repair after injurious ventilation.^{233,234} Fetal sheep (125 days GA; 0.85 of term²³³ and 110 days GA; 0.75 of term²³⁴) were exteriorised, ventilated for 2 h with an injurious ventilation strategy, then returned to the uterus for either 24 h or 15 days.^{233,234} In the absence of continued ventilation, lung tissues showed heterogenous histological injury 24 h after injurious ventilation that resolved by 15 days without any additional

interventions.^{233,234} It is undetermined if this was a tissue specific response, if the intrauterine environment contributed to this reversal of injury, or both.

Certainly, the placenta and umbilical cord are rich sources of stem and progenitor cell populations which have anti-inflammatory, angiogenic, and regenerative properties.^{175,235,236} With regards to the brain, the placenta is vital for regulation of neurosteroid precursors, neurosteroids, and neurotrophins during normal development, either via direct placental production of these factors or by placental transfer of maternal factors to the fetus.^{237,238} Neurosteroids (e.g. allopregnanolone) and neurotrophins (e.g. brain derived neurotrophic factor [BDNF] and nerve growth factor [NGF]) may have neuroprotective effects in the fetus besides their roles in fetal brain development processes such as neurogenesis, gliogenesis, myelination, and survival and maintenance.^{237–240} Maternal pro-inflammatory cytokines (e.g. IL-6) have been shown to be able to cross the placental barrier, although this is dependent on the cytokine.²⁴¹ There is minimal transfer of maternal IL-1 α and tumour necrosis factor (TNF) to the fetus,²⁴¹ and placental transfer of anti-inflammatory cytokines have been relatively unexplored. Indeed, little is known about healthy placental responses to a challenged fetus; a compromised fetus is more commonly the *consequence* of altered placenta function (e.g. inflammation of placental membranes and placental insufficiency). It is possible that the dampened systemic inflammatory response in our studies, in addition to the haemodynamic influence of the placental circulation, may be in response to maternal or placental mediators. This remains conjecture and warrants further investigation.

6.6. Limitations

In commencing these studies, it was evident that my animal models would need to induce detectable and reproducible changes to the white matter of the preterm brain, consistent with what has been observed in humans. This has not always been the case. Indeed, the methodology employed in this thesis has several strengths but is not without limitations.

6.6.1. Clinical relevance of the fetal ventilation model

While fetal ventilation models are useful for isolating individual ventilatory parameters (as in V_T in Chapters 3 and 4, and duration in Chapter 5), injury purely from ventilation without consideration of other factors is not a realistic representation of what happens in a clinical setting. There is abundant room for further progress in determining the role of mechanical ventilation in those contexts, by using the basic science findings in this thesis as a springboard for more complex studies with greater translational relevance. For example, ventilation may play an additive rather than main role in causing brain injury in infants exposed to adverse antenatal conditions (e.g. chorioamnionitis and fetal growth restriction) and will need be studied in that context. Furthermore, my results in Chapter 4 on the effects

of UCB cells need to be validated in postnatal models, where lambs are cared for more similarly to preterm infants.

6.6.2. Low tidal volumes

A key limitation of the studies in this thesis is that the V_T applied to the lambs was insufficient to achieve the aims of the studies. Nevertheless, this has provided vital insight to the importance of monitoring V_T in the delivery room setting (Section 6.2) and alluded to the possibility that maintaining low V_T during prolonged ventilation in the NICU may counter VIBI. Nonetheless, there are necessary alterations that need to be done to strengthen these fetal ventilation models before undertaking future work. Specifically, strategies to obtain a higher V_T are required. For example, surfactant administration before ventilation can increase lung compliance and allow for larger V_T . Increasing the upper limit of peak inspiratory pressure can also increase V_T but this should be undertaken with caution since excess pressure contributes to lung injury. In my studies, the maximum pressure was limited to prevent pneumothoraces.

6.6.3. Brain regions of interest and pathways of injury investigated

Another limitation is that assessments have been restricted to the PVWM and SCWM in an attempt to add depth rather than breadth to current literature. The PVWM and SCWM have consistently been shown to be vulnerable regions of the brain of preterm infants. However, the contribution of ventilation to injury in these regions is not well understood. Recent findings suggest subtle injury in other brain regions, such as the cortical grey matter and hippocampus, which may be the focus of future studies.

Similarly, the two pathways of VIBI evaluated in this thesis are those previously shown to be critically involved in the progression of VIBI. Collateral pathways of injury (e.g. oxidative stress) have not been investigated in this thesis. In particular, effects of oxidative stress pathways may not have been adequately reflected since room air was used for ventilation and there was negligible pulmonary gas exchange in the fetuses.

Microglia reactivity, astrocyte reactivity, changes in total oligodendrocyte numbers, and vascular protein extravasation were used as indicators of white matter wellbeing and injury in my studies. However, there are undoubtedly other critical cell types and responses important to the evolution of brain injury in the ventilated preterm infant. These include neurons, neuronal fibres, neuronal activity, myelin content, measurements of oxidative stress, as well as cell death pathways. Furthermore, I have only used common markers to assess the cell types in the white matter. For example, I have relied on oligodendrocyte-transcription 2 (Olig2) and myelin basic protein (MBP) to assess white matter integrity. Given the heightened vulnerability of preoligodendrocytes expected at this stage of brain maturity, it would be

useful to assess the different populations of oligodendrocyte lineage cells. Attempts to thoroughly characterise brain injury in sheep has often been limited by the reagents and working protocols available, but this is an essential area for investigations when techniques progress in the future.

6.6.4. Inherent issues with using sheep

This thesis has leveraged on the use of sheep as an experimental model for several reasons. Briefly, we can more closely replicate clinical equipment and conditions compared to using smaller animals (e.g. rodents, rabbits), with simpler ethical considerations and less extensive resources compared to using other large animal models (e.g. non-human primates). The physiology as well as brain development of fetal sheep are also well documented. Pregnant sheep are resilient to surgery, and the size of fetal sheep/lambs allows repeated blood sampling which is useful in characterising systemic inflammatory profiles. However, there are a few limitations associated with using sheep. Relatively small sample sizes (5-10 animals/group) have been used in this thesis, as is common with studies utilising large animals. This remains a challenge when accounting for variability. The species differences between human and sheep must also be part of this discussion. The brain-lung maturation mismatch was mentioned briefly in Chapter 5, in proposing the IUUV model. To reiterate, while the overall developmental timeline of white matter is comparable to humans, myelination occurs earlier in relation to birth in sheep, and advances more rapidly than lung development, relative to humans (i.e. in a preterm lamb of 125 days GA, lung development is comparable to a 26-28 week infant^{242,243} but cerebral white matter development is comparable to a 36-38 week infant^{203,204}). This is an important consideration for VIBI studies (see Appendix I).

6.7. Future direction

6.7.1. Umbilical cord blood cells and mechanical ventilation

The findings in Chapter 4 provide a strong justification to interrogate the interaction of UCB cells and mechanical ventilation. I speculate that with an optimised dosing regimen (dose, timing, route), UCB cells administration may not be detrimental and perhaps even has the potential to improve neurodevelopmental outcomes in ventilated preterm infants. However, my findings do show that if given at the wrong time and/or dose, UCB cells may in fact be harmful. Therefore, it is critical that future studies delineate the interplay between UCB cells and ventilation, as well as the overall inflammatory state of the newborn when UCB cells are given.

6.7.2. Further characterisation of the pathology and pathways of VIBI

The findings in Chapter 3 and 5 highlight the need to more comprehensively investigate the pathology of VIBI by characterising changes in different cell types and to expand investigations to other regions of the brain. Studies should also explore the contribution of the oxidative stress pathway of injury; this is feasible by isolating the influence of oxygenation (e.g. different fraction of inspired oxygen [FiO_2] levels) in the fetal ventilation models presented in this thesis.

6.7.3. Examining placental factors

As discussed above (Section 6.5), there is a need to better understand how the placenta may play a role in modulating ventilation-induced lung and brain injury. Future studies can explore the haemodynamic interaction between the placenta and fetus during ventilation. These studies can also include analysis of placental tissue to identify potential protective cell types or mediators. Furthermore, major initiatives such as the Human Placenta Project launched by the *Eunice Kennedy Shriver* National Institute of Child Health and Human Development (NICHD) will provide substantial clarifications on placenta development, structure, function, and role in health and disease.²⁴⁴

6.8. Conclusion

The studies presented in this thesis examine two specific ventilation situations preterm infants receive in the immediate neonatal period. Our knowledge of VIBI, which is vital for rational attempts at prevention or treatment, will remain incomplete without reliable preclinical models. This thesis explores the value of sheep as an appropriate tool for the ongoing investigation of VIBI. By mimicking physiological scenarios of acute injurious ventilation in the delivery room and prolonged controlled ventilation in the NICU, I clarified the pathways involved in VIBI, characterised histopathology of VIBI, and evaluated a therapeutic intervention (UCB cells) to prevent or reduce VIBI.

Recent advancements in neonatology have ensured that preterm infants can be supported at gestational ages earlier than ever before. Reducing VIBI and its sequelae is critical in ensuring that the improved survival of our tiniest, most vulnerable infants does not come at the expense of long-term neurodevelopmental morbidities. The work demonstrated in this thesis is a valuable contribution to this purpose.

References

1. Blencowe, H. *et al.* National, regional, and worldwide estimates of preterm birth rates in the year 2010 with time trends since 1990 for selected countries: A systematic analysis and implications. *Lancet* **379**, 2162–2172 (2012).
2. Ancel, P. Y. *et al.* Survival and morbidity of preterm children born at 22 through 34 weeks' gestation in France in 2011: results of the EPIPAGE-2 cohort study. *JAMA Pediatr.* **169**, 230–238 (2015).
3. Stoll, B. J. *et al.* Trends in care practices, morbidity, and mortality of extremely preterm Neonates, 1993–2012. *JAMA – J. Am. Med. Assoc.* **314**, 1039–1051 (2015).
4. Guillén, Ú. *et al.* Guidelines for the Management of Extremely Premature Deliveries: A Systematic Review. *Pediatrics* **136**, 343–50 (2015).
5. Gale, C., Statnikov, Y., Jawad, S., Uthaya, S. N. & Modi, N. Neonatal brain injuries in England: population-based incidence derived from routinely recorded clinical data held in the National Neonatal Research Database. *Arch. Dis. Child. – Fetal Neonatal Ed.* **103**, F301–F306 (2018).
6. Jarjour, I. T. Neurodevelopmental outcome after extreme prematurity: A review of the literature. *Pediatr. Neurol.* **52**, 143–152 (2015).
7. Marlow, N., Wolke, D., Bracewell, M. A., Samara, M. & EPICure Study Group. Neurologic and developmental disability at six years of age after extremely preterm birth. *N. Engl. J. Med.* **352**, 9–19 (2005).
8. Younge, N. *et al.* Survival and neurodevelopmental outcomes among periviable infants. *N. Engl. J. Med.* **376**, 617–628 (2017).
9. Khwaja, O. & Volpe, J. J. Pathogenesis of cerebral white matter injury of prematurity. *Arch. Dis. Child. – Fetal Neonatal Ed.* **93**, F153–F161 (2007).
10. Volpe, J. J. Dysmaturation of Premature Brain: Importance, Cellular Mechanisms, and Potential Interventions. *Pediatr. Neurol.* **95**, 42–66 (2019).
11. Chevallier, M. *et al.* Leading causes of preterm delivery as risk factors for intraventricular hemorrhage in very preterm infants: results of the EPIPAGE 2 cohort study. *Am. J. Obstet. Gynecol.* **216**, 518.e1–518.e12 (2017).

12. Kelly, C. E. *et al.* Moderate and late preterm infants exhibit widespread brain white matter microstructure alterations at term-equivalent age relative to term-born controls. *Brain Imaging Behav.* **10**, 41–49 (2016).
13. Pandit, A. S., Ball, G., Edwards, A. D. & Counsell, S. J. Diffusion magnetic resonance imaging in preterm brain injury. *Neuroradiology* **55 Suppl 2**, 65–95 (2013).
14. Bolisetty, S. *et al.* Intraventricular Hemorrhage and Neurodevelopmental Outcomes in Extreme Preterm Infants. *Pediatrics* **133**, 55–62 (2014).
15. Hintz, S. R. *et al.* Neuroimaging and Neurodevelopmental Outcome in Extremely Preterm Infants. *Pediatrics* **135**, e32–e42 (2015).
16. Blencowe, H. *et al.* Preterm birth-associated neurodevelopmental impairment estimates at regional and global levels for 2010. *Pediatr. Res.* **74 Suppl 1**, 17–34 (2013).
17. Institute of Medicine. *Preterm Birth: Causes, Consequences, and Prevention.* (2007).
18. Doyle, L. W., Roberts, G. & Anderson, P. J. Outcomes at age 2 years of infants < 28 weeks' gestational age born in Victoria in 2005. *J. Pediatr.* **156**, 49–53.e1 (2010).
19. Saigal, S. & Doyle, L. W. An overview of mortality and sequelae of preterm birth from infancy to adulthood. *Lancet* **371**, 261–269 (2008).
20. Cheong, J. L. Y. *et al.* Changing Neurodevelopment at 8 Years in Children Born Extremely Preterm Since the 1990s. **139**, (2017).
21. Teune, M. J. *et al.* A systematic review of severe morbidity in infants born late preterm. *Am. J. Obstet. Gynecol.* **205**, 374.e1–374.e9 (2011).
22. Petrini, J. R. *et al.* Increased Risk of Adverse Neurological Development for Late Preterm Infants. *J. Pediatr.* **154**, (2009).
23. Linsell, L. *et al.* Trajectories of behavior, attention, social and emotional problems from childhood to early adulthood following extremely preterm birth: a prospective cohort study. *Eur. Child Adolesc. Psychiatry* **28**, 531–542 (2019).
24. Petrou, S., Yiu, H. H. & Kwon, J. Economic consequences of preterm birth: a systematic review of the recent literature (2009–2017). *Arch. Dis. Child.* **104**, 456–465 (2019).
25. Johnston, K. M. *et al.* The economic burden of prematurity in Canada. *BMC Pediatr.* **14**, (2014).
26. Gilbert, W. M., Nesbitt, T. S. & Danielsen, B. The cost of prematurity: Quantification by gestational age and birth weight. *Obstet. Gynecol.* **102**, 488–492 (2003).

27. Access Economics. The Economic Impact of Cerebral Palsy in Australia in 2007 Report by Access Economics Pty Limited for Cerebral Palsy Australia. (2008).
28. Kruse, M. *et al.* Lifetime costs of cerebral palsy. *Dev. Med. Child Neurol.* **51**, 622–628 (2009).
29. Stolp, H. B., Liddelow, S. A., Sá-Pereira, I., Dziegielewska, K. M. & Saunders, N. R. Immune responses at brain barriers and implications for brain development and neurological function in later life. *Front. Integr. Neurosci.* **7**, 61 (2013).
30. Semple, B. D., Blomgren, K., Gimlin, K., Ferriero, D. M. & Noble-Haeusslein, L. J. Brain development in rodents and humans: Identifying benchmarks of maturation and vulnerability to injury across species. *Prog. Neurobiol.* **106–107**, 1–16 (2013).
31. Menassa, D. A. & Gomez-Nicola, D. Microglial dynamics during human brain development. *Front. Immunol.* **9**, (2018).
32. Reemst, K., Noctor, S. C., Lucassen, P. J. & Hol, E. M. The Indispensable Roles of Microglia and Astrocytes during Brain Development. *Front. Hum. Neurosci.* **10**, 1–28 (2016).
33. Pont-Lezica, L., Béchade, C., Belarif-Cantaut, Y., Pascual, O. & Bessis, A. Physiological roles of microglia during development. *J. Neurochem.* **119**, 901–908 (2011).
34. Monier, A., Evrard, P., Gressens, P. & Verney, C. Distribution and differentiation of microglia in the human encephalon during the first two trimesters of gestation. *J. Comp. Neurol.* **499**, 565–82 (2006).
35. Rezaie, P. Microglia in the Human Nervous System during Development. *Neuroembryology* **2**, 18–31 (2003).
36. Baburamani, A. A., Supramaniam, V. G., Hagberg, H. & Mallard, C. Microglia toxicity in preterm brain injury. *Reprod. Toxicol.* **48**, 106–112 (2014).
37. Orihuela, R., McPherson, C. A. & Harry, G. J. Microglial M1/M2 polarization and metabolic states. *Br. J. Pharmacol.* **173**, 649–65 (2016).
38. Mallard, C., Tremblay, M. E. & Vexler, Z. S. Microglia and Neonatal Brain Injury. *Neuroscience* **405**, 68–76 (2019).
39. Sofroniew, M. V. & Vinters, H. V. Astrocytes: Biology and pathology. *Acta Neuropathol.* **119**, 7–35 (2010).
40. Haddad-Tóvolli, R., Dragano, N. R. V., Ramalho, A. F. S. & Velloso, L. A. Development and function of the blood-brain barrier in the context of metabolic control. *Front. Neurosci.* **11**, 1–12 (2017).

41. Saunders, N. R., Liddelow, S. a. & Dziegielewska, K. M. Barrier mechanisms in the developing brain. *Front. Pharmacol.* **3 MAR**, 1–18 (2012).
42. Patra, A., Huang, H., Bauer, J. A. & Giannone, P. J. Neurological consequences of systemic inflammation in the premature neonate. *Neural Regen. Res.* **12**, 890–896 (2017).
43. Kuhn, S., Gritti, L., Crooks, D. & Dombrowski, Y. Oligodendrocytes in Development, Myelin Generation and Beyond. *Cells* **8**, 1–23 (2019).
44. Lee, H. S., Han, J., Bai, H. J. & Kim, K. W. Brain angiogenesis in developmental and pathological processes: Regulation, molecular and cellular communication at the neurovascular interface. *FEBS J.* **276**, 4622–4635 (2009).
45. Risau, W. & Wolburg, H. Development of the blood-brain barrier. *Trends Neurosci.* **13**, 174–8 (1990).
46. Badaut, J., Cohen, S. S., Virgintino, D. & Stonestreet, B. S. Development of the Blood-Brain Barrier. in *Fetal and Neonatal Physiology* (eds. Polin, R. A., Abman, S. H., Rowitch, D. H. & Benitz, W. E.) 1314–1325 (Elsevier, 2017).
47. Ballabh, P., Braun, A. & Nedergaard, M. Anatomic analysis of blood vessels in germinal matrix, cerebral cortex, and white matter in developing infants. *Pediatr. Res.* **56**, 117–124 (2004).
48. Brew, N., Walker, D. & Wong, F. Y. Cerebral vascular regulation and brain injury in preterm infants. *AJP Regul. Integr. Comp. Physiol.* **306**, R773–R786 (2014).
49. Licht, T., Dor-Wollman, T., Ben-Zvi, A., Rothe, G. & Keshet, E. Vessel maturation schedule determines vulnerability to neuronal injuries of prematurity. *J. Clin. Invest.* **125**, 1319–1328 (2015).
50. Volpe, J. J. Brain injury in the premature infant: Neuropathology, clinical aspects, and pathogenesis. *Ment. Retard. Dev. Disabil. Res. Rev.* **3**, 3–12 (1997).
51. Baburamani, A. A., Ek, C. J., Walker, D. W. & Castillo-Melendez, M. Vulnerability of the developing brain to hypoxic-ischemic damage: Contribution of the cerebral vasculature to injury and repair? *Front. Physiol.* **3 NOV**, 1–21 (2012).
52. Kuban, K. C. & Gilles, F. H. Human telencephalic angiogenesis. *Ann. Neurol.* **17**, 539–548 (1985).
53. Fumagalli, S., Ortolano, F. & De Simoni, M. G. A close look at brain dynamics: Cells and vessels seen by in vivo two-photon microscopy. *Prog. Neurobiol.* **121**, 36–54 (2014).

54. Zhao, Z., Nelson, A. R., Betsholtz, C. & Zlokovic, B. V. Establishment and Dysfunction of the Blood-Brain Barrier. *Cell* **163**, 1064–1078 (2015).
55. Greisen, G. Autoregulation of cerebral blood flow in newborn babies. *Early Hum. Dev.* **81**, 423–428 (2005).
56. Stamatovic, S. M., Johnson, A. M., Keep, R. F. & Andjelkovic, A. V. Junctional proteins of the blood-brain barrier: New insights into function and dysfunction. *Tissue Barriers* **4**, 1–12 (2016).
57. Ballabh, P., Hu, F., Kumarasiri, M., Braun, A. & Nedergaard, M. Development of tight junction molecules in blood vessels of germinal matrix, cerebral cortex, and white matter. *Pediatr. Res.* **58**, 791–798 (2005).
58. Virgintino, D. *et al.* Immunolocalization of tight junction proteins in the adult and developing human brain. *Histochem. Cell Biol.* **122**, 51–9 (2004).
59. Ek, C. J., Dziegielewska, K. M., Stolp, H. & Saunders, N. R. Functional Effectiveness of the Blood- Brain Barrier to Small Water-Soluble Molecules in Developing and Adult Opossum (*Monodelphis domestica*). **26**, 13–26 (2006).
60. Walsh, M. C. *et al.* Extremely low birthweight neonates with protracted ventilation: mortality and 18-month neurodevelopmental outcomes. *J. Pediatr.* **146**, 798–804 (2005).
61. Serenius, F. *et al.* Short-term outcome-after active perinatal management at 23-25 weeks of gestation. A study from two Swedish perinatal centres. Part 3: Neonatal morbidity. *Acta Paediatr. Int. J. Paediatr.* **93**, 1090–1097 (2004).
62. Gagliardi, L., Bellù, R., Zanini, R. & Dammann, O. Bronchopulmonary dysplasia and brain white matter damage in the preterm infant: A complex relationship. *Paediatr. Perinat. Epidemiol.* **23**, 582–590 (2009).
63. Soll, R. F. *et al.* Obstetric and neonatal care practices for infants 501 to 1500 g from 2000 to 2009. *Pediatrics* **132**, 222–228 (2013).
64. Chow, S. S. W., Creighton, P., Chambers, G. & Lui, K. *Report of the Australian and New Zealand Neonatal Network 2017. Annual Report* (ANZNN, 2019).
65. Cho, S. J., Shin, J. & Namgung, R. Initial resuscitation at delivery and short term neonatal outcomes in very-low-birth-weight infants. *J. Korean Med. Sci.* **30**, S45–S51 (2015).
66. Serenius, F. *et al.* Short-term outcome after active perinatal management at 23-25 weeks of gestation. A study from two Swedish tertiary care centres. Part 2: Infant survival. *Acta Paediatr. Int. J. Paediatr.* **93**, 1081–1089 (2004).

67. Bajaj, M. *et al.* Delivery Room Resuscitation and Short-Term Outcomes in Moderately Preterm Infants. *J. Pediatr.* **195**, 33-38.e2 (2018).
68. Hillman, N. H., Kallapur, S. G. & Jobe, A. H. Physiology of Transition from Intrauterine to Extrauterine Life. *Clin. Perinatol.* **39**, 769–783 (2012).
69. Australian and New Zealand Committee on Resuscitation. ANZCOR Guideline 13 . 4 – Airway Management and Mask Ventilation of the Newborn Infant. (2016).
70. Schmölzer, G. M., Te Pas, A. B., Davis, P. G. & Morley, C. J. Reducing lung injury during neonatal resuscitation of preterm infants. *J. Pediatr.* **153**, 741–745 (2008).
71. Hooper, S. B., Te Pas, A. B. & Kitchen, M. J. Respiratory transition in the newborn: a three-phase process. *Arch. Dis. Child. Fetal Neonatal Ed.* **101**, F266-71 (2016).
72. Aly, H. Is It Safer to Intubate Premature Infants in the Delivery Room? *Pediatrics* **115**, 1660–1665 (2005).
73. Choi, Y.-B., Lee, J., Park, J. & Jun, Y. H. Impact of Prolonged Mechanical Ventilation in Very Low Birth Weight Infants: Results From a National Cohort Study. *J. Pediatr.* **194**, 34-39.e3 (2018).
74. Lundqvist, P., Källén, K., Hallström, I. & Westas, L. H. Trends in outcomes for very preterm infants in the southern region of Sweden over a 10-year period. *Acta Paediatr. Int. J. Paediatr.* **98**, 648–653 (2009).
75. Vliegenthart, R. J. S., van Kaam, A. H., Aarnoudse-Moens, C. S. H., van Wassenae, A. G. & Onland, W. Duration of mechanical ventilation and neurodevelopment in preterm infants. *Arch. Dis. Child. Fetal Neonatal Ed.* **104**, F631–F635 (2019).
76. Curley, G. F., Laffey, J. G., Zhang, H. & Slutsky, A. S. Biotrauma and Ventilator-Induced Lung Injury: Clinical Implications. *Chest* **150**, 1109–1117 (2016).
77. Attar, M. A. & Donn, S. M. Mechanisms of ventilator-induced lung injury in premature infants. *Semin. Neonatol.* **7**, 353–360 (2002).
78. Jobe, A. H. & Ikegami, M. Mechanisms initiating lung injury in the preterm. *Early Hum. Dev.* **53**, 81–94 (1998).
79. Parker, J. C., Hernandez, L. A. & Peevy, K. J. Mechanisms of ventilator-induced lung injury. *Critical care medicine* **21**, 131–143 (1993).
80. Polglase, G. R. *et al.* Respiratory support for premature neonates in the delivery room: effects on cardiovascular function and the development of brain injury. *Pediatr. Res.* **75**, 682–688 (2014).

81. Björklund, L. J. *et al.* Manual ventilation with a few large breaths at birth compromises the therapeutic effect of subsequent surfactant replacement in immature lambs. *Pediatr. Res.* **42**, 348–355 (1997).
82. Schmölzer, G. M. *et al.* Airway obstruction and gas leak during mask ventilation of preterm infants in the delivery room. *Arch. Dis. Child. Fetal Neonatal Ed.* **96**, F254–F257 (2011).
83. Finer, N. N. & Rich, W. D. Unintentional variation in positive end expiratory pressure during resuscitation with a T-piece resuscitator. *Resuscitation* **82**, 717–719 (2011).
84. Schmolzer, G. *et al.* 8: Tidal Volume Delivery During Mask Ventilation and Brain Injury in Newborns <29 Weeks Gestation. *Paediatr. Child Health (Oxford)*. **20**, 33–34 (2015).
85. Poulton, D. A., Schmölzer, G. M., Morley, C. J. & Davis, P. G. Assessment of chest rise during mask ventilation of preterm infants in the delivery room. *Resuscitation* **82**, 175–179 (2011).
86. Tracy, M., Downe, L. & Holberton, J. How safe is intermittent positive pressure ventilation in preterm babies ventilated from delivery to newborn intensive care unit? *Arch. Dis. Child. Fetal Neonatal Ed.* **89**, F84–F87 (2004).
87. Schmölzer, G. M. *et al.* Assessment of tidal volume and gas leak during mask ventilation of preterm infants in the delivery room. *Arch. Dis. Child. Fetal Neonatal Ed.* **95**, 1–4 (2010).
88. van Vonderen, J. J., Hooper, S. B., Krabbe, V. B., Siew, M. L. & te Pas, A. B. Monitoring tidal volumes in preterm infants at birth: mask versus endotracheal ventilation. *Arch. Dis. Child. - Fetal Neonatal Ed.* **100**, F43–F46 (2015).
89. Tingay, D. G. *et al.* Surfactant before the first inflation at birth improves spatial distribution of ventilation and reduces lung injury in preterm lambs. *J. Appl. Physiol.* **116**, 251–258 (2014).
90. Vozzelli, M. A., Mason, S. N., Whorton, M. H. & Auten, R. L. Antimacrophage chemokine treatment prevents neutrophil and macrophage influx in hyperoxia-exposed newborn rat lung. *Am. J. Physiol. Cell. Mol. Physiol.* **286**, L488–L493 (2004).
91. Bohrer, B., Silveira, R. C., Neto, E. C. & Procianoy, R. S. Mechanical Ventilation of Newborns Infant Changes in Plasma Pro- and Anti-Inflammatory Cytokines. *J. Pediatr.* **156**, 16–19 (2010).
92. Carvalho, C. G., Silveira, R. C. & Procianoy, R. S. Ventilator-induced lung injury in preterm infants. *Rev. Bras. Ter. Intensiva* **25**, 319–326 (2013).
93. Kotecha, S., Wilson, L., Wangoo, A., Silverman, M. & Shaw, R. J. Increase in Interleukin (IL)-1 β and IL-6 in Bronchoalveolar Lavage Fluid Obtained from Infants with Chronic Lung Disease of Prematurity. *Pediatr. Res.* **40**, 250–256 (1996).

94. Bose, C. L. *et al.* Systemic inflammation associated with mechanical ventilation among extremely preterm infants. *Cytokine* **61**, 315–322 (2013).
95. Demauro, S. B. *et al.* Impact of delivery room resuscitation on outcomes up to 18 months in very low birth weight infants. *J. Pediatr.* **159**, 546–550.e1 (2011).
96. Barton, S. K. *et al.* Unraveling the links between the initiation of ventilation and brain injury in preterm infants. *Front. Pediatr.* **3**, 97 (2015).
97. Mian, Q. *et al.* Impact of delivered tidal volume on the occurrence of intraventricular haemorrhage in preterm infants during positive pressure ventilation in the delivery room. *Arch. Dis. Child. Fetal Neonatal Ed.* **104**, F57–F62 (2019).
98. Aly, H., Hammad, T. A., Essers, J. & Wung, J. T. Is mechanical ventilation associated with intraventricular hemorrhage in preterm infants? *Brain Dev.* **34**, 201–205 (2012).
99. Pahuja, A. *et al.* Relationship of resuscitation, respiratory function monitoring data and outcomes in preterm infants. *Eur. J. Pediatr.* **177**, 1617–1624 (2018).
100. Mian, Q. N. *et al.* Tidal volumes in spontaneously breathing preterm infants supported with continuous positive airway pressure. *J. Pediatr.* **165**, 702–706.e1 (2014).
101. Vento, M. *et al.* Using intensive care technology in the delivery room: a new concept for the resuscitation of extremely preterm neonates. *Pediatrics* **122**, 1113–6 (2008).
102. Lee, J. & Loepke, A. W. Does pediatric anesthesia cause brain damage? – Addressing parental and provider concerns in light of compelling animal studies and seemingly ambivalent human data. *Korean J. Anesthesiol.* **71**, 255–273 (2018).
103. Andropoulos, D. B. Effect of anesthesia on the developing brain: Infant and fetus. *Fetal Diagn. Ther.* **43**, 1–11 (2018).
104. Kumar, P., Denson, S. E. & Mancuso, T. J. Premedication for Nonemergency Endotracheal Intubation in the Neonate. *Pediatrics* **125**, 608–615 (2010).
105. Albertine, K. H. Brain Injury in Chronically Ventilated Preterm Neonates. *Clin. Perinatol.* **39**, 727–740 (2012).
106. Chow, S. S. W. *et al.* *Report of the Australian and New Zealand Neonatal Network 2015.* (2017).
107. Tsai, W. *et al.* Association between mechanical ventilation and neurodevelopmental disorders in a nationwide cohort of extremely low birth weight infants. *Res. Dev. Disabil.* **35**, 1544–50 (2014).

108. Behnke, J. *et al.* Non-Invasive Ventilation in Neonatology. *Dtsch. Arztebl. Int.* **116**, 177–183 (2019).
109. Rees, S. & Inder, T. Fetal and neonatal origins of altered brain development. *Early Human Development* **81**, 753–761 (2005).
110. Polglase, G. R. *et al.* Initiation of resuscitation with high tidal volumes causes cerebral hemodynamic disturbance, brain inflammation and injury in preterm lambs. *PLoS One* **7**, e39535 (2012).
111. Alahmari, D. M. *et al.* Diffusion tensor imaging detects ventilation-induced brain injury in preterm lambs. *PLoS One* **12**, e0188737 (2017).
112. Polglase, G. R. & Hooper, S. B. Role of Intra-Luminal Pressure in Regulating PBF in the Fetus and After Birth. *Curr. Pediatr. Rev.* **2**, 287–299 (2006).
113. Gilmore, M. M. *et al.* Relationship between cerebrovascular dysautoregulation and arterial blood pressure in the premature infant. *Journal of Perinatology* **31**, 722–729 (2011).
114. Del Toro, J., Louis, P. T. & Goddard-Finegold, J. Cerebrovascular regulation and neonatal brain injury. *Pediatr. Neurol.* **7**, 3–12 (1991).
115. Mayhan, W. G. & Heistad, D. D. Permeability of blood-brain barrier to various sized molecules. *Am. J. Physiol. – Hear. Circ. Physiol.* **17**, (1985).
116. du Plessis, A. J. The role of systemic hemodynamic disturbances in prematurity-related brain injury. *J. Child Neurol.* **24**, 1127–1140 (2009).
117. Verma, P. K., Panerai, R. B., Rennie, J. M. & Evans, D. H. Grading of cerebral autoregulation in preterm and term neonates. *Pediatr. Neurol.* **23**, 236–242 (2000).
118. Papile, L. A., Rudolph, A. M. & Heymann, M. A. Autoregulation of cerebral blood flow in the preterm fetal lamb. *Pediatr. Res.* **19**, 159–61 (1985).
119. Purves, M. J. & James, I. M. Observations on the control of cerebral blood flow in the sheep fetus and newborn lamb. *Circ. Res.* **25**, 651–67 (1969).
120. Müller, T. *et al.* Developmental changes in cerebral autoregulatory capacity in the fetal sheep parietal cortex. *J. Physiol.* **539**, 957–967 (2002).
121. Czynski, A. J. *et al.* Cerebral autoregulation is minimally influenced by the superior cervical ganglion in two-week-old lambs, and absent in preterm lambs immediately following delivery. *PLoS One* **8**, e82326 (2013).

122. Perlman, J. M., McMennamin, J. B. & Volpe, J. J. Fluctuating Cerebral Blood-Flow Velocity in Respiratory-Distress Syndrome. *N. Engl. J. Med.* **309**, 204–209 (1983).
123. Temesvári, P. & Kovács, J. Selective opening of the blood-brain barrier in newborn piglets with experimental pneumothorax. *Neurosci. Lett.* **93**, 38–43 (1988).
124. Stonestreet, B. S. *et al.* Effects of duration of positive-pressure ventilation on blood-brain barrier function in premature lambs. *J. Appl. Physiol.* **88**, 1672–1677 (2000).
125. Malaeb, S. & Dammann, O. Fetal Inflammatory Response and Brain Injury in the Preterm Newborn. *J. Child Neurol.* **24**, 1119–1126 (2009).
126. Turunen, R., Nupponen, I., Siitonen, S., Repo, H. & Andersson, S. Onset of mechanical ventilation is associated with rapid activation of circulating phagocytes in preterm infants. *Pediatrics* **117**, 448–454 (2006).
127. Sankowski, R., Mader, S. & Valdés-Ferrer, S. I. Systemic inflammation and the brain: novel roles of genetic, molecular, and environmental cues as drivers of neurodegeneration. *Front. Cell. Neurosci.* **9**, 28 (2015).
128. Threlkeld, S. W. *et al.* Ovine proinflammatory cytokines cross the murine blood-brain barrier by a common saturable transport mechanism. *Neuroimmunomodulation* **17**, 405–410 (2010).
129. Cohen, S. S. *et al.* Effects of Interleukin-6 on the Expression of Tight Junction Proteins in Isolated Cerebral Microvessels from Yearling and Adult Sheep. *Neuroimmunomodulation* **20**, 264–273 (2013).
130. Stoll, B. J. *et al.* Neurodevelopmental and growth impairment among extremely low-birth-weight infants with neonatal infection. *J. Am. Med. Assoc.* **292**, 2357–2365 (2004).
131. Shah, D. K. *et al.* Adverse neurodevelopment in preterm infants with postnatal sepsis or necrotizing enterocolitis is mediated by white matter abnormalities on magnetic resonance imaging at term. *J. Pediatr.* **153**, 170–5, 175.e1 (2008).
132. Polglase, G. R. *et al.* Inflammation in utero exacerbates ventilation-induced brain injury in preterm lambs. *Journal of Applied Physiology* **112**, 481–489 (2012).
133. Barton, S. K. *et al.* Differential short-term regional effects of early high dose erythropoietin on white matter in preterm lambs after mechanical ventilation. *J. Physiol.* **594**, 1437–49 (2016).
134. Skiöld, B. *et al.* Early detection of ventilation-induced brain injury using magnetic resonance spectroscopy and diffusion tensor imaging: An in vivo study in preterm lambs. *PLoS One* **9**, 1–8 (2014).

135. Barton, S. K. *et al.* Human amnion epithelial cells modulate ventilation-induced white matter pathology in preterm lambs. *Dev. Neurosci.* **37**, 338–348 (2015).
136. Stojanovska, V. *et al.* The Effect of Antenatal Betamethasone on White Matter Inflammation and Injury in Fetal Sheep and Ventilated Preterm Lambs. *Dev. Neurosci.* **40**, 497–507 (2018).
137. Probyn, M. E. *et al.* Effects of tidal volume and positive end-expiratory pressure during resuscitation of very premature lambs. *Acta Paediatr.* **94**, 1764–1770 (2005).
138. Alahmari, D. M. *et al.* Correlation between diffusion tensor imaging and histological brain injury in ventilated preterm lambs. *Imaging Med.* **9**, 67–76 (2017).
139. Stojanovska, V. *et al.* Effects of Intrauterine Inflammation on Cortical Gray Matter of Near-Term Lambs. *Front. Pediatr.* **6**, 1–10 (2018).
140. Alahmari, D. M. *et al.* Diffusion Tensor Imaging Colour Mapping Threshold for Identification of Ventilation-Induced Brain Injury after Intrauterine Inflammation in Preterm Lambs. *Front. Pediatr.* **5**, 1–13 (2017).
141. Bapat, R., Narayana, P. A., Zhou, Y. & Parikh, N. A. Magnetic resonance spectroscopy at term-equivalent age in extremely preterm infants: Association with cognitive and language development. *Pediatr. Neurol.* **51**, 53–59 (2014).
142. Hyodo, R. *et al.* Magnetic resonance spectroscopy in preterm infants: association with neurodevelopmental outcomes. *Arch. Dis. Child. Fetal Neonatal Ed.* **103**, F238–F244 (2018).
143. Loeliger, M. *et al.* High-Frequency Oscillatory Ventilation Is Not Associated With Increased Risk of Neuropathology Compared With Positive Pressure Ventilation: A Preterm Primate Model. *Pediatr. Res.* **66**, 545–550 (2009).
144. Dieni, S. *et al.* The pattern of cerebral injury in a primate model of preterm birth and neonatal intensive care. *J. Neuropathol. Exp. Neurol.* **63**, 1297–309 (2004).
145. Loeliger, M. *et al.* Developmental and neuropathological consequences of ductal ligation in the preterm baboon. *Pediatr. Res.* **65**, 209–214 (2009).
146. Rees, S. M. *et al.* Inhaled Nitric Oxide: Effects on Cerebral Growth and Injury in a Baboon Model of Premature Delivery. *Pediatr. Res.* **61**, 552–558 (2007).
147. Yoder, B. A., Siler-Khodr, T., Winter, V. T. & Coalson, J. J. High-frequency oscillatory ventilation: Effects on lung function, mechanics, and airway cytokines in the immature baboon model for neonatal chronic lung disease. *Am. J. Respir. Crit. Care Med.* **162**, 1867–1876 (2000).

148. Griffith, J. L. *et al.* MR imaging correlates of white-matter pathology in a preterm baboon model. *Pediatr. Res.* **71**, 185–191 (2012).
149. Verney, C. *et al.* Neuronal damage in the preterm baboon: Impact of the mode of ventilatory support. *J. Neuropathol. Exp. Neurol.* **69**, 473–482 (2010).
150. Allison, B. J. *et al.* Does growth restriction increase the vulnerability to acute ventilation-induced brain injury in newborn lambs? Implications for future health and disease. *J. Dev. Orig. Health Dis.* **8**, 556–565 (2017).
151. Brett Kothe, T. *et al.* Surfactant plus budesonide decreases lung and systemic inflammation in mechanically ventilated preterm sheep. *Am. J. Physiol. - Lung Cell. Mol. Physiol.* **316**, L888–L893 (2019).
152. Malhotra, A. *et al.* Neuropathology as a consequence of neonatal ventilation in premature growth-restricted lambs. *Am. J. Physiol. Integr. Comp. Physiol.* **315**, R1183–R1194 (2018).
153. Dekker, J. *et al.* Caffeine to improve breathing effort of preterm infants at birth: A randomized controlled trial. *Pediatr. Res.* **82**, 290–296 (2017).
154. Amaro, C. M. *et al.* Early Caffeine and Weaning from Mechanical Ventilation in Preterm Infants: A Randomized, Placebo-Controlled Trial. *J. Pediatr.* **196**, 52–57 (2018).
155. Barton, S. K. *et al.* Protective ventilation of preterm lambs exposed to acute chorioamnionitis does not reduce ventilation-induced lung or brain injury. *PLoS One* **9**, e112402 (2014).
156. Polglase, G. R. *et al.* Ventilation onset prior to umbilical cord clamping (physiological-based cord clamping) improves systemic and cerebral oxygenation in preterm lambs. *PLoS One* **10**, 1–13 (2015).
157. Bhatt, S. *et al.* Delaying cord clamping until ventilation onset improves cardiovascular function at birth in preterm lambs. *J. Physiol.* **591**, 2113–2126 (2013).
158. Polglase, G. R. *et al.* Physiologically based cord clamping stabilises cardiac output and reduces cerebrovascular injury in asphyxiated near-term lambs. *Arch. Dis. Child. Fetal Neonatal Ed.* **103**, F530–F538 (2018).
159. Chan, K. Y. Y. *et al.* Optimizing the Dose of Erythropoietin Required to Prevent Acute Ventilation-Induced Cerebral White Matter Injury in Preterm Lambs. *Dev. Neurosci.* **39**, 298–309 (2017).
160. Barton, S. K. *et al.* Ventilation-Induced Brain Injury in Preterm Neonates: A Review of Potential Therapies. *Neonatology* **110**, 155–62 (2016).

161. Allison, B. J. *et al.* Dose-dependent exacerbation of ventilation-induced lung injury by erythropoietin in preterm newborn lambs. *J. Appl. Physiol.* **126**, 44–50 (2019).
162. Juul, S. E. *et al.* Erythropoietin concentrations in cerebrospinal fluid of nonhuman primates and fetal sheep following high-dose recombinant erythropoietin. *Biol. Neonate* **85**, 138–144 (2004).
163. Polglase, G. R. *et al.* Prophylactic erythropoietin exacerbates ventilation-induced lung inflammation and injury in preterm lambs. *J. Physiol.* **592**, 1993–2002 (2014).
164. Melville, J. M. *et al.* Human amnion epithelial cells modulate the inflammatory response to ventilation in preterm lambs. *PLoS One* **12**, e0173572 (2017).
165. Hodges, R. J. *et al.* Human amnion epithelial cells reduce ventilation-induced preterm lung injury in fetal sheep. *Am. J. Obstet. Gynecol.* **206**, 448.e8–448.e15 (2012).
166. Weiss, M. L. & Troyer, D. L. Stem Cells in the Umbilical Cord. *Stem Cell Rev* **2**, 155–162 (2006).
167. McDonald, C. A., Castillo-Melendez, M., Penny, T. R., Jenkin, G. & Miller, S. L. Umbilical Cord Blood Cells for Perinatal Brain Injury: The Right Cells at the Right Time? in *Umbilical Cord Blood Banking for Clinical Application and Regenerative Medicine* (InTech, 2017). doi:10.5772/66647
168. Li, J., McDonald, C. A., Fahey, M. C., Jenkin, G. & Miller, S. L. Could cord blood cell therapy reduce preterm brain injury? *Front. Neurol.* **5**, (2014).
169. Verina, T., Fatemi, A., Johnston, M. V. & Comi, A. M. Pluripotent possibilities: Human umbilical cord blood cell treatment after neonatal brain injury. *Pediatr. Neurol.* **48**, 346–354 (2013).
170. Jaing, T.-H. Umbilical Cord Blood: A Trustworthy Source of Multipotent Stem Cells for Regenerative Medicine. *Cell Transplant.* **23**, 493–496 (2014).
171. McDonald, C. A., Fahey, M. C., Jenkin, G. & Miller, S. L. Umbilical cord blood cells for treatment of cerebral palsy; timing and treatment options. *Pediatr. Res.* **83**, 333–344 (2018).
172. Boltze, J. *et al.* Assessment of neuroprotective effects of human umbilical cord blood mononuclear cell subpopulations in vitro and in vivo. *Cell Transplant.* **21**, 723–737 (2012).
173. Takahata, Y. *et al.* CD25+CD4+ T cells in human cord blood: an immunoregulatory subset with naive phenotype and specific expression of forkhead box p3 (Foxp3) gene. *Exp. Hematol.* **32**, 622–629 (2004).

174. Maillacheruvu, P. F., Engel, L. M., Crum, I. T., Agrawal, D. K. & Peeples, E. S. From cord to caudate: Characterizing umbilical cord blood stem cells and their paracrine interactions with the injured brain. *Pediatr. Res.* **83**, 205–213 (2018).
175. Castillo-Melendez, M., Yawno, T., Jenkin, G. & Miller, S. L. Stem cell therapy to protect and repair the developing brain: A review of mechanisms of action of cord blood and amnion epithelial derived cells. *Front. Neurosci.* **7**, 1–14 (2013).
176. Melero-Martin, J. M. *et al.* In vivo vasculogenic potential of human blood-derived endothelial progenitor cells. *Blood* **109**, 4761–4768 (2007).
177. Liu, Y. *et al.* Vasculogenic and osteogenesis-enhancing potential of human umbilical cord blood endothelial colony-forming cells. *Stem Cells* **30**, 1911–1924 (2012).
178. Kögler, G., Sensken, S. & Wernet, P. Comparative generation and characterization of pluripotent unrestricted somatic stem cells with mesenchymal stem cells from human cord blood. *Exp. Hematol.* **34**, 1589–1595 (2006).
179. Caprnda, M. *et al.* Immunomodulatory effects of stem cells: Therapeutic option for neurodegenerative disorders. *Biomed. Pharmacother.* **91**, 60–69 (2017).
180. Gu, Y. *et al.* Endogenous IL-6 of mesenchymal stem cell improves behavioral outcome of hypoxic-ischemic brain damage neonatal rats by supressing apoptosis in astrocyte. *Sci. Rep.* **6**, 1–16 (2016).
181. Hernández, R. *et al.* Differentiation of human mesenchymal stem cells towards neuronal lineage: Clinical trials in nervous system disorders. *Biomol. Ther.* **28**, 34–44 (2020).
182. Urrutia, D. N. *et al.* Comparative study of the neural differentiation capacity of mesenchymal stromal cells from different tissue sources: An approach for their use in neural regeneration therapies. *PLoS One* **14**, 1–17 (2019).
183. Ahn, S. Y., Chang, Y. S. & Park, W. S. Stem Cells for Neonatal Brain Disorders. *Neonatology* **109**, 377–383 (2016).
184. Aridas, J. D. S. *et al.* Cord blood mononuclear cells prevent neuronal apoptosis in response to perinatal asphyxia in the newborn lamb. *J. Physiol.* **594**, 1421–1435 (2016).
185. Li, J. *et al.* Term vs. preterm cord blood cells for the prevention of preterm brain injury. *Pediatr. Res.* **82**, 1030–1038 (2017).
186. Drobyshevsky, A. *et al.* Human Umbilical Cord Blood Cells Ameliorate Motor Deficits in Rabbits in a Cerebral Palsy Model. *Dev. Neurosci.* **37**, 349–362 (2015).

187. Borlongan, C. V., Hadman, M., Sanberg, C. D. & Sanberg, P. R. Central nervous system entry of peripherally injected umbilical cord blood cells is not required for neuroprotection in stroke. *Stroke* **35**, 2385–2389 (2004).
188. Li, J. *et al.* Preterm white matter brain injury is prevented by early administration of umbilical cord blood cells. *Exp. Neurol.* **283**, 179–187 (2016).
189. Smith, M. J. *et al.* Umbilical Cord Blood Cells Do Not Reduce Ventilation Induced Lung Injury in Preterm Lambs. *J. Paediatr. Child Health* **55**, 49–49 (2019).
190. Clark, E. L. *et al.* A high resolution atlas of gene expression in the domestic sheep (*Ovis aries*). *PLOS Genet.* **13**, e1006997 (2017).
191. Livak, K. J. & Schmittgen, T. D. Analysis of relative gene expression data using real-time quantitative PCR and the 2- $\Delta\Delta$ CT method. *Methods* **25**, 402–408 (2001).
192. Johnson, J. I., Sudheimer, K. D., Davis, K. K., Kerndt, G. M. & Winn, B. M. The Sheep Brain Atlas. *Michigan State University Brain Biodiversity Bank* Available at: <https://msu.edu/~brains/brains/sheep/index.html>.
193. Riddle, A. Spatial Heterogeneity in Oligodendrocyte Lineage Maturation and Not Cerebral Blood Flow Predicts Fetal Ovine Periventricular White Matter Injury. *J. Neurosci.* **26**, 3045–3055 (2006).
194. Ito, D. *et al.* Microglia-specific localisation of a novel calcium binding protein, Iba1. *Mol. Brain Res.* **57**, 1–9 (1998).
195. Kettenmann, H., Hanisch, U.-K., Noda, M. & Verkhratsky, A. Physiology of Microglia. *Physiol. Rev.* **91**, 461–553 (2011).
196. Saunders, N. R., Dziegielewska, K. M., Møllgård, K. & Habgood, M. D. Markers for blood-brain barrier integrity: How appropriate is Evans blue in the twenty-first century and what are the alternatives? *Front. Neurosci.* **9**, 1–16 (2015).
197. Zhou, Q., Wang, S. & Anderson, D. J. Identification of a novel family of oligodendrocyte lineage-specific basic helix-loop-helix transcription factors. *Neuron* **25**, 331–343 (2000).
198. Harauz, G. & Boggs, J. M. Myelin management by the 18.5-kDa and 21.5-kDa classic myelin basic protein isoforms. *J. Neurochem.* **125**, 334–361 (2013).
199. Chang, H. H. *et al.* Preventing preterm births: Analysis of trends and potential reductions with interventions in 39 countries with very high human development index. *Lancet* **381**, 223–234 (2013).

200. Volpe, J. J. Brain injury in premature infants: a complex amalgam of destructive and developmental disturbances. *Lancet Neurol.* **8**, 110–124 (2009).
201. Back, S. A. & Rosenberg, P. A. Pathophysiology of glia in perinatal white matter injury. *Glia* **62**, 1790–1815 (2014).
202. Bel, F. Van, Roman, C., Klautz, R. J. M., Teitel, D. F. & Rudolph, A. M. Relationship between Brain Blood Flow and Carotid Arterial Flow in the Sheep Fetus. *Pediatr. Res.* **35**, 329–333 (1994).
203. Barlow, R. M. The foetal sheep: morphogenesis of the nervous system and histochemical aspects of myelination. *J. Comp. Neurol.* **135**, 249–262 (1969).
204. Back, S. A., Riddle, A. & Hohimer, A. R. Role of instrumented fetal sheep preparations in defining the pathogenesis of human periventricular white-matter injury. *J Child Neurol* **21**, 582–589 (2006).
205. Hillman, N. H. *et al.* Brief, large tidal volume ventilation initiates lung injury and a systemic response in fetal sheep. *Am. J. Respir. Crit. Care Med.* **176**, 575–581 (2007).
206. Winger, R. C., Koblinski, J. E., Kanda, T., Ransohoff, R. M. & Muller, W. A. Rapid Remodeling of Tight Junctions during Paracellular Diapedesis in a Human Model of the Blood–Brain Barrier. *J. Immunol.* **193**, 2427–2437 (2014).
207. Sobotka, K. S. *et al.* Single sustained inflation followed by ventilation leads to rapid cardiorespiratory recovery but causes cerebral vascular leakage in asphyxiated near-term lambs. *PLoS One* **11**, 1–14 (2016).
208. Signorelli, F. *et al.* Hemodynamic Stress, Inflammation, and Intracranial Aneurysm Development and Rupture: A Systematic Review. *World Neurosurg.* **115**, 234–244 (2018).
209. Paton, M. C. B. *et al.* Human umbilical cord blood therapy protects cerebral white matter from systemic LPS exposure in preterm fetal sheep. *Dev. Neurosci.* **40**, 258–270 (2018).
210. McDonald, C. A. *et al.* Effects of umbilical cord blood cells, and subtypes, to reduce neuroinflammation following perinatal hypoxic-ischemic brain injury. *J. Neuroinflammation* **15**, 1–14 (2018).
211. Paton, M. C. B. *et al.* Umbilical cord blood versus mesenchymal stem cells for inflammation-induced preterm brain injury in fetal sheep. *Pediatr. Res.* **86**, 165–173 (2019).
212. Hillman, N. H. *et al.* Inflammation and lung maturation from stretch injury in preterm fetal sheep. *Am. J. Physiol. Lung Cell. Mol. Physiol.* **300**, L232–L241 (2011).

213. Ransohoff, R. M. & Perry, V. H. Microglial Physiology: Unique Stimuli, Specialized Responses. *Annu. Rev. Immunol.* **27**, 119–145 (2009).
214. Hwang, S., Choi, J. I. & Kim, M. Y. Combining human umbilical cord blood cells with erythropoietin enhances angiogenesis/neurogenesis and behavioral recovery after stroke. *Front. Neurol.* **10**, 1–15 (2019).
215. Bernardo, M. E. & Fibbe, W. E. Mesenchymal stromal cells: Sensors and switchers of inflammation. *Cell Stem Cell* **13**, 392–402 (2013).
216. Burr, S. P., Dazzi, F. & Garden, O. A. Mesenchymal stromal cells and regulatory T cells: The Yin and Yang of peripheral tolerance. *Immunol. Cell Biol.* **91**, 12–18 (2013).
217. Kang, M. *et al.* Involvement of Immune Responses in the Efficacy of Cord Blood Cell Therapy for Cerebral Palsy. *Stem Cells Dev.* **24**, 2259–68 (2015).
218. Allison, B. J. *et al.* Ventilation of the very immature lung in utero induces injury and BPD-like changes in lung structure in fetal sheep. *Pediatr. Res.* **64**, 387–392 (2008).
219. O'Reilly, M. *et al.* Persistent bronchiolar remodeling following brief ventilation of the very immature ovine lung. *Am. J. Physiol. – Lung Cell. Mol. Physiol.* **297**, 992–1001 (2009).
220. Abdul Aziz, A. N. *et al.* Early inotropes use is associated with higher risk of death and/or severe brain injury in extremely premature infants. *J. Matern. Neonatal Med.* **0**, 1–8 (2019).
221. Brew, N. *et al.* Dobutamine treatment reduces inflammation in the preterm fetal sheep brain exposed to acute hypoxia. *Pediatr. Res.* **84**, 442–450 (2018).
222. Brew, N. *et al.* Dopamine treatment during acute hypoxia is neuroprotective in the developing sheep brain. *Neuroscience* **316**, 82–93 (2016).
223. Mellor, D. J., Diesch, T. J., Gunn, A. J. & Bennet, L. Fetal 'awareness' and 'pain': What precautions should be taken to safeguard fetal welfare during experiments? *Anim. Welf.* 79–83 (2008).
224. Blanco, C. E., Martin, C. B., Hanson, M. A. & McCooke, H. B. Breathing activity in fetal sheep during mechanical ventilation of the lungs in utero. *Eur. J. Obstet. Gynecol. Reprod. Biol.* **26**, 175–182 (1987).
225. Walther, F. J., Blanco, C. E., Houdijk, M. & Bevers, E. M. Single Versus Repetitive Doses of Natural Surfactant as Treatment of Respiratory Distress Syndrome in Premature Lambs. *Pediatr. Res.* **19**, 224–227 (1985).

226. Allison, B. J. *et al.* Pulmonary hemodynamic responses to in utero ventilation in very immature fetal sheep. *Respir. Res.* **11**, 1–11 (2010).
227. Heep, A. *et al.* Increased serum levels of interleukin 6 are associated with severe intraventricular haemorrhage in extremely premature infants. *Arch. Dis. Child. Fetal Neonatal Ed.* **88**, F501–4 (2003).
228. Bartha, A. I. *et al.* Neonatal encephalopathy: association of cytokines with MR spectroscopy and outcome. *Pediatr. Res.* **56**, 960–6 (2004).
229. Ellison, V. J. *et al.* The relationship of CSF and plasma cytokine levels to cerebral white matter injury in the premature newborn. *Pediatr. Res.* **57**, 282–286 (2005).
230. Schmölder, G. M., Morley, C. J. & Kamlin, O. C. O. F. Enhanced monitoring during neonatal resuscitation. *Semin. Perinatol.* **43**, 151177 (2019).
231. van Vonderen, J. J. *et al.* Cardiorespiratory Monitoring during Neonatal Resuscitation for Direct Feedback and Audit. *Front. Pediatr.* **4**, 1–7 (2016).
232. Schmölder, G. M. *et al.* Respiratory function monitor guidance of mask ventilation in the delivery room: A feasibility study. *J. Pediatr.* **160**, (2012).
233. Brew, N., Hooper, S. B., Allison, B. J., Wallace, M. J. & Harding, R. Injury and repair in the very immature lung following brief mechanical ventilation. *Am. J. Physiol. – Lung Cell. Mol. Physiol.* **301**, L917–L926 (2011).
234. Brew, N., Hooper, S. B., Zahra, V., Wallace, M. & Harding, R. Mechanical Ventilation Injury and Repair in Extremely and Very Preterm Lungs. *PLoS One* **8**, 1–10 (2013).
235. Pogozhykh, O., Prokopyuk, V., Figueiredo, C. & Pogozhykh, D. Placenta and Placental Derivatives in Regenerative Therapies: Experimental Studies, History, and Prospects. *Stem Cells Int.* **2018**, 4837930 (2018).
236. Silini, A. R., Cargnoni, A., Magatti, M., Pianta, S. & Parolini, O. The long path of human placenta, and its derivatives, in regenerative medicine. *Front. Bioeng. Biotechnol.* **3**, (2015).
237. Hodyl, N. A. *et al.* Child neurodevelopmental outcomes following preterm and term birth : What can the placenta tell us ? *Placenta* **57**, 79–86 (2017).
238. Hirst, J. J., Palliser, H. K., Yates, D. M., Yawno, T. & Walker, D. W. Neurosteroids in the fetus and neonate : Potential protective role in compromised pregnancies. **52**, 602–610 (2008).
239. Vu, T. T. *et al.* Changes in human placental 5 α -reductase isoenzyme expression with advancing gestation: effects of fetal sex and glucocorticoid exposure. *Reprod. Fertil. Dev.* **21**, 599 (2009).

- 240. Yawno, T., Hirst, J. J., Castillo-Melendez, M. & Walker, D. W. Role of neurosteroids in regulating cell death and proliferation in the late gestation fetal brain. *Neuroscience* **163**, 838–847 (2009).
- 241. Zaretsky, M. V., Alexander, J. M., Byrd, W. & Bawdon, R. E. Transfer of inflammatory cytokines across the placenta. *Obstet. Gynecol.* **103**, 546–550 (2004).
- 242. Schittny, J. C. Development of the lung. *Cell Tissue Res.* **367**, 427–444 (2017).
- 243. Alcorn, D. G., Adamson, T. M., Maloney, J. E. & Robinson, P. M. A morphologic and morphometric analysis of fetal lung development in the sheep. *Anat. Rec.* **201**, 655–67 (1981).
- 244. Guttmacher, A. E. & Spong, C. Y. Editorial The human placenta project : it ' s time for real time. *Am. J. Obstet. Gynecol.* **213**, S3–S5 (2015).

Afterword

I often marvel at the events that have culminated in this moment.

In the tattered map of any PhD student, there is the logical, linear route detailing the science to new knowledge – everything you’ve read in this book up to this point. And then there is everything around that route – the roads that led to the starting point, the side paths and detours from start to end, the messy maze of responsibilities and decisions, and the landscape littered with tiny red and white flags nobody talks about. I do not have the words to transcribe the entirety of this journey and attempting to do so would not do it justice. I have in fact rewritten this section more times than any other chapter, with varying degrees of resentment, acceptance, despair, hope, helplessness, invincibility, jadedness, excitement, frustration, and pride each time.

You see, there are things you want to do, and then there are things you have to do; over the course of four years, my PhD went from one to the other. The past four years have been an intellectually stimulating, emotionally exhausting adventure I was not prepared for but learnt to endure. In rare moments, I embraced it. I said at the start that the best view comes after the hardest climb. On some days they were mountains, but most others they were valleys and I was making my way back up to ground. Ultimately, I won’t miss the sum of it, but I certainly will treasure the good parts of this story – and there were many.

I always thought that at the end of it, this would feel much more. Perhaps a loud celebration at the end of a dark tunnel with an overwhelming sense of fulfilment. But in this moment, writing this, it feels more like relief that I can finally stop hitting myself with the hammer. Submitting this thesis amidst the chaos of a global pandemic is perhaps the perfect summary of this journey – that even when the world is crumbling around you, you trudge on because being mediocre is not enough in a world that requires your best.

Lastly, I have acknowledged those who have contributed to the making of this thesis, except the most important person. To me – thank you for making it this far despite wanting to give up every single day. I read somewhere that the problem with academic career goals is that you might not be enough of the same person when you reach them to have it be worthwhile. There have been days near the end where I caught the shadows of joy long lost. It was in those fleeting moments that I realised my fascination with all things babies and brains had not been completely eroded. The girl who genuinely believed she could change the world one experiment at a time was still there. I am so glad that I didn’t lose her. And

so, even if it's hard to feel on the day to day, hand on heart, old Kyra – all the versions of her – is very, very proud. We did it.

Appendices

This thesis includes three appendices, listed in order of the chapters they relate to:

Appendix	Article Title	Chapter
I	Respiratory support of the preterm neonate: Lessons about ventilation-induced brain injury from large animal models.	1
II	Diffusion tensor imaging detects ventilation-induced brain injury in preterm lambs.	3
III	Umbilical cord blood cells do not reduce ventilation-induced lung injury in preterm lambs.	4

Appendix I

This appendix relates to Chapter One: Introduction. As an extension of the literature review included in this thesis, I explored the relevance and importance of large preclinical models to investigate ventilation-induced brain injury and synthesised the information we have obtained from these experimental models to date. The review article is included below in manuscript form:

Chan KYY, Miller SL, Schmölzer GM, *Stojanovska V, *Polglase GR. Respiratory support of the preterm neonate: lessons about ventilation-induced brain injury from large animal models. [Submitted to *Front Neurol*, resubmitted with revisions after peer review (18/06/2020)]

N.B. This manuscript has since been accepted and published. The paper is available at:

Chan KYY, Miller SL, Schmölzer GM, *Stojanovska V, *Polglase GR. Respiratory support of the preterm neonate: lessons about ventilation-induced brain injury from large animal models. *Front Neurol* 2020;**11**:862.

Respiratory Support of the Preterm Neonate: Lessons about Ventilation-Induced Brain Injury from Large Animal Models

1 Kyra YY Chan¹, Suzanne L Miller¹, Georg M Schmölzer², #Vanesa Stojanovska¹ and **Graeme
2 R Polglase¹

3 ¹The Ritchie Centre, Hudson Institute of Medical Research and Department of Obstetrics and
4 Gynecology, Monash University, Clayton, Victoria, Australia.

5 ²Centre for the Studies of Asphyxia and Resuscitation, Neonatal Research Unit, Royal Alexandra
6 Hospital and Department of Pediatrics, University of Alberta, Edmonton, Alberta, Canada.

7 #Equal Contribution

8 * **Correspondence:**

9 A/Prof Graeme Polglase

10 27-31 Wright Street

11 Clayton VIC3168, Australia

12 Graeme.Polglase@monash.edu

13 +61 3 85722822

14 **Keywords: Ventilation, respiratory support, ventilation-induced brain injury,**
15 **neurodevelopment, preterm**

16 Abstract

17 Many preterm neonates require mechanical ventilation which increases the risk of cerebral
18 inflammation and white matter injury in the immature brain. In this review, we discuss the links
19 between ventilation and brain injury with a focus on the immediate period after birth, incorporating
20 respiratory support in the delivery room and subsequent mechanical ventilation in the neonatal
21 intensive care unit.

22 This review collates insight from large animal models in which acute injurious ventilation and
23 prolonged periods of ventilation have been used to create clinically relevant brain injury patterns.
24 These models are valuable resources in investigating the pathophysiology of ventilation-induced
25 brain injury and have important translational implications. We discuss the challenges of reconciling
26 lung and brain maturation in commonly used large animal models.

27 A comprehensive understanding of ventilation-induced brain injury is necessary to guide the way we
28 care for preterm neonates, with the goal to improve their neurodevelopmental outcomes.

1 Introduction

Respiratory support is a necessary life-saving intervention which has been associated with brain injury, especially in preterm neonates. Preterm birth, defined as birth prior to 37 completed weeks of gestation, is a major cause of perinatal mortality and morbidity (Blencowe et al., 2013; Chow et al., 2019). Almost 1 million preterm infants who survive the neonatal period suffer adverse neurodevelopmental outcomes (Blencowe et al., 2013) which, in addition to an individual burden, imposes enormous financial and social costs to their families and society. Many complications associated with prematurity are due to an interruption of normal organ development that would otherwise proceed to term *in utero*. For this reason, the distinction of babies by gestational age (GA) at birth – extremely preterm (<28 weeks), very preterm (28-<32 weeks), and moderate to late preterm (32-<37 weeks) – helps to identify infant populations which are most at risk of complications related to preterm birth (Blencowe et al., 2012). Notably, the lungs of very and extremely preterm infants are often too immature to provide adequate respiratory function required to sustain extrauterine life.

The lower the GA of the infant at birth, the less mature the lungs are, and the higher the requirement for respiratory support. An estimated 2.4 million babies are born very and extremely preterm worldwide each year (Blencowe et al., 2012) and approximately 60-95% of these infants will require respiratory support during their neonatal period (Serenius et al., 2004a; Walsh et al., 2005; Gagliardi et al., 2009; Soll et al., 2013; Chow et al., 2019). At the same time, the brains of these infants who require respiratory support are at a vulnerable stage of development and prone to injury. It is this combination of high requirements for respiratory support and the heightened vulnerability of their immature brains that increases the risk of ventilation-induced brain injury (VIBI) in extremely preterm infants.

Importantly, VIBI is likely to ensue as early as when respiratory support commences in the delivery room. Depending on GA, approximately 34 - 85% of preterm infants require intubation and positive pressure ventilation (PPV) to establish lung aeration immediately after birth (Serenius et al., 2004b; Cho et al., 2015; Stoll et al., 2015; Chow et al., 2019). These statistics exclude non-invasive forms of ventilation, meaning the total percentage of preterm infants who need respiratory support immediately after birth is substantially higher. Despite this high requirement, the limitations of equipment used in delivery suites mean that a significant proportion of babies receive inappropriate pressures or tidal volumes (V_T) (Schmölzer et al., 2010; van Vonderen et al., 2015), which can initiate pathways leading to VIBI (Barton et al., 2015b). Subsequent to this, the duration of ventilatory support in the neonatal intensive care unit (NICU) is proportional to the risk of neurodevelopmental impairment and disorders (Walsh et al., 2005; Tsai et al., 2014).

Respiratory support exacerbates key pathways of preterm brain injury: 1) cerebral inflammation and 2) cerebral hemodynamic instability (Polglase et al., 2012a, 2014b; Barton et al., 2015b), meaning ventilated preterm infants are in the unfortunate position of double jeopardy and are at an increased risk of brain injury. The nature of VIBI is not fully understood because it is difficult to determine clinically if brain injury is attributed solely or predominantly to ventilation. It is in this background that large animal models have played a vital role in improving our understanding of the pathogenesis of VIBI and to aid development of therapies.

In this review we will explore the issue of VIBI, how large animal models have been utilized to investigate VIBI, and the value of these models to develop much-needed therapies.

2 Preterm Birth, the Requirement for Respiratory Support, and How This May Be Injurious

Prematurity is the key contributor to the need for respiratory support in newborns. The majority of extremely preterm newborns will require respiratory support due to inadequate alveolarization, insufficient surfactant production, and impaired lung liquid clearance, together with reduced respiratory drive, weak chest muscles and flexible ribs (Hillman et al., 2012; Polglase et al., 2014b).

Our improved understanding of respiratory transition and lung function from fetal to newborn life has led to significant advances in neonatal respiratory care, many of which aim to reduce the risk of chronic lung diseases and adverse neonatal outcomes. Despite this, a significant proportion of preterm infants still develop long-term pulmonary and neurodevelopmental morbidities due to ventilation-induced injury. Various methods of respiratory support (e.g., nasal continuous positive airway pressure, PPV via face mask or endotracheal tube) have been linked to cerebral inflammation and neuropathologies in preterm infants, including cystic periventricular leukomalacia, diffuse white matter injury and intraventricular hemorrhage (IVH) (Rees and Inder, 2005; Albertine, 2012; Aly et al., 2012; Tsai et al., 2014; Mian et al., 2019). It is essential to clarify and address the effect ventilation has on the preterm infant.

2.1 Positive Pressure Ventilation in the Delivery Room

Most infants can independently transition from a fetus to a newborn, but many preterm infants will require assistance for this physiologically challenging process. Neonatal transition involves cardiovascular adaptations and, more importantly, respiratory adaptations since the newborn is no longer supported by the placenta for oxygenation (Hillman et al., 2012). Infants who cannot spontaneously breathe at birth will require PPV which is usually first delivered non-invasively via a facemask, and infants who are still unable to initiate stable respiration are intubated (Aly, 2005; Australian and New Zealand Committee on Resuscitation, 2016). Extremely preterm infants may be electively intubated in the delivery room in some centres although it has been suggested that individualized intubation strategies after establishing respiratory failure may be better to reduce morbidities (Lindner et al., 1999; Bajaj et al., 2018), given that the process of intubation may itself be injurious and is associated with neurodevelopmental impairments (Wallenstein et al., 2016).

A significant proportion of very and extremely infants require intubation in the delivery room. Despite decreasing percentages of infants requiring intubation in the delivery room over the past decades (Soll et al., 2013; Stoll et al., 2015), a staggering 31.6-77.7% of very low birth weight (VLBW) and/or extremely preterm infants continue to require this invasive intervention (Soll et al., 2013; Cho et al., 2015; Stoll et al., 2015; Chow et al., 2019). Early PPV in the delivery room has been associated with the development of severe IVH (Aly et al., 2012; Mian et al., 2019). VLBW infants, mostly born extremely preterm, who received PPV in the delivery room had a nearly three-fold increased likelihood of severe IVH (grades III and IV) than infants who did not receive PPV (Aly et al., 2012). However, it could be that the infants who require higher levels of intervention are sicker and more vulnerable to brain injury to begin with, hence it is challenging to accurately determine the extent to which advanced resuscitation is causal in the progression of brain injury in these infants.

Importantly, despite the high requirement of PPV in the delivery room, it is likely the least controlled respiratory support a neonate will ever receive, and this has proven to be inadvertently injurious to the immature brain (Schmölzer et al., 2010; Barton et al., 2015b; Mian et al., 2019). Current neonatal resuscitation guidelines in the delivery room rely on visual assessment of chest rise to deliver an

adequate V_T during PPV where pressure monitoring is unavailable (Tracy et al., 2004; Poulton et al., 2011; Australian and New Zealand Committee on Resuscitation, 2016). Besides being subjective, the ability to observe changes in chest wall movement is reduced when a preterm infant is covered to maintain body temperature during delivery room resuscitation, stabilization, and transportation (Tracy et al., 2004). It is challenging even for experienced clinicians to accurately estimate the V_T delivered (Schmölzer et al., 2010; Poulton et al., 2011) and a noticeably expanded chest wall from PPV may itself be a sign of lung overdistension. Excessively high V_T causes volutrauma – a major cause of lung inflammation and injury (Parker et al., 1993; Jobe and Ikegami, 1998; Attar and Donn, 2002; Schmölzer et al., 2008; Polglase et al., 2014b). Together, these factors contribute to a suboptimal ventilation situation that leads to injury of the lung and, consequently, the brain. Indeed, the use of excessive V_T has dire consequences on the immature brain. Preterm infants <29 weeks GA who received unintentional high V_T ventilation (>6 ml/kg, where median normal V_T is 4.2-5.8 ml/kg) in the delivery room had a nearly four-fold higher incidence of IVH than infants who received normal V_T (<6 ml/kg; 51% vs 13%) (Mian et al., 2014, 2019).

Other mechanisms by which PPV leads to lung injury are barotrauma (e.g., high airway pressure), atelectrauma (e.g., repeated opening and closing of collapsed airways), and biotrauma (Jobe and Ikegami, 1998; Attar and Donn, 2002; Schmölzer et al., 2008; Curley et al., 2016). Systemic inflammation secondary to lung injury can also initiate cerebral inflammation which is a major cause of brain injury. Inappropriate ventilation pressures and volumes can also trigger the hemodynamic pathway of injury to cause hemorrhagic brain injury (Barton et al., 2015b).

2.2 Mechanical Ventilation in the Neonatal Intensive Care Unit

Preterm infants often continue to require respiratory support after transfer to the NICU. In Australia and New Zealand, up to 95.0% of very and extremely preterm babies (<32 weeks GA) and 91.3% of moderate to late preterm infants (32-36 weeks GA) needed assisted ventilation in the NICU, with each baby receiving on average 8.8 days of assisted ventilation (Chow et al., 2019). A cohort study in South Korea reported that 38.5% of VLBW preterm infants received >7 days of mechanical ventilation (Choi et al., 2018). Importantly, the trends for long-term respiratory support in preterm infants do not seem to be decreasing (Lundqvist et al., 2009; Chow et al., 2019).

Prolonged periods of mechanical ventilation increases the risks of IVH (Serenius et al., 2004a; Aly, 2005), periventricular leukomalacia or white matter injury (Serenius et al., 2004a; Gagliardi et al., 2009; Albertine, 2012; Barnett et al., 2018; Choi et al., 2018), cerebral palsy (Tsai et al., 2014), and attention deficit hyperactivity disorder (Tsai et al., 2014) in preterm infants. In a retrospective analysis of extremely low birth weight infants, most of whom were extremely preterm, only 24% of infants who were ventilated for ≥ 60 days and 7% of those ventilated for ≥ 90 days survived without neurodevelopmental impairments (Walsh et al., 2005). All infants who had been ventilated for ≥ 120 days and survived suffered some form of neurodevelopmental impairment (Walsh et al., 2005).

Compared to the initiation of PPV in the delivery room, PPV in the NICU is much more controlled with sophisticated equipment and vigilant monitoring of ventilation parameters (Vento et al., 2008). The precise cause of VIBI in this setting has not been thoroughly investigated, with additional confounding factors such as analgesia and anesthetics (Kumar et al., 2010; Andropoulos, 2018; Lee and Loepke, 2018), oxygenation (Albertine, 2012), and a plethora of other NICU interventions for a range of primary and/or secondary complications that need to be considered. However, it is known that the duration of ventilation is an important determinant of neurodevelopmental morbidities (Walsh et al., 2005; Albertine, 2012; Vliegthart et al., 2019).

Attempts to shift management encouraging earlier extubation or less invasive ventilation strategies have not translated to improved neurological outcomes in preterm infants (Behnke et al., 2019). Furthermore, limiting the duration of mechanical ventilation to reduce complications is not always feasible with preterm infants. Therefore, it is imperative to devise treatments for unavoidable brain injury from prolonged respiratory support.

3 Using Animal Models to Investigate Ventilation-Induced Brain Injury

Clinical observations discussed above underpin the need to understand mechanisms through which respiratory support causes brain injury, to allow focused clinical strategies or new therapies aimed at improving outcomes. However, such investigations are not necessarily achievable in preterm infants since respiratory support cannot be studied in isolation. Herein lies the value of using animals for comprehensive characterization of VIBI through imaging, physiological, immunohistochemical, and molecular techniques. Animals can also be used to model various conditions such as growth restriction and chorioamnionitis to more closely interrogate VIBI under conditions of compromised pregnancies.

Studies using large animals, most often sheep, to model ventilation-induced injury can be categorized by experimental technique (fetal [head-out or *in utero* ventilation] or neonatal ventilation) and period/duration of ventilation (acute or chronic) [Figure 1]. These different experimental techniques enable replication of specific scenarios of preterm respiratory support, including the initial resuscitation in the delivery room and prolonged care in the NICU. However, with all models, an understanding of the strengths and limitations is essential for appropriate interpretation of the findings and potential replication in clinical trials.

3.1 Balance Between Lung and Brain Development in Large Animal Models

An inevitable limitation to using large animals to model neonatal conditions is the difference in developmental milestones of major organ systems and physiology compared to humans. The animal's age cannot be chosen based on gestation duration alone since an animal at 0.65 gestation is not necessarily developmentally equivalent to a human at 0.65 gestation. Instead, the crucial factor is the stage of development of the organ of interest. This proves challenging for models of VIBI as the developmental milestones of both the brain and lungs must be considered. Detailed comparisons of species-specific lung development and anatomical features have previously been compiled (Yoder and Coalson, 2014; Albertine, 2015; Schittny, 2017) and comparisons for brain development are summarized in Table 1. This presents a conundrum: how do we balance desired stage of brain development with lung maturation?

Non-human primate studies have used baboons (*Papio papio*; *Papio cynocephalus*) delivered at 125 days (term is 185 days; 0.68 gestation) which have similar lung development to an infant born at 26 weeks preterm age (Yoder and Coalson, 2014). At this stage, brain development is comparable to that of a 26-28 week-old extremely preterm human infant (Dieni et al., 2004). While these developmental stages are congruent, there are significant technical challenges as well as practical, financial and ethical concerns associated with the use of non-human primates (Phillips et al., 2014). Thus, even though they are the closest animal models to humans and offer vital insights to developmental studies (Phillips et al., 2014), non-human primate models of VIBI are relatively less commonly pursued.

Piglets (*Sus scrofa*) have been proposed to be suitable for studying neurodevelopment and cerebral consequences of early life insults (Conrad and Johnson, 2015). A piglet at 91-94 days gestation (term is 115 days; 0.8 gestation) is physiologically similar to a 23-25 week extremely preterm infant in

terms of lung development and the requirement for respiratory support for survival (Eiby et al., 2013). Neurodevelopment of the piglet at this GA is slightly more mature, comparable instead to a moderate to late preterm human infant (Sweasey et al., 1976; Conrad and Johnson, 2015). Besides this developmental mismatch, there are significant challenges in performing fetal surgery and chronic instrumentation in pigs due to relatively large litters and the large size of the sow. Hence, piglets have not been widely used in VIBI studies that require these techniques. The suitability of piglets in postnatal ventilation studies for VIBI has not been extensively explored.

Similarly, brain maturation in sheep (*Ovis aries*) advances more rapidly in late gestation than development of the lungs, relative to humans. Previous studies in preterm lambs that have investigated VIBI were performed at the earliest GA at which the lambs were viable with respiratory support (125 days where term is 148 days; 0.85 gestation; structural lung development comparable to a 26-28 week human infant (Alcorn et al., 1981; Schittny, 2017)). However, a limitation is that the fetal sheep brain development at 125 days gestation is comparable to a late preterm or term human fetus on the basis of white matter maturation (Barlow, 1969; Back et al., 2006). Studies using lambs at this gestation have investigated the effect of respiratory support for up to 4 weeks on chronic lung injury (Albertine et al., 1999), but have only looked at VIBI up to 24 h of ventilation (Malhotra et al., 2018).

3.2 Modelling of Acute VIBI

Animal studies to date have focused on VIBI downstream of lung injury resulting from volutrauma in the delivery room. The rationale behind these studies is that clinical findings have shown that variable V_T during delivery room resuscitation can be outside recommended limits (Schmölzer et al., 2010; Schilleman et al., 2013; van Vonderen et al., 2015).

Observed V_T during mask ventilation can range from 0-31 ml/kg (Schmölzer et al., 2010; Schilleman et al., 2013; van Vonderen et al., 2015) and V_T during endotracheal tube ventilation has been reported to be 3.9-9.6 ml/kg (van Vonderen et al., 2015). The upper ranges of these V_T are higher than the recommended 4-8 ml/kg for very and extremely preterm infants (Schmölzer et al., 2010). This is critical as we have known for decades that as few as six manual inflations of high V_T (35-40 ml/kg) are enough to induce injury in immature, surfactant-deficient lungs of preterm lambs (Björklund et al., 1997). Sheep studies that have investigated acute VIBI have similarly found that brief periods of high V_T ventilation resulted in detectable brain injury as early as 90 min after ventilation onset (Polglase et al., 2012a, 2012b, 2014b; Skiöld et al., 2014; Barton et al., 2015b, 2016a). Importantly, even if recommended V_T is delivered, the act of respiratory in itself can activate an immune response in immature respiratory units (Jobe and Ikegami, 1998; Attar and Donn, 2002; Curley et al., 2016).

To isolate this initial period of injurious respiratory support, akin to poorly regulated V_T in the delivery room, sheep studies have employed an acute high V_T ventilation strategy: 15 min injurious ventilation with stepwise increments of V_T to achieve a high target V_T of 10-15 ml/kg, which is 2-3 times the normal V_T of lambs for that GA (125 days of term 148 days; ~5-7 ml/kg) (Polglase et al., 2012a, 2012b, 2014b; Skiöld et al., 2014; Barton et al., 2015b, 2016a). Thereafter, lambs are sustained on appropriate respiratory support (neonatal model) or returned to the uterus (head-out model) to allow for the inflammation and injury pathways to manifest into gross lung/brain injury. These studies have provided valuable information on the pathology and mechanisms of acute VIBI (discussed in Section 4).

3.3 Chronic Models of VIBI

The majority of animal models used to model VIBI are acute, focusing on the initial hours after birth. This is mainly due to inherent problems with maintaining animals for long periods of time. In particular, the problem with maintaining respiratory support for long periods of time in newborn animal models is the inability to control for specific factors, due to the need to introduce increasing levels of neonatal intensive care – akin to that of looking after a chronically ventilated preterm infant. To get around this problem, animal models have utilized respiratory support via a head-out approach or entirely *in utero* [Figure 1]. Using these techniques, the intact placental circulation manages nutrition and gas exchange of the fetus, allowing subtle mechanisms of respiratory support to be examined. In the head-out approach, the fetus's head and chest are exteriorized, the fetus is intubated and ventilation with various strategies altering delivered volume, pressures, respiratory frequencies, or oxygen content, and then returned to the uterus (Hillman et al., 2007, 2010, 2011; Alahmari et al., 2017b; Kothe et al., 2018). *In utero* ventilation (IUV) studies require the fetus to be exteriorized and instrumented with ventilation tubes and equipment required for monitoring prior to being returned to the uterus. After a recovery period for the ewe and fetus, the fetus is ventilated via the externalized ventilation tubes for various times, although to date the longest has been 12 h (Allison et al., 2008, 2010; Hodges et al., 2012). IUV has been used in fetal sheep to study cardiopulmonary physiology (Iwamoto et al., 1993; Giraud et al., 1995), lung mechanics (Blanco et al., 1987), and ventilation-induced lung injury (Allison et al., 2008; O'Reilly et al., 2009; Hodges et al., 2012). While cerebral physiological responses to IUV have been investigated previously (Gleason et al., 1988), histopathology of brain injury after IUV has not been reported.

It is obvious that these *in utero* models are not designed with the intention to replicate clinical situations given that prolonged neonatal studies are more reflective of current clinical care. Instead, they provide the opportunity to manipulate specific ventilatory parameters in isolation so that we can better understand the contribution of a sole variable to lung and brain injury. Importantly, the IUV model allows ventilation of a fetus at a younger gestation than would be viable postnatally. This is advantageous, especially in ovine models, as the stage of brain development will be more comparable to that of extremely preterm infants.

4 Understanding VIBI from Injurious Respiratory Support in the Delivery Room

4.1 Animal Studies That Investigate Pathology of VIBI

Studies in preterm lambs have characterized acute white matter changes following 15 min of injurious high V_T ventilation (Polglase et al., 2012a, 2012b, 2014b; Skiöld et al., 2014; Barton et al., 2015b, 2015a, 2016a; Stojanovska et al., 2018b). High V_T ventilation causes a robust pulmonary inflammatory response which increases systemic and cerebral inflammation, characterized by elevated IL-6 and IL-8 messenger ribonucleic acid (mRNA) levels in the periventricular and subcortical white matter of the brain in ventilated preterm lambs (Polglase et al., 2012a; Barton et al., 2015a, 2016a). Increased microglial activation and aggregation, and a higher incidence of vascular protein extravasation (indicative of a compromised blood-brain barrier) and cerebral hemorrhage in the same regions were also observed (Polglase et al., 2012a; Barton et al., 2016a; Stojanovska et al., 2018b). Injurious ventilation did not alter expression of myelin basic protein (MBP; oligodendrocyte marker) in the internal capsule or neuronal nuclei (NeuN; neuron marker) in the thalamus (Alahmari et al., 2017a) and did not increase inflammation or injury in grey matter (Stojanovska et al., 2018a).

Importantly, pathology resultant from injurious ventilation can be visualized using non-invasive imaging such as magnetic resonance imaging (MRI) (Skiöld et al., 2014; Alahmari et al., 2017b, 2017c) and correlated with histopathology (Alahmari et al., 2017a). Magnetic resonance

spectroscopy (MRS) detected acute changes in brain metabolite peak-area ratios (Lactate/Creatine and Lactate/Choline) in preterm lambs that received high V_T although macroscopic injury was absent in structural MR images (T1,T2) (Skiöld et al., 2014). Alterations in MRS-detected metabolite levels relate to neuronal damage and potentially predict subsequent neurodevelopmental impairments (Bapat et al., 2014; Hyodo et al., 2018). Notably, these MRS changes were observed within 90 min of ventilation onset (Skiöld et al., 2014). Recent findings suggest that MRS-detectable changes persist 24 h after injurious ventilation (Alahmari et al., 2017b). Diffusion tensor imaging (DTI) perhaps offers the most sensitive measures of early brain injury. DTI detected decreased diffusivity measures in the frontal white matter (axial, radial, and mean) and internal capsule (axial) in preterm lambs 24 h after injurious ventilation (Alahmari et al., 2017b). These parameters have been suggested to correlate with myelination deficits (Alahmari et al., 2017b).

4.2 Mechanistic Insight from Animal Studies

Several explanations have been put forward to link ventilation and brain injury. Studies in ventilated preterm lambs have identified two major pathways of acute VIBI: cerebral inflammation and hemodynamic instability (Polglase et al., 2012a, 2014b; Barton et al., 2015b; Alahmari et al., 2017b). Both pathways are proposed to be downstream effects of the pulmonary consequences following ventilation (Polglase et al., 2012a, 2014b; Barton et al., 2015b). Incidentally, these key VIBI pathways mirror those of preterm brain injury – suggesting compounded risk of injury in preterm infants. These mechanisms have been reviewed previously (Barton et al., 2015b).

Briefly, the inflammatory pathway of VIBI involves upregulation of pro-inflammatory cytokines (e.g., IL-6, IL-8) and activation of microglia and astrocytes within the developing white matter of the brain (Khwaja and Volpe, 2007). Injurious ventilation initiates a profound pulmonary inflammatory response caused by volutrauma, barotrauma, atelectrauma, and/or biotrauma (Jobe and Ikegami, 1998; Attar and Donn, 2002; Schmölzer et al., 2008; Curley et al., 2016). This inflammatory cascade is associated with systemic inflammation and subsequent localized inflammation and injury in the white matter involving glia cells (Polglase et al., 2012a, 2014b; Barton et al., 2015b). Activated microglia and astrocytes are thought to mediate the destruction of cells in the oligodendrocyte lineage, contributing to hypomyelination and diffuse white matter injury that can underlie long-term neurological sequelae such as cerebral palsy (Khwaja and Volpe, 2007; Back and Rosenberg, 2014).

The hemodynamic pathway of injury refers to significant alterations, caused by PPV and atypical to hemodynamic changes during the transition at birth, to pulmonary blood flow and consequently cardiac output and cerebral blood flow (CBF) (Polglase et al., 2012a, 2014b). During PPV, applying a high pressure into the airways decreases pulmonary capillary transmural pressure, causing compression of intra-alveolar capillaries, hence increasing capillary resistance and decreasing pulmonary blood flow (Polglase et al., 2014b; Barton et al., 2015b). This reduces pulmonary venous return, left ventricular output, and accordingly alters CBF (Polglase et al., 2012a, 2014b; Barton et al., 2015b). Arterial blood pressure variability within a physiological range is not usually a problem because it is compensated by pressure-flow autoregulation to sustain a stable CBF. This involves constriction and dilation of arteries to alter cerebral vasculature resistance in response to changing perfusion pressures (Greisen, 2005). The autoregulatory plateau, bounded by lower and upper limits of arterial pressure, has been postulated to be narrower in preterm infants with decreasing GA (Verma et al., 2000; Greisen, 2005; du Plessis, 2009). Moreover, it has been suggested that preterm delivery or treatments reflective of clinical care of the preterm infant, including mechanical ventilation, affects cerebral autoregulation (Czynski et al., 2013). Prolonged CBF fluctuations for more than 10 to 20s has been defined as cerebral hemodynamic instability (Gilmore et al., 2011). The

initiation of ventilation in preterm lambs caused CBF instability in the initial 15 min, even when a gentle strategy was used (Polglase et al., 2012b); the variability in CBF amplified when an injurious high V_T strategy was used (Polglase et al., 2012a). Clinically, 91% of babies with respiratory distress syndrome who had fluctuating CBF after 12 h of life subsequently had an IVH (Perlman et al., 1983), highlighting the critical importance of preventing fluctuations in hemodynamics immediately after birth.

The relative contribution of each pathway towards the progression of white matter injury discussed in Section 4.1 is unknown although a recent study suggests that the hemodynamic pathway has an additive effect on the inflammatory pathway on injury progression, but the inflammatory pathway seems to dominate (Alahmari et al., 2017b).

5 Understanding VIBI from Ventilation in the Neonatal Intensive Care Unit

Ventilation studies in preterm baboons and lambs suggest that the brain injury underlying neurodevelopmental impairments in chronically ventilated preterm infants involves subtle diffuse white and grey matter lesions, often without intraventricular or germinal matrix hemorrhage and overt lesions or infarcts (Dieni et al., 2004; Rees et al., 2007; Loeliger et al., 2009b, 2009a; Albertine, 2012). This indicates a potentially distinct mechanism of injury to acute VIBI sustained in delivery room settings.

Preterm baboons have been used extensively to study the impact of prolonged mechanical ventilation (2-4 weeks) on the lungs (Coalson et al., 1999; Yoder et al., 2000; Albertine, 2015) and, more recently, the brain (Loeliger et al., 2006, 2009b; Verney et al., 2010). In these studies, preterm baboons (125 days of term 185 days; 0.68 gestation) are cared for with similar interventions to that of preterm infants in the NICU, including mechanical ventilation using a gentle strategy to maintain V_T at 4-6 ml/kg with adequate chest motion (Yoder et al., 2000; Dieni et al., 2004). While not investigating injury from ventilation per se, the brain injury observed in these animals is not from any direct insult or influenced by potentiating conditions associated with preterm birth or an adverse uterine environment. The subtle neuropathologies from preterm birth and subsequent intensive care alone closely resemble what is observed clinically (Dieni et al., 2004; Rees et al., 2007; Loeliger et al., 2009b; Griffith et al., 2012). After 14 days of ventilator support, preterm baboon brains had delayed gyrification (Rees et al., 2007; Loeliger et al., 2009a), reduced brain weight (Rees et al., 2007; Loeliger et al., 2009b, 2009a), reduced white and grey matter volumes (Loeliger et al., 2009b, 2009a), increased white and grey matter injury (Dieni et al., 2004), increased astrogliosis in the forebrain (Loeliger et al., 2009b), increased ramified microglia (Loeliger et al., 2009b), and a reduction of oligodendrocytes (Loeliger et al., 2009b, 2009a) compared to gestation-matched controls. These histopathological indices correlated with microstructural and macrostructural changes detected by *ex vivo* MRI (Griffith et al., 2012).

Additionally, the effects of shorter durations of controlled NICU respiratory support have been investigated in sheep. Preterm lambs (125 days of term 145 days; 0.85 gestation) ventilated with a non-injurious strategy (V_T at 5-7 ml/kg) had increased IL-8 and connective tissue growth factor (CTGF) mRNA levels and decreased vascular occludin protein density in the white matter after 2 h (Allison et al., 2017). When the length of ventilation was extended to 24 h, ventilated lambs had increased astrogliosis within cortical grey matter but otherwise no apparent neuropathology or changes in glial cell populations compared to unventilated control lambs (Malhotra et al., 2018).

Both the preterm baboon and lamb models discussed are neonatal ventilation models. However, as mentioned above, a disadvantage of the neonatal ventilation model is the intensive care requirements of maintaining a preterm animal for significant periods of time, making them more akin to human studies where individual parameters cannot be teased apart unless large numbers of animals are used, which is financially unviable. This is where the IUV model may be advantageous if used for extended periods beyond 24 h.

6 Influence of the Antenatal Environment on Respiratory Support and VIBI

Work explored in the previous sections have studied the pathology and mechanisms of VIBI in preterm but otherwise healthy animals. The ability to isolate effects of respiratory support with minimal confounding factors is vital and these findings provide a foundation to explore therapeutic options to minimize VIBI which will be discussed in section 6 of this review. However, it is important to consider that the clinical situation is much more complex – many preterm infants will have been exposed to adverse uterine environments which may increase their risk of VIBI.

6.1 Adverse Antenatal Conditions Alter Responses to Postnatal Respiratory Support

Adverse antenatal conditions such as fetal growth restriction and intrauterine inflammation have independently been associated with adverse neurodevelopmental outcomes in preterm infants (Miller et al., 2016; Sharma et al., 2016). Further, these infants often require respiratory support after birth, increasing the risk of brain injury. Yet, there is a paucity of information on how these antenatal conditions alter the response these infants have to ventilation and if this contributes to VIBI.

6.1.1 Fetal Growth Restriction and VIBI

Fetal growth restriction (FGR) is a condition where the fetus fails to reach its projected growth potential, often due to placenta insufficiency (Sharma et al., 2016). FGR fetuses are sometimes delivered preterm to prevent deterioration in an adverse *in utero* environment (Sharma et al., 2016), thus many will require respiratory support due to prematurity. FGR fetuses have altered cardiovascular and vascular function, most notably the characteristic “brain-sparing” phenomenon by redirecting blood flow and oxygen delivery to important organs including the heart, adrenals, and brain. These adaptations persist to early postnatal life and may affect how a growth-restricted infant responds to ventilation. Preterm growth-restricted lambs ventilated with a gentle non-injurious strategy for 24 h had disrupted interaction of astrocyte end-feet with cerebral blood vessels, increased microgliosis, and increased oxidative stress compared to their unventilated counterparts and to ventilated preterm appropriately-grown lambs (Malhotra et al., 2018). Notably, differences between growth-restricted and appropriately grown lambs were evident after 2 h of ventilation (Allison et al., 2017). This suggests that growth restricted infants may be at increased risk of VIBI, perhaps in part due to differences in the neurovascular unit and blood-brain barrier properties (Allison et al., 2017; Malhotra et al., 2018).

6.1.2 Intrauterine Inflammation and VIBI

Intrauterine inflammation, which most commonly presents as chorioamnionitis, is a major cause of preterm birth (Goldenberg et al., 2008). Antenatal inflammation alters the vulnerability and response of the immature brain to ventilation (Polglase et al., 2012b; Barton et al., 2014; Alahmari et al., 2017c). Lipopolysaccharide(LPS)-mediated inflammation *in utero* amplified cerebral hemodynamic instability during the initiation of ventilation in preterm lambs (Polglase et al., 2012b). Compared to saline controls, these lambs that had been exposed to LPS 2 or 4 days before preterm delivery had increased inflammation, vascular extravasation, and microhemorrhages in cerebral white matter

regions after ventilation (Polglase et al., 2012b). Further, injurious ventilation increased the number of apoptotic cells (TUNEL⁺ cells) in the subcortical white matter of LPS-exposed lambs, compared to their unventilated counterparts (Barton et al., 2014). Injurious ventilation had no obvious acute detrimental effects on white matter (Alahmari et al., 2017a) and grey matter (Stojanovska et al., 2018a) compared to injuriously ventilated healthy preterm lambs and to LPS-exposed lambs that received gentle ventilation. Brain macro- and microstructure as assessed by MRI and DTI were similarly not different (Alahmari et al., 2017a, 2017c). However, a novel DTI color map threshold technique detected lower diffusivity indices in white matter regions of the brain, indicative of subtle brain injury in the ventilated lambs that were exposed to inflammation prior to delivery (Alahmari et al., 2017c). Importantly, using a non-injurious ventilation strategy did not mitigate VIBI in the LPS-exposed lambs (Barton et al., 2014). Clinically, histologic chorioamnionitis is associated with a longer cumulative duration of mechanical ventilation in VLBW infants (Choi et al., 2018), thereby increasing the risk of VIBI. However, the combination of chorioamnionitis and prolonged ventilation has not been investigated in large animals and the potential cerebral effects are unknown.

6.2 Cerebral Effects of Antenatal Medical interventions

Corticosteroid administration is a common antecedent to preterm birth, where antenatal glucocorticoids (betamethasone and dexamethasone) are given to accelerate fetal lung maturation before preterm labor (Roberts et al., 2017). Clinically, antenatal glucocorticoid administration is suggested to reduce the incidence and severity of IVH (Roberts et al., 2017) and does not affect subsequent development of subsequent childhood mental and behavioral disorders in preterm infants (Räikkönen et al., 2020). However, information on its interaction with respiratory support is scant. A recent study found that antenatal betamethasone improved cerebral hemodynamic instability in preterm lambs that received 15 min of high V_T injurious ventilation followed by 75 min non-injurious ventilation (Stojanovska et al., 2018b). However, there was an increase in the percentage of amoeboid microglia in the periventricular white matter, the number of vessel profiles with protein extravasation in the subcortical white matter, and malondialdehyde levels in cerebrospinal fluid, suggesting increased inflammation and oxidative stress in betamethasone-treated animals than their saline-treated counterparts ventilated with the same protocol (Stojanovska et al., 2018b). This potential increased risk of VIBI following antenatal betamethasone administration may lie in the increased lung compliance and hence susceptibility of the lungs to volutrauma rather than a direct cerebral effect (Stojanovska et al., 2018b).

It is crucial to consider that antenatal glucocorticoid administration may have additional interactions with the conditions mentioned above; for example, growth restricted fetuses have different hemodynamic responses to antenatal glucocorticoids compared to appropriately grown fetuses (Miller and Wallace, 2013). Maternal betamethasone administration increased fetal cardiac output and blood flow to major organs whereas cardiac output was decreased and blood flow to major organs remained unchanged in control fetuses (Miller et al., 2009). Furthermore, there were transient decreases in carotid blood flow, an index for CBF, in both control and FGR fetuses. While CBF of control fetuses were stable after returning to baseline levels, FGR fetuses displayed a persistent rebound increase in carotid blood flow from 10 h after treatment (Miller et al., 2007). Whether these altered responses are beneficial or harmful in the context of VIBI needs to be ascertained. Indeed, little is known about the combined effects of adverse antenatal conditions, antenatal glucocorticoid administration, and postnatal respiratory support on brain injury in the preterm infant. Large animal models of VIBI may provide a means to address this.

7 Bench to Bedside

Establishing reliable animal models with reproducible neuropathology that is reflective of injury seen clinically expedites efforts to test novel potential interventions and/or therapeutic candidates. Potential treatments for VIBI and their mechanisms of actions have recently been discussed in detail by Barton *et al.* (Barton et al., 2016b) and this remains an active area of research.

In the delivery room setting, physiological-based cord clamping (PBCC) can stabilize pulmonary, systemic, and cerebral circulation in preterm (Bhatt et al., 2013; Polglase et al., 2015) and near-term lambs (Polglase et al., 2018), essentially mitigating the hemodynamic pathway of injury, but it is unlikely to prevent VIBI resultant from the inflammatory pathway. PBCC refers to delaying umbilical cord clamping until respiration has been initiated and established in the newborn or providing respiratory support prior to umbilical cord clamping (Bhatt et al., 2013; Polglase et al., 2015, 2018). Thus, a therapy that targets both pathways of VIBI, with a focus on modulating inflammation, is required. To date, animal experiments have investigated short-term effects of erythropoietin (EPO) and human amnion epithelial cells (hAECs) as prophylactic postnatal treatments for VIBI resultant from acute volutrauma (Barton et al., 2015a, 2016a; Chan et al., 2017). These treatments have proposed mechanisms of action that make them ideal candidates for neuroprotection. EPO has anti-inflammatory, anti-apoptotic, and neurotrophic properties while hAECs are anti-inflammatory and reparative (Barton et al., 2016b).

When administered to preterm lambs that received 15 min of injurious high V_T ventilation, single early low doses of 300 IU/kg and 1000 IU/kg human recombinant EPO did not reduce or exacerbate lung and brain injury (Chan et al., 2017; Allison et al., 2019), suggesting that EPO doses presently used in clinical trials appear to be safe for preterm infants receiving respiratory support. However, they appear to not be efficacious as a therapy for VIBI given the lack of therapeutic potential observed. High doses of EPO of 3000 IU/kg and 5000 IU/kg increased cerebrospinal fluid EPO levels to “neuroprotective levels” (>100 mU/ml (Juul et al., 2004)) within 2 h of administration (Barton et al., 2016a; Chan et al., 2017). These high doses respectively had a protective effect on blood-brain barrier integrity (Chan et al., 2017) and differential regional effects on white matter (Barton et al., 2016a) despite both doses amplifying lung inflammation and injury (Polglase et al., 2014a; Allison et al., 2019). Together, these data highlight a complex dose response with distinct effects on the lungs and brain, indicating that further investigation is required to elucidate the efficacy of EPO in the context of a preterm infant requiring respiratory support.

In a similar study, preterm lambs that received high V_T ventilation were administered an intratracheal infusion of 9×10^7 hAECs before ventilation onset and an additional intravenous dose of 9×10^7 hAECs within 5 min of delivery (total 1.8×10^8 hAECs) (Barton et al., 2015a; Melville et al., 2017). The cells were able to enter the brain within 2 h of administration, as detected by fluorescent cell labelling in the frontal and parietal periventricular and subcortical white matter of the brain (Barton et al., 2015a). Cell administration reduced microgliosis and vascular protein extravasation (Barton et al., 2015a), potentially as a downstream effect of reduced pulmonary inflammation (Melville et al., 2017). However, hAECs did not stabilize hemodynamic transition or modulate systemic inflammation within the brief period of the experiment, and conversely they induced an increase in pro-inflammatory cytokine mRNA levels within the brain (Barton et al., 2015a; Melville et al., 2017). Further long-term effects of hAECs on acute VIBI have not been investigated to accurately determine the interaction of hAECs and ventilation on the preterm brain.

Chronic ventilation studies in animals have so far focused on treatments to reduce lung rather than brain injury. Sheep fetuses ventilated *in utero* for 12 h and administered intratracheal infusion of 3×10^7 hAECs and an intravenous dose of 3×10^7 hAECs at 3 h and 6 h after ventilation onset (total

1.2x10⁸ hAECs) demonstrated a reduction in ventilation-induced lung injury (Hodges et al., 2012), and as such may have the potential to reduce VIBI but this remains a speculation.

While the above strategies have some promise, it is unlikely that a single strategy will prevent or reduce VIBI. The key might lie in a multipronged approach that involves reducing the requirement for or duration of respiratory support, optimizing how PPV is administered to avoid adverse effects, and reducing the sequelae of unpreventable adverse effects of PPV [Figure 2].

In this regard, researchers in The Netherlands have investigated the use of caffeine in the delivery room, showing improved respiratory efforts of preterm infants (24-30 weeks GA), potentially reducing the need for invasive respiratory support in this setting (Dekker et al., 2017). Further, spontaneous respiratory drive is a determinant of effective use of gentle non-invasive respiratory support (Amaro et al., 2018). However, caffeine administration to mechanically ventilated preterm infants (23-30 weeks GA) in the first 5 days of life did not encourage early extubation or decrease ventilation duration in the NICU (Amaro et al., 2018; Jain et al., 2019). The trial was terminated due to safety concerns, making it difficult to interpret results and secondary outcome findings of morbidities including BPD and IVH (Amaro et al., 2018; Jain et al., 2019). In contrast, caffeine had neuroprotective effects in very preterm infants when assessed at 18 months' corrected age (Schmidt et al., 2007; Lodha et al., 2019), in part attributed to earlier discontinuation of PPV and decreased rates of bronchopulmonary dysplasia (Schmidt et al., 2006; Lodha et al., 2015). The treatment benefits of caffeine administered in the first 10 days of life on neurobehavioral and functional cognitive outcomes were less pronounced at 5- and 11-years follow-up, with only slight but statistically significant improvements to motor outcomes observed (Schmidt et al., 2012, 2017; Mürner-Lavanchy et al., 2018). Earlier administration of caffeine within the first 2 days of life has been associated with improved neurodevelopmental outcomes at 18 to 24 months' corrected age compared to late administration (Lodha et al., 2019) but whether these benefits persist have not been reported. Certainly, these contradictory findings highlight the need to better understand the interaction of caffeine, respiratory support, and neurodevelopmental outcomes. Independently, caffeine has been postulated to have neuroprotective properties by reducing inflammation, reducing periventricular white matter injury, and stabilizing hemodynamics in preterm infants (Lodha et al., 2019).

Correspondingly, protective ventilation strategies have reduced brain inflammation and vascular protein extravasation but do not completely mitigate injury in preterm lambs (Polglase et al., 2012a, 2014b; Barton et al., 2014; Skiöld et al., 2014). Together, these indicate that our current efforts to minimize the need for respiratory support and, where respiratory support is necessary, improve the way PPV is administered are inadequate to prevent VIBI. Large animal models will likely play a key role in studies focusing on stimulating respiratory function at birth and optimizing the delivery of non-invasive respiratory support to minimize lung and brain inflammation and injury. Additionally, there is an apparent need to devise treatments and large animal models of VIBI provide a means to address this.

8 Summary

This review highlights the necessity of large animal models when investigating the relationship between invasive respiratory support, the lungs, and the brain in the preterm infant. These models provide a powerful research tool; a combination of physiological, histological, molecular and imaging techniques provides an integrated picture of the interactions between respiratory support and the immature brain which is difficult to obtain in a clinical setting.

553 Recognizing the consequences of respiratory support on the immature brain will encourage
554 development of effective therapies to prevent or treat VIBI in otherwise healthy preterm infants.
555 VIBI should also be considered when investigating treatments for other conditions such as fetal
556 growth restriction, chorioamnionitis, and hypoxic injury where the compromised infant will often
557 receive respiratory support.

558

559 **9 Conflict of Interest**

560 *The authors declare that the research was conducted in the absence of any commercial or financial*
561 *relationships that could be construed as a potential conflict of interest.*

562 **10 Author Contributions**

563 KYYC contributed to the conception the review and created the table. KYYC and GMS
564 conceptualized and created the figures. KYYC, SLM, GMS, VS, and GRP all contributed to
565 structuring, drafting, revising, and the final approval of the version to be published.

566 **11 Funding**

567 This work was supported by the National Health and Medical Research Council (NHMRC) and/or
568 National Heart Foundation of Australia and/or NHMRC Fellowships (VS: 1165935 and GRP:
569 1105526), and the Victorian Government's Operational Infrastructure Support Program.

570

12 References

- Åarström, K.-E. (1967). On the Early Development of the Isocortex in Fetal Sheep. *Prog. Brain Res.* 26, 1–59. doi:10.1016/S0079-6123(08)61418-1.
- Alahmari, D. M., Barton, S. K., Galinsky, R., Nitsos, I., Atik, A., Farrell, M., et al. (2017a). Correlation between diffusion tensor imaging and histological brain injury in ventilated preterm lambs. *Imaging Med.* 9, 67–76.
- Alahmari, D. M., Chan, K. Y. Y., Stojanovska, V., LaRosa, D., Barton, S. K., Nitsos, I., et al. (2017b). Diffusion tensor imaging detects ventilation-induced brain injury in preterm lambs. *PLoS One* 12, e0188737. doi:10.1371/journal.pone.0188737.
- Alahmari, D. M., Skiöld, B., Barton, S. K., Nitsos, I., McDonald, C., Miller, S. L., et al. (2017c). Diffusion Tensor Imaging Colour Mapping Threshold for Identification of Ventilation-Induced Brain Injury after Intrauterine Inflammation in Preterm Lambs. *Front. Pediatr.* 5, 1–13. doi:10.3389/fped.2017.00070.
- Albertine, K. H. (2012). Brain Injury in Chronically Ventilated Preterm Neonates. *Clin. Perinatol.* 39, 727–740. doi:10.1016/j.clp.2012.06.017.
- Albertine, K. H. (2015). Utility of large-animal models of BPD: chronically ventilated preterm lambs. *Am. J. Physiol. - Lung Cell. Mol. Physiol.* 308, L983–L1001. doi:10.1152/ajplung.00178.2014.
- Albertine, K. H., Jones, G. P., Starcher, B. C., Bohnsack, J. F., Davis, P. L., Cho, S. C., et al. (1999). Chronic lung injury in preterm lambs. Disordered respiratory tract development. *Am. J. Respir. Crit. Care Med.* 159, 945–58. doi:10.1164/ajrcm.159.3.9804027.
- Alcorn, D. G., Adamson, T. M., Maloney, J. E., and Robinson, P. M. (1981). A morphologic and morphometric analysis of fetal lung development in the sheep. *Anat. Rec.* 201, 655–67. doi:10.1002/ar.1092010410.
- Allison, B. J., Crossley, K. J., Flecknoe, S. J., Davis, P. G., Morley, C. J., Harding, R., et al. (2008). Ventilation of the very immature lung in utero induces injury and BPD-like changes in lung structure in fetal sheep. *Pediatr. Res.* 64, 387–392. doi:10.1203/PDR.0b013e318181e05e.
- Allison, B. J., Crossley, K. J., Flecknoe, S. J., Morley, C. J., Polglase, G. R., and Hooper, S. B. (2010). Pulmonary hemodynamic responses to in utero ventilation in very immature fetal sheep. *Respir. Res.* 11, 1–11. doi:10.1186/1465-9921-11-111.
- Allison, B. J., Hooper, S. B., Coia, E., Jenkin, G., Malhotra, A., Zahra, V., et al. (2017). Does growth restriction increase the vulnerability to acute ventilation-induced brain injury in newborn lambs? Implications for future health and disease. *J. Dev. Orig. Health Dis.* 8, 556–565. doi:10.1017/S204017441700037X.
- Allison, B. J., LaRosa, D. A., Barton, S. K., Hooper, S., Zahra, V., Tolcos, M., et al. (2019). Dose-dependent exacerbation of ventilation-induced lung injury by erythropoietin in preterm newborn lambs. *J. Appl. Physiol.* 126, 44–50. doi:10.1152/jappphysiol.00800.2018.
- Aly, H. (2005). Is It Safer to Intubate Premature Infants in the Delivery Room? *Pediatrics* 115, 1660–1665. doi:10.1542/peds.2004-2493.

- 610 Aly, H., Hammad, T. A., Essers, J., and Wung, J. T. (2012). Is mechanical ventilation associated with
611 intraventricular hemorrhage in preterm infants? *Brain Dev.* 34, 201–205.
612 doi:10.1016/j.braindev.2011.04.006.
- 613 Amaro, C. M., Bello, J. A., Jain, D., Ramnath, A., D’Ugard, C., Vanbuskirk, S., et al. (2018). Early
614 Caffeine and Weaning from Mechanical Ventilation in Preterm Infants: A Randomized,
615 Placebo-Controlled Trial. *J. Pediatr.* 196, 52–57. doi:10.1016/j.jpeds.2018.01.010.
- 616 Andropoulos, D. B. (2018). Effect of anesthesia on the developing brain: Infant and fetus. *Fetal*
617 *Diagn. Ther.* 43, 1–11. doi:10.1159/000475928.
- 618 Attar, M. A., and Donn, S. M. (2002). Mechanisms of ventilator-induced lung injury in premature
619 infants. *Semin. Neonatol.* 7, 353–360. doi:10.1053/siny.2002.0129.
- 620 Australian and New Zealand Committee on Resuscitation (2016). ANZCOR Guideline 13 . 4 –
621 Airway Management and Mask Ventilation of the Newborn Infant.
- 622 Back, S. A., Riddle, A., Dean, J., and Hohimer, A. R. (2012). The Instrumented Fetal Sheep as a
623 Model of Cerebral White Matter Injury in the Premature Infant. *Neurotherapeutics* 9, 359–370.
624 doi:10.1007/s13311-012-0108-y.
- 625 Back, S. A., Riddle, A., and Hohimer, A. R. (2006). Role of instrumented fetal sheep preparations in
626 defining the pathogenesis of human periventricular white-matter injury. *J Child Neurol* 21, 582–
627 589. doi:10.1177/08830738060210070101.
- 628 Back, S. A., and Rosenberg, P. A. (2014). Pathophysiology of glia in perinatal white matter injury.
629 *Glia* 62, 1790–1815. doi:10.1002/glia.22658.
- 630 Bajaj, M., Natarajan, G., Shankaran, S., Wyckoff, M., Laptook, A. R., Bell, E. F., et al. (2018).
631 Delivery Room Resuscitation and Short-Term Outcomes in Moderately Preterm Infants. *J.*
632 *Pediatr.* 195, 33-38.e2. doi:10.1016/j.jpeds.2017.11.039.
- 633 Bapat, R., Narayana, P. A., Zhou, Y., and Parikh, N. A. (2014). Magnetic resonance spectroscopy at
634 term-equivalent age in extremely preterm infants: Association with cognitive and language
635 development. *Pediatr. Neurol.* 51, 53–59. doi:10.1016/j.pediatrneurol.2014.03.011.
- 636 Barlow, R. M. (1969). The foetal sheep: morphogenesis of the nervous system and histochemical
637 aspects of myelination. *J. Comp. Neurol.* 135, 249–262.
- 638 Barnett, M. L., Tusor, N., Ball, G., Chew, A., Falconer, S., Aljabar, P., et al. (2018). Exploring the
639 multiple-hit hypothesis of preterm white matter damage using diffusion MRI. *NeuroImage Clin.*
640 17, 596–606. doi:10.1016/j.nicl.2017.11.017.
- 641 Barton, S. K., McDougall, A. R. A., Melville, J. M., Moss, T. J. M., Zahra, V. A., Lim, T., et al.
642 (2016a). Differential short-term regional effects of early high dose erythropoietin on white
643 matter in preterm lambs after mechanical ventilation. *J. Physiol.* 594, 1437–49.
644 doi:10.1113/JP271376.
- 645 Barton, S. K., Melville, J. M., Tolcos, M., Polglase, G. R., McDougall, A. R. a., Azhan, A., et al.
646 (2015a). Human amnion epithelial cells modulate ventilation-induced white matter pathology in
647 preterm lambs. *Dev. Neurosci.* 37, 338–348. doi:10.1159/000371415.
- 648 Barton, S. K., Moss, T. J. M., Hooper, S. B., Crossley, K. J., Gill, A. W., Kluckow, M., et al. (2014).

- 649 Protective ventilation of preterm lambs exposed to acute chorioamnionitis does not reduce
650 ventilation-induced lung or brain injury. *PLoS One* 9, e112402.
651 doi:10.1371/journal.pone.0112402.
- 652 Barton, S. K., Tolcos, M., Miller, S. L., Christoph-Roehr, C., Schmölzer, G. M., Moss, T. J. M., et al.
653 (2016b). Ventilation-Induced Brain Injury in Preterm Neonates: A Review of Potential
654 Therapies. *Neonatology* 110, 155–62. doi:10.1159/000444918.
- 655 Barton, S. K., Tolcos, M., Miller, S. L., Roehr, C. C., Schmölzer, G. M., Davis, P. G., et al. (2015b).
656 Unraveling the links between the initiation of ventilation and brain injury in preterm infants.
657 *Front. Pediatr.* 3, 97. doi:10.3389/fped.2015.00097.
- 658 Behnke, J., Lemyre, B., Czernik, C., Zimmer, K.-P., Ehrhardt, H., and Waitz, M. (2019). Non-
659 Invasive Ventilation in Neonatology. *Dtsch. Arztebl. Int.* 116, 177–183.
660 doi:10.3238/arztebl.2019.0177.
- 661 Bhatt, S., Alison, B. J., Wallace, E. M., Crossley, K. J., Gill, A. W., Kluckow, M., et al. (2013).
662 Delaying cord clamping until ventilation onset improves cardiovascular function at birth in
663 preterm lambs. *J. Physiol.* 591, 2113–2126. doi:10.1113/jphysiol.2012.250084.
- 664 Björklund, L. J., Ingimarsson, J., Curstedt, T., John, J., Robertson, B., Werner, O., et al. (1997).
665 Manual Ventilation with a Few Large Breaths at Birth Compromises the Therapeutic Effect of
666 Subsequent Surfactant Replacement in Immature Lambs. *Pediatr. Res.* 42, 348–355.
667 doi:10.1203/00006450-199709000-00016.
- 668 Blanco, C. E., Martin, C. B., Hanson, M. A., and McCooke, H. B. (1987). Breathing activity in fetal
669 sheep during mechanical ventilation of the lungs in utero. *Eur. J. Obstet. Gynecol. Reprod. Biol.*
670 26, 175–182. doi:10.1016/0028-2243(87)90054-2.
- 671 Blencowe, H., Cousens, S., Oestergaard, M. Z., Chou, D., Moller, A. B., Narwal, R., et al. (2012).
672 National, regional, and worldwide estimates of preterm birth rates in the year 2010 with time
673 trends since 1990 for selected countries: A systematic analysis and implications. *Lancet* 379,
674 2162–2172. doi:10.1016/S0140-6736(12)60820-4.
- 675 Blencowe, H., Lee, A. C. C., Cousens, S., Bahalim, A., Narwal, R., Zhong, N., et al. (2013). Preterm
676 birth-associated neurodevelopmental impairment estimates at regional and global levels for
677 2010. *Pediatr. Res.* 74 Suppl 1, 17–34. doi:10.1038/pr.2013.204.
- 678 Chan, K. Y. Y., LaRosa, D. A., Tolcos, M., Li, A., Zahra, V. A., Polglase, G. R., et al. (2017).
679 Optimizing the Dose of Erythropoietin Required to Prevent Acute Ventilation-Induced Cerebral
680 White Matter Injury in Preterm Lambs. *Dev. Neurosci.* 39, 298–309. doi:10.1159/000459620.
- 681 Chi, J. G., Dooling, E. C., and Gilles, F. H. (1977). Gyral development of the human brain. *Ann.*
682 *Neurol.* 1, 86–93. doi:10.1002/ana.410010109.
- 683 Cho, S. J., Shin, J., and Namgung, R. (2015). Initial resuscitation at delivery and short term neonatal
684 outcomes in very-low-birth-weight infants. *J. Korean Med. Sci.* 30, S45–S51.
685 doi:10.3346/jkms.2015.30.S1.S45.
- 686 Choi, Y.-B., Lee, J., Park, J., and Jun, Y. H. (2018). Impact of Prolonged Mechanical Ventilation in
687 Very Low Birth Weight Infants: Results From a National Cohort Study. *J. Pediatr.* 194, 34-
688 39.e3. doi:10.1016/j.jpeds.2017.10.042.

- 689 Chow, S. S. W., Creighton, P., Chambers, G., and Lui, K. (2019). *Report of the Australian and New*
690 *Zealand Neonatal Network 2017*. Sydney: ANZNN.
- 691 Coalson, J. J., Winter, V. T., Siler-Khodr, T., and Yoder, B. A. (1999). Neonatal chronic lung disease
692 in extremely immature baboons. *Am. J. Respir. Crit. Care Med.* 160, 1333–1346.
693 doi:10.1164/ajrccm.160.4.9810071.
- 694 Conrad, M. S., and Johnson, R. W. (2015). The Domestic Piglet: An Important Model for
695 Investigating the Neurodevelopmental Consequences of Early Life Insults. *Annu. Rev. Anim.*
696 *Biosci.* 3, 245–264. doi:10.1146/annurev-animal-022114-111049.
- 697 Counsell, S. J., Rutherford, M. A., Cowan, F. M., and Edwards, A. D. (2003). Magnetic resonance
698 imaging of preterm brain injury. *Arch Dis Child Fetal Neonatal Ed* 88, F269-74.
699 doi:10.1136/fn.88.4.F269.
- 700 Curley, G. F., Laffey, J. G., Zhang, H., and Slutsky, A. S. (2016). Biotrauma and Ventilator-Induced
701 Lung Injury: Clinical Implications. *Chest* 150, 1109–1117. doi:10.1016/j.chest.2016.07.019.
- 702 Czynski, A. J., Terry, M. H., Deming, D. D., Power, G. G., Buchholz, J. N., and Blood, A. B. (2013).
703 Cerebral autoregulation is minimally influenced by the superior cervical ganglion in two-week-
704 old lambs, and absent in preterm lambs immediately following delivery. *PLoS One* 8, e82326.
705 doi:10.1371/journal.pone.0082326.
- 706 Dekker, J., Hooper, S. B., Van Vonderen, J. J., Witlox, R. S. G. M., Lopriore, E., and Te Pas, A. B.
707 (2017). Caffeine to improve breathing effort of preterm infants at birth: A randomized
708 controlled trial. *Pediatr. Res.* 82, 290–296. doi:10.1038/pr.2017.45.
- 709 Dieni, S., Inder, T., Yoder, B., Briscoe, T., Camm, E., Egan, G., et al. (2004). The pattern of cerebral
710 injury in a primate model of preterm birth and neonatal intensive care. *J. Neuropathol. Exp.*
711 *Neurol.* 63, 1297–309. doi:10.1093/jnen/63.12.1297.
- 712 du Plessis, A. J. (2009). The role of systemic hemodynamic disturbances in prematurity-related brain
713 injury. *J. Child Neurol.* 24, 1127–1140. doi:10.1177/0883073809339361.
- 714 Eiby, Y. A., Wright, L. L., Kalanjati, V. P., Miller, S. M., Bjorkman, S. T., Keates, H. L., et al.
715 (2013). A pig model of the preterm neonate: anthropometric and physiological characteristics.
716 *PLoS One* 8, e68763. doi:10.1371/journal.pone.0068763.
- 717 Gagliardi, L., Bellù, R., Zanini, R., and Dammann, O. (2009). Bronchopulmonary dysplasia and
718 brain white matter damage in the preterm infant: A complex relationship. *Paediatr. Perinat.*
719 *Epidemiol.* 23, 582–590. doi:10.1111/j.1365-3016.2009.01069.x.
- 720 Gilmore, M. M., Stone, B. S., Shepard, J. A., Czosnyka, M., Easley, R. B., and Brady, K. M. (2011).
721 Relationship between cerebrovascular dysautoregulation and arterial blood pressure in the
722 premature infant. *J. Perinatol.* 31, 722–729. doi:10.1038/jp.2011.17.
- 723 Giraud, G., Morton, M., Reid, D., Reller, M., and Thornburg, K. (1995). Effects of ductus arteriosus
724 occlusion on pulmonary artery pressure during in utero ventilation in fetal sheep. *Exp. Physiol.*
725 80, 129–139. doi:10.1113/expphysiol.1995.sp003828.
- 726 Gleason, C. A., Jones, M. D., Traystman, R. J., and Notter, R. H. (1988). Fetal cerebral responses to
727 ventilation and oxygenation in utero. *Am. J. Physiol. Integr. Comp. Physiol.* 255, R1049–R1054.

- 728 doi:10.1152/ajpregu.1988.255.6.R1049.
- 729 Goldenberg, R. L., Culhane, J. F., Iams, J. D., and Romero, R. (2008). Epidemiology and causes of
730 preterm birth. *Lancet* 371, 75–84. doi:10.1016/S0140-6736(08)60074-4.
- 731 Greisen, G. (2005). Autoregulation of cerebral blood flow in newborn babies. *Early Hum. Dev.* 81,
732 423–428. doi:10.1016/j.earlhumdev.2005.03.005.
- 733 Griffith, J. L., Shimony, J. S., Cousins, S. A., Rees, S. E., McCurnin, D. C., Inder, T. E., et al. (2012).
734 MR imaging correlates of white-matter pathology in a preterm baboon model. *Pediatr. Res.* 71,
735 185–191. doi:10.1038/pr.2011.33.
- 736 Hagberg, H., Peebles, D., and Mallard, C. (2002). Models of white matter injury: Comparison of
737 infectious, hypoxic-Ischemic, and excitotoxic insults. *Ment. Retard. Dev. Disabil. Res. Rev.* 8,
738 30–38. doi:10.1002/mrdd.10007.
- 739 Hillman, N. H., Kallapur, S. G., and Jobe, A. H. (2012). Physiology of Transition from Intrauterine to
740 Extrauterine Life. *Clin. Perinatol.* 39, 769–783. doi:10.1016/j.clp.2012.09.009.
- 741 Hillman, N. H., Kallapur, S. G., Pillow, J. J., Moss, T. J. M., Polglase, G. R., Nitsos, I., et al. (2010).
742 Airway Injury From Initiating Ventilation in Preterm Sheep. *Pediatr. Res.* 67, 60–65.
743 doi:10.1203/PDR.0b013e3181c1b09e.
- 744 Hillman, N. H., Moss, T. J. M., Kallapur, S. G., Bachurski, C., Pillow, J. J., Polglase, G. R., et al.
745 (2007). Brief, large tidal volume ventilation initiates lung injury and a systemic response in fetal
746 sheep. *Am. J. Respir. Crit. Care Med.* 176, 575–581. doi:10.1164/rccm.200701-051OC.
- 747 Hillman, N. H., Polglase, G. R., Pillow, J. J., Saito, M., Kallapur, S. G., and Jobe, A. H. (2011).
748 Inflammation and lung maturation from stretch injury in preterm fetal sheep. *Am. J. Physiol.*
749 *Lung Cell. Mol. Physiol.* 300, L232–L241. doi:10.1152/ajplung.00294.2010.
- 750 Hodges, R. J., Jenkin, G., Hooper, S. B., Allison, B., Lim, R., Dickinson, H., et al. (2012). Human
751 amnion epithelial cells reduce ventilation-induced preterm lung injury in fetal sheep. *Am. J.*
752 *Obstet. Gynecol.* 206, 448.e8–448.e15. doi:10.1016/j.ajog.2012.02.038.
- 753 Hyodo, R., Sato, Y., Ito, M., Sugiyama, Y., Ogawa, C., Kawai, H., et al. (2018). Magnetic resonance
754 spectroscopy in preterm infants: association with neurodevelopmental outcomes. *Arch. Dis.*
755 *Child. Fetal Neonatal Ed.* 103, F238–F244. doi:10.1136/archdischild-2016-311403.
- 756 Inder, T., Neil, J., Yoder, B., and Rees, S. (2005). Patterns of Cerebral Injury in a Primate Model of
757 Preterm Birth and Neonatal Intensive Care. *J. Child Neurol.* 20, 965–967.
758 doi:10.1177/08830738050200120601.
- 759 Iwamoto, H. S., Teitel, D. F., and Rudolph, A. M. (1993). Effects of lung distension and spontaneous
760 fetal breathing on hemodynamics in sheep. *Pediatr. Res.* 33, 639–644. doi:10.1203/00006450-
761 199306000-00021.
- 762 Jain, V. G., Saroha, V., Patel, R. M., and Jobe, A. (2019). Is early caffeine therapy safe and effective
763 for ventilated preterm infants? *J. Perinatol.* 39, 754–757. doi:10.1038/s41372-019-0336-7.
- 764 Jobe, A. H., and Ikegami, M. (1998). Mechanisms initiating lung injury in the preterm. *Early Hum.*
765 *Dev.* 53, 81–94. doi:10.1016/S0378-3782(98)00045-0.

- 766 Juul, S. E., McPherson, R. J., Farrell, F. X., Jolliffe, L., Ness, D. J., and Gleason, C. A. (2004).
767 Erythropoietin concentrations in cerebrospinal fluid of nonhuman primates and fetal sheep
768 following high-dose recombinant erythropoietin. *Biol. Neonate* 85, 138–144.
769 doi:10.1159/000074970.
- 770 Khwaja, O., and Volpe, J. J. (2007). Pathogenesis of cerebral white matter injury of prematurity.
771 *Arch. Dis. Child. - Fetal Neonatal Ed.* 93, F153–F161. doi:10.1136/ad.2006.108837.
- 772 Kothe, T. B., Royse, E., Kemp, M. W., Schmidt, A., Salomone, F., Saito, M., et al. (2018). Effects of
773 budesonide and surfactant in preterm fetal sheep. *Am. J. Physiol. Cell. Mol. Physiol.* 315, L193–
774 L201. doi:10.1152/ajplung.00528.2017.
- 775 Kumar, P., Denson, S. E., and Mancuso, T. J. (2010). Premedication for Nonemergency Endotracheal
776 Intubation in the Neonate. *Pediatrics* 125, 608–615. doi:10.1542/peds.2009-2863.
- 777 Lee, J., and Loepke, A. W. (2018). Does pediatric anesthesia cause brain damage? – Addressing
778 parental and provider concerns in light of compelling animal studies and seemingly ambivalent
779 human data. *Korean J. Anesthesiol.* 71, 255–273. doi:10.4097/kja.d.18.00165.
- 780 Lindner, W., Vossbeck, S., Hummler, H., and Pohlandt, F. (1999). Delivery room management of
781 extremely low birth weight infants: spontaneous breathing or intubation? *Pediatrics* 103, 961–7.
782 Available at: <http://www.ncbi.nlm.nih.gov/pubmed/10224173>.
- 783 Lodha, A., Entz, R., Synnes, A., Creighton, D., Yusuf, K., Lapointe, A., et al. (2019). Early Caffeine
784 Administration and Neurodevelopmental Outcomes in Preterm Infants. *Pediatrics* 143,
785 e20181348. doi:10.1542/peds.2018-1348.
- 786 Lodha, A., Seshia, M., McMillan, D. D., Barrington, K., Yang, J., Lee, S. K., et al. (2015).
787 Association of early caffeine administration and neonatal outcomes in very preterm neonates.
788 *JAMA Pediatr.* 169, 33–38. doi:10.1001/jamapediatrics.2014.2223.
- 789 Loeliger, M., Inder, T., Cain, S., Ramesh, R. C., Camm, E., Thomson, M. A., et al. (2006). Cerebral
790 Outcomes in a Preterm Baboon Model of Early Versus Delayed Nasal Continuous Positive
791 Airway Pressure. *Pediatrics* 118, 1640–1653. doi:10.1542/peds.2006-0653.
- 792 Loeliger, M., Inder, T. E., Dalitz, P. A., Cain, S., Camm, E. J., Yoder, B., et al. (2009a).
793 Developmental and neuropathological consequences of ductal ligation in the preterm baboon.
794 *Pediatr. Res.* 65, 209–214. doi:10.1203/PDR.0b013e31818d6d0b.
- 795 Loeliger, M., Inder, T. E., Shields, A., Dalitz, P., Cain, S., Yoder, B., et al. (2009b). High-Frequency
796 Oscillatory Ventilation Is Not Associated With Increased Risk of Neuropathology Compared
797 With Positive Pressure Ventilation: A Preterm Primate Model. *Pediatr. Res.* 66, 545–550.
798 doi:10.1203/PDR.0b013e3181bb0cc1.
- 799 Lundqvist, P., Källén, K., Hallström, I., and Westas, L. H. (2009). Trends in outcomes for very
800 preterm infants in the southern region of Sweden over a 10-year period. *Acta Paediatr. Int. J.*
801 *Paediatr.* 98, 648–653. doi:10.1111/j.1651-2227.2008.01155.x.
- 802 Malhotra, A., Castillo-Melendez, M., Allison, B. J., Sutherland, A. E., Nitsos, I., Pham, Y., et al.
803 (2018). Neuropathology as a consequence of neonatal ventilation in premature growth-restricted
804 lambs. *Am. J. Physiol. Integr. Comp. Physiol.* 315, R1183–R1194.
805 doi:10.1152/ajpregu.00171.2018.

- 806 McIntosh, G. H., Baghurst, K. I., Potter, B. J., and Hetzel, B. S. (1979). Foetal brain development in
807 the sheep. *Neuropathol. Appl. Neurobiol.* 5, 103–114.
- 808 Melville, J. M., McDonald, C. A., Bischof, R. J., Polglase, G. R., Lim, R., Wallace, E. M., et al.
809 (2017). Human amnion epithelial cells modulate the inflammatory response to ventilation in
810 preterm lambs. *PLoS One* 12, e0173572. doi:10.1371/journal.pone.0173572.
- 811 Mian, Q., Cheung, P.-Y., O'Reilly, M., Barton, S. K., Polglase, G. R., and Schmölzer, G. M. (2019).
812 Impact of delivered tidal volume on the occurrence of intraventricular haemorrhage in preterm
813 infants during positive pressure ventilation in the delivery room. *Arch. Dis. Child. Fetal*
814 *Neonatal Ed.* 104, F57–F62. doi:10.1136/archdischild-2017-313864.
- 815 Mian, Q. N., Pichler, G., Binder, C., O'Reilly, M., Aziz, K., Urlesberger, B., et al. (2014). Tidal
816 volumes in spontaneously breathing preterm infants supported with continuous positive airway
817 pressure. *J. Pediatr.* 165, 702–706.e1. doi:10.1016/j.jpeds.2014.06.047.
- 818 Miller, S. L., Chai, M., Loose, J., Castillo-Meléndez, M., Walker, D. W., Jenkin, G., et al. (2007).
819 The effects of maternal betamethasone administration on the intrauterine growth-restricted fetus.
820 *Endocrinology* 148, 1288–1295. doi:10.1210/en.2006-1058.
- 821 Miller, S. L., Huppi, P. S., and Mallard, C. (2016). The consequences of fetal growth restriction on
822 brain structure and neurodevelopmental outcome. *J. Physiol.* 594, 807–823.
823 doi:10.1113/JP271402.
- 824 Miller, S. L., Supramaniam, V. G., Jenkin, G., Walker, D. W., and Wallace, E. M. (2009).
825 Cardiovascular responses to maternal betamethasone administration in the intrauterine growth-
826 restricted ovine fetus. *Am. J. Obstet. Gynecol.* 201, 613.e1-613.e8.
827 doi:10.1016/j.ajog.2009.07.028.
- 828 Miller, S. L., and Wallace, E. M. (2013). Effect of Antenatal Steroids on Haemodynamics in the
829 Normally Grown and Growth Restricted Fetus. *Curr. Pediatr. Rev.* 9, 67–74.
830 doi:10.2174/1573396311309010014.
- 831 Mürner-Lavanchy, I. M., Doyle, L. W., Schmidt, B., Roberts, R. S., Asztalos, E. V., Costantini, L., et
832 al. (2018). Neurobehavioral Outcomes 11 Years After Neonatal Caffeine Therapy for Apnea of
833 Prematurity. *Pediatrics* 141, e20174047. doi:10.1542/peds.2017-4047.
- 834 O'Reilly, M., Hooper, S. B., Allison, B. J., Flecknoe, S. J., Snibson, K., Harding, R., et al. (2009).
835 Persistent bronchiolar remodeling following brief ventilation of the very immature ovine lung.
836 *Am. J. Physiol. - Lung Cell. Mol. Physiol.* 297, 992–1001. doi:10.1152/ajplung.00099.2009.
- 837 Parker, J. C., Hernandez, L. A., and Peevy, K. J. (1993). Mechanisms of ventilator-induced lung
838 injury. *Crit. Care Med.* 21, 131–143.
- 839 Patterson, D. S. P., Sweasey, D., and Hebert, C. N. (1971). Changes Occurring in the Chemical
840 Composition of the Central Nervous System During Foetal and Post-Natal Development of the
841 Sheep. *J. Neurochem.* 18, 2027–2040. doi:10.1111/j.1471-4159.1971.tb05062.x.
- 842 Perlman, J. M., McMenamin, J. B., and Volpe, J. J. (1983). Fluctuating Cerebral Blood-Flow
843 Velocity in Respiratory-Distress Syndrome. *N. Engl. J. Med.* 309, 204–209.
844 doi:10.1056/NEJM198307283090402.

- 845 Phillips, K. A., Bales, K. L., Capitanio, J. P., Conley, A., Czoty, P. W., 't Hart, B. A., et al. (2014).
846 Why primate models matter. *Am. J. Primatol.* 76, 801–827. doi:10.1002/ajp.22281.
- 847 Polglase, G. R., Barton, S. K., Melville, J. M., Zahra, V., Wallace, M. J., Siew, M. L., et al. (2014a).
848 Prophylactic erythropoietin exacerbates ventilation-induced lung inflammation and injury in
849 preterm lambs. *J. Physiol.* 592, 1993–2002. doi:10.1113/jphysiol.2013.270348.
- 850 Polglase, G. R., Blank, D. A., Barton, S. K., Miller, S. L., Stojanovska, V., Kluckow, M., et al.
851 (2018). Physiologically based cord clamping stabilises cardiac output and reduces
852 cerebrovascular injury in asphyxiated near-term lambs. *Arch. Dis. Child. Fetal Neonatal Ed.*
853 103, F530–F538. doi:10.1136/archdischild-2017-313657.
- 854 Polglase, G. R., Dawson, J. A., Kluckow, M., Gill, A. W., Davis, P. G., Te Pas, A. B., et al. (2015).
855 Ventilation onset prior to umbilical cord clamping (physiological-based cord clamping)
856 improves systemic and cerebral oxygenation in preterm lambs. *PLoS One* 10, 1–13.
857 doi:10.1371/journal.pone.0117504.
- 858 Polglase, G. R., Miller, S. L., Barton, S. K., Baburamani, A. A., Wong, F. Y., Aridas, J. D. S., et al.
859 (2012a). Initiation of resuscitation with high tidal volumes causes cerebral hemodynamic
860 disturbance, brain inflammation and injury in preterm lambs. *PLoS One* 7, 1–8.
861 doi:10.1371/journal.pone.0039535.
- 862 Polglase, G. R., Miller, S. L., Barton, S. K., Kluckow, M., Gill, A. W., Hooper, S. B., et al. (2014b).
863 Respiratory support for premature neonates in the delivery room: effects on cardiovascular
864 function and the development of brain injury. *Pediatr. Res.* 75, 682–688.
865 doi:10.1038/pr.2014.40.
- 866 Polglase, G. R., Nitsos, I., Baburamani, A. A., Crossley, K. J., Slater, M. K., Gill, A. W., et al.
867 (2012b). Inflammation in utero exacerbates ventilation-induced brain injury in preterm lambs. *J.*
868 *Appl. Physiol.* 112, 481–489. doi:10.1152/jappphysiol.00995.2011.
- 869 Poulton, D. A., Schmölzer, G. M., Morley, C. J., and Davis, P. G. (2011). Assessment of chest rise
870 during mask ventilation of preterm infants in the delivery room. *Resuscitation* 82, 175–179.
871 doi:10.1016/j.resuscitation.2010.10.012.
- 872 Räikkönen, K., Gissler, M., and Kajantie, E. (2020). Associations Between Maternal Antenatal
873 Corticosteroid Treatment and Mental and Behavioral Disorders in Children Supplemental
874 content. *Jama* 323, 1924–1933. doi:10.1001/jama.2020.3937.
- 875 Rees, S., and Inder, T. (2005). Fetal and neonatal origins of altered brain development. *Early Hum.*
876 *Dev.* 81, 753–761. doi:10.1016/j.earlhumdev.2005.07.004.
- 877 Rees, S. M., Camm, E. J., Loeliger, M., Cain, S., Dieni, S., McCurnin, D., et al. (2007). Inhaled
878 Nitric Oxide: Effects on Cerebral Growth and Injury in a Baboon Model of Premature Delivery.
879 *Pediatr. Res.* 61, 552–558. doi:10.1203/pdr.0b013e318045be20.
- 880 Rees, S. M., Loeliger, M. M., Munro, K. M., Shields, A., Dalitz, P. A., Dieni, S., et al. (2009).
881 Cerebellar Development in a Baboon Model of Preterm Delivery. *J. Neuropathol. Exp. Neurol.*
882 68, 605–615. doi:10.1097/NEN.0b013e3181a39b3f.
- 883 Riddle, A. (2006). Spatial Heterogeneity in Oligodendrocyte Lineage Maturation and Not Cerebral
884 Blood Flow Predicts Fetal Ovine Periventricular White Matter Injury. *J. Neurosci.* 26, 3045–

- 885 3055. doi:10.1523/JNEUROSCI.5200-05.2006.
- 886 Roberts, D., Brown, J., Medley, N., and Dalziel, S. R. (2017). Antenatal corticosteroids for
887 accelerating fetal lung maturation for women at risk of preterm birth. *Cochrane database Syst.*
888 *Rev.* 3, Art. No.: CD004454. doi:10.1002/14651858.CD004454.pub3.
- 889 Romanes, G. J. (1947). The prenatal medullation of the sheep's nervous system. *J. Anat.* 81, 64–81.
890 Available at: <http://www.ncbi.nlm.nih.gov/pubmed/17105021>.
- 891 Schilleman, K., Van Der Pot, C. J. M., Hooper, S. B., Lopriore, E., Walther, F. J., and Te Pas, A. B.
892 (2013). Evaluating manual inflations and breathing during mask ventilation in preterm infants at
893 birth. *J. Pediatr.* 162, 457–463. doi:10.1016/j.jpeds.2012.09.036.
- 894 Schittny, J. C. (2017). Development of the lung. *Cell Tissue Res.* 367, 427–444. doi:10.1007/s00441-
895 016-2545-0.
- 896 Schmidt, B., Anderson, P. J., Doyle, L. W., Dewey, D., Grunau, R. E., Asztalos, E. V., et al. (2012).
897 Survival without disability to age 5 years after neonatal caffeine therapy for apnea of
898 prematurity. *JAMA* 307, 275–82. doi:10.1001/jama.2011.2024.
- 899 Schmidt, B., Roberts, R. S., Anderson, P. J., Asztalos, E. V., Costantini, L., Davis, P. G., et al. (2017).
900 Academic Performance, Motor Function, and Behavior 11 Years After Neonatal Caffeine
901 Citrate Therapy for Apnea of Prematurity. *JAMA Pediatr.* 171, 564.
902 doi:10.1001/jamapediatrics.2017.0238.
- 903 Schmidt, B., Roberts, R. S., Davis, P., Doyle, L. W., Barrington, K. J., Ohlsson, A., et al. (2006).
904 Caffeine Therapy for Apnea of Prematurity. *N. Engl. J. Med.* 354, 2112–2121.
905 doi:10.1056/NEJMoa054065.
- 906 Schmidt, B., Roberts, R. S., Davis, P., Doyle, L. W., Barrington, K. J., Ohlsson, A., et al. (2007).
907 Long-Term Effects of Caffeine Therapy for Apnea of Prematurity. *N. Engl. J. Med.* 357, 1893–
908 1902. doi:10.1056/NEJMoa073679.
- 909 Schmölzer, G. M., Kamlin, O. C. O. F., O'Donnell, C. P. F., Dawson, J. A., Morley, C. J., and Davis,
910 P. G. (2010). Assessment of tidal volume and gas leak during mask ventilation of preterm
911 infants in the delivery room. *Arch. Dis. Child. Fetal Neonatal Ed.* 95, 1–4.
912 doi:10.1136/adc.2009.174003.
- 913 Schmölzer, G. M., Te Pas, A. B., Davis, P. G., and Morley, C. J. (2008). Reducing lung injury during
914 neonatal resuscitation of preterm infants. *J. Pediatr.* 153, 741–745.
915 doi:10.1016/j.jpeds.2008.08.016.
- 916 Serenius, F., Ewald, U., Farooqi, A., Holmgren, P. Å., Håkansson, S., and Sedin, G. (2004a). Short-
917 term outcome-after active perinatal management at 23-25 weeks of gestation. A study from two
918 Swedish perinatal centres. Part 3: Neonatal morbidity. *Acta Paediatr. Int. J. Paediatr.* 93, 1090–
919 1097. doi:10.1080/08035250410027760.
- 920 Serenius, F., Ewald, U., Farooqi, A., Holmgren, P. Å., Håkansson, S., and Sedin, G. (2004b). Short-
921 term outcome after active perinatal management at 23-25 weeks of gestation. A study from two
922 Swedish tertiary care centres. Part 2: Infant survival. *Acta Paediatr. Int. J. Paediatr.* 93, 1081–
923 1089. doi:10.1080/08035250410027751.

- 924 Sharma, D., Shastri, S., and Sharma, P. (2016). Intrauterine Growth Restriction: Antenatal and
925 Postnatal Aspects. *Clin. Med. Insights. Pediatr.* 10, 67–83. doi:10.4137/CMPed.S40070.
- 926 Skiöld, B., Wu, Q., Hooper, S. B., Davis, P. G., McIntyre, R., Tolcos, M., et al. (2014). Early
927 detection of ventilation-induced brain injury using magnetic resonance spectroscopy and
928 diffusion tensor imaging: An in vivo study in preterm lambs. *PLoS One* 9, 1–8.
929 doi:10.1371/journal.pone.0095804.
- 930 Soll, R. F., Edwards, E. M., Badger, G. J., Kenny, M. J., Morrow, K. A., Buzas, J. S., et al. (2013).
931 Obstetric and neonatal care practices for infants 501 to 1500 g from 2000 to 2009. *Pediatrics*
932 132, 222–228. doi:10.1542/peds.2013-0501.
- 933 Stojanovska, V., Atik, A., Nitsos, I., Skiöld, B., Barton, S. K., Zahra, V. A., et al. (2018a). Effects of
934 Intrauterine Inflammation on Cortical Gray Matter of Near-Term Lambs. *Front. Pediatr.* 6, 1–
935 10. doi:10.3389/fped.2018.00145.
- 936 Stojanovska, V., Barton, S. K., Tolcos, M., Gill, A. W., Kluckow, M., Miller, S. L., et al. (2018b).
937 The Effect of Antenatal Betamethasone on White Matter Inflammation and Injury in Fetal Sheep
938 and Ventilated Preterm Lambs. *Dev. Neurosci.* 40, 497–507. doi:10.1159/000496466.
- 939 Stoll, B. J., Hansen, N. I., Bell, E. F., Walsh, M. C., Carlo, W. A., Shankaran, S., et al. (2015).
940 Trends in care practices, morbidity, and mortality of extremely preterm Neonates, 1993-2012.
941 *JAMA - J. Am. Med. Assoc.* 314, 1039–1051. doi:10.1001/jama.2015.10244.
- 942 Sweasey, D., Patterson, D. S. P., and Glancy, E. M. (1976). Biphasic Myelination and the Fatty Acid
943 Composition of Cerebrosides and Cholesterol Esters in the Developing Central Nervous System
944 of the Domestic Pig. *J. Neurochem.* 27, 375–380. doi:10.1111/j.1471-4159.1976.tb12256.x.
- 945 Tracy, M., Downe, L., and Holberton, J. (2004). How safe is intermittent positive pressure ventilation
946 in preterm babies ventilated from delivery to newborn intensive care unit? *Arch. Dis. Child.*
947 *Fetal Neonatal Ed.* 89, F84–F87. doi:10.1136/fn.89.1.F84.
- 948 Tsai, W., Hwang, Y., Hung, T., Weng, S., Lin, S.-J., and Chang, W.-T. (2014). Association between
949 mechanical ventilation and neurodevelopmental disorders in a nationwide cohort of extremely
950 low birth weight infants. *Res. Dev. Disabil.* 35, 1544–50. doi:10.1016/j.ridd.2014.03.048.
- 951 van Vonderen, J. J., Hooper, S. B., Krabbe, V. B., Siew, M. L., and te Pas, A. B. (2015). Monitoring
952 tidal volumes in preterm infants at birth: mask versus endotracheal ventilation. *Arch. Dis. Child.*
953 *- Fetal Neonatal Ed.* 100, F43–F46. doi:10.1136/archdischild-2014-306614.
- 954 Vento, M., Aguar, M., Leone, T. A., Finer, N. N., Gimeno, A., Rich, W., et al. (2008). Using
955 intensive care technology in the delivery room: a new concept for the resuscitation of extremely
956 preterm neonates. *Pediatrics* 122, 1113–6. doi:10.1542/peds.2008-1422.
- 957 Verma, P. K., Panerai, R. B., Rennie, J. M., and Evans, D. H. (2000). Grading of cerebral
958 autoregulation in preterm and term neonates. *Pediatr. Neurol.* 23, 236–242. doi:S0887-
959 8994(00)00184-3 [pii].
- 960 Verney, C., Rees, S., Biran, V., Thompson, M., Inder, T., and Gressens, P. (2010). Neuronal damage
961 in the preterm baboon: Impact of the mode of ventilatory support. *J. Neuropathol. Exp. Neurol.*
962 69, 473–482. doi:10.1097/NEN.0b013e3181dac07b.

- 963 Vliegthart, R. J. S., van Kaam, A. H., Aarnoudse-Moens, C. S. H., van Wassenae, A. G., and
964 Onland, W. (2019). Duration of mechanical ventilation and neurodevelopment in preterm
965 infants. *Arch. Dis. Child. Fetal Neonatal Ed.* 104, F631–F635. doi:10.1136/archdischild-2018-
966 315993.
- 967 Wallenstein, M. B., Birnie, K. L., Arain, Y. H., Yang, W., Yamada, N. K., Huffman, L. C., et al.
968 (2016). Failed endotracheal intubation and adverse outcomes among extremely low birth weight
969 infants. *J. Perinatol.* 36, 112–115. doi:10.1038/jp.2015.158.
- 970 Walsh, M. C., Morris, B. H., Wragge, L. A., Vohr, B. R., Poole, W. K., Tyson, J. E., et al. (2005).
971 Extremely low birthweight neonates with protracted ventilation: mortality and 18-month
972 neurodevelopmental outcomes. *J. Pediatr.* 146, 798–804. doi:10.1016/j.jpeds.2005.01.047.
- 973 Workman, A. D., Charvet, C. J., Clancy, B., Darlington, R. B., and Finlay, B. L. (2013). Modeling
974 Transformations of Neurodevelopmental Sequences across Mammalian Species. *J. Neurosci.*
975 33, 7368–7383. doi:10.1523/JNEUROSCI.5746-12.2013.
- 976 Yoder, B. A., and Coalson, J. J. (2014). Animal models of bronchopulmonary dysplasia. The preterm
977 baboon models. *Am. J. Physiol. Lung Cell. Mol. Physiol.* 307, L970-7.
978 doi:10.1152/ajplung.00171.2014.
- 979 Yoder, B. A., Siler-Khodr, T., Winter, V. T., and Coalson, J. J. (2000). High-frequency oscillatory
980 ventilation: Effects on lung function, mechanics, and airway cytokines in the immature baboon
981 model for neonatal chronic lung disease. *Am. J. Respir. Crit. Care Med.* 162, 1867–1876.
982 doi:10.1164/ajrccm.162.5.9912145.
- 983

13 Table

Table 1. Comparative gestational ages for key brain development processes in the human, baboon, and sheep.

Developmental process	Human (term 40 weeks)	Baboon (term 185 days)	Sheep (term 145 days)
Weight			
Growth spurt	26-28 wk	125-140 d	85-100 d
Cortical folding			
Primary	<i>ev</i> 26-28 wk	<i>ev</i> 125 d	<i>ev</i> 71-89 d
Secondary	<i>ev</i> 32-34 wk	<i>ev</i> 140 d	n.d.
Tertiary	<i>ev</i> 40-44wk	<i>ev</i> 160 d	n.d.
Six distinct cortical layers	<i>ev</i> 28 wk	<i>ev</i> 125 d	<i>ev</i> 89 d
Neurogenesis and Gliogenesis			
Main neuronal multiplication	10-15 wk	n.d.	40-80 d
Main glial multiplication	36-40 wk	n.d.	95-130 d
Myelination			
Periventricular white matter (preOL predominant)	23-28 wk	n.d.	93-99 d
Internal capsule	<i>ev</i> 32 wk	<i>ev</i> 125 d	<i>ev</i> 78-96 d
Superior temporal gyrus	Mature at 48 wk	Moderate at 160 d	n.d.
Cerebellum	<i>ev</i> 28 wk	<i>ev</i> 125d	<i>ev</i> 80 d

d days; *ev* evident at; *n.d.* not determined; *OL* oligodendrocytes; *wk* weeks.

Note that there is often heterogeneity in development not just between different regions in the brain, but within each region. Compiled from refs human and cross-species comparisons (Chi et al., 1977; Hagberg et al., 2002; Counsell et al., 2003; Albertine, 2012; Workman et al., 2013), baboon (Dieni et al., 2004; Inder et al., 2005; Rees et al., 2009), sheep (Romanes, 1947; Åarström, 1967; Barlow, 1969; Patterson et al., 1971; McIntosh et al., 1979; Back et al., 2006, 2012; Riddle, 2006).

14 Figure Legends

Figure 1. Experimental models of ventilation-induced injury in sheep outlining the major advantages and disadvantages of each model.

Figure 2. A multipronged approach is likely necessary to prevent or reduce ventilation-induced brain injury. Only strategies discussed in-text have been included in the diagram. PPV positive pressure ventilation; PBCC physiological-based cord clamping; hAECs human amnion epithelial cells; EPO erythropoietin.

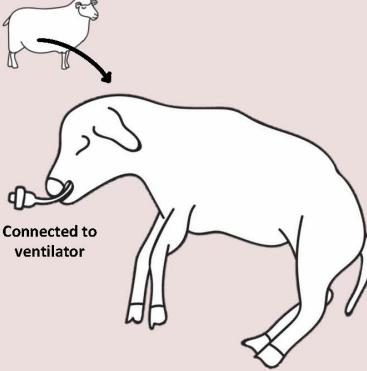
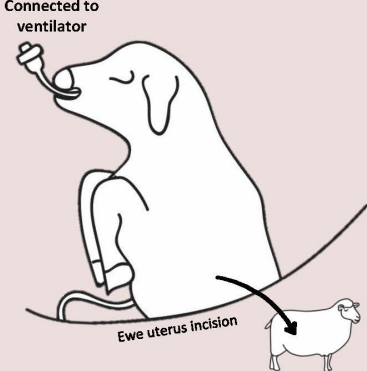
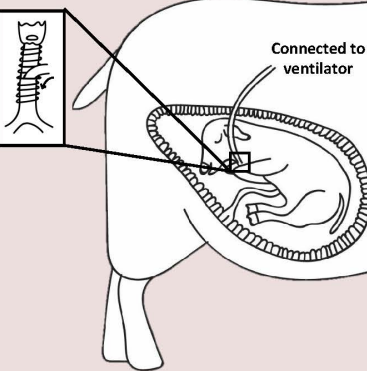
NEONATAL VENTILATION	FETAL HEAD-OUT VENTILATION	FETAL <i>IN UTERO</i> VENTILATION
 <p>Connected to ventilator</p> <p>Lamb delivered, then ventilated</p> <ul style="list-style-type: none"> ✓ Most closely resembles clinical care ✗ Prolonged anaesthetic, increased exposure to oxygen, nutrients supplementation are potential confounders ✗ Viability of animal limited by lung maturation, brain may be relatively more mature and less relevant 	 <p>Connected to ventilator</p> <p>Ewe uterus incision</p> <p>Fetus ventilated in surgery, then returned to uterus.</p> <ul style="list-style-type: none"> ✓ Placenta supports fetus, removes need for supplementary nutrients and oxygenation; able to isolate effects of ventilation and/or alter specific parameters ✓ Younger gestational age possible ✗ Exposure to anaesthetics during ventilation ✗ Only short periods of ventilation possible 	 <p>Connected to ventilator</p> <p>Fetus instrumented in surgery with tubing for ventilation, returned to uterus, then ventilated <i>in utero</i> via externalised tubing</p> <ul style="list-style-type: none"> ✓ Placenta supports fetus, removes need for supplementary nutrients and oxygenation; able to isolate effects of ventilation and/or alter specific parameters ✓ Younger gestational age possible ✓ Not exposed to anaesthetics during ventilation period ✓ Extended periods of ventilation possible ✗ Least clinically relevant

Figure 1. Experimental models of ventilation-induced injury in sheep outlining the major advantages and disadvantages of each model.

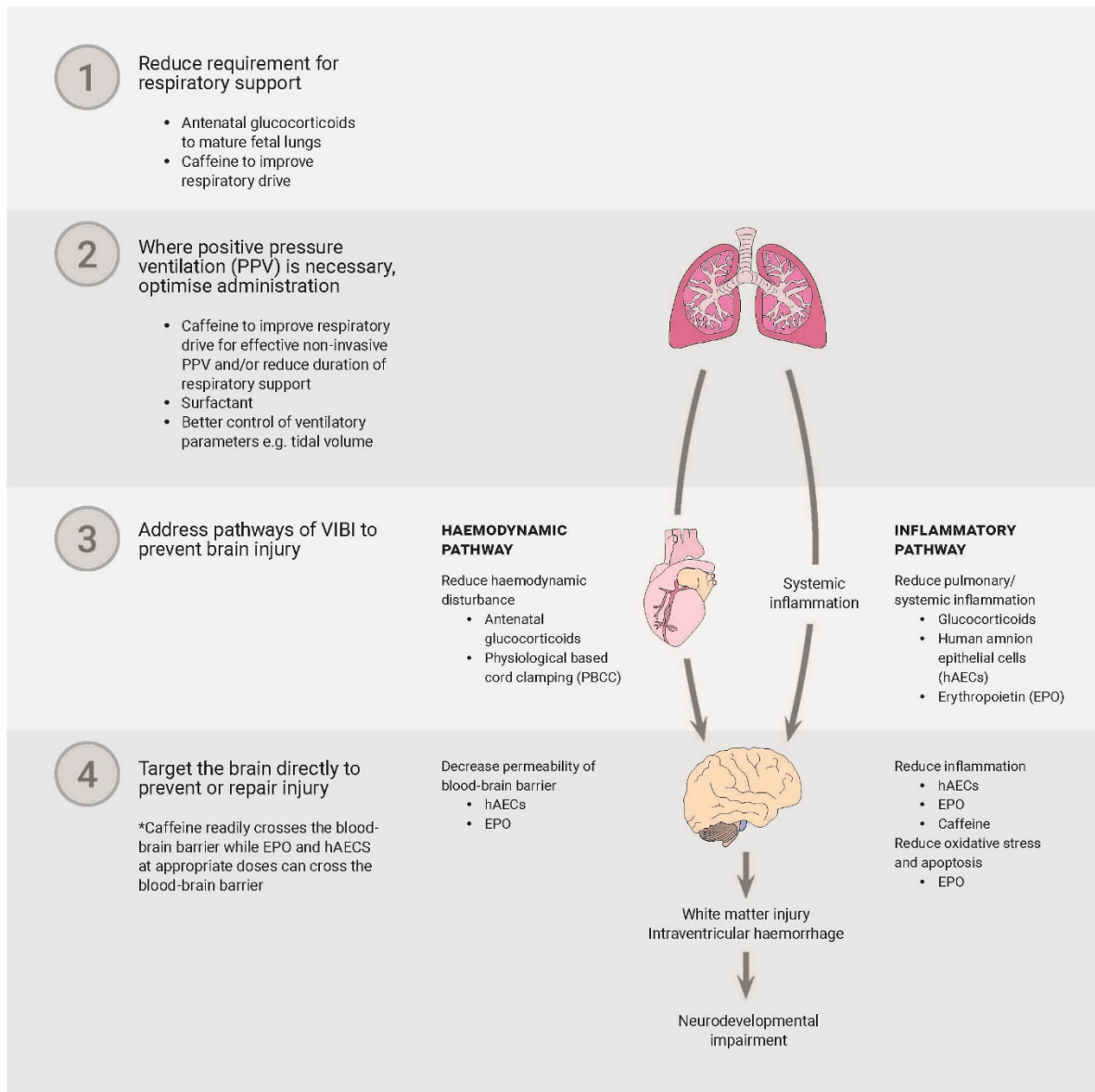


Figure 2. A multipronged approach is likely necessary to prevent or reduce ventilation-induced brain injury. Only strategies discussed in-text have been included in the diagram. *PPV* positive pressure ventilation; *PBCC* physiological-based cord clamping; *hAECs* human amnion epithelial cells; *EPO* erythropoietin.

Appendix II

This appendix relates to Chapter Three: Isolating Pathways of Ventilation-Induced Brain Injury (VIBI) and presents the magnetic resonance imaging results from a subset of those animals [Table A2]. The key finding of this study was that VIBI can be detected by diffusion tensor imaging colour mapping threshold techniques 24 h after injurious ventilation. Additionally, white matter injury detected by this approach was more severe in the animals subjected to both major pathways of injury (INJ+UCO group in paper; INJ_{INF+HAE} group in Chapter 3) compared to animals exposed to the inflammatory pathway only (INJ group in paper; INJ_{INF} group in Chapter 3).

Table A2. Comparison of corresponding experimental groups in Appendix II and Chapter 3.

Synonymous groups in		Group description
Appendix II	Chapter 3	
Cont (n=6)	UNOP (n=7)	Lambs did not undergo initial fetal surgery or ventilation
Sham (n=5)	SHAM (n=5)	Lambs underwent fetal surgery but did not receive ventilation
INJ (n=5)	INJ _{INF} (n=7)	Lambs received 15 min of high tidal volume (V _T) ventilation initiating predominantly the inflammatory pathway of VIBI
INJ+UCO (n=7)	INJ _{INF+HAE} (n=7)	Lambs received 15 min of high V _T ventilation with umbilical cord occluded, initiating the inflammatory and haemodynamic pathways of VIBI

The original article is included below, reproduced under the terms of the Creative Commons Attribution 4.0 International License:

Alahmari DM, **Chan KYY**, Stojanovska V, LaRosa DA, Barton SK, Nitsos I, Zahra VA, Barbuto J, Farrell M, Yamaoka S, Pearson JT, Polglase GR. Diffusion tensor imaging detects ventilation-induced brain injury in preterm lambs. *PLoS One* 2017;**12(12)**: e0188737.

RESEARCH ARTICLE

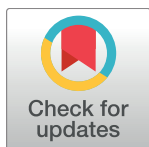
Diffusion tensor imaging detects ventilation-induced brain injury in preterm lambs

Dhafer M. Alahmari^{1,2,3}, Kyra Y. Y. Chan⁴, Vanesa Stojanovska⁴, Domenic LaRosa⁴, Samantha K. Barton⁴, Ilias Nitsos⁴, Valerie Zahra⁴, Jade Barbuto⁴, Michael Farrell^{1,2}, Shigeo Yamaoka⁴, James T. Pearson^{2,5,6}, Graeme R. Polglase⁴*

1 Monash Biomedicine Discovery Institute and Department of Medical Imaging and Radiation Sciences, Monash University, Clayton, VIC, Australia, **2** Monash Biomedical Imaging, Monash University, Clayton, VIC, Australia, **3** Department of Diagnostic Imaging, King Saud Medical City, Riyadh, Saudi Arabia, **4** The Ritchie Centre, Hudson Institute of Medical Research and Department of Obstetrics and Gynaecology, Monash University, Clayton, VIC, Australia, **5** Department of Physiology, Monash University, Clayton, VIC, Australia, **6** Department of Cardiac Physiology, National Cerebral and Cardiovascular Center, Suita, Osaka, Japan

* These authors contributed equally to this work.

* graeme.polglase@monash.edu



OPEN ACCESS

Citation: Alahmari DM, Chan KYY, Stojanovska V, LaRosa D, Barton SK, Nitsos I, et al. (2017) Diffusion tensor imaging detects ventilation-induced brain injury in preterm lambs. PLoS ONE 12(12): e0188737. <https://doi.org/10.1371/journal.pone.0188737>

Editor: Damir Janigro, Cleveland Clinic, UNITED STATES

Received: June 6, 2017

Accepted: November 13, 2017

Published: December 6, 2017

Copyright: © 2017 Alahmari et al. This is an open access article distributed under the terms of the [Creative Commons Attribution License](https://creativecommons.org/licenses/by/4.0/), which permits unrestricted use, distribution, and reproduction in any medium, provided the original author and source are credited.

Data Availability Statement: All relevant data are within the paper and its Supporting Information files.

Funding: This research was supported by the National Institutes of Health (R01HD072848-04), a joint National Heart Foundation of Australia and National Health and Medical Research Council (NH&MRC) Career Development Fellowship (1105526), National Health and Medical Research Council (AU)-Australian Research Council Dementia Research Development Fellowship (SKB);

Abstract

Purpose

Injurious mechanical ventilation causes white matter (WM) injury in preterm infants through inflammatory and haemodynamic pathways. The relative contribution of each of these pathways is not known. We hypothesised that *in vivo* magnetic resonance imaging (MRI) can detect WM brain injury resulting from mechanical ventilation 24 h after preterm delivery. Further we hypothesised that the combination of inflammatory and haemodynamic pathways, induced by umbilical cord occlusion (UCO) increases brain injury at 24 h.

Methods

Fetuses at 124±2 days gestation were exposed, instrumented and either ventilated for 15 min using a high tidal-volume (V_T) injurious strategy with the umbilical cord intact (INJ; inflammatory pathway only), or occluded (INJ+UCO; inflammatory and haemodynamic pathway). The ventilation groups were compared to lambs that underwent surgery but were not ventilated (Sham), and lambs that did not undergo surgery (unoperated control; Cont). Fetuses were placed back *in utero* after the 15 min intervention and ewes recovered. Twenty-four hours later, lambs were delivered, placed on a protective ventilation strategy, and underwent MRI of the brain using structural, diffusion tensor imaging (DTI) and magnetic resonance spectroscopy (MRS) techniques.

Results

Absolute MRS concentrations of creatine and choline were significantly decreased in INJ+UCO compared to Cont lambs ($P = 0.03$, $P = 0.009$, respectively); no significant differences were detected between the INJ or Sham groups and the Cont group. Axial diffusivities in the internal capsule and frontal WM were lower in INJ and INJ+UCO compared to Cont lambs ($P = 0.05$, $P = 0.04$, respectively). Lambs in the INJ and INJ+UCO groups had lower

1110040) and Victorian Government's Operational Infrastructure Support Program. The funders had no role in study design, data collection and analysis, decision to publish, or preparation of the manuscript.

Competing interests: The authors have declared that no competing interests exist.

mean diffusivities in the frontal WM compared to Cont group ($P = 0.04$). DTI colour mapping revealed lower diffusivity in specific WM regions in the Sham, INJ, and INJ+UCO groups compared to the Cont group, but the differences did not reach significance. INJ+UCO lambs more likely to exhibit lower WM diffusivity than INJ lambs.

Conclusions

Twenty-four hours after injurious ventilation, DTI and MRS showed increased brain injury in the injuriously ventilated lambs compared to controls. DTI colour mapping threshold approach provides evidence that the haemodynamic and inflammatory pathways have additive effects on the progression of brain injury compared to the inflammatory pathway alone.

Introduction

Brain injury is a worldwide problem in preterm infants and is associated with a high risk of morbidity and mortality [1]. Children born very preterm have higher rates of cerebral palsy, educational disabilities and respiratory illnesses [2–4]. These lifelong morbidities cause substantial economic costs for individuals and countries [4,5]. Of 70% of surviving preterm infants, 58% have severe overall disability or mild disability with neuromotor abnormalities [6]. Despite significant improvements to neonatal care resulting in increased preterm survival, efforts to reduce or prevent neonatal morbidity and subsequent physical and neurodevelopmental disabilities have had little success so far.

The perinatal period is a critical time for heightened risk of preterm brain injury [7]. The transition from fetus to independent life in preterm infants is complicated by the immaturity of respiratory and cardiovascular systems, which can make the brain vulnerable to injury [8]. The requirement for respiratory support in the delivery room, which is extremely common in these infants [9], has been identified as a potential cause of preterm brain injury; termed ventilation-induced brain injury (VIBI) [10]. The risk of VIBI is amplified in infants who receive high tidal volumes (V_T) in the delivery room, which occurs in up to 80% of infants in the delivery room receiving positive pressure ventilation [11]. Our studies have demonstrated that as little as 15 min of high V_T ventilation can increase early markers of brain injury through two key pathways: 1) initiation of a systemic inflammatory cascade resulting in cerebral inflammation and injury; and 2) haemodynamic instability resulting in fluctuations in cerebral blood flow and pressure [10,12]. Early markers of brain injury can be detected within 1–2 h after birth using histological techniques [12] as well as advanced magnetic resonance imaging (MRI) [13,14]. However, it is unlikely that infants can undergo MRI so soon after birth. It is not known whether the pathology observed within two hours of delivery manifests into gross brain injury 24 h later. Further, the relative contribution of the inflammatory or haemodynamic pathways of VIBI is not known.

To investigate how VIBI evolves over time we aimed to examine whether 15 min of high V_T ventilation results in significant microstructural brain injury 24 h later. Since VIBI occurs through two major pathways [12], we also aimed to determine the relative contribution of each pathway to brain injury. We hypothesised that structural brain injury evolves and is detectable by non-invasive MRI techniques on clinical 3T scanners at 24 h after high V_T ventilation induced to the fetal *in utero*. Further, we hypothesised that activation of the haemodynamic and inflammatory pathways would result in levels of WM injury that exceed levels of damage associated with the inflammatory pathway alone.

Methods

Ethics statement

The experimental protocol was approved by the Monash Medical Centre 'A' animal ethics committee at Monash University and conducted according to guidelines established by the National Health and Medical Research Council of Australia.

Ventilation strategy, preterm delivery and stabilisation

Under sterile conditions, pregnant ewes at 124 ± 2 days of gestation (term ~ 148 days) were anaesthetised via intravenous injection of thiopentone sodium (20 mg/kg; Jurox, NSW, Australia), followed by tracheal intubation and delivery of inhalational anesthesia (isoflurane 1.5–2.5% in oxygenated air; Bomac Animal Health, NSW, Australia). Fetuses were exposed via laparotomy, and were instrumented for the placement of catheters into the left jugular vein and carotid artery as described previously [10,12]. The fetal chest was exteriorised and the fetus dried, intubated (4.0 mm cuffed endotracheal tube), lung liquid drained and randomised to one of three groups:

1. INJ: Lambs ($n = 5$) received 15 min of high V_T ventilation (targeting 12–15 mL/kg) initiating predominately the inflammatory pathway of VIBI.
2. INJ+UCO: Lambs ($n = 7$) received 15 min of high V_T ventilation (targeting 12–15 mL/kg) during which the umbilical cord was occluded. The removal of the placental circulation simulates umbilical cord clamping and triggers the cardiovascular transition at birth and its associated instability [15] resulting in initiation of the inflammatory and haemodynamic pathways of VIBI. At the end of the 15 minutes of injurious ventilation the occluder was removed and placental blood flow restored to the fetus.
3. Sham: The sham surgery group ($n = 5$) underwent catheterisation and intubation but did not receive mechanical ventilation.

A fourth group of lambs did not undergo the initial surgery or ventilation and were used as un-operated group (Cont; $n = 6$) to control for the surgical intervention.

Ventilation was conducted using a neonatal positive pressure ventilator (Babylog 8000+, Dräger, Lübeck, Germany) using heated, humidified air (Fisher and Paykel). Peak inflation pressure (PIP) was limited to 45 cmH₂O with a positive end expiratory pressure (PEEP) of 5 cmH₂O [15]. Ventilated lambs received a V_T of 7 mL/kg at 5 min, escalated to 10 mL/kg at 10 min and targeting 12–15 mL/kg (the PIP was limited to 45 cmH₂O) by 15 min. Fetal blood-gas variables and oxygenation were monitored and maintained within normal newborn parameters. The ventilation was conducted under sterile conditions to prevent infection of the fetus.

After ventilation, the fetus was returned to the uterus and it was sutured closed. The jugular vein and carotid artery catheters were externalised through the ewe's flank via a small incision [16] to allow periodic blood sampling. The abdominal and flank incisions were sutured closed and the ewe allowed to recover. Analgesia was provided to the ewe via buprenorphine (300ug/ml i.v., Reckitt Benckiser, UK) and a fentanyl patch (75 mg/h, Janssen-Cilag, NSW, Australia). At regular intervals over the proceeding 24 h, fetal arterial blood samples were collected to ensure fetal health by assessing the partial pressure of arterial carbon dioxide (PaCO₂), oxygen (PaO₂), oxygen saturation (SaO₂), and pH (ABL30, Radiometer, Copenhagen, Denmark).

Twenty-four hours later, ewes were again anaesthetised as above, the fetus exteriorised via the same incision site, intubated, and ventilation initiated using volume guarantee set at 7 mL/kg and PEEP of 5 cmH₂O. Lambs were ventilated for 3 minutes before the umbilical cord was

clamped and surfactant (100 mg/kg, Curosurf^R, Chiesi Pharma, Italy) was administered within the first 15 min of ventilation. The fraction of inspired oxygen was adjusted to maintain arterial oxygen saturation between 88–95%. The umbilical cord was cut 15 min after ventilation onset and the lambs transferred to the MRI. Ewes were euthanised immediately after the lamb was removed; lambs were euthanised after the MRI (sodium pentobarbitone 100 mg/kg i.v.).

Magnetic resonance imaging

MRI acquisition protocols were conducted as per previously published [13,14]. Following stabilisation, lambs were transferred to the 3T MRI system (Siemens Skyra, Erlangen, Germany) at Monash Biomedical Imaging (Clayton, Australia), with a 15-channel radio frequency coil for transmission and reception. Lambs were placed in supine position, and ventilation was maintained using a BabyPAC portable and MR-compatible ventilator (Pneupac, Smiths Medical, UK). Brain MRI included structural imaging sequences (T1, T2), susceptibility-weighted imaging (SWI), DTI, and single-voxel MRS [13,14]. The total acquisition time was about 40 min.

We acquired images for anatomical localisation and identification of gross brain injury, including infarcts and haemorrhages. Whole-brain DTI was acquired using a single-shot, echo-planar imaging sequence with the following image parameters: repetition time (TR) = 11,400 ms; echo time (TE) = 99 ms; slice thickness = 1.2 mm; field of view = 154×154 mm; acquisition matrix = 128×128, giving a voxel size of 1.2×1.2×1.2 mm³, for five $b = 0$. Diffusion-encoding gradients were acquired in 30 directions with a b value of 1,000 s/mm². The diffusion-weighted imaging was performed twice; five $b = 0$ volumes were acquired. A single-voxel spin-echo sequence was used to acquire MRS, localised on the supratentorial deep grey matter and central WM (TR = 2,000 ms, TE = 270 ms) with a voxel size of 15×15×20 mm³.

MRI data analysis

All data were analysed using the FMRIB Software Library (FSL, FMRIB, Oxford, UK [17]). First, the FDT toolbox was used to correct all DTI data for eddy-current distortion, and then DTI parametric maps of fractional anisotropy (FA), axial diffusivity (AD), radial diffusivity (RD), and mean diffusivity (MD) were created with the FMRIB Diffusion Toolbox. All maps were co-registered with high-resolution T2 images of the brains using the Linear Image Registration Tool (FLIRT [18]), with the $b = 0$ image used as a reference [14].

ROIs were defined manually on the high-resolution T2 images of each lamb and then transformed to the corresponding FA, AD, MD, and RD maps to calculate the mean regional values for each lamb [13,14]. ROIs were placed in the thalamus (Th), periventricular white matter (PVWM), IC, frontal white matter (FWM), and cerebellum (CB) vermis, targeting the stalk and midline WM (S1 Fig). The mean value of the adjacent 4–5 slices that defined a given ROI volume was calculated for each ROI to test between-animal diffusivity variability. MATLAB R2013a (Mathworks, MA, USA) was then used to calculate the standard deviation (SD) for the ROIs of each region of the lamb brains to test within-animal variability (heterogeneity in DTI).

MRS data were processed with TARQUIN software to implement spectral fitting in the time domain [13,14]. Peak-area ratios for lactate (Lac) relative to NAA (total N-acetylaspartate and N-acetylaspartylglutamate), creatine (Cr, total phosphocreatine and free creatine), and choline (Cho, total glycerophosphocholine and phosphocholine) were calculated, along with major peak areas (Cr, NAA, Lac, and Cho).

DTI-ROI data showed more heterogeneity in the specified white matter regions of the lamb brains. To further examine this we utilised a colour-map threshold technique to determine

where the low-diffusivity voxels were distributed in the DTI volumes, as previously described [14]. The total pixel intensity distribution for each brain was compared between the minimum and maximum intensities for 256 bins in all DTI images (S2 Fig) to produce the frequency distribution of MRI voxel intensity levels at each position [14]. Here, we applied a threshold to the mapped intensities in the overlay in all groups (width, 10%); the upper threshold (S2 Fig, green dashed line) was manually set at an intensity where voxels were almost completely absent across the brain in Cont lambs, but coloured voxels were still evident at the edges of the brain mask. The upper threshold was consistent with the 90th percentile of intensities in the Cont lambs, with 3–5% overlap in observed pixel intensities among the groups (S2 Fig). This process permitted mapping and quantification of low-diffusivity voxels for AD, RD, and MD colour-map images.

Statistical analyses

Physiological data were compared using a two-way repeated measure ANOVA and Holm-Sidak post-hoc analyses to determine significant interactions (Sigmaplot, Systat Software Inc). The mean and SEM of ROI voxel intensities were calculated, as well as one-way ANOVA was used to compare treatment groups with a significance level of $P < 0.05$. Data are presented as means (box 5–95% CIs of mean) with maximum–minimum error bars. The SD was calculated for the ROIs in each brain to test within-animal variability and the heterogeneity of DTI diffusivities for differences between groups.

Results

Physiological parameters

Fetal blood gases parameters at the time of intubation and cord clamping, body weight and sex were not different between groups (Table 1). Blood gases and haemodynamic data were recorded throughout the MRI examination. In brief, at 10 and 15 minutes after delivery INJ +UCO lambs required a higher fraction of inspired oxygen (FiO_2) compared to the Cont group ($P = 0.02$ and $P = 0.007$, respectively; Fig 1A). However, pH, PaO_2 and PaCO_2 were not different between groups ($P = 0.8$, $P = 0.1$ and $P = 0.2$, respectively; Fig 1B–1D). Peak inflation pressure and positive end-expiratory pressure were not different between groups ($P = 0.09$ and $P = 0.2$, respectively). Alveolar-arterial differences in oxygen (AaDO_2) were not different between groups at any time point ($P = 0.1$).

Table 1. Fetal characteristics at the time of intervention at 124 days of gestation.

Variable	Cont	Sham	INJ	INJ+UCO	P value
Sex (M/F)	5 / 1	3 / 2	4 / 1	1 / 6	-
Gestational age (d)	126 ± 1	126 ± 1	126 ± 1	126 ± 1	0.2
Body weight (kg)	3.4 ± 0.4	3.3 ± 0.2	3.6 ± 0.3	3.2 ± 0.4	0.3
SaO_2 (%)	48.2 ± 23.1	33.9 ± 19.2	42.8 ± 10.2	34.9 ± 16.5	0.5
pH	7.27 ± 0.04	7.31 ± 0.17	7.37 ± 0.05	7.35 ± 0.10	0.4
PaCO_2 (mm Hg)	59.0 ± 7.8	53.5 ± 20.9	49.5 ± 5.6	52.3 ± 8.2	0.3
PaO_2 (mm Hg)	36.7 ± 17.7	24.0 ± 8.1	27.0 ± 4.3	28.3 ± 8.8	0.3

Characteristics of the Cont, Sham, INJ and INJ+UCO lambs groups in this study and their fetal blood gases at the time of intubation and cord clamping. Data are presented as mean ± SD.

<https://doi.org/10.1371/journal.pone.0188737.t001>

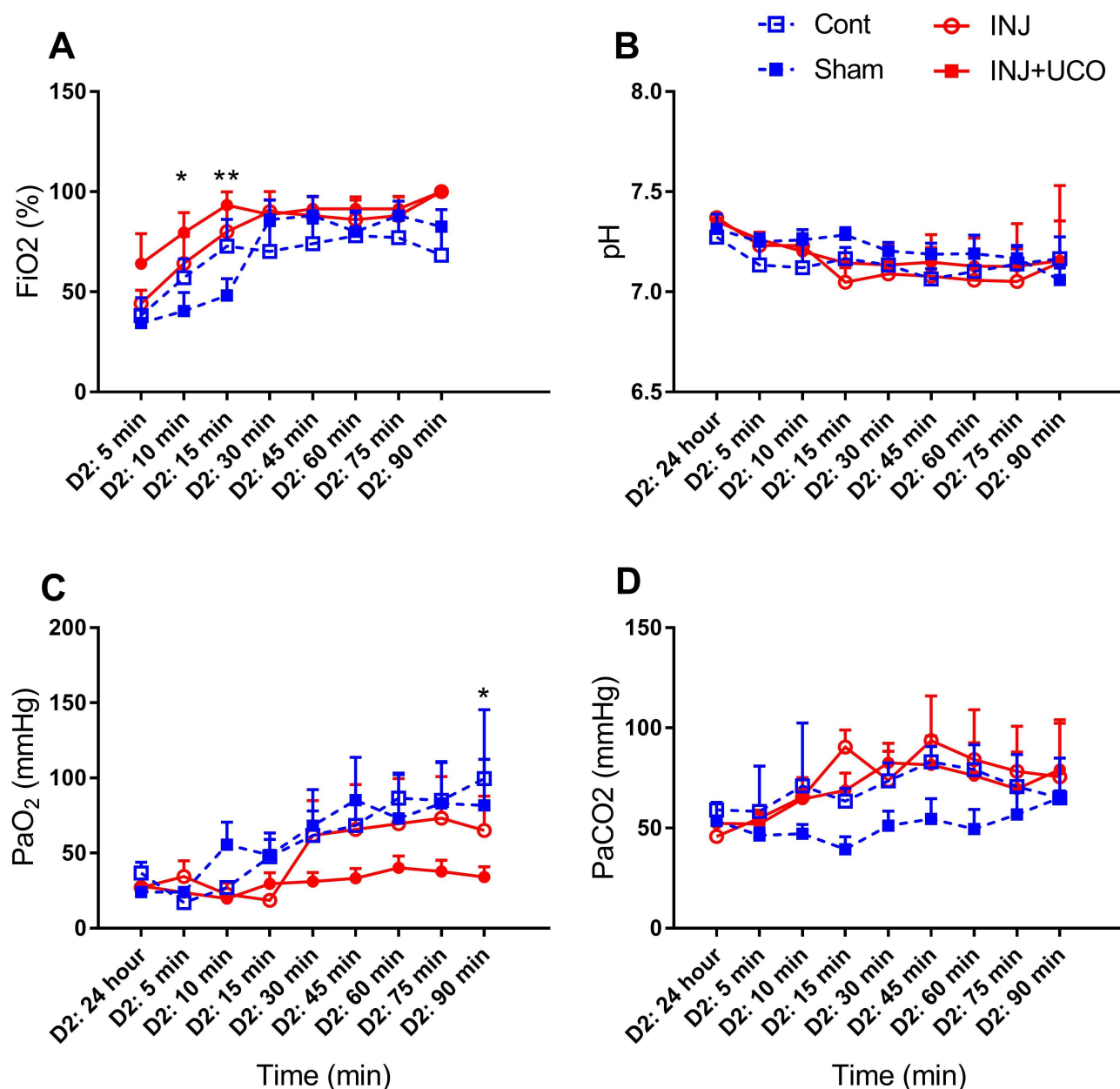


Fig 1. Physiological parameters. (A) Fraction of inspired oxygen (FiO₂) in the unoperated control (Cont; blue open squares n = 6), sham surgery (Sham; blue closed squares n = 5), injurious ventilation (INJ; red open circles n = 5), and INJ + umbilical cord occlusion (INJ+UCO; red closed circles n = 7) groups. (B) pH. (C) Partial pressure of arterial oxygen (PaO₂) and (D) carbon dioxide (PaCO₂). * $P < 0.01$, ** $P < 0.001$ vs INJ+UCO.

<https://doi.org/10.1371/journal.pone.0188737.g001>

Structural MRI

There was no overt structural injury evident on T1, T2, or SWI images in any group. However, MRS and DTI showed subtle brain injury, as detailed below.

Magnetic resonance spectroscopy

The MRS peak-area ratios of Lac to other metabolites, Cr, NAA, and Cho at 24 h were not different between groups (S3 Fig). However, absolute concentrations of Cr and Cho were

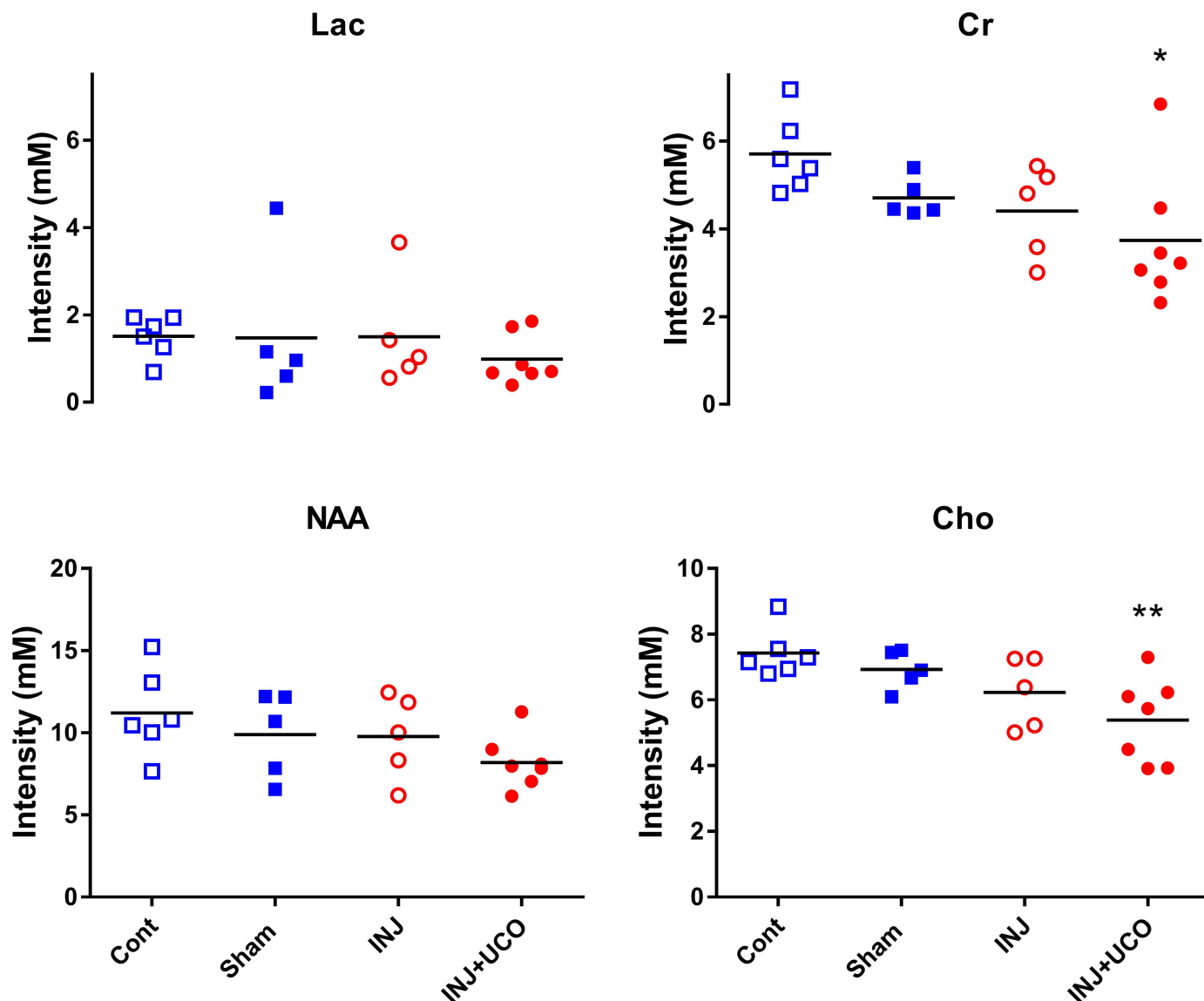


Fig 2. Absolute magnetic resonance spectroscopy (MRS) concentrations of metabolites in the preterm lamb brain. Individual absolute concentrations of lactate (Lac), creatine (Cr), choline (Cho), and N-acetylaspartate (NAA) using a single-voxel MRS encompassing supratentorial central white matter and deep grey matter in the unoperated control (Cont; blue open squares $n = 6$), sham surgery (Sham; blue closed squares $n = 5$), injurious ventilation (INJ; red open circles $n = 5$), and INJ + umbilical cord occlusion (INJ+UCO; red closed circles $n = 7$) groups. One way ANOVA comparisons tests relative to the Cont group were used with $P < 0.05$ was considered statistically significant. * $P < 0.01$, ** $P < 0.001$ vs INJ+UCO.

<https://doi.org/10.1371/journal.pone.0188737.g002>

significantly lower in the INJ+UCO group than the Cont group ($P = 0.03$, $P = 0.009$, respectively); no other differences were detected between the groups. Absolute concentrations of Lac and NAA at 24 h were not different between groups (Fig 2).

Region of interest analysis for diffusion tensor imaging

DTI-ROI analysis for each area conducted in six Cont, five Sham, five INJ, and seven INJ+UCO lambs. AD was significantly decreased in the IC and FWM in INJ and INJ+UCO compared to Cont lambs ($P = 0.05$, $P = 0.04$, respectively), as shown in Fig 3. A trend was evident for lower RD in the FWM of INJ and INJ+UCO lambs compared to Cont lambs ($P = 0.07$).

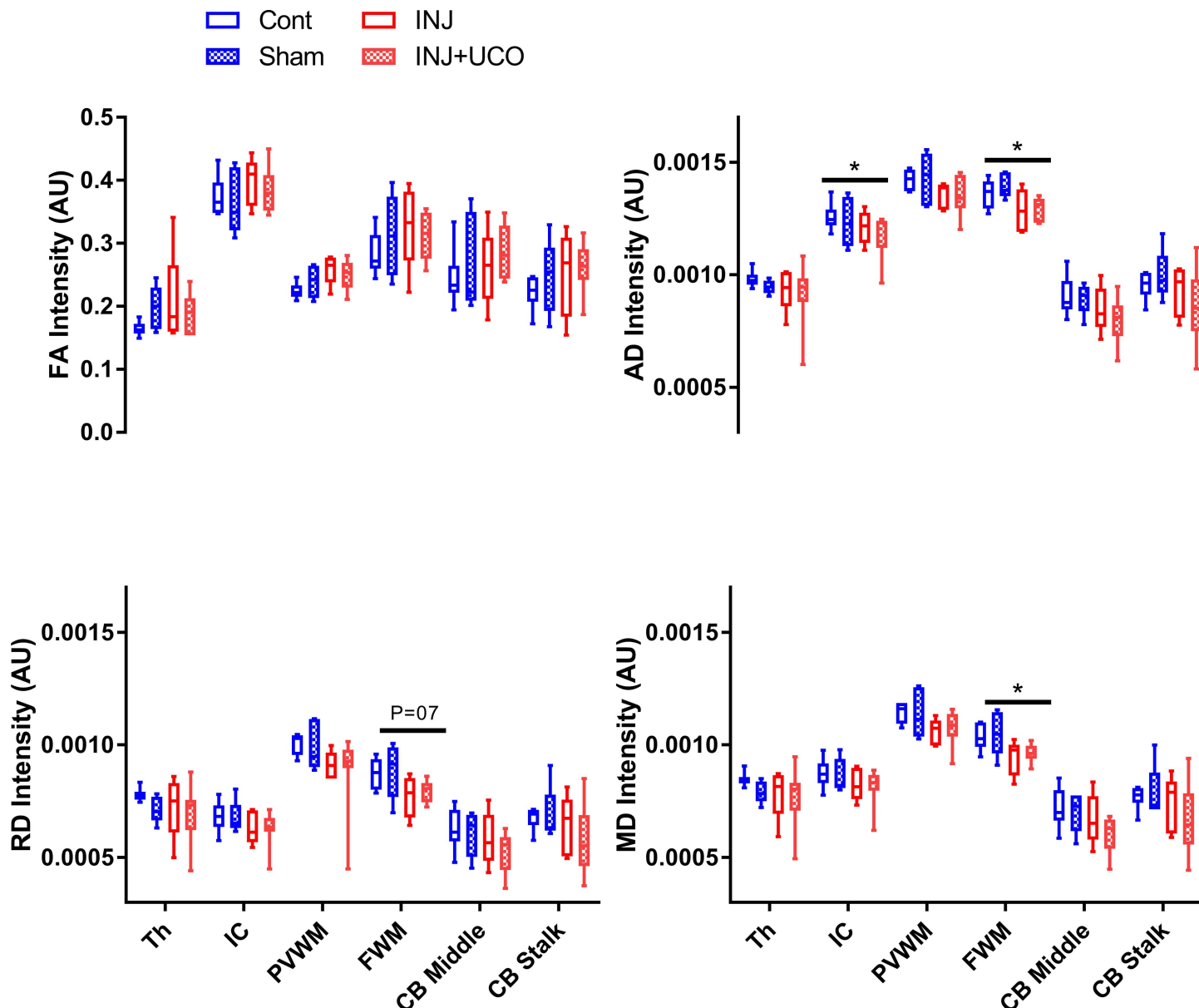


Fig 3. Mean and confidence intervals of DTI measurements for the small regions of interest analyses. Mean fractional anisotropy (FA), axial diffusivity (AD), radial diffusivity (RD), and mean diffusivity (MD) measurements for each region of interest (ROI) in the unoperated control (Cont $n = 6$), sham surgery (Sham $n = 5$), injurious ventilation (INJ $n = 5$), and INJ + umbilical cord occlusion (INJ+UCO $n = 7$) groups. The ROIs shown in S1 Fig were located in the thalamus (Th), internal capsule (IC), periventricular white matter (PVWM), frontal white matter (FWM), middle cerebellum (CB), and CB stalk. * $P < 0.01$, ** $P < 0.001$ vs INJ+UCO.

<https://doi.org/10.1371/journal.pone.0188737.g003>

MD significantly decreased in the FWM of the INJ and INJ+UCO compared to the Cont group ($P = 0.04$), while mean AD, RD, and MD indices were lower in some INJ and INJ+UCO lambs compared to the Cont group (Fig 3). There were no mean differences in the Th, PVWM, middle CB, or CB stalk between groups. However, INJ+UCO, INJ, and Sham lambs showed significantly increased heterogeneity of diffusivity in the PVWM and CB stalk regions (S4 Fig).

Table 2. Percentage of lambs found to have AD, RD, and MD in the selected WM regions of each group below the colour map threshold intensity 90% confidence interval of the Cont group.

	Cont <i>n</i> = 6			Sham <i>n</i> = 5			INJ <i>n</i> = 5			INJ+UCO <i>n</i> = 7		
	AD	RD	MD	AD	RD	MD	AD	RD	MD	AD	RD	MD
Th	0	0	0	20	80	60	20	80	60	43	86	86
IC	0	0	0	0	80	80	20	60	60	29	86	86
PVWM	0	0	0	0	20	0	20	80	40	14.3	86	43
FWM	0	0	0	0	20	20	40	80	60	43	86	71.4
CB	16.6	16.6	16.6	40	40	40	80	80	60	86	86	43

Thalamus (Th), internal capsule (IC), white matter (WM), periventricular WM (PVWM), frontal WM (FWM), and cerebellum (CB) vermis. DTI parameters: axial diffusivity (AD), radial diffusivity (RD), and mean diffusivity (MD). The DTI colour-mapping technique revealed the number of lambs found to have lower diffusivities from the total number (*n*) in each group. Therefore, there were different degrees of red colour (threshold range) between the lamb groups. Data are given as percentage of each group.

<https://doi.org/10.1371/journal.pone.0188737.t002>

Whole brain intensity analysis

Whole-brain intensity distribution analysis was employed to describe the tensor orientation in the WM tract direction. This technique revealed lower AD, RD, and MD values that were closely occurred with the specific WM regions in this study (Table 2).

AD, RD, and MD histogram distributions for the whole brains of individual lambs are plotted in S2 Fig. In the low-diffusivity maps, there were different degrees of red colour (threshold range) within each specific brain region. We observed that the red shading was more visible in the Th of AD, RD and MD maps (Figs 4–6) in the INJ+UCO and INJ lambs, while the lowest diffusivity values were almost absent in the same region in the Cont group. Further, lower diffusivity values were more widespread in the surrounding areas of the Th of the INJ+UCO group than the INJ group and Sham group (Figs 4–6). Likewise, DTI diffusivities were reduced in the IC, PVWM, FWM and CB of some INJ+UCO and INJ lambs, but rarely in the Cont group (Table 2). Finally, quantifying the low-diffusivity voxels in each ROI, we compared voxel counts between all groups (Fig 7). We found evidence of reduced diffusivity in all WM regions in the INJ+UCO and INJ groups compared with Cont lambs. Interestingly, more lambs in the INJ+UCO group had some evidence of reduced AD, RD and MD values compared to the lambs INJ lambs (Fig 7), but this did not reach statistical significance.

Discussion

Brain injury remains a significant burden for preterm infants, resulting in chronic neurological pathology including cerebral palsy [19], disrupted brain microstructures, and chronic myelination disturbances [20]. We demonstrated previously that injurious ventilation of preterm neonates upon delivery causes cerebral inflammation and haemodynamic instability [12], resulting in early markers of WM injury, detectable within the first 1–2 h after delivery with clinical 3T MRI [13,14]. While the previous study demonstrated early mechanisms of brain injury so soon after birth, it is not known whether these early markers of ventilation induced brain injury manifest as gross injury 24 h later. This is important given that the earliest clinical MRIs are likely to be achieved is at this 24h time-point. Since VIBI occurs through two major pathways, we also aimed to determine the relative contribution of each pathway to brain injury. We found no differences in indices of brain injury between the groups using conventional MRI techniques, including T1 and SWI. However, DTI-ROI analysis provides evidence that both the INJ and INJ+UCO groups had increased injury compared to controls. Further,

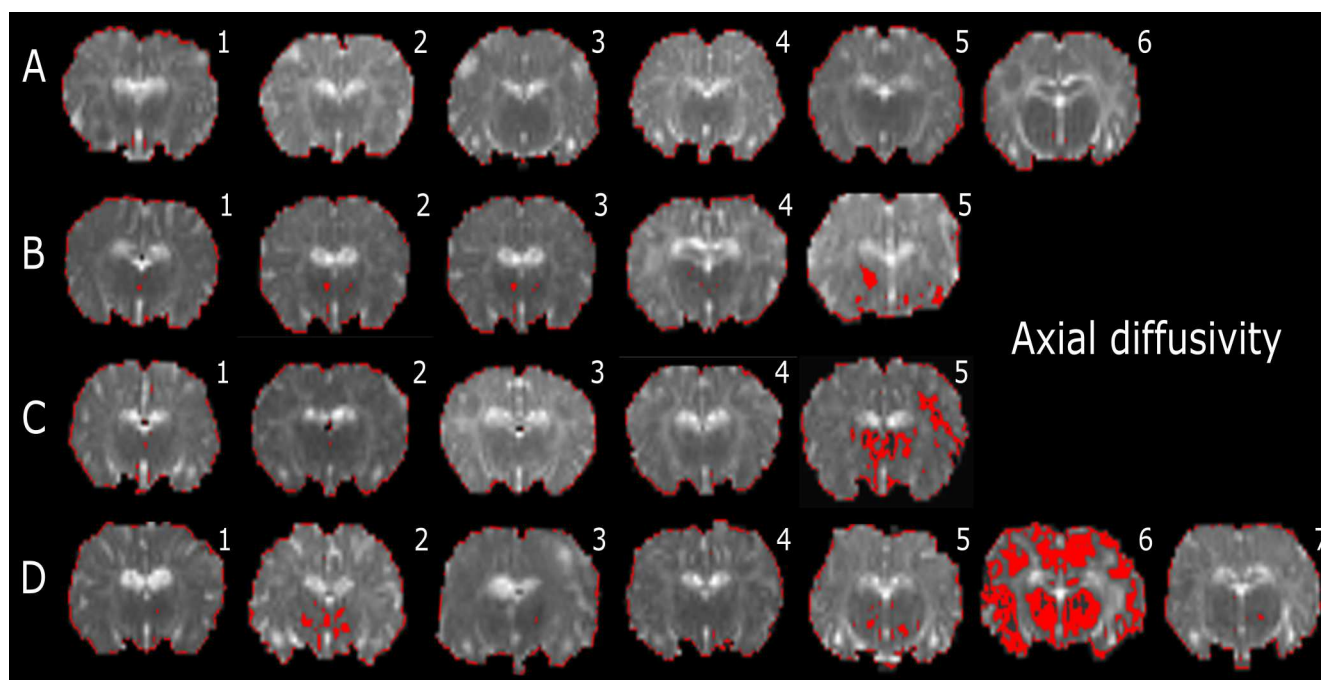


Fig 4. Representative slices of whole-brain DTI colour maps of the thalamus (Th) for axial diffusivity (AD). Voxel diffusivity intensities falling below the low threshold are shown as red for AD measurements for all lamb brains. All low-diffusion maps are overlaid on diffusion images for a slice passing through the thalamus (Th). In the injurious ventilation (INJ $n = 5$; C) and umbilical cord occlusion (INJ+UCO $n = 7$; D) groups, red indicates lower values in the range of the threshold, while black indicates values below the threshold (see explanation in S2 Fig). One sham surgery (Sham $n = 5$; B), one INJ, and three INJ+UCO lambs had widespread lower diffusivity values in the Th than unoperated control lambs (Cont $n = 6$; A).

<https://doi.org/10.1371/journal.pone.0188737.g004>

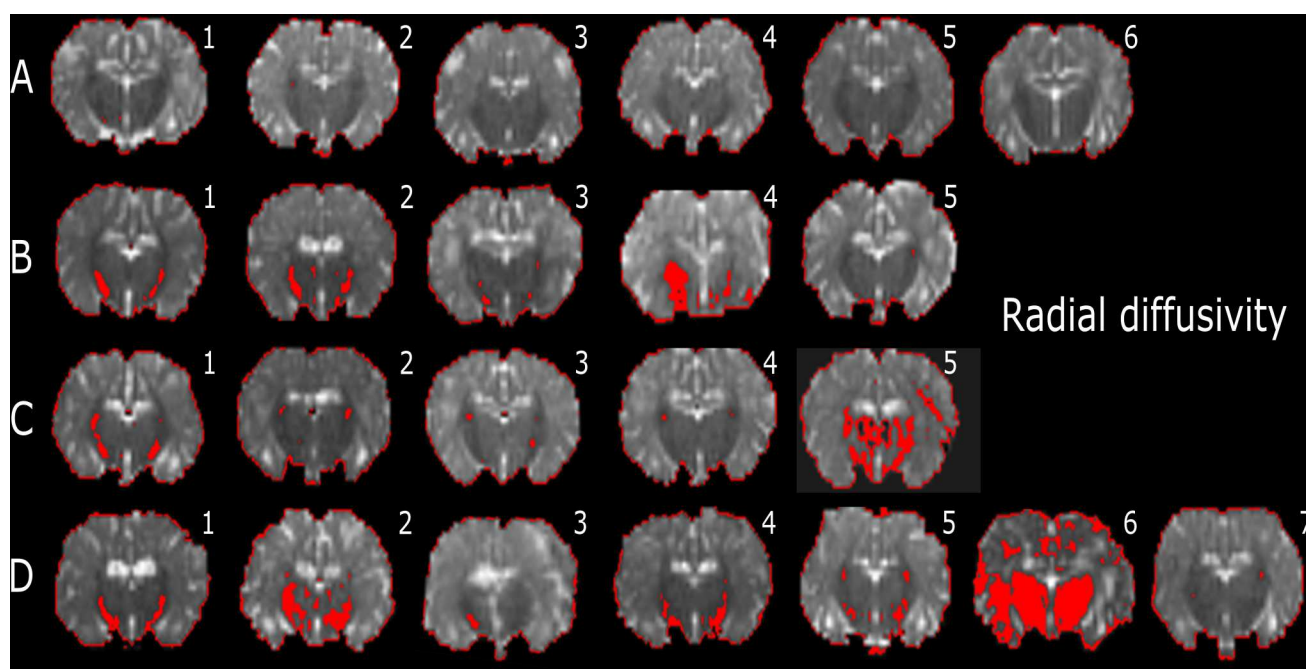


Fig 5. Representative slices of whole-brain DTI colour maps of the thalamus (Th) for radial diffusivity (RD). Voxel diffusivity intensities falling below the low threshold are shown in red for RD measurements for all lamb brains. All low-diffusion maps are overlaid on diffusion images for a slice passing through the Th. All lambs in the unoperated control (Cont $n = 6$; A) group had no low RD values in the Th, but low RD values appeared in the Th of 4 lambs following sham surgery (Sham $n = 5$; B), 4 lambs following injurious ventilation (INJ $n = 5$; C), and 6 lambs following umbilical cord occlusion (INJ+UCO $n = 7$; D).

<https://doi.org/10.1371/journal.pone.0188737.g005>

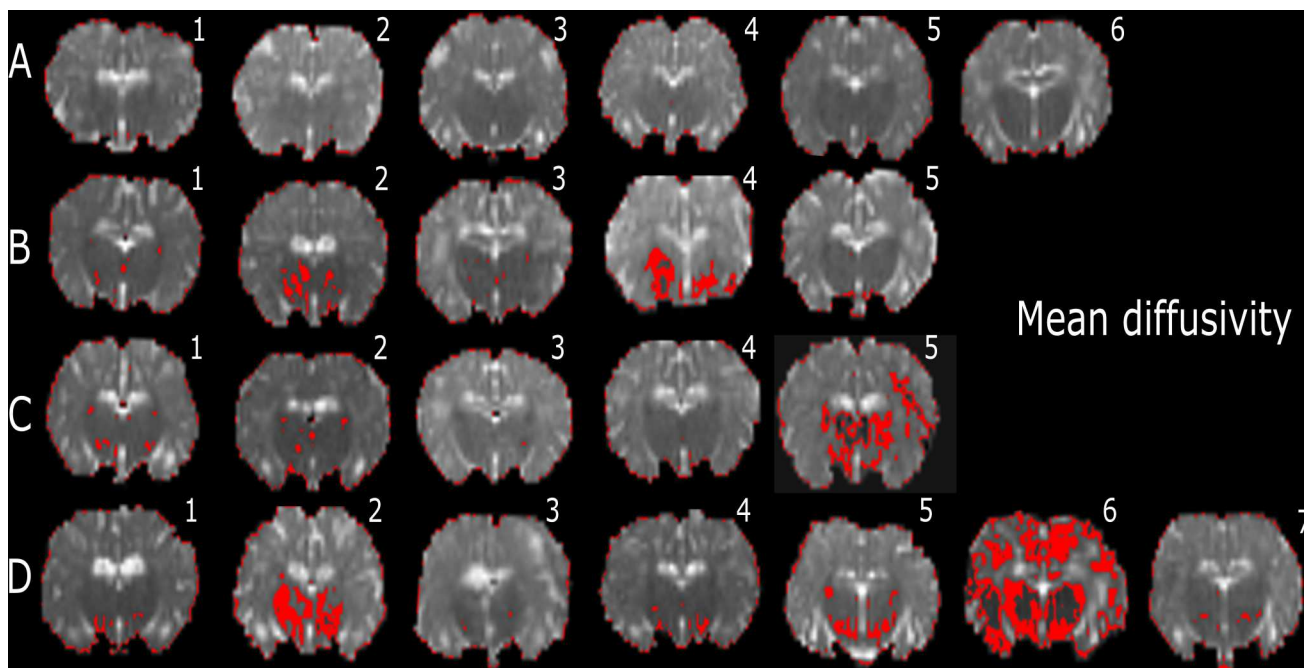


Fig 6. Representative slices of whole-brain DTI colour maps of the thalamus (Th) for mean diffusivity (MD). Voxel diffusivity intensities falling below the low threshold are shown in red for MD measurements for all lamb brains. All low-diffusion maps are overlaid on diffusion images for a slice passing through the Th. All lambs in the unoperated control (Cont $n = 6$; A) group had no low MD values in the Th, but low MD values appeared in the Th of about lambs following sham surgery (Sham $n = 5$; B), lambs following injurious ventilation (INJ $n = 5$; C), and lambs following umbilical cord occlusion (INJ+UCO $n = 7$; D).

<https://doi.org/10.1371/journal.pone.0188737.g006>

the analysis of the whole brain using colour mapping threshold approach revealed evidence of worse pathology in the INJ+UCO lambs compared to INJ alone.

The initiation of ventilation using an injurious strategy results in acute brain inflammation and injury through two major pathways: an inflammatory cascade and haemodynamic instability. In order to isolate the relative contribution of the two pathways, we initiated ventilation in preterm lambs with or without an intact umbilical cord. Ventilating whilst maintaining placental blood supply prevents rapid swings in pulmonary and carotid blood pressures and flows and stabilizes cardiac output upon transition at birth [15]. The resulting injury from this ventilation strategy can be attributed to the inflammatory pathway only. Occluding the cord simulates immediate cord clamping at ventilation onset [15], which initiates both the inflammatory and haemodynamic pathways of brain injury. Any additional injury above that of the INJ group can therefore be attributed to the haemodynamic pathway.

DTI can provide microstructural information about the integrity of axons and myelin in the preterm infant brain; along the fiber tract (i.e., AD), decreased water diffusion indicates axonal degeneration, while perpendicular to the fiber tract (i.e., RD), decreased water diffusion indicates myelin loss [21]. Similar to Bassi et al. [22], who previously observed FWM lesions in preterm infants scanned in the neonatal period, we found DTI-ROI were able to detect decreased AD, RD and MD in the FWM due to injurious ventilation, with and without cord occlusion. Further, we found evidence of decreased AD in the IC in the INJ and INJ+UCO groups, which may indicate axonal loss [23] and may be associated with motor dysfunction later in development [24]. Further, subsequent studies have confirmed that decreased AD was observed with dysmyelination and demyelination [25,26]. We did not observe any significant changes in the thalamus, PVWM or CB in any lambs groups.

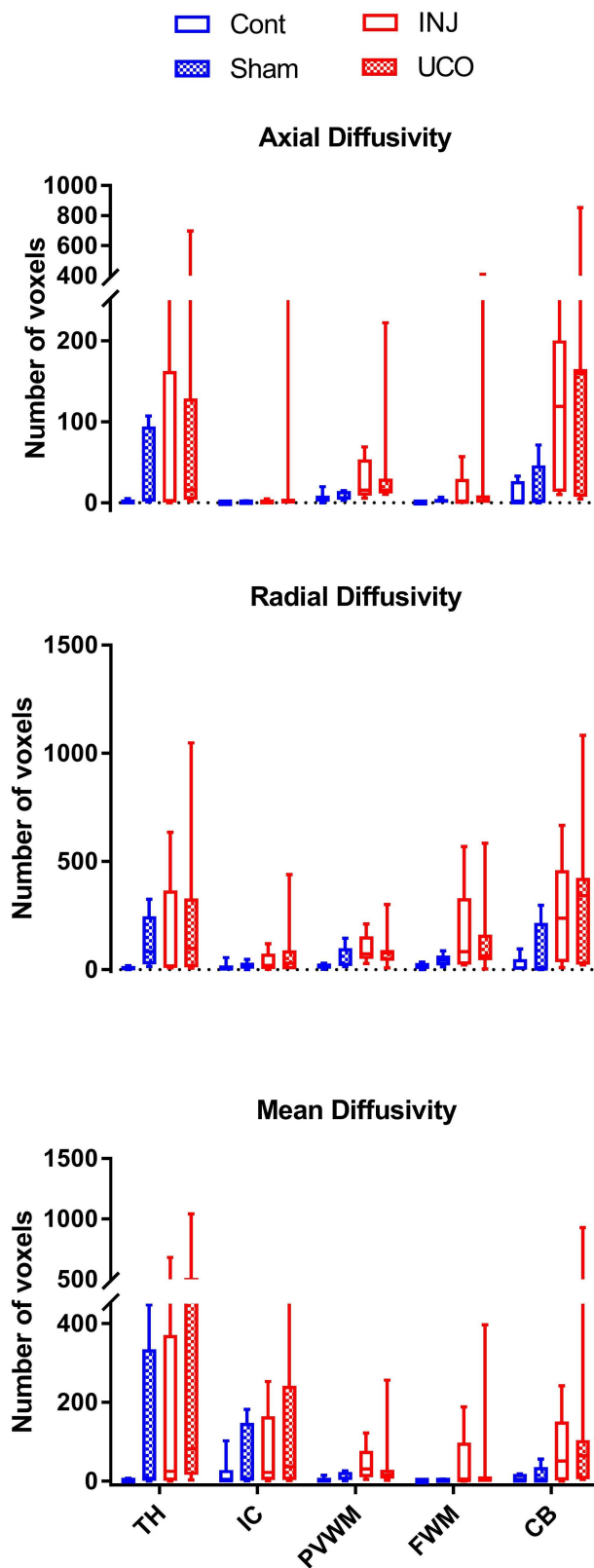


Fig 7. Comparison of voxel-based colour-map images for the whole brain. Images were compared for axial diffusivity (AD), radial diffusivity (RD), and mean diffusivity (MD) values below the threshold for specified regions in the lamb brain in all groups. The white matter (WM) regions were located in the thalamus (Th),

internal capsule (IC), periventricular WM (PVWM), frontal WM (FWM), and cerebellum (CB) vermis. There were widespread lower AD, RD, and MD intensities in all WM regions in the umbilical cord occlusion (INJ+UCO $n = 7$; red closed circles) and injurious ventilation (INJ $n = 5$; red open circles) groups, but this did not reach statistical significance. While there were few lower diffusivities in WM regions in the sham surgery (Sham $n = 5$; blue closed squares) group the unoperated control (Cont $n = 6$; blue open squares) lambs showed very few voxels of low AD, RD, and MD intensities.

<https://doi.org/10.1371/journal.pone.0188737.g007>

In contrast to the DTI-based ROI approach, whole-brain analysis is more sensitive to detect subtle brain injury, particularly axonal and myelin injury [27]. In this study, INJ+UCO lambs had the lowest AD, RD, and MD values in the WM regions compared to the other groups (Table 2). This suggests that activation of the inflammatory and haemodynamic pathways of injury had an additive effect on WM injury [28,29]. Importantly, it also suggests that improving the haemodynamic transition at birth (delayed cord occlusion) only reduces a portion of VIBI, if ventilation is delivered in an injurious fashion [12]. Therefore, simply improving the haemodynamic transition at birth is not enough to reduce VIBI—future therapies need to target the inflammatory cascade resultant from ventilation.

In-vivo MRS provides non-invasive metabolic information about the newborn's brain [30]. Cr, Cho, Lac and NAA are the most readily determined resonances (peaks) using MRS [30]. The putative roles of Cr, Cho, Lac and NAA have been reported in many MRS studies. For instance, Cr is often used as an internal reference, but since it has been shown to change with neurological conditions and disease, changes in total Cr must always be considered [31]. A ^1H -MRS study in infants within the first 4 days after birth demonstrated that a reduction in absolute brain Cr was associated with both the normal/mild and severe/fatal outcome groups, and may reflect reduced overall cellularity in neonatal encephalopathy groups compared with controls [32]. Cho is frequently used for the investigation of normal cell function and as a marker for cell membrane metabolism [33,34], and hence reduced Cho reflects reduced cellularity [35], impairments with myelination or altered cell types [36]. NAA is considered as a marker of neuronal density and function [37], and it is diffused along the axons; however, it breaks down in oligodendrocytes. Thus reductions in NAA may reflect neuronal or axonal degeneration [31]. Lac is an indicator of anaerobic metabolism. The elevated levels of brain Lac are thought to be due to major cell death events resulting from tumours and ischaemic diseases [38,39]. For any biomarker, the sensitivity of the MRS recordings and the sample size acquired are important considerations as to whether absolute concentrations and/or the metabolic ratios are used for quantification of neural metabolic changes [40]. In this study, we found that INJ+UCO lambs had significantly reduced absolute Cr and Cho values compared to controls, but no significant differences in Lac or NAA, at 24 h. An early decline in absolute brain Cr in this study might reflect impending tissue loss, as suggested first in a study on shaken baby syndrome [41]. MRS recordings on babies with shaken baby syndrome showed a decline in Cr and NAA concentration and a delayed, but pronounced increase in Lac, indicative of tissue loss and reduced cellularity, which was able to be measured at a much earlier stage than with conventional MRI [41]. The INJ+UCO lambs had lower Cho levels than the control group. Others have previously associated low Cho levels in the brain with reduced myelination [42]. We have previously shown that alterations in DTI measurements at the time of preterm delivery correlated with impairment of neuron and myelination as a result of injurious mechanical ventilation [43]. Measuring myelination was outside the scope of this study, but the loss of oligodendrocyte progenitors has been well characterized in models of prematurity [44], HIE [45], and ventilation [7]. Lactate concentrations were not significantly different between the lamb groups at 24 h in this study. Others have also reported that there was no significant Lac elevation in preterm infant brains [46]. Furthermore, we found no significant

differences in MRS peak-area metabolite ratios at 24 h, which might reflect the relative insensitivity of these indices in detecting the early onset of brain injury. Others also failed to detect an effect of magnesium sulfate, which was expected to decrease the severity of delayed cerebral energy failure in infants with cerebral ischaemia, on the MRS peak-area ratios of Lac to other metabolites within the first 1–2 days of postnatal life [47]. Our metabolite concentration findings greatly improve our understanding for pathological interpretation compared with that provided by peak-area ratios.

We did not observe obvious lesions that have been detected in animal models with conventional MRI at 24 h [48]. However, this does not rule out the possibility such lesions might manifest in the following days. Brown et al. [49] reported that there was a direct relationship between poor behavioural performance and severe microstructural WM abnormalities on MRI findings at 5–7 days of age, and at two years of age in preterm infants. An ultimate aim of our research is to identify a marker of preterm brain injury before it manifests to allow a window for treatment. Our previous study did not observe DTI changes using DTI-based ROI approach at one hour after delivery [14]. Identification of DTI-based ROI approach with subsequent structural injury in longer-termed studies will be critical to validate this technique as a reliable early marker of brain injury [50,51].

The DTI findings in this study confirm and extend our previous investigations of neuropathology in preterm neonate brains. However, we acknowledge that the study has important limitations. Histological examination of the lamb brains in this study was not undertaken to confirm inflammatory markers or subtle WM injury. However, we have previously demonstrated that alterations in fractional anisotropy and diffusivity at the time of preterm delivery correlated with impairment of myelination as a result of injurious mechanical ventilation [43]. This study and previous studies [14,43], show that MRI can be quantitative for microstructural changes in specific anatomical structures in the preterm brain, providing potentially useful biomarkers for preterm delivery-associated neuropathology in the clinic. A further limitation, is that the surgery in of itself is injurious, since there was mild injury observed in the sham lambs compared to the Cont group. This is likely due to using twins exposed to longer isoflurane which is harmful to the preterm brain [52].

In conclusion, both DTI and colour-map threshold technique revealed that VIBI is associated with very low AD, RD, and MD intensities observed in the WM of preterm lambs 24 h after ventilation. When both pathways of injury were initiated WM injury was amplified compared to the inflammatory pathway alone, demonstrating the importance for targeting of both pathways of injury for any therapeutic strategy focused on reducing VIBI.

Supporting information

S1 Fig. Magnetic resonance imaging (MRI) data analysis regions of interest (ROIs). Examples of ROIs in specific regions of (A) the thalamus (Th), (B) internal capsule (IC), (C) periventricular white matter (PVWM), (D) frontal white matter (FWM), and the cerebellum (CB) vermis, targeting (E) midline and (F) stalk white matter for DTI analysis. Figure is reproduced from Alahmari et al. [14].

(TIF)

S2 Fig. DTI histogram distributions for individual lambs. Histogram distribution plots of axial diffusivity (AD), radial diffusivity (RD), and mean diffusivity (MD) for the whole brains from each group. Blue lines represent the unoperated control (Cont) group; blue dashed lines represent the sham surgery (Sham) group. Red lines represent the injurious ventilation (INJ) group, while red dashed lines represent the lambs exposed to umbilical cord occlusion (INJ +UCO) during the initial 15 min of high tidal-volume (V_T) ventilation. The black

box represents the 75% confidence interval (CI) of all voxel intensities observed in the distribution in Cont lamb brains. Threshold (green dashed line) applied to the mapped intensities in the overlay in all groups.

(TIF)

S3 Fig. Peak-area magnetic resonance spectroscopy (MRS) lactate metabolite ratios. Individual MRS peak-area metabolite ratios utilising a single-voxel encompassing supratentorial central white matter and deep grey matter in the unoperated control (Cont; blue open squares), sham surgery (Sham; blue closed squares), injurious ventilation (INJ; red open circles), and injurious ventilation with umbilical cord occlusion (INJ+UCO; red closed circles) groups. Lac: lactate; Cr: creatine; Cho: choline; NAA: N-acetylaspartate.

(TIF)

S4 Fig. Standard deviation of DTI measurements. The standard deviation of the distribution of voxel intensities within each region of interest ROI for each animal was calculated for fractional anisotropy (FA), axial diffusivity (AD), radial diffusivity (RD), and mean diffusivity (MD) measurements in the unoperated control (Cont), sham surgery (Sham), injurious ventilation (INJ), and umbilical cord occlusion (INJ+UCO) groups. The means of the standard deviations were tested for differences between the four groups of lambs using one-way ANOVA. The ROIs shown in S1 Fig were located in the thalamus (Th), internal capsule (IC), periventricular white matter (PVWM), frontal white matter (FWM), cerebellum (CB) middle and cerebellum (CB) stalk. * $P < 0.01$ and ** $P < 0.001$ group effect.

(TIF)

Author Contributions

Conceptualization: Dhafer M. Alahmari, Kyra Y. Y. Chan, Domenic LaRosa, Samantha K. Barton, Michael Farrell, Shigeo Yamaoka, James T. Pearson, Graeme R. Polglase.

Data curation: Dhafer M. Alahmari, Kyra Y. Y. Chan, Vanesa Stojanovska, Domenic LaRosa, Samantha K. Barton, Ilias Nitsos, Valerie Zahra, Jade Barbuto, Michael Farrell, Shigeo Yamaoka, James T. Pearson, Graeme R. Polglase.

Formal analysis: Dhafer M. Alahmari, Kyra Y. Y. Chan, Vanesa Stojanovska, Domenic LaRosa, Samantha K. Barton, Ilias Nitsos, Valerie Zahra, Jade Barbuto, Michael Farrell, Shigeo Yamaoka, James T. Pearson, Graeme R. Polglase.

Funding acquisition: Samantha K. Barton, James T. Pearson, Graeme R. Polglase.

Investigation: Dhafer M. Alahmari, Kyra Y. Y. Chan, Vanesa Stojanovska, Domenic LaRosa, Samantha K. Barton, Ilias Nitsos, Valerie Zahra, Jade Barbuto, Michael Farrell, Shigeo Yamaoka, James T. Pearson, Graeme R. Polglase.

Methodology: Dhafer M. Alahmari, Kyra Y. Y. Chan, Vanesa Stojanovska, Samantha K. Barton, Ilias Nitsos, Valerie Zahra, Jade Barbuto, Michael Farrell, James T. Pearson, Graeme R. Polglase.

Project administration: Dhafer M. Alahmari, Vanesa Stojanovska, Domenic LaRosa, Samantha K. Barton, Ilias Nitsos, Valerie Zahra, Michael Farrell, James T. Pearson, Graeme R. Polglase.

Resources: Dhafer M. Alahmari, Kyra Y. Y. Chan, Vanesa Stojanovska, Domenic LaRosa, Samantha K. Barton, Ilias Nitsos, Valerie Zahra, Jade Barbuto, Michael Farrell, Shigeo Yamaoka, James T. Pearson, Graeme R. Polglase.

Supervision: James T. Pearson, Graeme R. Polglase.

Validation: Dhafer M. Alahmari, James T. Pearson, Graeme R. Polglase.

Visualization: Dhafer M. Alahmari, James T. Pearson, Graeme R. Polglase.

Writing – original draft: Dhafer M. Alahmari, James T. Pearson, Graeme R. Polglase.

Writing – review & editing: Dhafer M. Alahmari, Kyra Y. Y. Chan, Vanesa Stojanovska, Domenic LaRosa, Samantha K. Barton, Ilias Nitsos, Valerie Zahra, Jade Barbuto, Michael Farrell, Shigeo Yamaoka, James T. Pearson, Graeme R. Polglase.

References

1. Fanaroff AA, Stoll BJ, Wright LL, Carlo WA, Ehrenkranz RA, Stark AR, et al. (2007) Trends in neonatal morbidity and mortality for very low birthweight infants. *American Journal of Obstetrics and Gynecology* 196: 147.e141–147.e148.
2. Grether JK, Cummins SK, Nelson KB (1992) The California Cerebral Palsy Project. *Paediatric and Perinatal Epidemiology* 6: 339–351. PMID: [1635884](#)
3. Nelson KB (2002) The epidemiology of cerebral palsy in term infants. *Mental Retardation and Developmental Disabilities Research Reviews* 8: 146–150. <https://doi.org/10.1002/mrdd.10037> PMID: [12216058](#)
4. Wen SW, Smith G, Yang Q, Walker M (2004) Epidemiology of preterm birth and neonatal outcome. *Seminars in Fetal and Neonatal Medicine* 9: 429–435. <https://doi.org/10.1016/j.siny.2004.04.002> PMID: [15691780](#)
5. Petrou S (2005) The economic consequences of preterm birth during the first 10 years of life. *BJOG: An International Journal of Obstetrics & Gynaecology* 112: 10–15.
6. Serenius F, Kallen K, Blennow M, Ewald U, Fellman V, Holmstrom G, et al. (2013) Neurodevelopmental outcome in extremely preterm infants at 2.5 years after active perinatal care in Sweden. *Jama* 309: 1810–1820. <https://doi.org/10.1001/jama.2013.3786> PMID: [23632725](#)
7. Khwaja O, Volpe JJ (2008) Pathogenesis of cerebral white matter injury of prematurity. *Archives of Disease in Childhood—Fetal and Neonatal Edition* 93: F153–F161. <https://doi.org/10.1136/adc.2006.108837> PMID: [18296574](#)
8. Hillman NH, Moss TJ, Nitsos I, Jobe AH (2012) Moderate tidal volumes and oxygen exposure during initiation of ventilation in preterm fetal sheep. *Pediatr Res* 72: 593–599. <https://doi.org/10.1038/pr.2012.135> PMID: [23037872](#)
9. Finer NN, Carlo WA, Walsh MC, Rich W, Gantz MG, Laptook AR, et al. (2010) Early CPAP versus surfactant in extremely preterm infants. *N Engl J Med* 362: 1970–1979. <https://doi.org/10.1056/NEJMoa0911783> PMID: [20472939](#)
10. Barton SK, Moss TJM, Hooper SB, Crossley KJ, Gill AW, Kluckow M, et al. (2014) Protective ventilation of preterm lambs exposed to acute chorioamnionitis does not reduce ventilation-induced lung or brain injury. *PLoS One* 9: e112402. <https://doi.org/10.1371/journal.pone.0112402> PMID: [25379714](#)
11. Poulton DA, Schmölzer GM, Morley CJ, Davis PG (2011) Assessment of chest rise during mask ventilation of preterm infants in the delivery room. *Resuscitation* 82: 175–179. <https://doi.org/10.1016/j.resuscitation.2010.10.012> PMID: [21074926](#)
12. Polglase GR, Miller SL, Barton SK, Baburamani AA, Wong FY, Aridas JD, et al. (2012) Initiation of resuscitation with high tidal volumes causes cerebral hemodynamic disturbance, brain inflammation and injury in preterm lambs. *PLoS One* 7: e39535. <https://doi.org/10.1371/journal.pone.0039535> PMID: [22761816](#)
13. Skiöld B, Wu Q, Hooper SB, Davis PG, McIntyre R, Tolcos M, et al. (2014) Early detection of ventilation-induced brain injury using magnetic resonance spectroscopy and diffusion tensor imaging: an in vivo study in preterm lambs. *PLoS One* 9: e95804. <https://doi.org/10.1371/journal.pone.0095804> PMID: [24759765](#)
14. Alahmari DM, Skiöld B, Barton SK, Nitsos I, McDonald C, Miller SL, et al. (2017) Diffusion tensor imaging colour mapping threshold for identification of ventilation-induced brain injury after intrauterine inflammation in preterm lambs. *Frontiers in Pediatrics* 5.
15. Bhatt S, Alison BJ, Wallace EM, Crossley KJ, Gill AW, Kluckow M, et al. (2013) Delaying cord clamping until ventilation onset improves cardiovascular function at birth in preterm lambs. *The Journal of Physiology* 591: 2113–2126. <https://doi.org/10.1113/jphysiol.2012.250084> PMID: [23401615](#)

16. Polglase GR, Wallace MJ, Grant DA, Hooper SB (2004) Influence of fetal breathing movements on pulmonary hemodynamics in fetal sheep. *Pediatr Res* 56: 932–938. <https://doi.org/10.1203/01.PDR.0000145254.66447.C0> PMID: 15470203
17. Jenkinson M, Beckmann CF, Behrens TEJ, Woolrich MW, Smith SM (2012) FSL. *NeuroImage* 62: 782–790. <https://doi.org/10.1016/j.neuroimage.2011.09.015> PMID: 21979382
18. Jenkinson M, Bannister P, Brady M, Smith S (2002) Improved optimization for the robust and accurate linear registration and motion correction of brain images. *NeuroImage* 17: 825–841. PMID: 12377157
19. Bax M, Tydeman C, Flodmark O (2006) Clinical and MRI correlates of cerebral palsy: The european cerebral palsy study. *JAMA* 296: 1602–1608. <https://doi.org/10.1001/jama.296.13.1602> PMID: 17018805
20. Volpe JJ (1998) Neurologic outcome of prematurity. *Archives of Neurology* 55: 297–300. PMID: 9520002
21. Song S-K, Sun S-W, Ju W-K, Lin S-J, Cross AH, Neufeld AH (2003) Diffusion tensor imaging detects and differentiates axon and myelin degeneration in mouse optic nerve after retinal ischemia. *NeuroImage* 20: 1714–1722. PMID: 14642481
22. Bassi L, Chew A, Merchant N, Ball G, Ramenghi L, Boardman J, et al. (2011) Diffusion tensor imaging in preterm infants with punctate white matter lesions. *Pediatr Res* 69: 561–566. <https://doi.org/10.1203/PDR.0b013e3182182836> PMID: 21386750
23. Cheong JL, Thompson DK, Wang HX, Hunt RW, Anderson PJ, Inder TE, et al. (2009) Abnormal white matter signal on MR imaging is related to abnormal tissue microstructure. *AJNR Am J Neuroradiol* 30: 623–628. <https://doi.org/10.3174/ajnr.A1399> PMID: 19131414
24. Woodward LJ, Anderson PJ, Austin NC, Howard K, Inder TE (2006) Neonatal MRI to predict neurodevelopmental outcomes in preterm infants. *N Engl J Med* 355: 685–694. <https://doi.org/10.1056/NEJMoa053792> PMID: 16914704
25. Tyszkja JM, Readhead C, Bearer EL, Pautler RG, Jacobs RE (2006) Statistical diffusion tensor histology reveals regional dysmyelination effects in the shiverer mouse mutant. *NeuroImage* 29: 1058–1065. <https://doi.org/10.1016/j.neuroimage.2005.08.037> PMID: 16213163
26. Harsan LA, Poulet P, Guignard B, Steibel J, Parizel N, de Sousa PL, et al. (2006) Brain dysmyelination and recovery assessment by noninvasive in vivo diffusion tensor magnetic resonance imaging. *J Neurosci Res* 83: 392–402. <https://doi.org/10.1002/jnr.20742> PMID: 16397901
27. Duerden EG, Foong J, Chau V, Branson H, Poskitt KJ, Grunau RE, et al. (2015) Tract-based spatial statistics in preterm-born neonates predicts cognitive and motor outcomes at 18 months. *American Journal of Neuroradiology* 36: 1565–1571. <https://doi.org/10.3174/ajnr.A4312> PMID: 25929880
28. Nitsos I, Newnham JP, Rees SM, Harding R, Moss TJM (2014) The Impact of chronic intrauterine inflammation on the physiologic and neurodevelopmental consequences of intermittent umbilical cord occlusion in fetal sheep. *Reproductive Sciences* 21: 658–670. <https://doi.org/10.1177/1933719111399928> PMID: 21421894
29. Rabe H, Diaz-Rossello JL, Duley L, Dowswell T (2012) Effect of timing of umbilical cord clamping and other strategies to influence placental transfusion at preterm birth on maternal and infant outcomes. *Cochrane Database Syst Rev*: Cd003248. <https://doi.org/10.1002/14651858.CD003248.pub3> PMID: 22895933
30. Soares DP, Law M (2009) Magnetic resonance spectroscopy of the brain: review of metabolites and clinical applications. *Clin Radiol* 64: 12–21. <https://doi.org/10.1016/j.crad.2008.07.002> PMID: 19070693
31. Van der Graaf M (2010) In vivo magnetic resonance spectroscopy: basic methodology and clinical applications. *European Biophysics Journal: EBJ* 39: 527–540. <https://doi.org/10.1007/s00249-009-0517-y> PMID: 19680645
32. Cheong JLY, Cady EB, Penrice J, Wyatt JS, Cox IJ, Robertson NJ (2006) Proton MR spectroscopy in neonates with perinatal cerebral hypoxic-ischemic injury: Metabolite peak-area ratios, relaxation times, and absolute concentrations. *American Journal of Neuroradiology* 27: 1546. PMID: 16908578
33. Zeisel SH (2000) Choline: needed for normal development of memory. *J Am Coll Nutr* 19: 528s–531s. PMID: 11023003
34. Zeisel SH (2006) Choline: Critical role during fetal development and dietary requirements in adults. *Annual Review of Nutrition* 26: 229–250. <https://doi.org/10.1146/annurev.nutr.26.061505.111156> PMID: 16848706
35. Roelants-Van Rijn AM, van der Grond J, de Vries LS, Groenendaal F (2001) Value of (1)H-MRS using different echo times in neonates with cerebral hypoxia-ischemia. *Pediatr Res* 49: 356–362. <https://doi.org/10.1203/00006450-200105000-00015> PMID: 11228261

36. Alkan A, Kutlu R, Yakinci C, Sigirci A, Aslan M, Sarac K (2003) Delayed myelination in a rhizomelic chondrodysplasia punctata case: MR spectroscopy findings. *Magn Reson Imaging* 21: 77–80. PMID: [12620550](#)
37. Urenjak J, Williams SR, Gadian DG, Noble M (1992) Specific expression of N-acetylaspartate in neurons, oligodendrocyte-type-2 astrocyte progenitors, and immature oligodendrocytes in vitro. *J Neurochem* 59: 55–61. PMID: [1613513](#)
38. Penrice J, Lorek A, Cady EB, Amess PN, Wylezinska M, Cooper CE, et al. (1997) Proton magnetic resonance spectroscopy of the brain during acute hypoxia-ischemia and delayed cerebral energy failure in the newborn piglet. *Pediatr Res* 41: 795–802. <https://doi.org/10.1203/00006450-199706000-00001> PMID: [9167191](#)
39. Rothman DL, Howseman AM, Graham GD, Petroff OA, Lantos G, Fayad PB, et al. (1991) Localized proton NMR observation of [3-13C]lactate in stroke after [1-13C]glucose infusion. *Magn Reson Med* 21: 302–307. PMID: [1745129](#)
40. Hoch SE, Kirov II, Tal A (2017) When are metabolic ratios superior to absolute quantification? A statistical analysis. *NMR in Biomedicine*: e3710-n/a.
41. Haseler LJ, Arcinue E, Danielsen ER, Bluml S, Ross BD (1997) Evidence from proton magnetic resonance spectroscopy for a metabolic cascade of neuronal damage in shaken baby syndrome. *Pediatrics* 99: 4–14. PMID: [8989330](#)
42. Hüppi P KR, Zientara G, Holling E, Maier S, Boesch C, Volpe J, Jolesz F (1998) Regional maturation of the human brain assessed by 1H-MRS and diffusion tensor imaging. Effects of prematurity and ischemic injury.. *International Society for Magnetic Resonance in Medicine* 1:94.
43. Alahmari Dhafer M, Barton Samantha K, Galinsky Robert, Nitsos Ilias, Atik Anzari, Farrell Michael, et al. (2017) Correlation between diffusion tensor imaging and histological brain injury in ventilated preterm lambs. *Imaging in Medicine* 9(3): 67–76.
44. Salmaso N, Jablonska B, Scafidi J, Vaccarino FM, Gallo V (2014) Neurobiology of premature brain injury. *Nat Neurosci* 17: 341–346. <https://doi.org/10.1038/nn.3604> PMID: [24569830](#)
45. Raymond M, Li P, Mangin J-M, Huntsman M, Gallo V (2011) Chronic perinatal hypoxia reduces GLAST function in astrocytes through the JAK/STAT pathway. *The Journal of Neuroscience* 31: 17864–17871. <https://doi.org/10.1523/JNEUROSCI.3179-11.2011> PMID: [22159101](#)
46. Leth H, Toft PB, Pryds O, Peitersen B, Lou HC, Henriksen O (1995) Brain lactate in preterm and growth-retarded neonates. *Acta Pædiatrica* 84: 495–499. PMID: [7633142](#)
47. Penrice J, Amess PN, Punwani S, Wylezinska M, Tyszczuk L, D'Souza P, et al. (1997) Magnesium sulfate after transient hypoxia-ischemia fails to prevent delayed cerebral energy failure in the newborn piglet. *Pediatr Res* 41: 443–447. <https://doi.org/10.1203/00006450-199703000-00025> PMID: [9078550](#)
48. Lodygensky GA, Inder TE, Neil JJ (2008) Application of magnetic resonance imaging in animal models of perinatal hypoxic-ischemic cerebral injury. *International journal of developmental neuroscience: the official journal of the International Society for Developmental Neuroscience* 26: 13–25.
49. Brown NC, Inder TE, Bear MJ, Hunt RW, Anderson PJ, Doyle LW (2009) Neurobehavior at term and white and gray matter abnormalities in very preterm infants. *J Pediatr* 155: 32–38, 38.e31. <https://doi.org/10.1016/j.jpeds.2009.01.038> PMID: [19394041](#)
50. Miller SP, Ferriero DM, Leonard C, Piecuch R, Glidden DV, Partridge JC, et al. (2005) Early brain injury in premature newborns detected with magnetic resonance imaging is associated with adverse early neurodevelopmental outcome. *The Journal of Pediatrics* 147: 609–616. <https://doi.org/10.1016/j.jpeds.2005.06.033> PMID: [16291350](#)
51. Inder TE, Anderson NJ, Spencer C, Wells S, Volpe JJ (2003) White matter injury in the premature infant: a comparison between serial cranial sonographic and MR findings at term. *American Journal of Neuroradiology* 24: 805–809. PMID: [12748075](#)
52. Wise-Faberowski L, Quinonez ZA, Hammer GB (2014) Anesthesia and the developing brain: relevance to the pediatric cardiac surgery. *Brain Sciences* 4: 295–310. <https://doi.org/10.3390/brainsci4020295> PMID: [24961762](#)

Appendix III

This appendix relates to Chapter Four: Early Umbilical Cord Blood Cells (UCBC) Exacerbates VIBI and presents findings of ventilation-induced lung injury (VILI) from the same animals [Table A3]. The key findings of this study were that brief injurious ventilation caused significant lung injury, which was not reduced by the administration of UCBC 1 h post-ventilation.

Table A3. Comparison of corresponding experimental groups in Appendix III and Chapter 4. In both studies, the UNOP and SHAM groups were pooled to form CONT for histological analyses.

Synonymous groups in		Group description
Appendix III	Chapter 4	
UNOP (n=7)	UNOP (n=7)	#Lambs did not undergo initial fetal surgery or ventilation
SHAM (n=5)	SHAM (n=5)	#Lambs underwent fetal surgery but did not receive ventilation
VILI (n=7)	INJ (n=7)	Lambs received 15 min of high tidal volume (V_T) ventilation
VILI _{CELLS} (n=7)	INJ+UCBC (n=7)	Lambs received 15 min of high V_T ventilation with umbilical cord blood cells

Pooled control group CONT (n=12)

The original article is included below, reproduced under the terms of the Creative Commons Attribution 4.0 International License:

Smith M, **Chan KYY**, Papagianis PC, Nitsos I, Zahra VA, Allison BJ, Polglase GR, McDonald CA. Umbilical cord blood cells do not reduce ventilation-induced lung injury in preterm lambs. *Front Physiol* 2020;**11**:119.



Umbilical Cord Blood Cells Do Not Reduce Ventilation-Induced Lung Injury in Preterm Lambs

Madeleine J. Smith¹, Kyra Y. Y. Chan¹, Paris Papagianis^{1,2}, Ilias Nitsos¹, Valerie Zahra¹, Beth Allison¹, Graeme R. Polglase^{1*} and Courtney A. McDonald^{1*}

¹ The Ritchie Centre, Department of Obstetrics and Gynaecology, Hudson Institute of Medical Research, Monash University, Melbourne, VIC, Australia, ² Chronic Infectious and Inflammatory Diseases Research, School of Health and Biomedical Sciences, RMIT University, Bundoora, VIC, Australia

OPEN ACCESS

Edited by:

John T. Fisher,
Queen's University School of
Medicine, Canada

Reviewed by:

Michael Stark,
Women's and Children's Hospital,
Australia
Jennifer J. P. Collins,
Erasmus University Medical Center,
Netherlands
David Warburton,
Children's Hospital Los Angeles –
The Saban Research Institute,
United States

*Correspondence:

Graeme R. Polglase
graeme.polglase@monash.edu
Courtney A. McDonald
courtney.mcdonald@hudson.org.au;
courtney.mcdonald@monash.edu

Specialty section:

This article was submitted to
Respiratory Physiology,
a section of the journal
Frontiers in Physiology

Received: 23 October 2019

Accepted: 03 February 2020

Published: 21 February 2020

Citation:

Smith MJ, Chan KYY,
Papagianis P, Nitsos I, Zahra V,
Allison B, Polglase GR and
McDonald CA (2020) Umbilical Cord
Blood Cells Do Not Reduce
Ventilation-Induced Lung Injury
in Preterm Lambs.
Front. Physiol. 11:119.
doi: 10.3389/fphys.2020.00119

Background: Preterm infants often have immature lungs and, consequently, many require respiratory support at birth. However, respiratory support causes lung inflammation and injury, termed ventilation-induced lung injury (VILI). Umbilical cord blood (UCB) contains five cell types that have been shown to reduce inflammation and injury. The aim of this study was to determine whether UCB cells can reduce VILI in preterm lambs.

Methods: We assessed lung inflammation and injury, with and without UCB cell administration. Fetal lambs at 125 ± 1 days gestation underwent sterile surgery and were randomly allocated to one of four groups; unoperated controls (UNOP), sham controls (SHAM), injuriously ventilated lambs (VILI), and injuriously ventilated lambs that received UCB cells via the jugular vein 1 h after ventilation (VILI_{CELLS}). Ventilated lambs received an injurious ventilation strategy for 15 min, before they were returned to the uterus and the lamb and ewe recovered for 24 h. After 24 h, lambs were delivered via caesarean section and euthanized and the lungs were collected for histological and molecular assessment of inflammation and injury.

Results: VILI led to increased immune cell infiltration, increased cellular proliferation, increased tissue wall thickness, and significantly reduced alveolar septation compared to controls. Further, extracellular matrix proteins collagen and elastin had abnormal deposition following VILI compared to control groups. Administration of UCB cells did not reduce any of these indices.

Conclusion: Administration of UCB cells 1 h after ventilation onset did not reduce VILI in preterm lambs.

Keywords: lung, ventilation-induced lung injury, bronchopulmonary dysplasia, preterm, umbilical cord blood cells, inflammation, stem cells

INTRODUCTION

Preterm birth is associated with increased risk of infant morbidity and mortality (Blencowe et al., 2012), with a major contributor being lung disease (Moss, 2006). Preterm infants have structurally and functionally immature lungs and therefore, the majority of preterm infants <32 weeks gestational age (GA) require respiratory support at birth (Sharon, 2016). While life-saving, the

initiation of respiratory support at birth can cause lung inflammation and injury, particularly if excessive tidal volumes (V_T) are used (Hillman et al., 2011). Although respiratory support is well-controlled in the Neonatal Intensive Care Unit (NICU), a recent study showed that up to 85% of infants requiring respiratory support in the delivery room received higher V_T than recommended (Schmölzer et al., 2010). Indeed, as few as 6 high V_T breathes are enough to initiate lung inflammation and injury, known as ventilation-induced lung injury (VILI) (Jobe et al., 2008; Hillman et al., 2010). This detrimental lung injury caused by excess V_T in the delivery room may contribute to the progression to chronic lung disease (bronchopulmonary dysplasia) with lifelong consequences (Doyle et al., 2017).

Bronchopulmonary dysplasia (BPD) is a severe lung disease, with the main risk factors being preterm birth and mechanical ventilation for 7 or more days. Additionally, there is a correlation between chorioamnionitis and BPD (Jobe, 2011). Despite significant improvements in the care of preterm infants, Doyle et al. (2017) has shown that BPD rates are increasing. BPD is associated with additional adverse outcomes including pulmonary hypertension, cardiovascular disease, and adverse neurological outcomes (Kinsella et al., 2006). VILI is a major antecedent of BPD (Jobe, 2011). VILI is caused by mechanisms including barotrauma, volutrauma, and atelectrauma, but the main component is believed to be volutrauma (Dreyfuss and Saumon, 1992). The initiation of respiratory support with high tidal volumes leads to lung inflammation and injury via an upregulation of pro-inflammatory cytokines and injury response genes (Jobe et al., 2008; Hillman et al., 2011). There are currently no effective therapies to treat or prevent VILI but targeting the pro-inflammatory cascade may be an effective target for reducing or preventing VILI.

There is increasing interest in the therapeutic potential of stem cells in the reduction of inflammation and injury, in particular lung injury. One promising source of stem cells is umbilical cord blood (UCB), which is usually discarded at birth and is an abundant source of stem and progenitor cells. Studies using both UCB mononuclear cells and individual cell types found within UCB have shown promising results in the attenuation of lung injury following hyperoxia (Mills et al., 2017; Monz et al., 2013). Further, individual UCB cell types have reduced lung injury in various experimental models including mesenchymal stem cells (MSCs) (Chang et al., 2009), T regulatory cells (Tregs) (Garibaldi et al., 2013), and hematopoietic stem cells (De Paepe et al., 2011; Huang et al., 2014). However, there is a lack of evidence to the effectiveness of UCB using large animal models of VILI. In addition, previous studies have administered cell therapies in the days following lung injury, allowing inflammation and tissue remodeling to be well established before treatment. To date, no studies have assessed the therapeutic potential of early or prophylactic UCB within the first hour after birth to reduce VILI.

In this study we assessed whether administration of UCB 1 h after 15 min of injurious ventilation (volutrauma) can reduce lung inflammation and remodeling 24 h later. We hypothesized that UCB cells would reduce histological and molecular indices of

lung inflammation and injury when administered intravenously 1 h following volutrauma in preterm lambs.

MATERIALS AND METHODS

Ethics

All animal experimental protocols were approved by the Monash Medical Centre Animal Ethics Committee. All methods were carried out in accordance with the relevant guidelines and regulations as described by the National Health and Medical Research Council of Australia.

Experimental Design

Sterile fetal surgery was conducted on pregnant ewes at 125 ± 1 (SD) days gestation (term ~148 days GA). Lambs were randomized to one of four groups; unoperated controls (UNOP) ($n = 7$), sham surgical controls ($n = 5$), injuriously ventilated ($n = 7$: VILI), and injuriously ventilated with UCB cells ($n = 7$: VILI_{CELLS}). The experimental protocol spanned 24 h and was conducted at the Monash Biomedical Imaging facility. All UCB-treated animals received cells via intravenous route through the jugular vein catheter. This route was chosen as the cells were given 1 h after injury when ventilation had ceased, intratracheal tubes had been removed and the fetuses had been returned to the uterus.

Animal Surgery

Pregnant ewes were anesthetized by intravenous injection of thiopentone sodium (20 mg/kg, i.v.; Jurox, NSW, Australia) and were subsequently intubated and anesthesia maintained by inhalational isoflurane (1.5–2.5% in oxygen; Bomac Animal Health, NSW, Australia) delivered via positive pressure ventilation. Polyvinyl catheters (inner diameter 0.86 mm, outer diameter 1.52 mm; Dural Plastics & Engineering, NSW, Australia) were inserted into the left carotid artery and jugular vein of the fetus to measure blood pressure and obtain blood samples and to administer UCB cells, respectively. An ultrasonic flow probe (3PS; Transonic Systems, Ithaca, NY, United States) was placed around the right carotid artery to record carotid blood flow – a pseudo measure of cerebral blood flow (Rudolph, 1983). The incision was sutured using polyvinyl silk. The fetus's chest was exteriorized, the fetus was dried, and intubated with a 4.5 mm cuffed endotracheal tube and lung liquid was passively drained. SHAM animals remained intubated for 15 min while VILI and VILI_{CELLS} lambs were ventilated using a ventilation strategy aiming to cause volutrauma (Babylog 8000+; Dräger, Lübeck, Germany) by targeting 10–15 ml/kg for a total of 15 min as described previously (Hillman et al., 2007; Barton et al., 2015). Following ventilation, fetuses were returned to the uterus, the incisions closed, and the fetus and ewes recovered. At 1 h post-ventilation, 80 million ovine UCB cells suspended in 3 ml of phosphate-buffered saline were administered to the fetus via the fetal jugular vein catheter (see below). The catheter was flushed with 3 ml of sterile heparinized saline to ensure all the cells were administered. Ewes were monitored overnight and regular blood gases were taken to ensure fetal well-being.

Twenty-four hours after the surgery, ewes were anesthetized as above and the lamb was exteriorized through the same incision site. The lamb was dried, intubated, and ventilated (Vt 7 ml/kg PEEP 5 cm H₂O) for ~5 min prior to umbilical cord clamping. A transcutaneous oximeter (Masimo, CA, United States) was attached to its tail. FiO₂ was initially set at 0.4 and adjusted to maintain SaO₂ between 88 and 95%. Intratracheal surfactant (240 mg in 3 ml; Curosurf®; Chiesi Pharmaceuticals, Parma, Italy) was administered within the first 10 min to improve lung compliance and sustained inflations were applied to recruit the lung if necessary. For unoperated control (UNOP) lambs, the ewe and lambs underwent the surgery, catheterization, and ventilation as described above.

Once the lamb was stabilized, the umbilical cord was clamped and the lamb was transferred to an MRI-compatible ventilator (Pneupac babyPAC™; Pneupac, Smiths Medical, United Kingdom). Lambs were scanned for 60 min in a 3T MRI scanner to assess brain structure, spectroscopy, and diffusion imaging. At the end of scanning lambs were euthanized with an overdose of sodium pentobarbitone (>100 mg/kg, i.v. Valabarb Euthanasia Solution; Jurox, NSW, Australia). Ewes were similarly euthanized immediately after delivery of the lamb.

Umbilical Cord Blood Cell Preparation

Ovine allogeneic term (141 days gestation) UCB sample was obtained from a separate group of animals as previously described (Aridas et al., 2016). Briefly, after clamping of the cord, UCB was collected via the two umbilical veins and approximately 90 ml of blood was collected from each ovine fetus. The mononuclear layer of cells was obtained by centrifuging the blood at 1000 × g for 12 min with no brake and cells were suspended in phosphate-buffered saline (PBS; Gibco, Waltham, MA, United States). Red blood cells were lysed using red blood cell lysis buffer (155 nM ammonium chloride, 10 mM potassium bicarbonate, and 0.1 mM EDTA in MilliQ water). The lysis reaction was stopped with excess media [16.5% fetal bovine serum (FBS) in DMEM:F13, Gibco, Waltham, MA, United States]. Cells were manually counted and their viability was assessed using trypan blue exclusion dye (Gibco, Waltham, MA, United States) and a hemocytometer. UCB cells were cryopreserved in dimethyl sulfoxide (10% DMSO, Sigma in FBS) and stored in liquid nitrogen for subsequent administration to lambs. UCB cells were thawed as previously described and have shown that administration of immediately thawed cells is effective at reducing inflammation and cell death (Aridas et al., 2016; Li et al., 2017; Paton et al., 2018; Paton et al., 2019). Briefly, cells were rapidly thawed in a 37°C water bath with 10 ml media, centrifuged for 5 min at 300 × g and then supernatant was removed and cells resuspended in media and counted using a hemocytometer and trypan blue. Cells were then left on ice until administration.

Histological Analysis

At postmortem the lungs were dissected from the chest and the right upper lobe was pressure fixed at 20 cm H₂O by inflation with 10% neutral buffered formalin (pH 7.4) for histological examination. The lobe was cut into 5 mm slices and cut into

2 cm² sections and three sections of lung were randomly chosen and embedded in paraffin. Five micrometers of sections were stained and a total of 15 random high-power images were taken for each stain. Sections were stained with Hematoxylin and Eosin (H&E), Hart's resorcin-fuchsin stain to identify elastin or picrosirius red to stain for type I and III collagen. H&E sections were scored for alveolar wall thickness, as described previously (Hillman et al., 2010; Polglase et al., 2017). Elastin and collagen density was measured by image analysis (ImagePro Plus) using five random fields of view per section using a 40× objective lens. Staining density was adjusted for tissue area. Analysis was performed using Image Pro Premier software. The total area of collagen/elastin within each image was calculated and normalized to the area of tissue. To determine the number of secondary septal crests present in the HART's stained sections, the image processing package Fiji was used, with a grid overlay with 1131 dots was placed over each image. The number of dots landing on tissue, airspace, and secondary septal crests were counted. The number of secondary septal crests was divided by the area of tissue and multiplied by 100 to yield a secondary septal crest percentage.

Immunohistochemical Analysis

Proliferating cells were visualized using Ki67 (1:200, Thermo Fisher Scientific, Cat#MA5-14520) immunohistochemistry. Immune cells were visualized using CD45 (1:500, AbCam, Cat#ab10558). Stained lung sections were analyzed in duplicate images, with each lung section imaged across five fields of view per slide. Briefly, for each immunohistochemical stain, lung sections were dewaxed through xylene-alcohol series. Antigen retrieval was performed (Ki67; in 0.1 M citrate buffer, CD45; DAKO PT Link in 1 × DAKO Target Retrieval Solution). Sections were then blocked (Ki67; 5% BSA in 1% triton X PBS, CD45; DAKO Protein Block). All sections were incubated with primary antibody overnight at 4°. The sections were then incubated in secondary antibody (Ki67; 1:200 biotinylated goat anti-rabbit IgG antibody, Thermo Scientific, CD45; 1:500, Dako) for 1 h. Staining was revealed with 3,3'-diaminobenzidine (Pierce Biotechnology, Rockford, IL, United States). Ki67 sections were counterstained with Harris hematoxylin. All slides were then cleared and cover-slipped using mounting medium (DPX, Merck, Kilsyth, Australia). Slides were dried then visualized using light microscopy (Ki67; Olympus Microscope, Japan, CD45; Leica ScanScope AT Turbo and captured using Leica Scanner Console version 102.7.5). Cell counts were performed using Image J (NIH, Bethesda, MD, United States) at 400× magnification.

Gene Analysis

The lower lobe of the right lung was chopped into small pieces and immediately snap-frozen in liquid nitrogen. Twenty milligrams of lung tissue was homogenized and total RNA isolated (RNeasy Midi Extraction Kit, Qiagen, Australia) and reverse-transcribed into cDNA (SuperScript III reverse transcriptase; Invitrogen). Genes of interest were measured by qPCR/Taqman. Five microliters of cDNA from each sample was plated onto a 96-well PCR plate and submitted to the MHTP

Genomics Facility, Hudson Institute of Medical Research. Quality control testing was performed using Sybr chemistry for the housekeeping gene 18s (ABI 7900 HT qPCR). This was followed by preamplification, then taqman analysis of the seven genes listed in **Table 1**. Relative mRNA levels of gene expression are expressed relative to the mean of the UNOP group.

Statistical Analysis

Fetal parameters were compared using one-way ANOVA. Ventilation parameters were compared using two-way repeated measures ANOVA and Holm-Sidak *post hoc* analysis, using SigmaStat. Indices of lung inflammation and injury were analyzed by using GraphPad Prism 7. Data were analyzed using one-way ANOVA or Kruskal-Wallis, as appropriate, with Tukey' or Dunn's multiple comparisons test, respectively. Data are expressed as mean \pm standard error of the mean (SEM). Statistical significance was considered as $p < 0.05$.

RESULTS

Fetal Physiological Parameters

Fetal parameters are summarized in **Table 2**. There were more males in each group compared to females but no difference between groups was observed. Birth weight and lung weights were not different between groups. There was no difference in fetal blood gas parameters, pH, PaCO₂, PaO₂, and SaO₂ between groups.

TABLE 1 | List of ovine specific probes for TaqMan Gene Array.

Gene/probe	Assay ID
18s (housekeeping gene)	Oa4906333_g1
IL-6	Oa04656315_m1
IL-8	Bt03211906_m1
IL-10	Oa03212724_m1
IL-1 β	Oa04656322_m1
CTGF	Oa04659069_g1
CYR61	Oa04673852_g1
EGR1	Oa03237885_m1

TABLE 2 | Baseline fetal data for all groups recorded prior to ventilation for all groups except UNOP, which was recorded before delivery.

	UNOP	SHAM	VILI	VILI _{CELLS}
Number	7	5	7	7
Sex (male)	6 (86%)	3 (60%)	5 (71%)	4 (57%)
Birth weight (kg)	3.4 \pm 0.2	3.3 \pm 0.1	3.4 \pm 0.2	3.4 \pm 0.2
Lung weight (g)	150.5 \pm 33	137.9 \pm 46	147.0 \pm 41	141.6 \pm 37
Birth order 1st (%)	6 (86%)	4 (80%)	7 (100%)	7 (100%)
pH	7.27 \pm 0.02	7.27 \pm 0.02	7.25 \pm 0.02	7.27 \pm 0.01
PaO ₂	36.7 \pm 7.2	33.0 \pm 2.7	51.2 \pm 8.8	34.1 \pm 1.3
PaCO ₂	59.0 \pm 3.2	64.0 \pm 5.8	57.3 \pm 3.1	59.2 \pm 1.6
SaO ₂	48.2 \pm 9.4	46.4 \pm 5.7	67.5 \pm 6.6	49.0 \pm 2.9

Data are expressed as mean \pm SD.

Ventilation

Ventilation parameters (**Figure 1**) during the volutrauma, including PIP, V_T, and mean airway pressure were not different between VILI and VILI_{CELLS}. V_T significantly increased with time throughout the 15 min ventilation strategy in both groups reaching a peak of 8.1 and 8.4 ml/kg for the VILI and VILI_{CELLS} group, respectively ($P < 0.001$ for both groups).

Blood Gas Parameters

Partial pressure of oxygen (PaO₂), partial pressure of carbon dioxide (PaCO₂), arterial saturation of oxygen (SaO₂), and pH were measured regularly. PaO₂ was significantly higher in the VILI group at the onset of ventilation compared to the SHAM group ($P = 0.017$; **Figure 2A**). During recovery there was no significant difference between groups. At 24 h during the MRI, PaCO₂ was significantly lower in the SHAM group compared to VILI ($P = 0.04$) and VILI_{CELLS} ($P = 0.036$) lambs (**Figure 2B**). There was no significant different in SaO₂ (**Figure 2C**) or pH (**Figure 2D**) across the experiment.

Assessment of Lung Injury

For all molecular and histological measures of lung inflammation and injury there was no significant difference between the UNOP and SHAM group; therefore, these groups were pooled (Controls).

Alveolar wall thickness (**Figures 3A,D-F**), inflammatory cell infiltration (**Figures 3B,G-I**), and proliferating cells (**Figures 3C,J-L**) were significantly increased in both the VILI ($P = 0.0017$, $P < 0.0001$, and $P = 0.0367$, respectively) and VILI_{CELLS} ($P = 0.002$, $P < 0.0001$, and $P = 0.0014$, respectively) groups compared to controls. There was no difference in these parameters between VILI and VILI_{CELLS}. There was no difference in hyaline membranes, epithelial sloughing, and hemorrhage between the groups.

Assessment of Lung Structure of Composition

Quantitative assessment of elastin showed no difference between groups for the percentage of elastin in tissue (**Figures 4A,D-I**). The number of secondary septal crests was significantly decreased in the VILI and VILI_{CELLS} groups compared to controls ($P = 0.0247$ and $P = 0.0021$, respectively, **Figures 4B,J-L**). Qualitative observation showed that elastin fibers were more elongated and relocated to airway walls in the ventilated (VILI and VILI_{CELLS}) groups (**Figures 4G-I**) rather than being localized to the septal crests as observed in control lungs.

Quantitative assessment of collagen showed that the VILI_{CELLS} group had significantly less collagen in tissue compared to the control group ($P = 0.0302$, **Figure 4C**). There was no significant difference in collagen between the VILI and control groups. Again, qualitative observation showed that collagen fibers were more elongated in the ventilated (VILI and VILI_{CELLS}) groups (**Figures 4K,L**).

Assessment of Gene Expression

mRNA levels of proinflammatory cytokines interleukin (IL)-1 β , IL-6, IL-8, and anti-inflammatory cytokine IL-10 and early

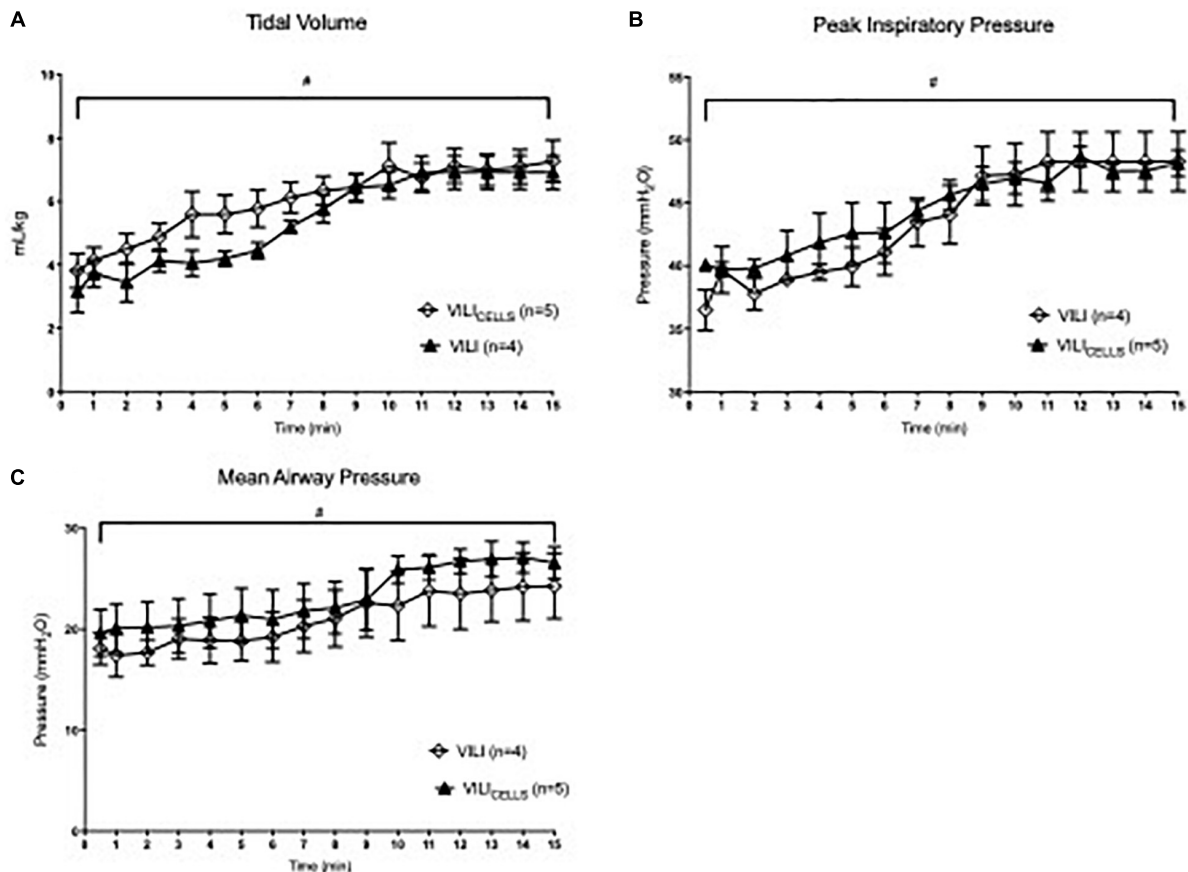


FIGURE 1 | Ventilation parameters for the two ventilated groups; VILI and VILI_{CELLS}. **(A)** Tidal volume, **(B)** peak inspiratory pressure, and **(C)** mean airway pressure. # indicates that time had a significant effect on the given ventilation parameter ($p < 0.05$).

response genes (CYR61, EGR1, and CTGF) were not different between groups as seen in **Figure 5**.

DISCUSSION

Preterm infants that require resuscitation in the delivery room may inadvertently receive higher tidal volumes than recommended, resulting in VILI, a major cause of BPD (Schmölzer et al., 2010). Similar to previous studies (Hillman et al., 2007), 15 min of volutrauma caused lung inflammation and injury and profound changes to lung structure. UCB cells have inherent properties which we hypothesized would reduce lung inflammation and injury. However, our study showed that the administration of UCB cells, 1 h after volutrauma, did not reduce lung inflammation or injury suggesting that early administration of UCB cells may not be efficacious at reducing or preventing VILI.

We investigated UCB cells because previous studies using UCB cells have demonstrated their anti-inflammatory and anti-fibrotic properties and their ability to aid alveolar epithelial reconstitution (Chang et al., 2009; De Paepe et al., 2011; Garibaldi et al., 2013; Monz et al., 2013; Huang et al., 2014;

Mills et al., 2017). In our study UCB cells were unable to reduce the increase in alveolar wall thickness and the number of infiltrating immune cells or prevent the loss of secondary septal crests from VILI. The mononuclear cell layer from UCB blood was chosen in this study over individual cell types. A study from our group has directly compared individual cell types and the UCB mononuclear cell fraction, showing that both reduced deficits and inflammation following brain injury (McDonald et al., 2018). Further, a large number of cells was required for this model and to use individual cell types, several cord blood units would be required. In the future, when cell expansion technologies are more advanced and larger doses of individual UCB stem cells can be generated, it would be interesting to examine different cell types in a similar experiment. UCB cells have never been studied for the treatment of VILI in a large animal model, so our chosen dose was based on previous studies treating brain injury in fetal sheep. In these studies, dosages of 25 million UCB cells/kg were able to attenuate hypoxic ischemic term and preterm brain injury and showed that both autologous and allogeneic UCB cell administration were effective at reducing inflammation and cell death (Aridas et al., 2016; Li et al., 2016). Although studies have not used UCB cells for lung injury in fetal sheep, the same dose of hAECs alleviates both brain and

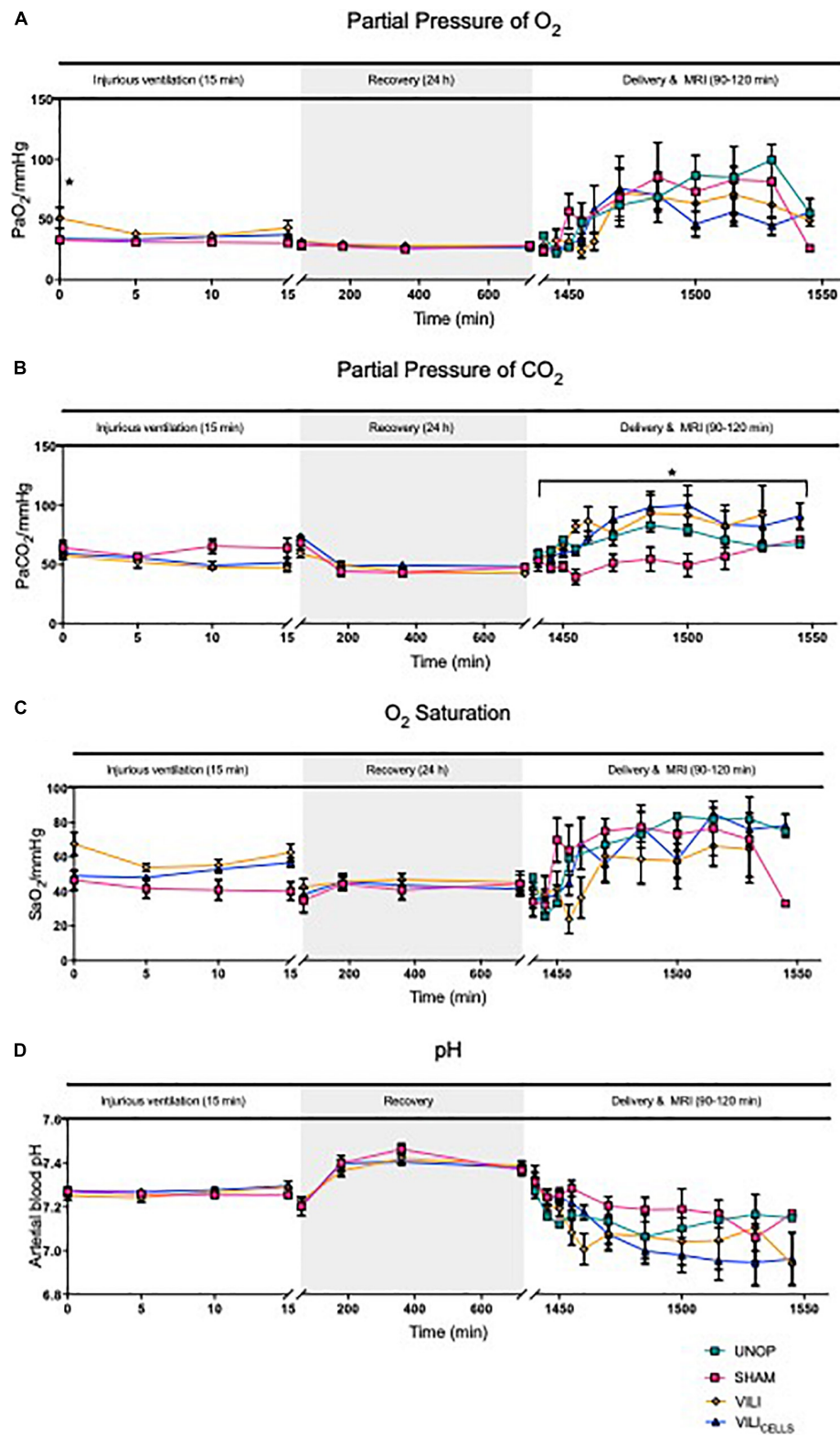


FIGURE 2 | Blood gas parameters between SHAM, VILI, and VILI_{CELLS} for the injurious ventilation period and recovery period and between UNOP, SHAM, VILI, and VILI_{CELLS} for delivery and MRI; partial pressure of (A) O₂, (B) CO₂, (C) saturation of oxygen, and (D) pH. Asterisk in panel (A) indicates significant difference in PaO₂ at time 0 between VILI and SHAM groups. Asterisk in panel (B) indicates difference in PaCO₂ during delivery and MRI, with SHAM significantly lower than VILI and VILI_{CELLS} groups, **P* < 0.05.

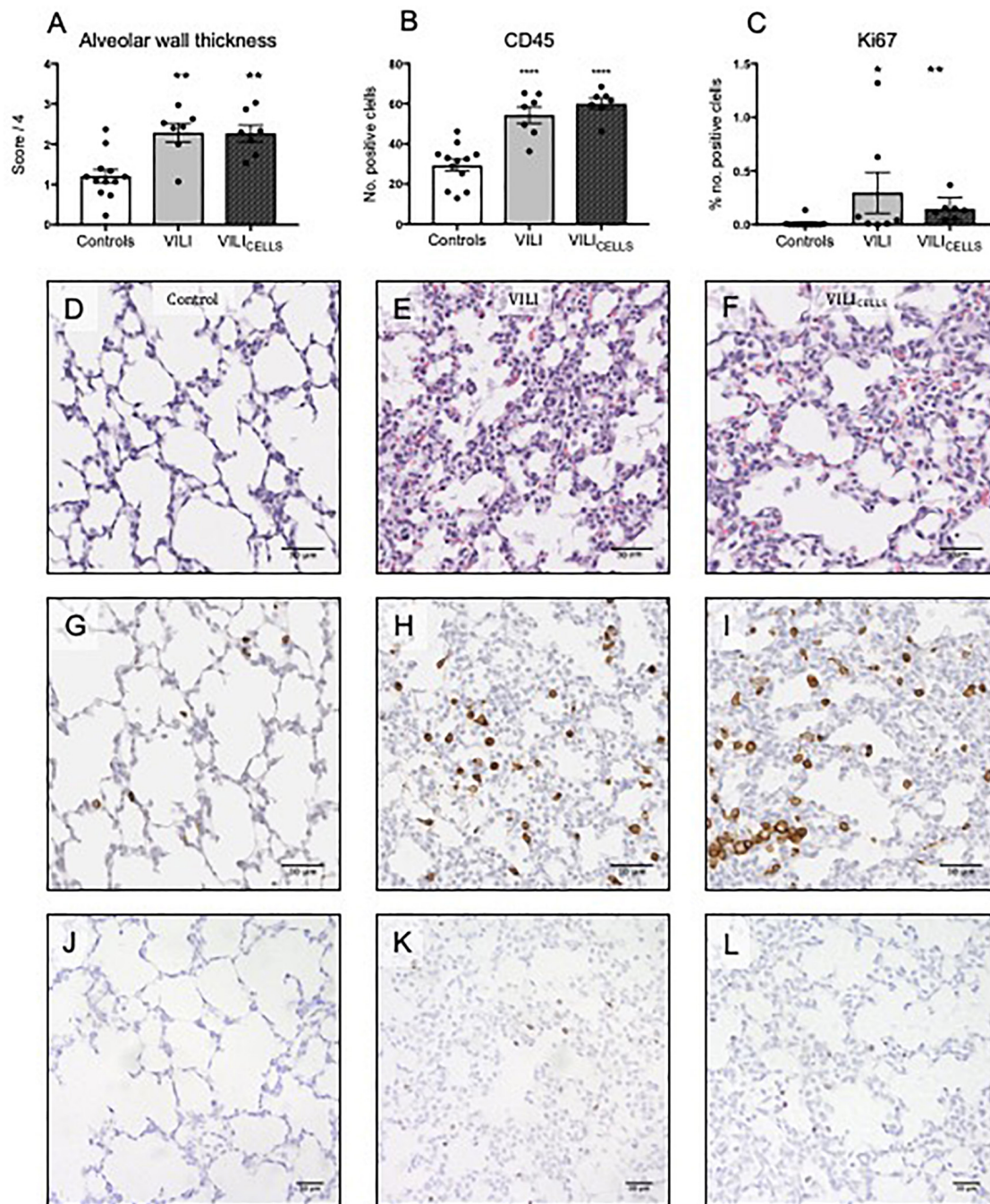


FIGURE 3 | (A) Alveolar wall thickness expressed a score out of 4, **(B)** Immune cell infiltration expressed as the number of positive cells per field of view, **(C)** number of proliferating cells expressed as the percentage of positive cells. Scale bars show 50 μm . $^*P < 0.05$, $^{**}P < 0.01$, $^{****}P < 0.0001$ compared to controls. **(D–F)** Representative lung sections stained with Hematoxylin and Eosin to assess alveolar wall thickness in **(D)** control, **(E)** VILI, and **(F)** VILI_{CELLS} lambs. **(G–I)** Representative lung sections demonstrating immune cell presence using CD45 immunohistochemistry. **(J–L)** Representative lung sections demonstrating cellular proliferation using Ki67 immunohistochemistry. Scale bar shows 30 μm .

lung injury in fetal sheep (Vosdoganes et al., 2011; Yawno et al., 2013). Our dose was based on an estimate of 3.2 kg fetal weight. Our average birth weight of 3.4 kg meant an average dose of ~ 23.5 million cells/kg was delivered. It is unlikely the marginally lower dose delivered in this study would have altered the findings.

However, as this is the first study to assess the effectiveness of UCB cells in a large animal model of lung injury, it is likely that future studies will need to assess different doses. The UCB cells used in this study were from sheep UCB, due to the limited availability of sheep-specific antibodies, we were unable

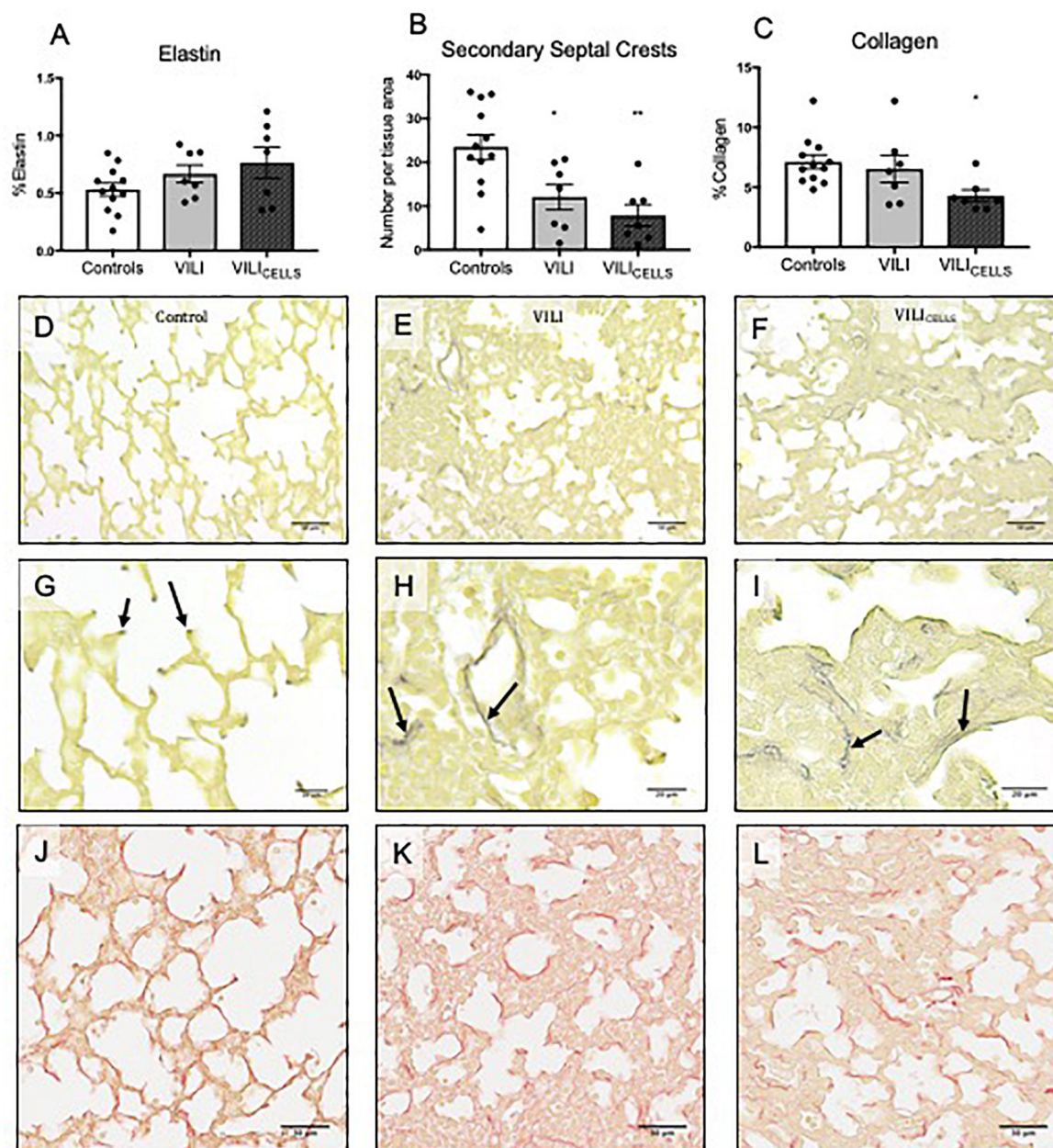


FIGURE 4 | (A) %Elastin content in tissue. **(B)** Density of secondary septal crests expressed as number per tissue area. **(C)** %Collagen content in tissue. * $P < 0.05$, ** $P < 0.01$ compared to controls. **(D–L)** Representative lung sections stained with HARTs to view elastin (black staining) in **(D,G)** control **(E,H)** VILI, and **(F,I)** VILI_{CELLS}. Arrows indicate elastin deposition at the points of septa in control lambs, which is irregular in the VILI and VILI_{CELLS} lambs. **(J–L)** Representative lung sections stained with picrosirius red to view collagen (dark red staining).

to identify the proportion of various cell types within the UCB samples. However, previous studies have shown UCB cells from autologous and allogeneic sheep to be efficacious in a sheep model of preterm brain injury (Li et al., 2017).

Umbilical cord blood cells were administered 1 h after volutrauma, which is known to be the peak of the pulmonary and systemic pro-inflammatory cascade resultant from injurious respiratory support (Hillman et al., 2011). This time point for stem cell administration has not been explored before. It was

our primary goal to see whether UCBs given at this peak inflammatory time could dampen the inflammatory response, thus reducing or preventing the subsequent progression of lung injury. Given the lack of efficacy, it is important to consider whether introducing the cells into a profound pro-inflammatory environment could alter the efficacy of UCB cells. Although the majority of studies that use cells such as MSCs, a stem cell subset present in UCB, have shown reduced inflammation (Curley et al., 2012; Hayes et al., 2015; Lai et al., 2015), there

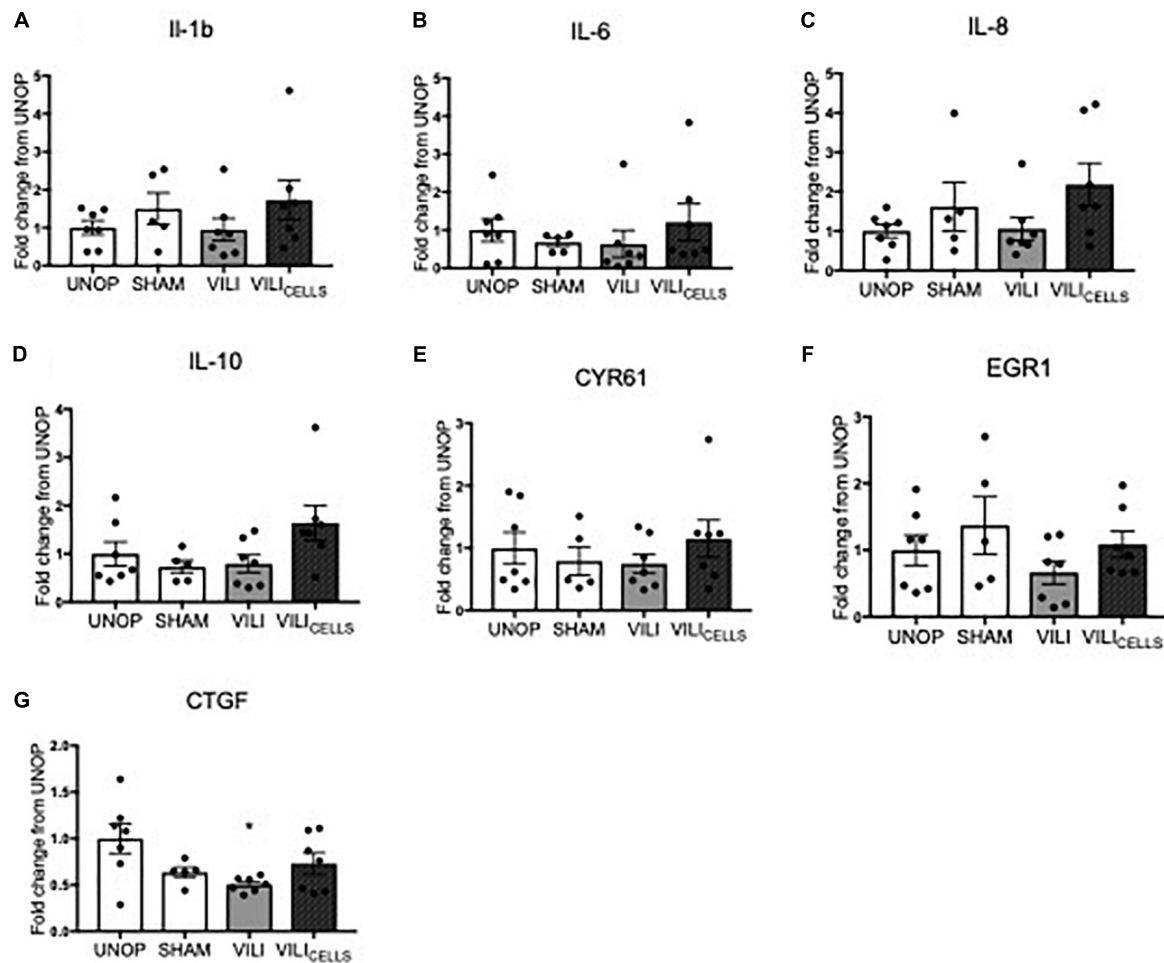


FIGURE 5 | Relative fold increase of (A) interleukin (IL)-1 β , (B) IL-6, (C) IL-8, (D) IL-10, (E) cysteine rich 61 (CYR61), (F) early growth response 1 (EGR1), (G) connective tissue growth factor (CTGF) expression between treatment groups expressed as a fold increase from UNOP.

are some studies that have shown that MSCs can exacerbate the inflammatory response if incorporated into an established pro-inflammatory environment (Bernardo and Fibbe, 2013). It has also been shown that bone marrow-derived MSCs are able to stimulate mononuclear cell types to produce pro-inflammatory cytokines IL-6 and IFN- γ (Rasmusson et al., 2007). Although we did not see any differences in inflammation at 24 h, it is likely that we missed the cytokine increases given they are largely resolved at this time (Hillman et al., 2011). Importantly, our results indicate that the UCB cells are not effective during this peak inflammatory period. Previous studies have administered human amnion epithelial cells prior to the onset of ventilation (Melville et al., 2017), 3 and 6 h (Hodges et al., 2012) into ventilation. Further, previous studies administered MSCs prior to the onset of ventilation (Chimenti et al., 2012) or 14 days after lung hyperoxia (Hansmann et al., 2012). This is the first study to assess cell administration at 1 h following lung injury, suggesting that cell administration may be efficacious in the resolution or prevention of inflammation and injury may not be efficacious when given at the peak of the pro-inflammatory

cascade. Future studies may be necessary to avoid this time point by administering cells prophylactically at the onset of ventilation or 6 h after the cessation of ventilation.

We used an exteriorized model of VILI to test the UCBs as described previously by others (Hillman et al., 2011). This model was chosen due to its ability to isolate the initial volutrauma from subsequent inflammation and injury that would occur over the proceeding 24 h with maintaining these lambs *ex utero*, including the need for ongoing respiratory support, nutrition, and neonatal intensive care. Instead, the ewe (via the placenta) provides all of the respiratory and nutritional requirements of the fetus. One potential problem with this model is that the presence of a fetal circulation, which means that only 12% of combined ventricular output passes through the pulmonary circulation (Rudolph, 1983). Normally when cells are given intravenously after birth, they can become passively trapped within the lungs, for a few days/weeks after administration (Anjos-Afonso et al., 2004; Kean et al., 2013). It has been postulated that this may actually be one of the mechanisms where by stem cells are effective for reducing lung injury (Inamdar and Inamdar, 2013). However, it is known

that actual engraftment and differentiation of UCB cells occurs at very low rates, or not at all, at the site of injury (Paton et al., 2018). Instead, they act systemically to reduce inflammation and can act at immune organs such as the spleen and lymph nodes (McDonald et al., 2018). In this study we did not label the UCB cells so we were unable to determine if there was cell engraftment within the lung parenchyma. However, studies by Vosdoganes et al. (2011) showed that i.v. administration of hAECs to the fetus reduced the pulmonary inflammatory response in an LPS model of lung injury. Although in this study combined intratracheal and i.v. administration was most effective, both administration routes alone were able to attenuate injury. A study by Cargnoni et al. (2009) using a bleomycin-induced lung injury mouse model showed that both i.v. and intratracheal hAEC administration was able to attenuate lung injury. The optimal route of cell administration needs to be investigated further.

While UCB cell administration did not reduce VILI in this study, the potential of UCB administration should not be dismissed out of hand. A multiple dosing scheme may be more effective at reducing inflammation and injury, since UCB cells unexposed to inflammation will be given at multiple time points, potentially overcoming a loss of efficacy following inflammation exposure. UCB cell administration at 1 h following initiation of ventilation is ineffective; therefore, a study comparing other or even multiple time points may show benefit.

CONCLUSION

We demonstrated that an acute period of volutrauma resulted in profound changes to lung architecture that can be observed 24 h after the insult, confirming the importance of the initial resuscitation period in the delivery room to the progression and severity of VILI. This highlights the importance of better monitoring and/or control of tidal volume during the initial resuscitation of preterm infants, and also the importance of this

critical window for therapeutic targeting. UCB cells administered 1 h after volutrauma were unable to reduce VILI in preterm fetal sheep. Future studies will be needed to determine the optimal timing, dosing, or administration scheme before UCB cells can be seen as a potential prophylactic therapy for VILI in preterm infants.

DATA AVAILABILITY STATEMENT

The datasets generated for this study are available on request to the corresponding author.

ETHICS STATEMENT

The animal study was reviewed and approved by the Monash University Animal Ethics Committee.

AUTHOR CONTRIBUTIONS

MS, KC, PP, IN, GP, and CM had input into the conception and design of the work. MS, KC, PP, VZ, IN, BA, GP, and CM were involved with data acquisition, analysis and interpretation of data for the work, drafting and revising the work, and approved the content for publication.

FUNDING

This work was supported by the National Health and Medical Research Council (NHMRC) Fellowships (GP: 1105526 and CM: APP1110195), a Heart Foundation of Australia Future Leaders Fellowship (GP), Cerebral Palsy Alliance of Australia Fellowship (CM), and the Victorian Government's Operational Infrastructure Support Program.

REFERENCES

- Anjos-Afonso, F., Siapati, E. K., and Bonnet, D. (2004). *In vivo* contribution of murine mesenchymal stem cells into multiple cell-types under minimal damage conditions. *J. Cell Sci.* 117(Pt 23), 5655–5664.
- Aridas, J. D., McDonald, C. A., Paton, M. C., Yawno, T., Sutherland, A. E., Nitsos, I., et al. (2016). Cord blood mononuclear cells prevent neuronal apoptosis in response to perinatal asphyxia in the newborn lamb. *J. Physiol.* 594, 1421–1435. doi: 10.1113/JP271104
- Barton, S. K., Melville, J. M., Tolcos, M., Polglase, G. R., McDougall, A. R., Azhan, A., et al. (2015). Human amnion epithelial cells modulate ventilation-induced white matter pathology in preterm lambs. *Dev. Neurosci.* 37, 338–348. doi: 10.1159/000371415
- Bernardo, M. E., and Fibbe, W. E. (2013). Mesenchymal stromal cells: sensors and switchers of inflammation. *Cell Stem Cell* 13, 392–402. doi: 10.1016/j.stem.2013.09.006
- Blencowe, H., Cousens, S., Oestergaard, M. Z., Chou, D., Moller, A. B., Narwal, R., et al. (2012). National, regional, and worldwide estimates of preterm birth rates in the year 2010 with time trends since 1990 for selected countries: a systematic analysis and implications. *Lancet* 379, 2162–2172. doi: 10.1016/S0140-6736(12)60820-4
- Cargnoni, A., Gibelli, L., Tosini, A., Signoroni, P. B., Nassuato, C., Arienti, D., et al. (2009). Transplantation of allogeneic and xenogeneic placenta-derived cells reduces bleomycin-induced lung fibrosis. *Cell Transplant.* 18, 405–422. doi: 10.3727/096368909788809857
- Chang, Y. S., Oh, W., Choi, S. J., Sung, D. K., Kim, S. Y., Choi, E. Y., et al. (2009). Human umbilical cord blood-derived mesenchymal stem cells attenuate hyperoxia-induced lung injury in neonatal rats. *Cell Transplant.* 18, 869–886. doi: 10.3727/096368909X471189
- Chimenti, L., Luque, T., Bonsignore, M. R., Ramirez, J., Navajas, D., and Farre, R. (2012). Pre-treatment with mesenchymal stem cells reduces ventilator-induced lung injury. *Eur. Respir. J.* 40, 939–948.
- Curley, G. F., Hayes, M., Ansari, B., Shaw, G., Ryan, A., Barry, F., et al. (2012). Mesenchymal stem cells enhance recovery and repair following ventilator-induced lung injury in the rat. *Thorax* 67, 496–501. doi: 10.1136/thoraxjnl-2011-201059
- De Paepe, M. E., Mao, Q., Ghanta, S., Hovanesian, V., and Padbury, J. F. (2011). Alveolar epithelial cell therapy with human cord blood-derived hematopoietic progenitor cells. *Am. J. Pathol.* 178, 1329–1339.
- Doyle, L. W., Carse, E., Adams, A. M., Ranganathan, S., Opie, G., and Cheong, J. L. Y. (2017). Ventilation in extremely preterm infants and respiratory function at 8 years. *N. Engl. J. Med.* 377, 329–337. doi: 10.1056/NEJMoa1700827

- Dreyfuss, D., and Saumon, G. (1992). Barotrauma is volutrauma, but which volume is the one responsible? *Intensive Care Med.* 18, 139–141.
- Garibaldi, B. T., D'Alessio, F. R., Mock, J. R., Files, D. C., Chau, E., Eto, Y., et al. (2013). Regulatory T cells reduce acute lung injury fibroproliferation by decreasing fibrocyte recruitment. *Am. J. Respir. Cell Mol. Biol.* 48, 35–43. doi: 10.1165/rcmb.2012-0198OC
- Hansmann, G., Fernandez-Gonzalez, A., Aslam, M., Vitali, S. H., Martin, T., Mitsialis, S. A., et al. (2012). Mesenchymal stem cell-mediated reversal of bronchopulmonary dysplasia and associated pulmonary hypertension. *Pulm. Circ.* 2, 170–181. doi: 10.4103/2045-8932.97603
- Hayes, M., Curley, G. F., Masterson, C., Devaney, J., O'Toole, D., and Laffey, J. G. (2015). Mesenchymal stromal cells are more effective than the MSC secretome in diminishing injury and enhancing recovery following ventilator-induced lung injury. *Intensive Care Med. Exp.* 3:29. doi: 10.1186/s40635-015-0065-y
- Hillman, N. H., Kallapur, S. G., Pillow, J. J., Moss, T. J., Polglase, G. R., Nitsos, I., et al. (2010). Airway injury from initiating ventilation in preterm sheep. *Pediatr. Res.* 67, 60–65. doi: 10.1203/PDR.0b013e3181c1b09e
- Hillman, N. H., Moss, T. J., Kallapur, S. G., Bachurski, C., Pillow, J. J., Polglase, G. R., et al. (2007). Brief, large tidal volume ventilation initiates lung injury and a systemic response in fetal sheep. *Am. J. Respir. Crit. Care Med.* 176, 575–581.
- Hillman, N. H., Polglase, G. R., Pillow, J. J., Saito, M., Kallapur, S. G., and Jobe, A. H. (2011). Inflammation and lung maturation from stretch injury in preterm fetal sheep. *Am. J. Physiol. Lung Cell. Mol. Physiol.* 300, L232–L241. doi: 10.1152/ajplung.00294.2010
- Hodges, R. J., Jenkin, G., Hooper, S. B., Allison, B., Lim, R., Dickinson, H., et al. (2012). Human amnion epithelial cells reduce ventilation-induced preterm lung injury in fetal sheep. *Am. J. Obstet. Gynecol.* 206, 448.e8–448.e15. doi: 10.1016/j.ajog.2012.02.038
- Huang, X., Sun, K., Zhao, Y. D., Vogel, S. M., Song, Y., Mahmud, N., et al. (2014). Human CD34+ progenitor cells freshly isolated from umbilical cord blood attenuate inflammatory lung injury following LPS challenge. *PLoS One* 9:e88814. doi: 10.1371/journal.pone.0088814
- Inamdar, A. C., and Inamdar, A. A. (2013). Mesenchymal stem cell therapy in lung disorders: pathogenesis of lung diseases and mechanism of action of mesenchymal stem cell. *Exp. Lung Res.* 39, 315–327. doi: 10.3109/01902148.2013.816803
- Jobe, A. H. (2011). The new bronchopulmonary dysplasia. *Curr. Opin. Pediatr.* 23, 167–172. doi: 10.1097/MOP.0b013e3283423e6b
- Jobe, A. H., Hillman, N., Polglase, G., Kramer, B. W., Kallapur, S., and Pillow, J. (2008). Injury and inflammation from resuscitation of the preterm infant. *Neonatology* 94, 190–196. doi: 10.1159/000143721
- Kean, T. J., Lin, P., Caplan, A. I., and Dennis, J. E. (2013). MSCs: delivery routes and engraftment, cell-targeting strategies, and immune modulation. *Stem Cells Int.* 2013:732742. doi: 10.1155/2013/732742
- Kinsella, J. P., Greenough, A., and Abman, S. H. (2006). Bronchopulmonary dysplasia. *Lancet* 367, 1421–1431.
- Lai, T. S., Wang, Z. H., and Cai, S. X. (2015). Mesenchymal stem cell attenuates neutrophil-predominant inflammation and acute lung injury in an in vivo rat model of ventilator-induced lung injury. *Chin. Med. J.* 128, 361–367. doi: 10.4103/0366-6999.150106
- Li, J., Yawno, T., Sutherland, A., Loose, J., Nitsos, I., Allison, B. J., et al. (2017). Term vs. preterm cord blood cells for the prevention of preterm brain injury. *Pediatr. Res.* 82, 1030–1038. doi: 10.1038/pr.2017.170
- Li, J., Yawno, T., Sutherland, A., Loose, J., Nitsos, I., Bischof, R., et al. (2016). Preterm white matter brain injury is prevented by early administration of umbilical cord blood cells. *Exp. Neurol.* 283(Pt A), 179–187. doi: 10.1016/j.expneurol.2016.06.017
- McDonald, C. A., Penny, T. R., Paton, M. C. B., Sutherland, A. E., Nekkanti, L., Yawno, T., et al. (2018). Effects of umbilical cord blood cells, and subtypes, to reduce neuroinflammation following perinatal hypoxic-ischemic brain injury. *J. Neuroinflamm.* 15:47. doi: 10.1186/s12974-018-1089-5
- Melville, J. M., McDonald, C. A., Bischof, R. J., Polglase, G. R., Lim, R., Wallace, E. M., et al. (2017). Human amnion epithelial cells modulate the inflammatory response to ventilation in preterm lambs. *PLoS One* 12:e0173572. doi: 10.1371/journal.pone.0173572
- Mills, D. R., Mao, Q., Chu, S., Falcon Girard, K., Kraus, M., Padbury, J. F., et al. (2017). Effects of human umbilical cord blood mononuclear cells on respiratory system mechanics in a murine model of neonatal lung injury. *Exp. Lung Res.* 43, 66–81. doi: 10.1080/01902148.2017.1300713
- Monz, D., Tutdibi, E., Mildau, C., Shen, J., Kasoha, M., Laschke, M. W., et al. (2013). Human umbilical cord blood mononuclear cells in a double-hit model of bronchopulmonary dysplasia in neonatal mice. *PLoS One* 8:e74740. doi: 10.1371/journal.pone.0074740
- Moss, T. J. M. (2006). Respiratory consequences of preterm birth. *Clin. Exp. Pharmacol. Physiol.* 33, 280–284.
- Paton, M. C. B., Allison, B. J., Fahey, M. C., Li, J., Sutherland, A. E., Pham, Y., et al. (2019). Umbilical cord blood versus mesenchymal stem cells for inflammation-induced preterm brain injury in fetal sheep. *Pediatr. Res.* 86, 165–173. doi: 10.1038/s41390-019-0366-z
- Paton, M. C. B., Allison, B. J., Li, J., Fahey, M. C., Sutherland, A. E., Nitsos, I., et al. (2018). Human umbilical cord blood therapy protects cerebral white matter from systemic LPS exposure in preterm fetal sheep. *Dev. Neurosci.* 40, 258–270. doi: 10.1159/000490943
- Polglase, G. R., Barbuti, J., Allison, B. J., Yawno, T., Sutherland, A. E., Malhotra, A., et al. (2017). Effects of antenatal melatonin therapy on lung structure in growth-restricted newborn lambs. *J. Appl. Physiol.* 123, 1195–1203. doi: 10.1152/japplphysiol.00783.2016
- Rasmussen, I., Le Blanc, K., Sundberg, B., and Ringden, O. (2007). Mesenchymal stem cells stimulate antibody secretion in human B cells. *Scand. J. Immunol.* 65, 336–343.
- Rudolph, A. M. (1983). Circulatory changes during the perinatal period. *Pediatr. Cardiol.* 4(Suppl. 2), 17–20.
- Schmölzer, G. M., Kamlin, O. C. O. F., O'Donnell, C. P. F., Dawson, J. A., Morley, C. J., and Davis, P. G. (2010). Assessment of tidal volume and gas leak during mask ventilation of preterm infants in the delivery room. *Arch. Dis. Child.* 95, F393–F397. doi: 10.1136/adc.2009.174003
- Sharon, S. W. (2016). *Chow, Prudence Creighton, Vinosan Kander, Ross Haslam, Lui K. Australian and New Zealand Neonatal Network.* Sydney: ANZNN.
- Vosdoganes, P., Hodges, R. J., Lim, R., Westover, A. J., Acharya, R. Y., Wallace, E. M., et al. (2011). Human amnion epithelial cells as a treatment for inflammation-induced fetal lung injury in sheep. *Am. J. Obstet. Gynecol.* 205, 156.e26–156.e33. doi: 10.1016/j.ajog.2011.03.054
- Yawno, T., Schuilwerf, J., Moss, T. J., Vosdoganes, P., Westover, A. J., Afandi, E., et al. (2013). Human amnion epithelial cells reduce fetal brain injury in response to intrauterine inflammation. *Dev. Neurosci.* 35, 272–282. doi: 10.1159/000346683

Conflict of Interest: The authors declare that the research was conducted in the absence of any commercial or financial relationships that could be construed as a potential conflict of interest.

Copyright © 2020 Smith, Chan, Papagianis, Nitsos, Zahra, Allison, Polglase and McDonald. This is an open-access article distributed under the terms of the Creative Commons Attribution License (CC BY). The use, distribution or reproduction in other forums is permitted, provided the original author(s) and the copyright owner(s) are credited and that the original publication in this journal is cited, in accordance with accepted academic practice. No use, distribution or reproduction is permitted which does not comply with these terms.

This page is intentionally blank.

End